A DIGITAL RELAYING ALGORITHM FOR INTEGRATED POWER SYSTEM PROTECTION AND CONTROL

A Thesis

Submitted to the College of Graduate Studies and Research

in Partial Fulfillment of the Requirements

For the Degree of

Doctor of Philosophy

in the Department of Electrical Engineering

University of Saskatchewan

Saskatoon, Saskatchewan

by

Elemer Demeter

PERMISSION TO USE

In presenting this thesis in partial fulfillment of the requirements for a Postgraduate degree from the University of Saskatchewan, the author has agreed that the Libraries of this University may make it freely available for inspection. The author further has agreed that permission for copying of this thesis in any manner, in whole or in part, for scholarly purposes may be granted by the professor or professors who supervised this thesis work or, in their absence, by the Head of the Department or the Dean of the College in which this thesis work was done. It is understood that any copying or publication or use of this thesis or parts thereof for financial gain shall not be allowed without the author's written permission. It is also understood that due recognition shall be given to the author and to the University of Saskatchewan in any scholarly use which may be made of any material in this thesis.

Request for permission to copy or to make other use of material in this thesis in whole or part should be addressed to:

Head of the Department of Electrical Engineering
University of Saskatchewan
57 Campus Drive
Saskatoon, Saskatchewan, Canada
S7N 5A9

ABSTRACT

Recent developments in data packets based high speed digital communications have opened the door for new types of applications in power system protection and control. Intelligent Electronic Devices (IEDs) are equipped with various communication capabilities that make their functional integration a natural next step. Existing integration of substation equipment is not capable of clustering with the purpose of pooling hardware resources.

Presently, every electric device requiring protection has its dedicated hardware performing the predetermined set of protective functions. A new function-based protection and control philosophy is proposed, based on an open-system solution. In the proposed system, the resources of the protective and control hardware are pooled, and as a clustered system provide each protected unit (line, transformer, breaker, etc) with functions required for complete direct and backup protection.

The work presented in this thesis identifies the performance requirements of a digital relaying algorithm for processing samples that are sent across Ethernet-based communication channels. The work shows the shortcomings and unstable performance of widely used protective algorithms in accommodating data samples that are out of step from their proper position due to variable time delays of the communications media. A new digital relaying algorithm was developed that is able to extract the amplitude and phase angle of signals from data samples received across Ethernet networks with variable jitter.

The performance of the algorithm was tested by using the recovered phasor amplitude and phase angle information in protective solutions. The results show that there is significant flexibility in the algorithm that can be used to facilitate less performant communication channels, or, to take advantage of faster communications channels by reducing the response time of the protective function.

The results show that the algorithm works well with variable length data windows, and variable sampling frequencies. Higher sampling rates make communications problems more visible, but the presented algorithm is able to compensate for wide variations in network performance, effectively maintaining sampled signal phase and amplitude information during network performance fluctuations.

ACKNOWLEDGEMENTS

The author would like to express his gratitude to Dr. S.O. Faried and Dr. T.S. Sidhu for their continuous guidance and encouragement during the course of this research. Without their support this work would not had been possible.

TABLE OF CONTENTS

LIST OF TABLES

LIST OF FIGURES

LIST OF ABBREVIATIONS

AC	Alternating Current
CB	Circuit Breaker
CDPD	Cellular Digital Packet Data
CRC	Cyclic Redundancy Check
CSMA/CD	Carrier Sense Multiple Access and Collision Detection
CT	Current Transformer
DAU	Data Acquisition Unit
DFR	Digital Fault Recorder
DNP	Distributed Network Protocol
EIA	Electronic Industries Alliance
EPRI	Electric Power Research Institute
FACTS	Flexible Alternating Current Transmission Systems
FF	Full Cycle Fourier
FTP	File Transfer Protocol
GOMSFE	General Object Models for Substation and Field Equipment
GOOSE	Generic Object Oriented Substation Event
GPS	Global Positioning System
GPS-LSE	Global Positioning System Least Square Error
HF	Half Cycle Fourier
HTTP	Hypertext Transport Protocol
IEC	International Electrotechnical Commission
IED	Intelligent Electronic Device
IEEE	Institute of Electrical and Electronics Engineers
ISO	International Organization for Standardization
IP	Internet Protocol
I/O	Input/Output
Kb	Kilobit

LAN	Local Area Network
LG	Line-to-Ground
LL	Line-to-Line
LLL	3-Line
LSE	Least Square Error
MAC	Media Access Control Protocol
Mb	Megabit
Mbps	Megabits per second
MMS	Manufacturing Message Specification
NFS	Network File System
NIC	Network Interface Card
OLE	Object Linking and Embedding
OPC	Object Linking and Embedding for Process Control
OSI	Open Systems Interconnection
PLC	Power Line Carrier
PMU	Phasor Measurement Unit
PQ	Power Quality
PSTN	Public Switched Telephone Network
PT	Potential Transformer
QOS	Quality of Service
RMS	Root Mean Square
RS/EIA-232	Recommended Standard EIA-232
RS/EIA-485	Recommended Standard EIA-485
RTU	Remote Terminal Unit
SCADA	Supervisory Control and Data Acquisition
SOE	Sequence of Events
TCP	Transmission Control Protocol
TX	Transformer
UCA	Utility Communications Architecture
UDP	User Datagram Protocol
UPFC	Unified Power Flow Controller

CHAPTER 1

INTRODUCTION

Between the multitude of new inventions and innovations, toward the end of the nineteenth century, there were a few that had the most significant influence on the means by which today's modern societies fuel their energy needs. The alternating current (AC) applications seamed to have a bleak future before Nicholas Tesla's work on the polyphase AC electrical machines [1].

The competition between Thomas Edison's direct current generation and distribution, and the alternating current solution proposed by Westinghouse came to an end: with the help of the AC transformers, efficient electrical power transmission and distribution over long distances became reality [1]. With the construction of the Niagara Hydro generating stations and the Hamilton distribution facilities, Canada was in the forefront of making use of long distance electrical power transmission.

During the first half of the last century, a multitude of electrical power generating and distributing companies have emerged across North America that were focused on providing electrical service over limited geographical areas. With the integration of these utilities, large transmission systems were developed to allow a more effi-

cient power production and distribution. Further integration of power utilities led to province and state-wide service providers. To increase reliability and system security during operations, utilities have interconnected their grids, covering most of the inhabited areas of the North American continent.

1.1 Alternating current - benefits and challenges

Economic development and population growth are two of the main causes behind the exponential load increase, which in turn has driven the long term planning for developing proper generation and transmission capacities. Due to social and economic factors, project's lead time or the time between identifying the need for a major facility and the actual in-service date, has been increasing over the years. This increase, together with the continuous load growth, have resulted in ever smaller capacity margins for transmission facilities.

By the end of the last century, the way society viewed electrical power shifted from considering electrical power a vital service, to the more commercial interpretation of a commodity. This change has resulted in the deregulation of the electrical power production and transmission in certain jurisdictions. Unlike other commodities, electrical power is not storable in significant amount, and needs to be produced, transferred, distributed at the same instant at which is consumed.

As a consequence of deregulation, the North American electrical grid is being used in ways for which it was not designed. In the deregulated market, transmission

capacities are sold to the highest bidder, and transmission lines are operated closer and closer to their limits.

During emergency situations, significant reconfiguration of the grid may be required to provide the extra power needed for disturbance control, while, at the same time, not interrupting "power wheeling" across the lines, since some other utility's grid stability may depend on it. To accommodate such changes, an entire new approach to grid operations and monitoring is required, transforming the dynamics of the system operation, protection and control. The benefits of having large, interconnected AC transmission systems are challenged by the requirement to have a flexible, adaptable transmission grid.

1.2 Technically possible versus economically feasible

The theory of current division between parallel electrical circuits is also valid when transferring electrical power between the generating plants and load. More current will flow toward the path with smaller impedance. During system fault events, the load impedance is short circuited by a much lower fault impedance. As a result, as seen in Fig.(1.1), transmission lines can see the amplitude of the current carried during fault increase many times as compared to the amplitude of the regular load current.

The high currents observed during fault events are produced and transmitted using the same infrastructure as for the regular load currents. In theory, it would be possible

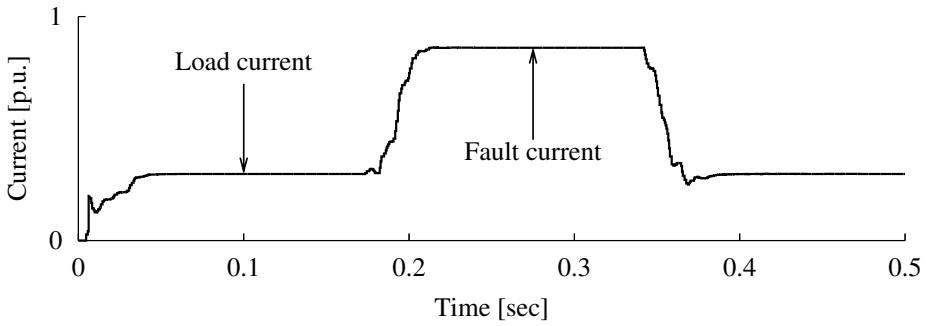

Figure 1.1: Fault current and load current amplitudes

to build over sized equipment that can handle the extra fault current, but such an approach would make the production and transmission of electrical power financially impossible. Ever since the first commercial applications, the adopted solution was to size the equipment for the load current with extra margin that provides a short time overloading capacity during which the faulted section of the system is to be de-energized and removed from service.

To reduce the area of the grid that is removed from service during a fault event, the system is sectionalized with the help of circuit breakers and zones of protection, as seen in Fig.(1.2). By opening breakers as close to the fault as possible, the extent of an outage to customers can be reduced.

1.3 Protecting the AC power system

Protective equipment is installed in switching stations to identify and isolate possible system faults and disturbances. Protective relays continuously monitor the state of the equipment and system they are meant to protect from damage [2, 3]. Providing

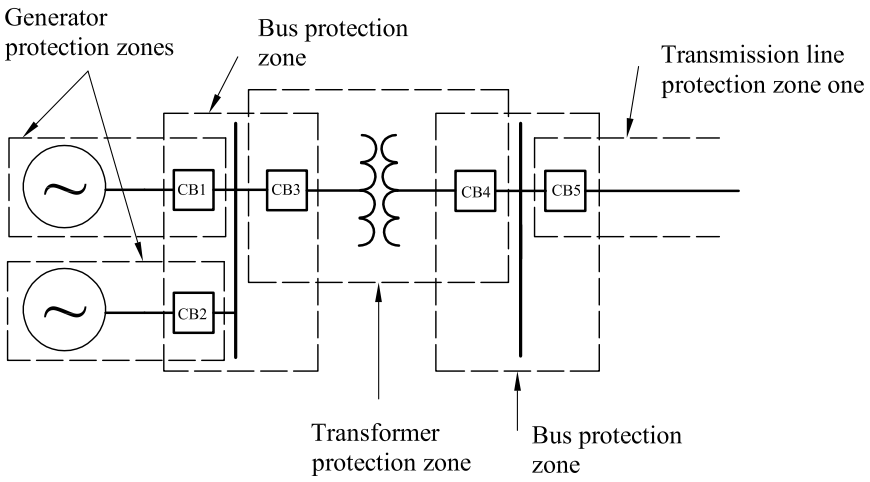

Figure 1.2: Section of power system with protection zones marked

information on the location and type of fault, or disturbance, is a secondary function of the protective relay.

Depending on the equipment they protect, there are numerous relay applications that monitor physical and chemical characteristics, or any other observable effect. The research presented in this thesis focuses on applications that monitor electrical values, voltages and currents, and their characteristics, while providing protection to various parts of the electrical grid.

An example of how relays can be connected to the transmission system they protect is presented in Fig.(1.3). The bus represents an energized, conducting structure to which lines, transformers and other apparatus are connected. The potential and current transformers (PT and CT, respectively) reduce the high voltage and current levels of the transmission line to signals that can be further processed using low power instrumentation. The circuit breaker (CB) has the ability to interrupt the high current during a fault condition.

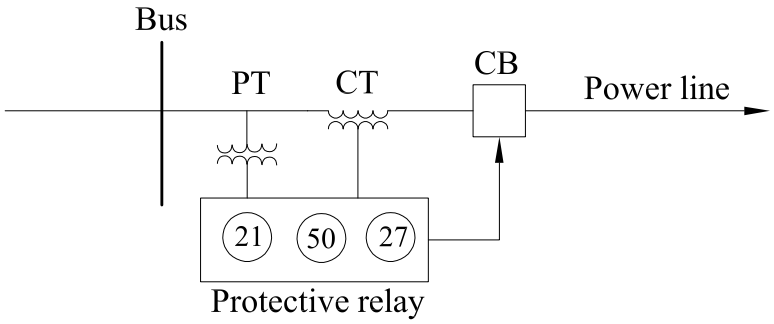

Figure 1.3: Typical application of a relay for line protection

Protection systems are designed using more than one protective device or function. In Fig.(1.3), the numbers 21, 50, 27 are representing standard IEEE protective functions describing the principles on which the protective relay or relays operate. The function 21 describes the presence of a distance or impedance element which operates when the circuit admittance, impedance or reactance increases or decreases beyond predetermined values. The element 50 is depicting an instantaneous overcurrent function that operates instantaneously on an excessive value of the current or an excessive rate-of-rise of the current. The under-voltage element 27 is meant to operate at a given value of under voltage. With the combination of different functions, a wide range of system faults and instability conditions can be detected and isolated.

The protective relay processes the information received through the CT and PT to decide if the system is in a condition that would indicate the presence of a fault or an unstable system condition. If decision is reached to remove the protected zone from service, it is done by opening the circuit breakers that completely isolate the faulted element from the rest of the system.

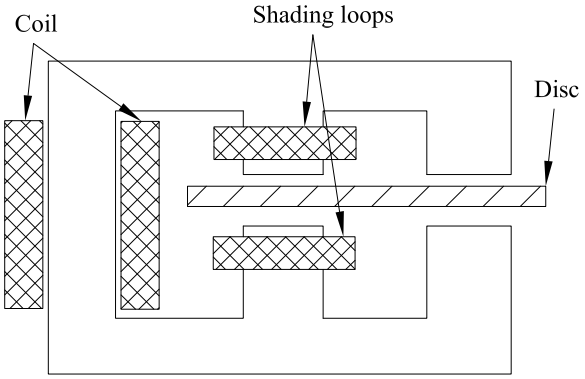

Figure 1.4: Induction-type overcurrent relay

1.3.1 Electromechanical relays

To better understand the new directions in the development of modern protective relaying, one has to understand its origins. Electromechanical relays were among the first types of devices utilized to protect electrical power systems. Their sensitivity to shock and vibration had significant effect on their performance. Different types of electromechanical relays have been developed. Most of them are based on the phenomena of electromagnetic attraction and electromagnetic induction [2].

Armature relays are the most extensively used electromechanical relays. The schematic structure of a shaded-pole relay is presented in Fig.(1.4). It operates under the same principles as the induction machine. Without the shading loops, the fluxes in the two magnetic paths passing through the disk would be in phase, and due to the sinusoidal signal in the coil, the disk would vibrate. Due to the shading loops, out-of-phase magnetic fluxes will be produced, and as a result, a constant force will be rotating the disk if the disk centre is not between the two points were the fluxes pierce the disk. Since the size characteristics of the relay are pre-determined by its

design, the monitored and controlling electrical signal is the current passing through the coil. The force acting on the disk is proportional to the amplitude of the current in the coil. With the help of a movement-opposing spring, various characteristics can be derived from this electromechanical structure. Overcurrent protection is the most frequent application to which shaded-pole relays are employed. They provide good primary protection for radial feeders, and can also be used for transformer backup protection [4].

A more complex relay is obtained if the effect of the current passing through the current coil is restrained with the voltage measured at the relay location. In the electromagnetic relay, this can be achieved by balancing the torque produced by the current element with the torque produced by the voltage element, as depicted in Fig.(1.5). During balanced condition, the torques produced by the voltage and current components would have to be equal, if the effect of the control spring is neglected.

$$T = k_1 I^2 - k_2 V^2 = 0 \tag{1.1}$$

In Eq.(1.1), T is the total torque acting on the disk, V and I are the measured voltage and current, respectively, while k_1 and k_2 are numerical coefficients. Equation (1.1) can be written as:

$$\frac{V}{I} = \sqrt{\frac{k_1}{k_2}} = Z \tag{1.2}$$

In other words, the relay is about to operate when the ratio of the voltage and

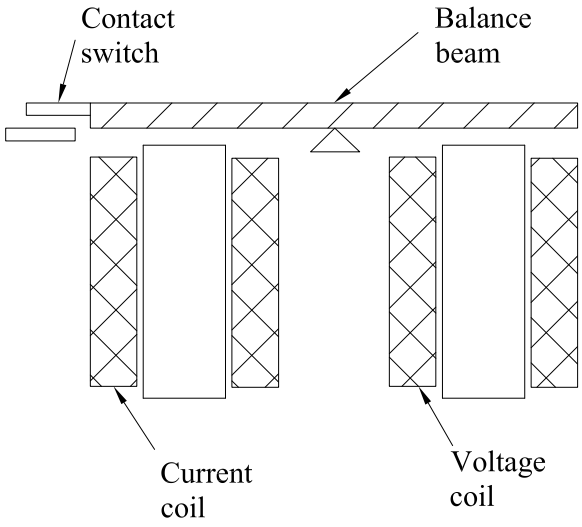

Figure 1.5: Impedance relay

current, or the equivalent impedance, is above a preset value. Considering Eq.(1.2), the operating characteristic of the impedance relay is depicted in Fig.(1.6).

The relay operating characteristic can also be depicted in the resistance and reactance plane, which is much more descriptive in representing the relay performance. The operating characteristic of the relay in the $R-X$ plane is depicted in Fig.(1.7).

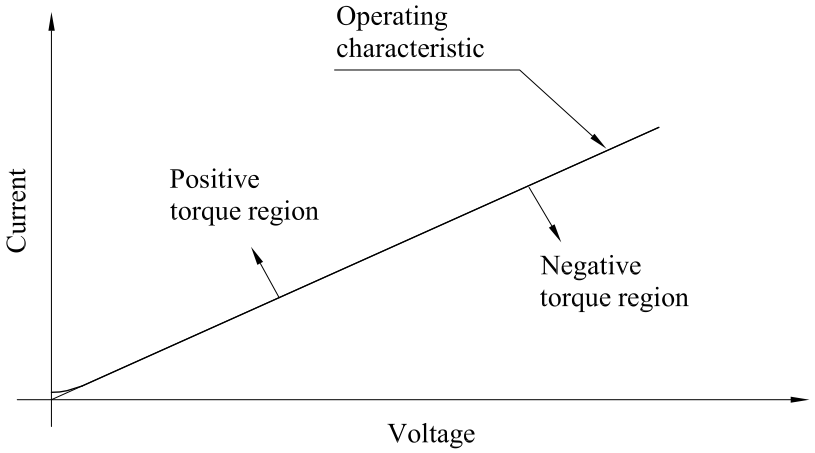

Figure 1.6: Impedance relay characteristic in the $V-I$ plane

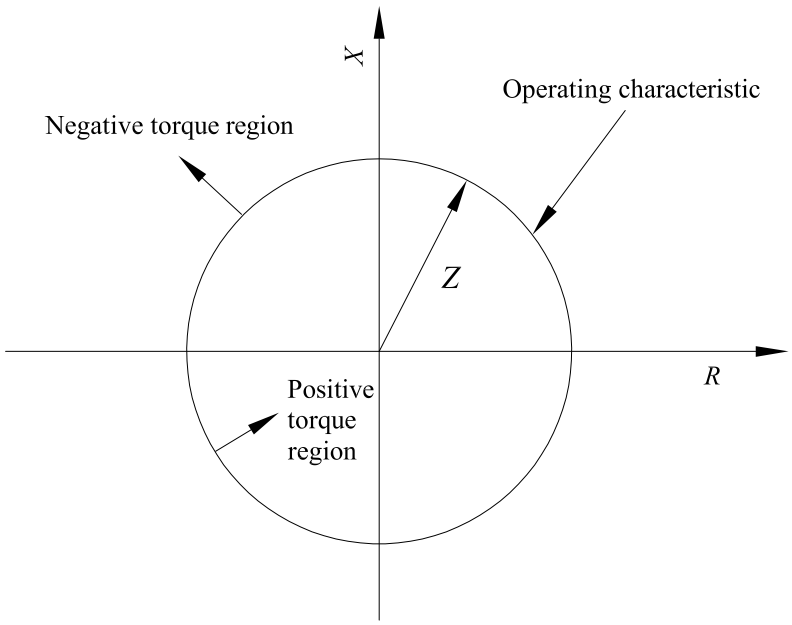

Figure 1.7: Impedance relay characteristic in the $R - X$ plane

The relay will experience positive torque for values inside the circle, and negative torque for values outside the circle. When the ratio between the voltage and current amplitudes is on the circle, the relay is on the verge of operating.

By selecting different polarizing voltages and with the help of restraining springs, complex operating characteristics can be obtained. The mho relay is a distance relay extensively used in transmission lines protection. As it can be seen in Fig.(1.8), its operating characteristic is a shifted circle and it has inherent directionality, being able to differentiate between faults on the protected line, and faults behind the line. Extensive research has been done in the area of transmission lines protection using impedance-, or distance elements [5–16].

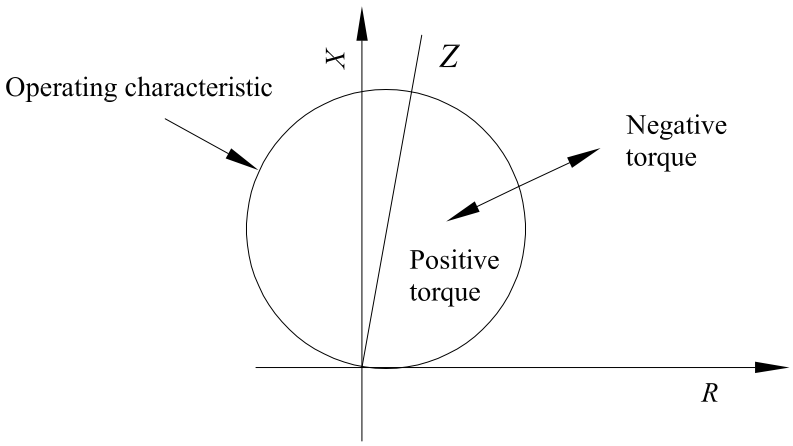

Figure 1.8: Mho relay characteristic in the $R - X$ plane

1.3.2 Solid-state relays

The stability and performance of induction-type electromechanical relays has made their replacement a slow process over the years. Solid-state solutions for power systems protection are well established. They are mostly analogue electronic devices, that in the beginning were designed to mimic the characteristics of the earlier electromechanical relays, which they could directly substitute in existing applications.

The main advantage of solid-state relays is that they allow complex multi-function schemes to be incorporated into one equipment. By measuring the voltage and current at the point of connection and using the characteristics of the protected power system segment, complex protection schemes can be developed. Since it is much more practical to process and store information in digital format, at some stage during the signal processing done by the solid-state relay, the analogue signals can be converted into digital information.

1.3.3 The digital age in power system protection

Protection solutions based on digital information processing have become widely utilized with the introduction of microprocessor-based relays [17–25]. Computations in solid-state relaying can be done mostly in parallel, as compared to microprocessor relays, which are doing calculations sequentially.

Some of the most significant drawbacks to adopting sooner microprocessor-based solutions were the stability and performance of these applications as compared to electromechanical and solid-state relays.

The continuously increasing performance and reduced costs have made the microprocessor relays the solution of choice [26,27]. Since information is processed digitally, a large number of functions can be built into one device. Backup protection solutions can be installed locally by simply installing dual-layer redundant protective systems. By selecting different make and model relays, the risk of maloperation due to common design or manufacturing defects is minimized. The structure of a microprocessor relay is presented in Fig.(1.9).

1.4 Active power flow control in transmission lines

Due to the continuous load increase and limited transmission capacities, combined with variable power wheeling requirements as a result of contractual obligations, active power flow control in the transmission grid is required. Power flow control can be done with the help of voltage and phase angle regulation, or by modifying

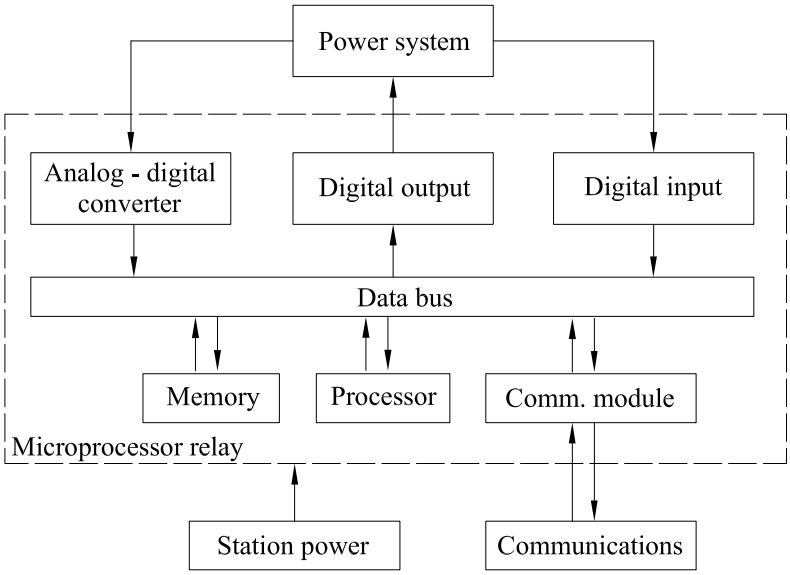

Figure 1.9: Microprocessor relay functional diagram

apparent system characteristics with the help of FACTS devices [28–36].

Protective solutions with static settings make extensive system reconfigurations difficult. One of the existing solutions that allows changes to relay settings is adaptive relaying, where the settings of protective relays are modified depending on the configuration of the transmission system. Such an approach provides a local solution. It does not address the problem of possible system disturbances created as a result of the transmission line reconfigurations. It lacks the ability to predict system-wide instabilities, since the relays monitor mainly local electrical values and have very limited features that would provide system level wide-area protection.

1.5 New challenges for power systems protection and control

Pressures from stakeholders force utilities to maximize their return on investment. As a result, transmission and distribution facilities are operated at ever higher levels of power transfer. Large blackouts, such as the one in the Northeast U.S. and Canada during August 2003, can result in a significant push to upgrade equipment and increase transfer capacity, which in turn, leads to even more pressure on transmission facilities, completing the circle.

Researchers have recognized that only fundamental change in the way power systems are designed and operated can reduce significantly the risk of large scale blackouts. Wide-area protection application have been identified as having great potential in minimizing future large scale outages.

The electromechanical relays presented in the previous section cannot be used effectively for wide-area protection because they lack the capability to receive and process information from other locations. What the previous apparatus have in common is that they are directly connected to the equipment they protect via CTs and PTs. Information cannot be transmitted over significant distances using the analogue signals in the low-voltage side of the PTs and CTs, since the information quality is affected by the length and electrical characteristics of the cabling between the instrumentation and the protective device. Minimizing the electrical burden is one of the design criteria for protective installations.

The need for wide-area protection has been recognized by numerous researchers

and regulators. In order to provide efficient wide-area protection to large segments of the power system, a significant number of electrical values (voltages and currents) have to be known from various locations. Since transferring analogue signals across large areas is not possible, existing solutions make use of digital communications. The amount of data processing required is significant, and effective protective functions require the use of information technology solutions.

Information technology applications have adopted the Ethernet networking as primary communications solution. Due to its performance and flexibility, the Ethernet has been included in a number of substation automation standards.

Existing digital relaying algorithms are not designed to accommodate the variations and changes in the performance of communications channels that are a characteristic of packet-based networks.

1.6 Research objectives

The objective of the research presented in this thesis is to develop the principles of an open-system solution based on information technology, that can be applied both to local device-focused protection schemes and also to wide-area protection, monitoring and control.

A digital relaying algorithm is developed that can be utilized using information technology communications media. The viability of the proposed system is tested on various protective applications.

1.7 Proposed outline

The first chapter is an introduction to power systems protection with examples on how it evolved from electromechanical relays to microprocessor-based complex protection systems. It places the research area in the big picture of power system protection solutions.

Information requirements during the operation of protection systems are outlined in the beginning of the second chapter. Early solutions for relay communications and supervisory control and data acquisition applications are presented. Protocols used in substations and operational communications are described, and the case is made for the need for real-time system data for wide-area power system protection functions. The Ethernet networking and its performance as a process bus is presented together with a model suitable for integration into power system simulations.

A complete open-system approach to protection and control integration based on information technology applications is proposed in chapter three. The advantages and benefits of the proposed solution are outlined.

Chapter four presents digital relaying algorithms used in microprocessor relays. The case is made that due to their characteristics, these algorithms cannot be used directly in the proposed open system Ethernet-based data transfer applications. The performance requirements of a digital relay algorithm capable of performing with delayed and missing samples is described.

The new digital relaying algorithm is developed in chapter five. The proposed so-

lution overcomes the drawbacks of Ethernet-based communications for synchrophasor transmission.

Chapter six presents the results obtained from testing the new digital relaying algorithm during various system conditions. The testing is done using the Matlab modelling environment. The Ethernet networking is included into the power system model together with the new digital relaying algorithm to allow for an integrated performance evaluation. The algorithm is tested as part of three protective functions during different types of faults. A parallel is made between the performance of the proposed solution and the widely used Full-cycle Fourier algorithm.

In chapter seven, conclusions are drawn based on the performance of the proposed digital relaying algorithm and the open-system integrated protection and control philosophy. Directions are proposed as possible continuation for the research work presented in this thesis.

CHAPTER 2

COMMUNICATIONS IN THE SUBSTATION

2.1 The need for information in substation applications

The first applications of communicating data in the substation are as old as the power systems protection. The scope of data communications in power systems can be either monitoring, recording, protection or control oriented [37–40].

At the beginning, substation communications consisted of electric cables transferring analogue values between the instrumentation installed on the lines and the corresponding electromechanical relays that were performing basic protective functions, as depicted in Fig.(2.1).

With the invent of high speed communications, such as power line carriers (PLC), microwave, radio, fibre optics, the performance of protective installations were significantly improved using teleprotection. For example, in Fig.(2.2), clearing of a fault along the transmission line can be done in high speed, from both ends, with the help of the communications channel.

Depending on the type of signals sent and on the operations logic, there are

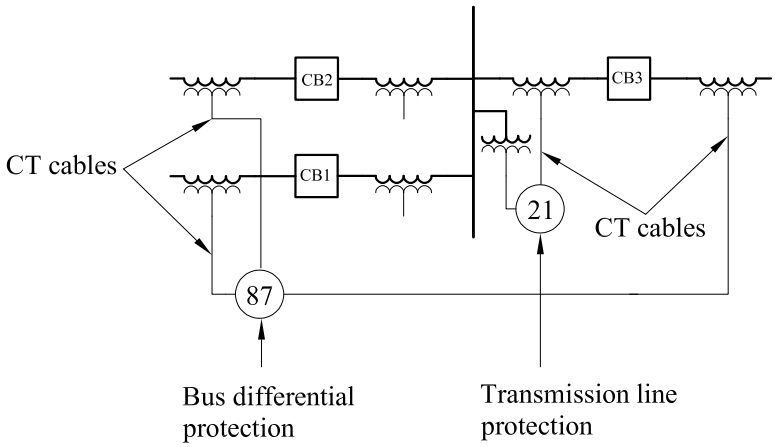

Figure 2.1: Instrumentation cabling in the substation

various teleprotection schemes that can be implemented for protecting transmission lines using communications equipment. Detailed system studies and performance requirements determine which specific solution is to be applied. One of the most common schemes for the example presented in Fig.(2.2) is the permissive under-reach. At the occurrence of a fault, the relay operating CB1 will see the fault in zone 2, since its zone 1 reach ends prior to where the fault took place. Without

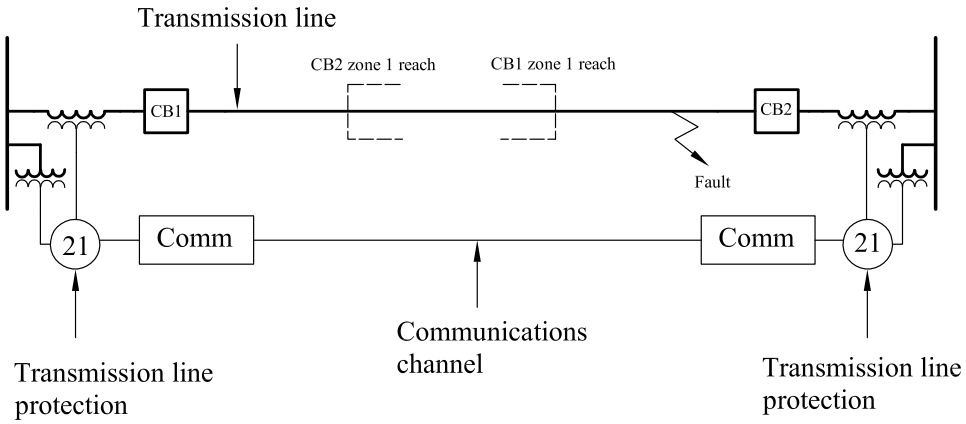

Figure 2.2: Transmission line protection coordination using communications

the help of teleprotection, the fault would be cleared as per the zone 2 time delay, which can lead to significant risks for the system. In this scheme, with the help of the communications channel, the relay operating CB2 is able to signal the opposite relay that a faulted condition exists in its zone 1 coverage, and CB1 can also clear the line in high-speed operation, giving the system a better chance to recover after the fault. Other teleprotection schemes used for transmission lines include permissive over-reach and blocking logic [4]. The advantage of blocking schemes over permissive under-reach schemes is that the signal does not have to travel through a faulted line in case that power line carrier (PLC) is used as communications media: the line will be cleared in high speed for all zones, unless a blocking signal is received.

2.2 Supervisory control and data acquisition

Supervisory control and data acquisition (SCADA) applications are built upon an extensive communications infrastructure, and can include a combination of communications media, as seen in Fig.(2.3). The requirements of SCADA communications is different than the ones that are protection oriented. Speed, bandwidth, reliability are extremely sensitive characteristics of a teleprotection system. On the other hand, loss of signal from a Remote Terminal Unit (RTU) for a short time is not an uncommon event in a system control centre.

Some of the main purposes of a power utility SCADA installation are to allow monitoring of the overall system, transfer equipment status and condition to a central

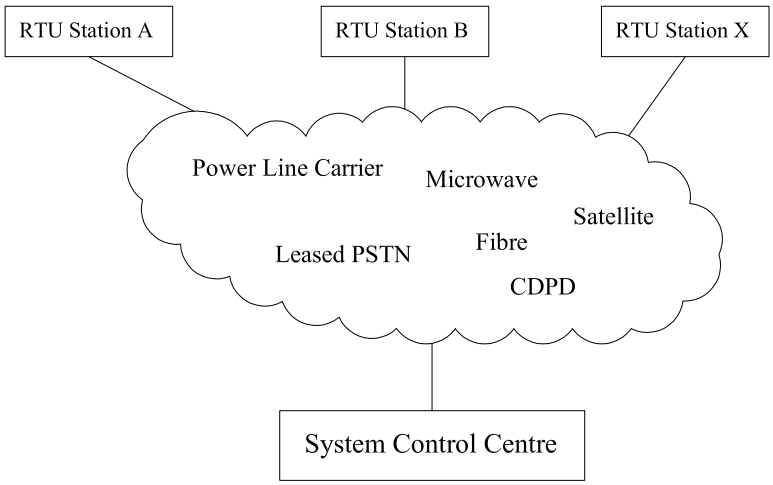

Figure 2.3: RTU connection to the System Control Centre

location, evaluate on-line and off-line the system condition, anticipate emergency situations, plan for preventive operations and execute system operations.

An example of substation SCADA installation that includes analogue input, digital status input/output (I/O) is presented in Fig.(2.4). The analogue module receives

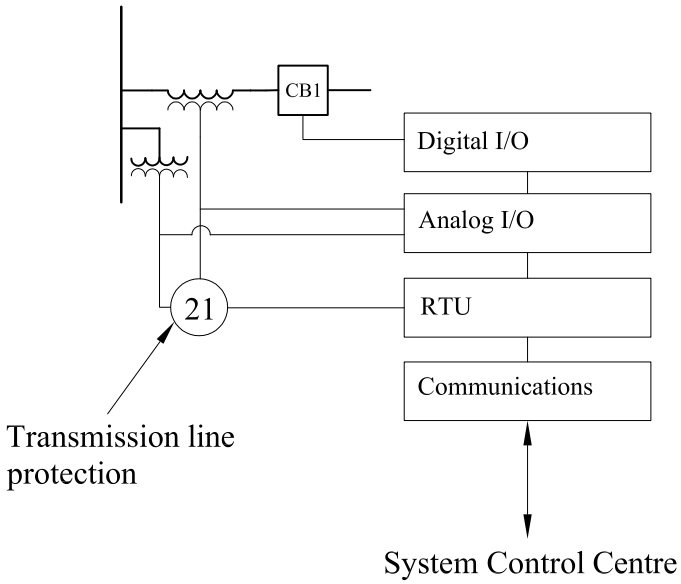

Figure 2.4: Data acquisition and control in the substation

input from the secondary circuits of the station instrumentation. Both current and voltage information is passed to the RTU by the analogue input subsystem. The analogue subsystem is also able to produce analogue output signal that can be used by other instrumentation and control equipment in the station.

Digital input values can include information related to the status of breakers, transformer tap position indication, station alarms, etc. Digital output signals can be used to operate the circuit breakers from the system control centre, either to open or close circuits or to execute routine remote switching in the station.

With the continuous progress in circuit integration, a large number of functions can be incorporated into protective, monitoring and control equipment in the substation. An Intelligent Electronic Device (IED) is able to perform much more than its primary function: it is able to do monitoring, control and diagnostic functions.

Interconnecting multipurpose equipment inside the substation was the next step in the development of substation control and monitoring applications. Intelligent electronic devices can be connected using combinations of three basic topologies. Star-connected IEDs are depicted in Fig.(2.5). This type of connection offers the advantage that different speeds of communication and protocols can be used on each of the connected device. The ring-type connection is depicted in Fig.(2.6), and it offers the advantage that the communications system can be kept operational to each device in case that any one segment of the communications cable is cut or malfunctioning. In case of the star configuration, the loss of one connection makes the IED connected

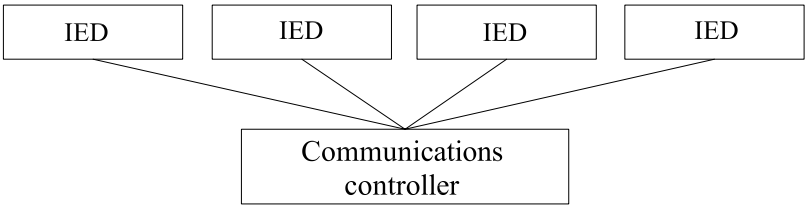

Figure 2.5: Star-connected IED devices

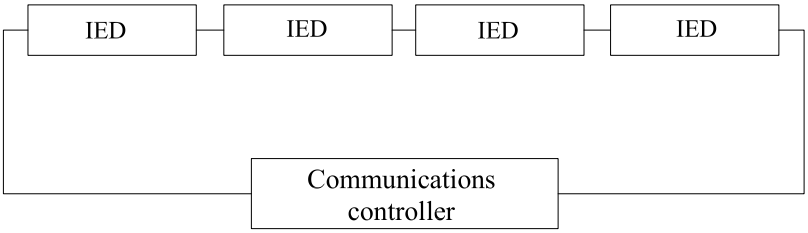

Figure 2.6: Ring-connected IED devices

to it unreachable.

A more advanced bus-type connection configuration is presented in Fig.(2.7). The bus-type configuration offers the advantage of reduced cabling and all IEDs can be accessed using the same communications port. In this type of connection, the communication channel is shared between many devices and requires advanced addressing capabilities from the communications protocol.

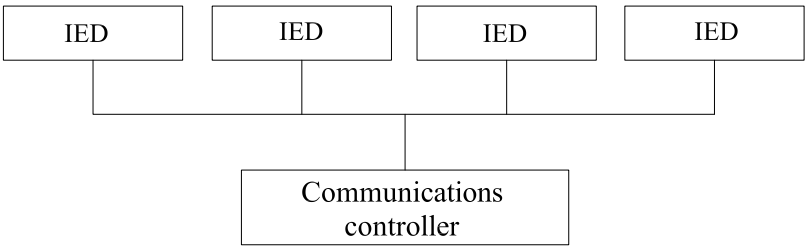

Figure 2.7: Bus-connected IED devices

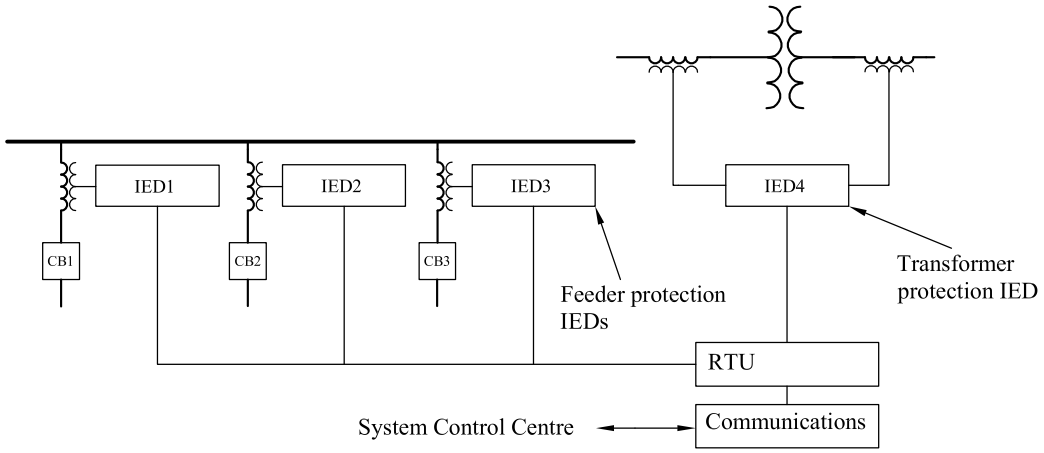

Figure 2.8: Connection of protective IEDs to the RTU in a typical substation

A combination of the star and bus type connections in a typical substation installation can be seen in Fig.(2.8). The recloser controllers installed on the distribution feeders connect to the RTU using a data bus type Ethernet network, while the transformer protection IED is directly connected to the central unit using a serial, dedicated connection.

2.3 Protocols used in SCADA applications

Communication is possible and available when two IED devices can "speak the same language". Standardized protocols help protection and control devices integrate into power system protection and control systems.

In widely used configurations, one of the IEDs will act as a central device that controls the other IEDs in the station in a master/slave or server/client configuration. The interconnected equipment should understand at least one communications protocol, and the master or server device has to understand each protocol used by

different slave IEDs. In device connections that share the same hardware, all devices connected must be able to understand the same protocol at the same baud rate. These requirements can determine the specific configuration in which IEDs are connected in a substation and the utilized protocols.

One of the most frequently utilized protocols in North America is the Distributed Network Protocol, or DNP. It started as a proprietary protocol and was later moved into the public domain. It is widely used for communicating with, and between, remote terminal units and IEDs. It can be used over a number of communications media and standards, including serial (RS-232 and RS-485) and Ethernet. Its operating principle is based on the master-slave configuration and has an object-oriented structure. The master unit is able to poll other slave IEDs in the network, which respond to the poll by sending the requested analogue, status and indication information. The protocol supports also control operations on devices connected to slave IEDs.

Unsolicited responses are possible using DNP. During an unsolicited event such as a breaker operation due to emergency system conditions, the slave terminal is able to send an unsolicited message to the master device upon certain pre-programmed status change. The protocol supports time synchronization between master and slave devices, which makes it a convenient tool to update date and time information on remote terminal units from the master station [41–45].

With the development of Ethernet technology inside the substations, IEDs are

able to connect to substation local area networks (LAN). The DNP protocol has been implemented both over Transport Control Protocol (TCP) and User Datagram Protocol (UDP). The substation LAN-based DNP presents great benefits when applied to high number of IEDs. Polling can be done in multicast and broadcast modes to solicit new values from all the remote units by issuing only one command. The responding units Internet Protocol (IP) and DNP addresses uniquely identify the source of the returned data packets.

The master-slave relationship of a typical peer-to-peer communications model is common to most of the SCADA protocols. Other protocols developed specifically for monitoring and control purposes, such as Modbus and Object Linking and Embedding for Process Control (OPC) have similar features [46, 47].

2.4 The need for real-time monitoring

Reasons behind the integration of electrical power systems have been discussed in previous sections. Reliable operation of these systems is dependent on proper assessment of system conditions at critical locations. In SCADA applications, due to the length and multitude of communications channels between the source and destination of the data, there could be several seconds delay between the time when a poll is sent and the moment when the requested values are received from the remote terminal. Such delays are not a concern when the system control feedback loop includes human interpretation and action, as in supervisory control of power systems.

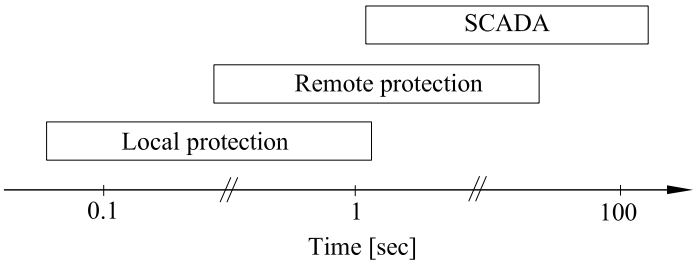

Figure 2.9: Communications speed performance requirements

2.4.1 Interprocess signalling

When IEDs are installed for monitoring and control automation, algorithms running in any given device could be dependent on the outputs or measurements made by other devices. In applications where operations are executed and control decisions are reached hundreds of times per second, delays in transmitting data can lead to the breakdown of the primary functions of the IED.

2.4.2 Protocols used for interprocess signalling

The Manufacturing Messaging Specification (MMS), was developed as a protocol for manufacturing automation, used to interconnect intelligent electronic devices, computers, programmable logic controllers, robots, etc on the shop floor. It is an object oriented messaging standard, aimed at sharing supervisory and real-time data between devices connected to the network [48].

The MMS has been adopted as an ISO standard for interprocess signalling. It is generic in nature, therefore, wide range of applications in different industries can be interconnected using this standard. It provides a unique communications environment

where data can be shared and provided exactly in the same manner, regardless of the type of device accessing it.

The MMS protocol is based on the concept of Messaging Service. Before data and control information could be exchanged, connection is established between the two communicating devices at logical level. This level of communication provides the syntax rules, services and objects available during the exchange of information, which represents the mechanics of the communications process.

The semantics or the meaning of the data and control objects communicated are defined in the next layer of the communications protocol. For power utility communications, the Utility Communications Architecture version 2 (UCA2) is a suite of standards that define the semantic rules required for two compliant devices to communicate. The UCA2 was developed by the Electric Power Research Institute (EPRI), as an open standard aimed for the power utility industry. The UCA2 uses the MMS for real time control signalling between two devices that communicate peer-to-peer. Object models called General Object Models for Substation and Field Equipment (GOMSFE) are used for the representation of physical or logical objects. With the help of the unsolicited event support of the MMS, UCA2 has implemented the unsolicited event reporting between communicating devices as a Generic Object Oriented Substation Event (GOOSE) message.

The International Electrotechnical Commission (IEC) continued the work started by EPRI, building on the UCA2 and developed the IEC 61850 standard. The IEC

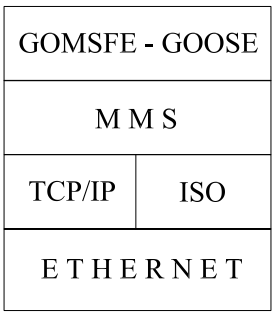

Figure 2.10: The UCA2 utility communications architecture

61850 standard provides a common reference for the interconnection of IEDs starting with substation applications up to inter-utility communications [49, 50].

2.5 Ethernet as a process bus

The Ethernet technology has experienced an exponential development and growth in almost every area where data transmission is involved. Continuous innovations in this networking technology make it very attractive to industrial applications [51–54].

The structure of the UCA2 protocol is shown in Fig.(2.10). Both UCA2 and IEC 61850 support Ethernet communications. Due to the characteristics of this type of networking, precise timing requirements are set on the communications media. The UCA2 standard requires a 4 ms target performance for communicating messages from single to multiple devices.

In order to present how latency occurs associated with the Ethernet-based communications, the ISO seven layer model for networking will be described. The ISO created a simple model for networking, the Open Systems Interconnection (OSI),

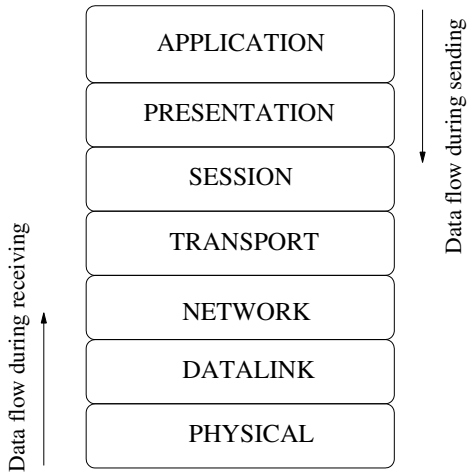

Figure 2.11: The ISO networking model

grouped in layers, one layer upon the other. Figure (2.11) presents the ISO seven layers model.

For transmission, the data will be passed from the top of the networking model, starting with the Application Layer, to the base of the model. The direction of data in the stack for receiving purposes is from the lower end to the top of the stack.

At the base of the model stands the network's physical structure, which gets packets to and from the network. The Data Link Layer determines how data is grouped. When Ethernet is utilized, it represents the Physical and Data Link Layers.

The Network Layer is responsible for getting the packets from point A to point B. The Internet Protocol, or IP, can be used as Network Layer.

The next layer will provide the transmission control. It will make sure that data is packed in properly sized data packets, and that packets arrive to the destination. The Transmission Control Protocol (TCP) is one possible solution that can do trans-

mission control. The TCP will monitor the receiving of the packets, and in case that a packet did not arrive, the transport layer will make sure that the missing packet is sent again. The User Datagram Protocol, or UDP, does not monitor the receiving of the packets, and it is up to the Application Layer at the receiving end to request a new transmission of the missing packet. The Session and the Presentation Layers will control the creation and the lifetime of connections and data formats.

The Application Layer resides at the top of the network model. It is the application that requests and sends the data across the network. Typical applications at this level of the networking model could include: File Transfer Protocol (FTP), Hypertext Transport Protocol (HTTP), Network File System (NFS), etc. The enormous advantage of this type of networking over the serial communications routinely used by power utilities is that a multitude of devices, protocols and applications can share the same communications hardware. The Application Layer in the UCA2 and IEC 61850 networking is represented by the MMS, together with the GOMSFE-GOOSE model.

Each of the above discussed layers will introduce a specific delay or latency in the data transmission. For the purpose of this discussion, the focus is on the total latency introduced by the communication process, and how to overcome this delay in protective relaying.

2.6 Modelling the Ethernet data transfer performance

The foundation block of the Ethernet networking philosophy is the equitable access of multiple devices to a common communications media. Each device connected to a network segment, while in a common collision domain, will have to share access time with all other devices in the same collision domain [55].

The Ethernet specifications determine the structure of the data frame shown in Fig.(2.12). The frame starts with 8 bytes of preamble, which are required to allow the network to synchronize with the frame by the time the next part of the frame arrives. The preamble is required only in the 10 Mbps network, and was kept for compatibility only in the faster versions of the network. The start-up losses are avoided using more complex mechanisms in the newer version of the Ethernet standard. The destination address contains the network card address of the destination device, while the source address is the network card address of the frame's originating interface.

The 4 bytes long type field contains information about what type of high-level protocol data is carried in the data field. The next 46 to 1500 bytes are the "payload" of the frame. The size of the data "payload" can be set by the user. Its size can determine the virtual utilization levels of the network. The performance of the network can be tuned for certain type of data by modifying the size of the data field.

The Ethernet frame ends with the cyclic redundancy check (CRC) information that is calculated by the sending interface. The destination interface calculates the CRC again, and accepts the frame as correct in case that the new CRC number is similar to the one embedded in the frame by the source card.

In half-duplex operation, the Media Access Control Protocol (MAC) implemented

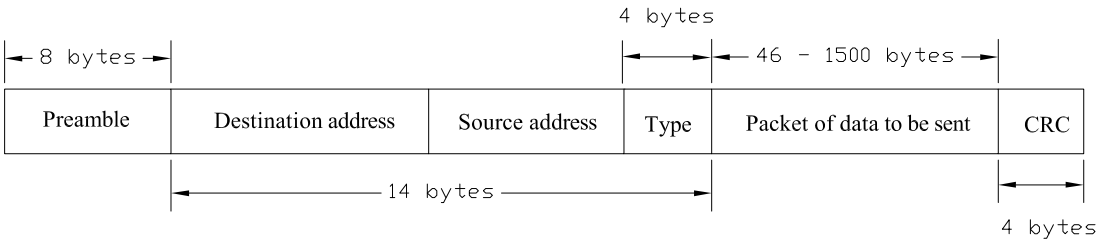

Figure 2.12: Ethernet frame structure

in each network card contains a set of rules that will give each device equitable access to the network. In Ethernet networking, the MAC mechanism is implemented using the Carrier Sense Multiple Access and Collision Detection (CSMA/CD) protocol.

The process of transmitting data is described by the logical diagram in Fig.(2.13). When a network interface card is ready to send data, and there is no other transmission in progress, it waits for a length of time equal to the inter-frame delay of the network. For 10 Mbps networks, this time is 9.6 μs. After this delay, the frame is sent into the network and the counter N is reset. All network interface cards will receive the transmission, but only the ones that are the destination end of the data frame will pick up the data, other cards will discard it.

It could happen that two devices on the network have sensed the free channel and have started transmitting data at the same instance. In this case, a collision occurs. The "collision" name can be misleading, since it is a feature of the network and not a failure of the transmission process to account for the possibility of colliding packets. The CSMA/CD protocol will recognize the data collision and execute a random delay after which the transmission is started again. The random number R, shown in Fig.(2.13), is determined based on how many previous collisions have occurred for the same data frame. As seen in the logic diagram, the time delay

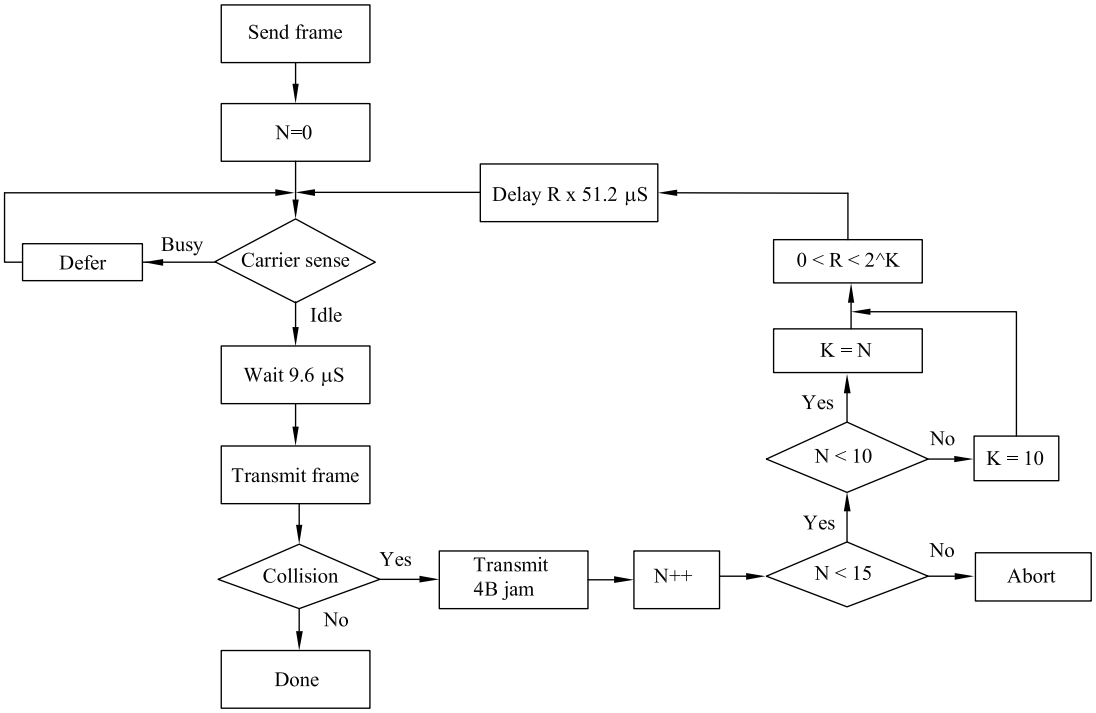

Figure 2.13: Collision detection and multiple access logic

is randomly selected from a set of numbers that increase exponentially after each collision.

The probability is very low to have the same two packets from the same two network interface cards collide several times. After 16 attempts the data frame is discarded. It is up to the higher layer in the networking model to make sure that discarded packets of data are sent again. As discussed, there are protocols that monitor the delivery of data, such as the TCP, and there are others that do not monitor data delivery, such as UDP. Evidently, since the UDP is a connection-less data delivery process, it is much faster than the TCP, but the application that uses it has to make provisions for missing information in the data stream.

The numbers representing definite time delays in Fig.(2.13) are characteristic to the 10 Mbps Ethernet channel. The 100 and 1000 Mbps network numbers are reduced

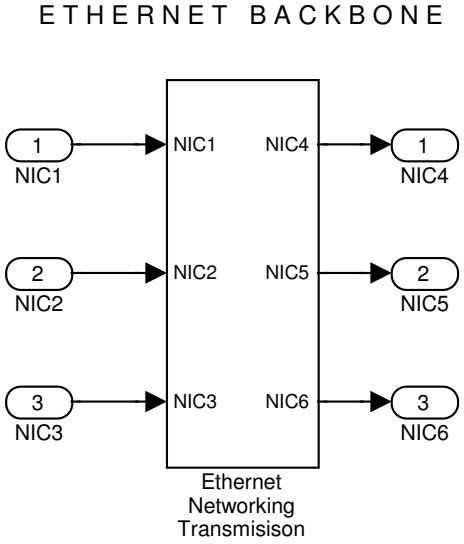

Figure 2.14: Ethernet networking system model

by the corresponding magnitude [55].

The Ethernet model will have to account for both delayed and discarded data frames. The delay experienced during data transmission has been extensively studied in the literature [55–59]. The models that best describe the overall performance of the transmission process are using the same random access approach. The delays caused by the upper layers in the networking model are considered also, since microprocessors are able to process data sequentially, and various applications are competing for resources.

The system model considered for investigating the performance of the process-bus application is shown in Fig.(2.14). The Network Interface Cards (NIC) are the Physical Layer of the ISO networking model representation, and are the input and output points at the sending and receiving ends, respectively. A detailed representation of the Ethernet transmission model is shown in Fig.(2.15).

The time delay distributions due to the Ethernet networking process are shown

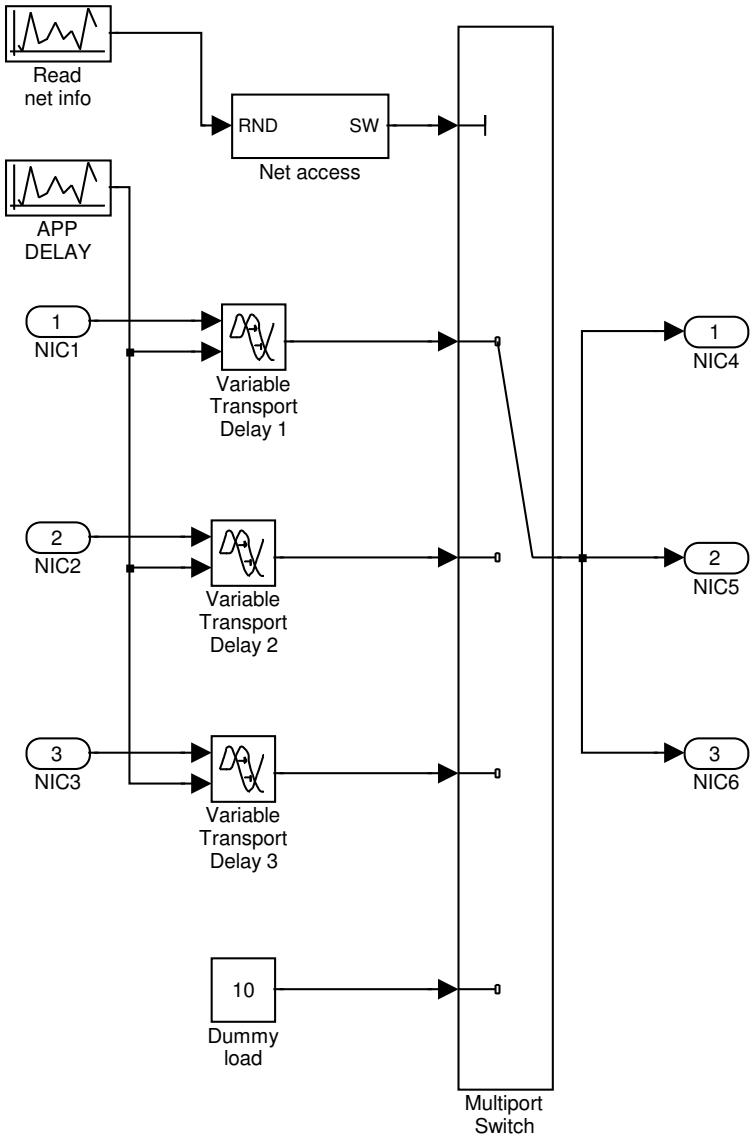

Figure 2.15: Detail of the Ethernet networking model

in Figs.(2.16) and (2.17). It can be seen that the fast network has a more consistent performance, while the slow network has delays distributed over a larger interval of time. The input parameters can be adjusted so that slow and fast network's performance can be modelled. The number of devices that are competing for the transmission media has been determined by researchers to be of great importance to

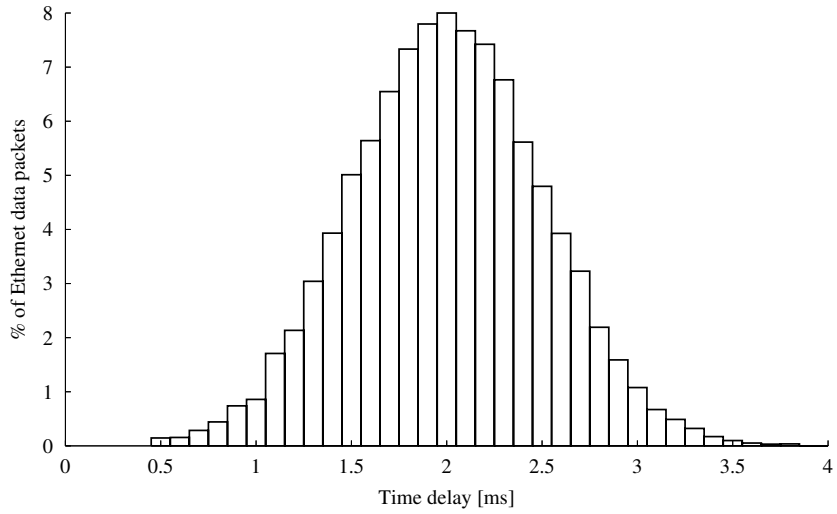

Figure 2.16: Time delay distribution of Ethernet data packets on fast network

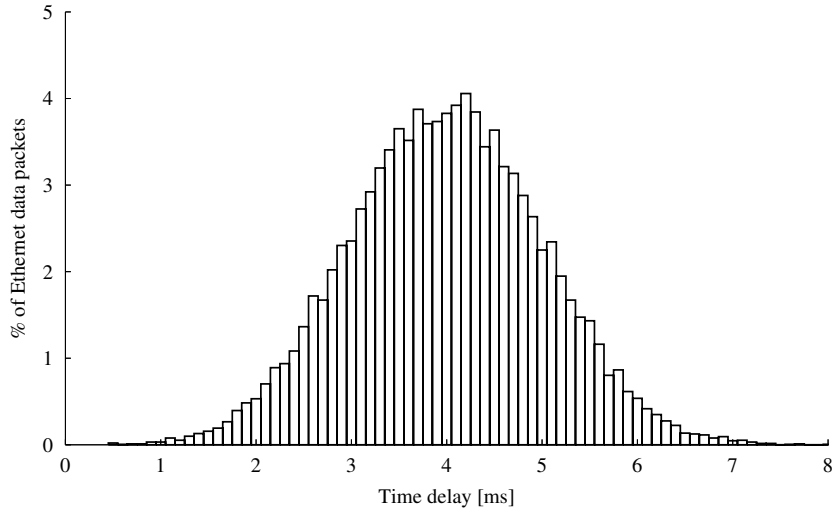

Figure 2.17: Time delay distribution of Ethernet data packets on slow network

the overall performance of the network, and can be preset in the proposed model.

The model can be used in Matlab simulations to reproduce a wide range of performance characteristics of Ethernet networks. To test the proposed digital relaying algorithm in accommodating variable network jitters, it is desirable to reproduce the worst possible time delays and data frame combinations that could occur during the

Ethernet networking. The results in Fig.(2.18) show two extreme operating conditions of the network. The reduced jitter transmission is specific to redundant transmission channels with high speed communications media, while the large jitter is specific to slow, congested data transmission on a single channel. The developed Ethernet model is capable of reproducing both.

Existing digital relaying algorithms depend on the constant flow of information received from the monitored signals. Protective applications that are to make use of data transmitted over Ethernet networks have to be able to accommodate the variable transport delay.

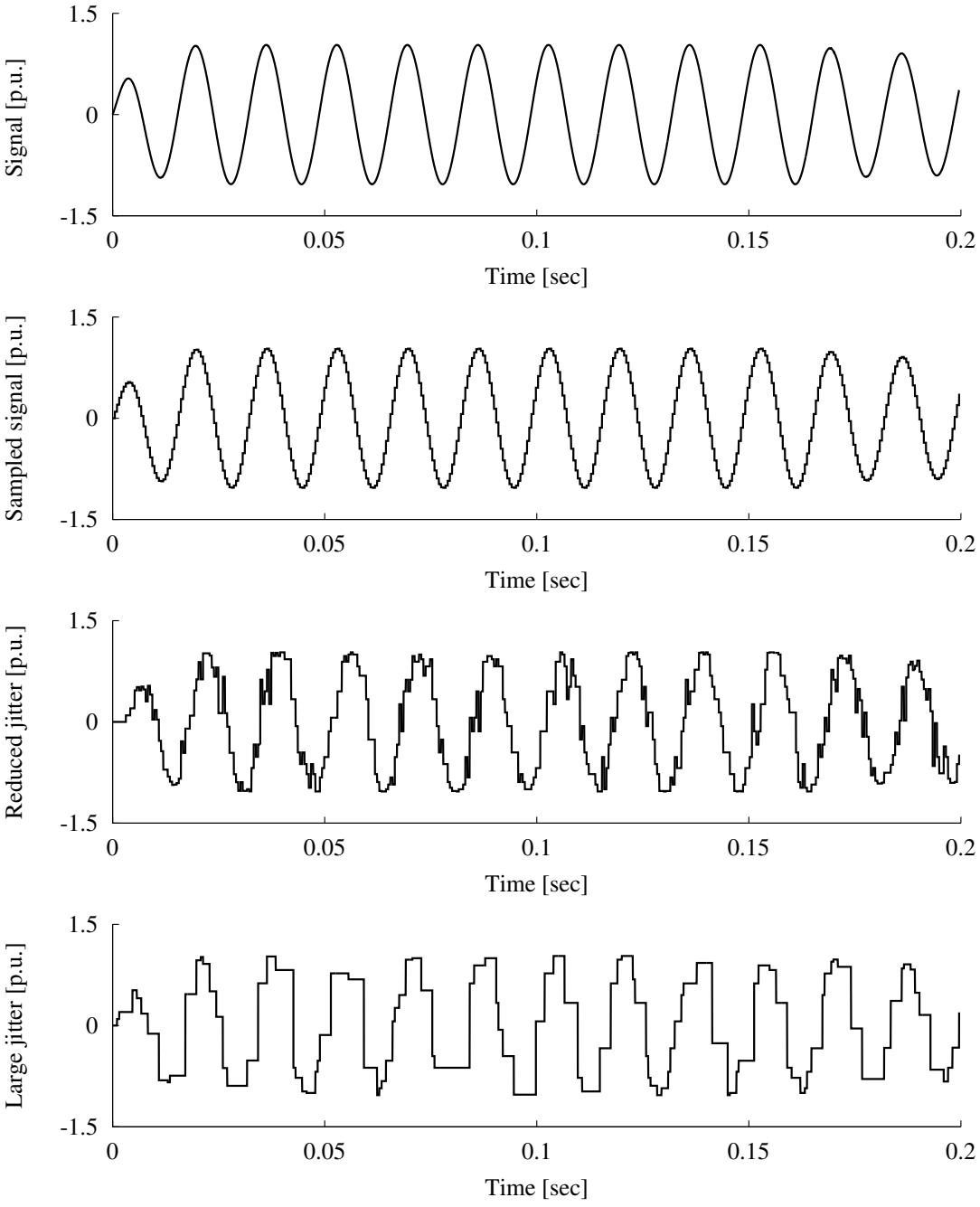

Figure 2.18: Ethernet networking performance

CHAPTER 3

THE INTEGRATED OPEN-SYSTEM PROTECTION

Application-level communications with, and between digital apparatus in substations is mainly limited to remote configuration and Supervisory Control and Data Acquisition (SCADA). For limited functionality, slow RS/EIA-232 and RS/EIA-485 standard serial communications are used to exchange SCADA data between substation monitoring, protection and control equipment.

Small changes to the substation configuration usually result in extensive changes of the communications infrastructure, and in configuration software. Present practices have resulted in a pyramidal structure with a multitude of data concentrators, remote terminal units, protocol converters, data archiving computers controlling and monitoring field devices connected through a web of cables. Such a structure makes high speed monitoring and control practically impossible.

Microprocessor-based digital protection and control relays offer a multitude of advantages over their analogue counterparts. Beside being able to perform a full range of protective and control functions, they offer numerous monitoring, analyzing and recording capabilities. The fact that information is processed and stored digitally,

makes their interconnection a natural step. Market forces and the lack of coordination between manufacturers in the past have resulted in numerous proprietary applications aimed at interconnecting digital protection, control and monitoring apparatus.

Ethernet networking inside the substation is providing an alternative solution to this problem, shifting focus from the hardware to the software, transforming the power system into a flexible, service oriented application.

The reason why information technology (IT) and Ethernet applications in power system protection and control have experienced a slower acceptance curve include the data delivery characteristics, lack of industrial components, physical media, security concerns and the lack of an application layer standard. Recent developments have started addressing these issues, making the Ethernet the solution of choice [60–62].

3.1 Substation automation

The first integrated substation protection and control application was proposed and implemented as a joint venture between the Electrical Power Research Institute (EPRI) and members of the utility industry [63, 64]. The project was a success story of integrating protection and control with the help of microprocessors or computers. The conclusion included numerous recommendations and future directions for similar projects. In the proposed implementation, at the lowest level of the functional structure, the data acquisition units (DAU), collected analogue and digital input values close to the protected power apparatus in order to minimize wiring. The sampled

values were converted to digital representation and transmitted using fibre networks. The control operation was transmitted on separate return fibre installations. The DAU transmitted data at 1 Mbps rate. The second level of the functional structure was represented by microprocessor controlled devices operating as protective relays, installed two per protected zone. At the top of the substation automation structure was a computer that connected to each microprocessor controlled device via serial communication.

The conclusions of the pilot project were that substation automation integrating protection and control apparatus can reduce substantially construction needs and will result in significant time savings, maintenance cost reduction due to the self monitoring features of microprocessor controlled applications, reduced costs due to simple modifications, and a multitude of new functions and monitoring features previously not available. Both IEEE and IEC have invested significant effort in developing standards to help substation automation development.

Most of the present day substation automation applications have followed the same structure as the initial EPRI project. Microprocessor-based IEDs are performing monitoring, metering and protection, while communicating, mostly SCADA data to local communications concentrators. The newest solutions are using a process bus to stream information from digital instrumentation to protective relays and other IEDs. The trend is toward further integration in the substation, with continuous pressure to reduce cost and increase reliability [65–76].

High speed digital processors are capable of performing the operations required for one given protective function using only a very small part of their computing capabilities. New digital relays are taking advantage of the extra speed by incorporating multiple functions in the same relay. For example, all functions required to protect a transformer now come packed into a single digital relay. The industry is proposing feeder management relays, underlining that the product is capable of much more than one given protective function. The overall trend is towards integration of protective functions, creating a digital revolution in the substation.

3.2 Industrial IT in the substation

Digital computer relaying has gained significant acceptance in utility applications. Between the most cited benefits are greater reliability, new functions, economy, etc. The first computer-based system for which the present digital protection algorithms were developed featured 100 nsec instruction time and 1 Mb memory. It was considered as the building block of adaptive relaying and synchrophasor protection [77].

More recently, Sciacca and Block identified the possibility of interconnecting digital protective relays to a substation controller via high speed communications channels, as a solution to the requirements of future protective and SCADA challenges [42]. Since then, significant progress has been made in developing faster and more reliable computers. New algorithms and applications should harness the extra computational power available.

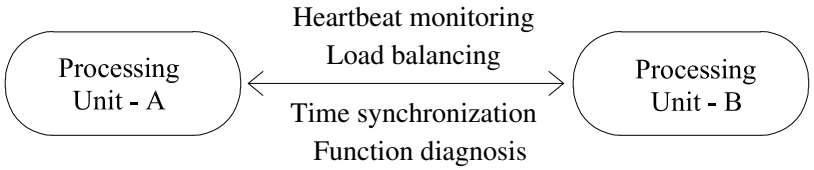

Figure 3.1: Clustered processing equipment

The main building block of the modern digital IED is very similar to industrial grade computers. In many cases, it is an industrial grade computer running specific software incorporating the relaying algorithm. The number of computations done by a digital protective relay, after each new sample received, is relatively small when the relay is performing standard protective algorithms. The computing performance of these relays, on the other hand, has increased exponentially.

There has been significant progress in the mission critical information technology applications. Separate, multiprocessor units can perform parallel processing at the same time while running function-, and device diagnostics on self and other members of the clustered hardware, as shown in Fig.(3.1). This type of operation implemented in protective hardware applications would be partly similar to installing redundant, dual layer protective systems. The difference is that in the existing solutions redundancy is achieved by the means of duplicating the hardware and the function for each protected unit, while in the new approach, the redundancy is obtained by duplicating the processing units, as part of a clustered environment.

In the proposed model, digital current and potential transformers broadcast real time samples across a common Ethernet-based data bus, as depicted in Fig.(3.2),

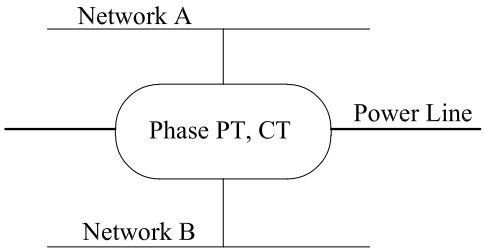

Figure 3.2: Digital instrumentation in the substation

while processing units receive the information and perform all the protection, control and monitoring operations for the entire substation. Control signals to operate substation equipment are transmitted on the same communications channels capable of multiple protocols.

The speed requirements for transmitting streaming analogue values from current and voltage transformers to protective and other IED equipment have been investigated and reported as part of the IEEE effort to standardize substation communications [40]. By using two, completely separate and redundant data buses, networks A and B, as shown in Fig.(3.3), the integrity of the data transmission system is preserved in case of malfunctions inside any single data collision domain.

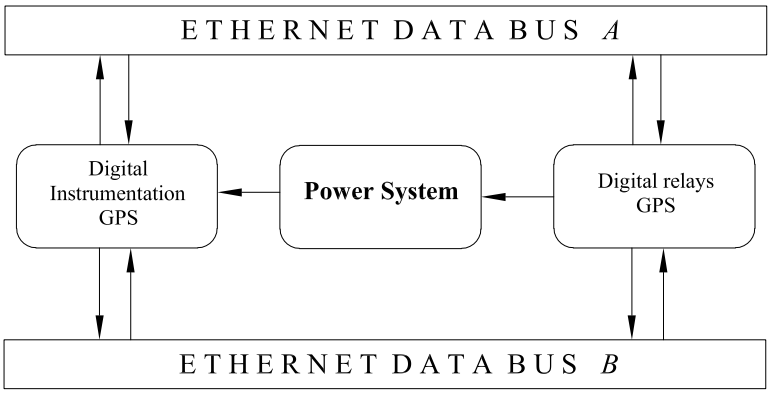

Figure 3.3: Open-system protection and control integration into the power system

3.3 Pooling the hardware resources

Integrated, multi-computer protection and control systems have been proposed as early as 1988 [78]. The main reason behind the need for interconnection was the distribution of processing power to a number of devices to accommodate for all functions and requirements in the stations. The idea was based on the same three level substation automation approach as proposed by EPRI [66]. By distributing the processing effort, the slower computers available at that time were able to cope with the amount of processing required for protecting and controlling a substation.

Multi-core microprocessors and multiprocessor systems on a single chip are the next step in integrating computing applications [79]. Real-time clustering of mission critical applications is becoming possible at software level. Wide-area, system level protection requires extensive processing of a large amount of data. Pooling hardware resources for parallel processing provides both speed and redundancy to the application.

Significant progress has been made in clustering information processing hardware resources, where a number of units can be made to operate as one. Internally, resources are shared and made available to functions and processes as required, based on predefined, priority-based process queueing. The redundancy of these systems is provided by the fact that in case of failure of, or in, any given unit, the other members of the cluster can take over the functions performed by the failed unit. Externally, at application level, the failure of any hardware unit does not affect the performance of the entire cluster. The failure is reported, and the failed cluster element replaced, on-line, without the need for an outage.

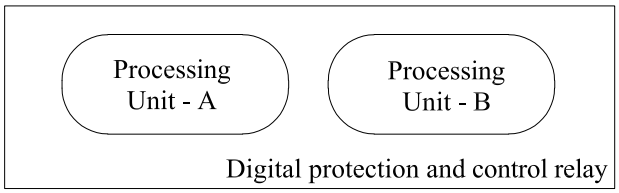

Figure 3.4: Clustered open-system concept for a digital protective relay

Hardware clustering features are well developed in information processing applications. Protective functions are performed by software in microprocessor-based relays, and they can be running on clustered platforms for redundancy and security. In these new applications, the software is the relay.

The proposed solution breaks from the standard configuration where the device performing the protective function is physically and functionally attached to the power system equipment it protects, and rather, it stands as a central protective processing unit, bringing the notion of parallel and clustered processing from the information technology world into the power system protection and control environment. The software performing the protective functions is not linked to any of the units that make up the clustered hardware. Specialized system software monitors the cluster, dedicating more or less computing power, as required, from the pooled resources. As a result, the computing effort, or load, can be balanced between the available resources. The concept of the proposed open-system relay is shown in Fig.(3.4).

Signal samples taken by digital instrumentation are transmitted via a process bus. The process-bus solution has the advantage that samples taken at different locations are available to any device that is connected to the common data bus. The process-bus model implemented in Matlab is shown in Fig.(3.5). It can be seen that all three source signals are available to both receiving systems. There is no need to send the

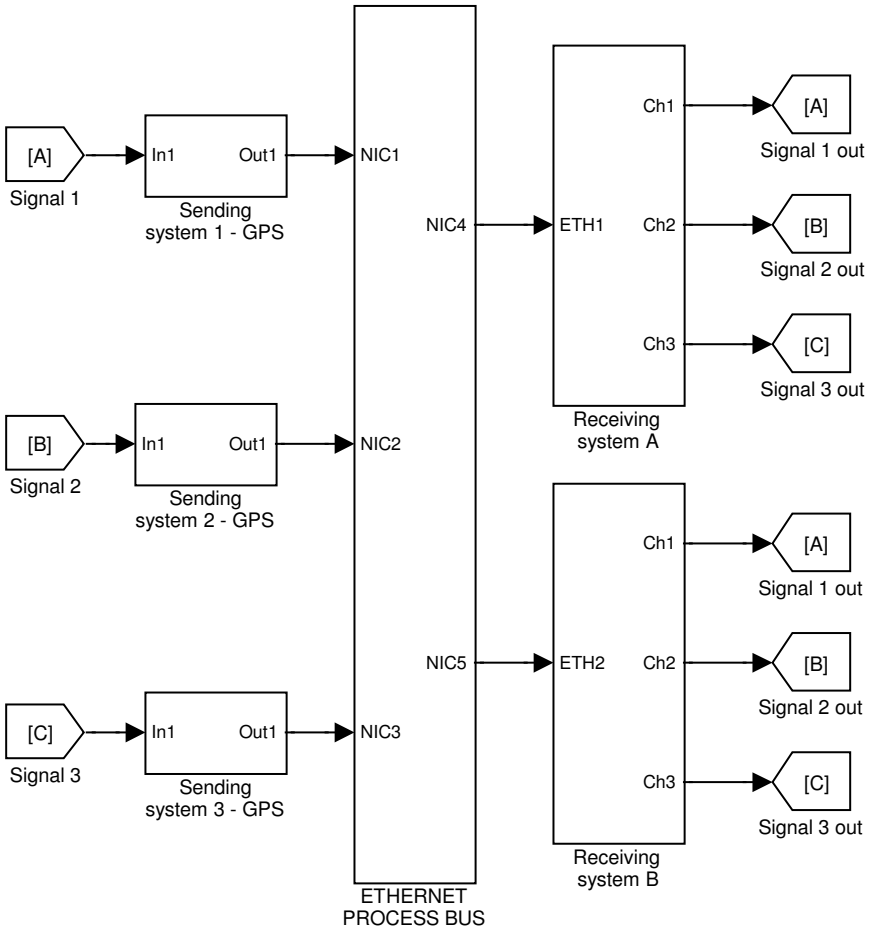

Figure 3.5: Ethernet process-bus model

data separately to each location, since the transmission is done in broadcast mode, and any device that is connected to the process bus can "tune in" and receive the data stream.

In order to make use of the information, at each receiving point, the sampled signals need to be synchronized.

3.4 Synchronized phasor measurement

When instantaneous information regarding currents and voltages is required at remote location, the electrical signals are sampled and transmitted via communication channels. Regardless of the medium of choice, the data transmission will experience delays. These delays are caused by the time required to process the information and by the communication path characteristics [80, 81].

In power systems applications with sensitive timing, a single data sample received later than anticipated can result in damaged equipment. In the Ethernet network, there is no way to determine the sequence in which packets of data will arrive to the destination. To use such an environment to transmit values obtained from sequentially sampled signals, care must be taken not to lose information that could bring the measurement error above the acceptable limits.

3.4.1 Implied sequential sampling

When using sequential communications, the data samples that arrive from the remote end are considered to be in proper sequence [82]. The protection and control applications that are using such communications channels do not time stamp the samples, but imply that the samples are in sequential order: every sample is considered to have been taken after the previously received value, and before the sample that will arrive next. Any communications breakdown, even for the duration of one sample, will result in losing the functions of the relay or relays.

3.4.2 Time-stamped sampling

The proposed application would represent a significant departure from existing solutions in which relaying algorithms process data samples obtained and received using implied sequential sampling.

In a different type of data transmission, the data samples taken from voltages and currents are time stamped and tagged. The attached time stamp represents the moment at which the sample was taken, as obtained through the Global Positioning System (GPS). Other data related to the acquisition system are embedded in each packet for transmission.

With a properly designed system, dropped packets are rare, and are mainly the result of failing communication media. Inside a network segment, data transmitted in broadcast mode is available to all listening devices simultaneously, therefore, with digital instrumentation in place, the data packets containing sampled values of currents and voltages can be made simultaneously available to any field device on the network segment.

The solution that can overcome the jitters in the networked data transmission is proposed at the Application Layer level of the Ethernet communication, offering maximum flexibility in setting up hardware resources. With the proposed approach, industrial information technology can bring clustered processing reliability, with load balancing and hardware backup into the substation. Using the described system, wide-area measurement and dynamic power system state monitoring and control can be developed for increasingly larger areas.

3.4.3 The data packet

When trying to align time-stamped phasors, several problems can influence the precision of the measurement. A possible solution is to keep track of the methods used to obtain the specific phasor, sample windows, and other information that may influence the results, and embed them into a data packet together with the information about the sampled signal, which would then be transmitted. Such an approach can create other problems, where for example, the specific digital algorithm used to obtain the phasor is not known to the computer or digital relay where the information received is to be employed for analysis or other protective functions.

The location where the given time stamp is placed in the filter window can have significant effect on the precision of the measurement. The effect of placing the samples at the end, at the middle or at the front of the data window was compared to the phase shift experienced in analogue filtering [83]. Requirements and performance of synchronized phasor measurements are well addressed in the literature [84, 85].

At the receiving end of the transmission channel, the information is processed using digital relaying algorithms. The amplitude and phase angle of the sampled signals are calculated. The following chapter starts with investigating the performance of common digital relaying algorithms in processing data samples received across an Ethernet process bus.

CHAPTER 4

CHARACTERISTICS OF DIGITAL RELAYING ALGORITHMS

A significant drawback to adopting Ethernet for real-time data transmission is the networks "best-effort data transmission". Existing digital relaying algorithms require that the transmission of the data to take place inside the time frame between two consecutive samples. This strict timing requirement places limitations on what types of protective functions Ethernet data transmission can be applied to.

During normal operation, digital relaying algorithms are continuously processing data representing samples taken from the measurement of instantaneous voltages and currents. Using sequential samples, the algorithm can extract information about the measured values, such as amplitude and phase angle. Faulted or other system conditions can be determined by comparing the measured values to predetermined settings.

4.1 Mann and Morrison algorithm

The Mann and Morrison algorithm is based on one sample and one derivative [3]. If the assumption is made that the voltage and current maintains sinusoidal form after the fault, the amplitude and phase of the signal can be obtained using only a limited number of samples.

If the samples are obtained from a sinusoidal signal described by:

$$v(t) = V_1 \sin(\omega_0 t) \tag{4.1}$$

then, the derivative of the signal is:

$$v'(t) = \omega_0 V_1 \cos(\omega_0 t) \tag{4.2}$$

where:

$$v'(t) = \frac{d}{dt}[v(t)] \tag{4.3}$$

From Eqs.(4.1) and (4.2):

$$(v(t))^2 = V_1^2(\sin(\omega_0 t))^2 \tag{4.4}$$

$$\left(\frac{v'(t)}{\omega_0}\right)^2 = V_1^2(\cos(\omega_0 t))^2 \tag{4.5}$$

The peak value of the sinusoidal signal can be expressed as:

$$V_1 = \sqrt{v(t)^2 + \left(\frac{v'(t)}{\omega_0}\right)^2} \tag{4.6}$$

The above equations are valid for any instant. The derivative of the signal can be obtained if, between two consecutive samples, the signal is considered linear. In this case, the derivative will be the slope of the linear segment of the signal, and can be calculated as:

$$v'[k] = \frac{\Delta v}{\Delta t} = \frac{v[k+1] - v[k]}{\Delta t} \tag{4.7}$$

where Δt is the time interval between the instances when the two samples were taken.

The amplitude and the phase angle of the signal can therefore be calculated after each new sample using the following two equations:

$$V[k] = \sqrt{v[k]^2 + \left(\frac{v[k+1] - v[k]}{\omega_0 \Delta t}\right)^2} \tag{4.8}$$

$$\phi[k] = \tan^{-1}\left(\frac{v[k]\omega_0 \Delta t}{v[k+1] - v[k]}\right) \tag{4.9}$$

For the type of applications that use Ethernet data transfer, the short length of the filter window of the Mann and Morrison algorithm is a significant disadvantage. Missing or delayed samples would make the output of this algorithm unstable.

4.2 Rockefeller and Udren algorithm

By using the first and second derivative, the Rockefeller and Udren algorithm is one sample longer than the previous solution, and it can reduce errors due to the decaying DC component [3]. Using the same notations as for the previous algorithm, the first and second derivatives of the sinusoidal signal expressed in Eq.(4.1) are:

$$v'[k] = \frac{v[k+1] - v[k-1]}{2\Delta t} \tag{4.10}$$

$$v''[k] = \frac{v[k+1] - 2v[k] + v[k-1]}{(\Delta t)^2} \tag{4.11}$$

The amplitude and the phase angle of the sampled signal can be obtained as:

$$V[k] = \frac{1}{\omega_0}\sqrt{(v'[k])^2 + \left(\frac{v''[k]}{\omega_0}\right)^2} \tag{4.12}$$

and

$$\phi[k] = -\tan^{-1}\left(\frac{v''[k]}{\omega_0 v'[k]}\right) \tag{4.13}$$

What the previous digital relaying algorithms have in common, is that they utilize only two or three data samples. Same as other short window algorithms, such as Miki-Makino or Gilbert-Shovlin, which also use two or three samples, Rockefeller and Udren has the same problems with delayed packets of data [3]. A delayed sample would look at destination as if the sampling rate was modified. The previous algorithms are extremely sensitive to deviations of the apparent sampling rate. Utilizing these classical solutions for processing non-sequential samples is not possible, as it can be seen from the equations representing the amplitude and phase angle of the sampled signals.

In order to accommodate for non-sequential and delayed samples, algorithms that use larger number of samples are required. One of the most stable and widely used solution in digital protection relaying is the discrete Fourier algorithm. The performance of this algorithm in processing data received across Ethernet networks is presented in the next section.

4.3 Full-cycle Fourier algorithm

The Full-cycle Fourier (FF) algorithm is one of the most stable algorithms that can extract the amplitude or Root Mean Square (RMS) value, and the phase angle of a signal. It is immune to any DC component of the signals, and it can filter out harmonics [18, 20].

If the measured voltage signal is considered periodic, it can be expanded into its Fourier series representation [86].

$$v(t) = a_0 + \sum_{n=1}^{\infty} a_n \cos(n\omega_0 t) + \sum_{n=1}^{\infty} b_n \sin(n\omega_0 t) \tag{4.14}$$

The values of the coefficients a_0, a_n and b_n can be obtained as:

$$a_0 = \frac{1}{T}\int_{t_0}^{t_0+T} v(t)dt \tag{4.15}$$

$$a_n = \frac{2}{T}\int_{t_0}^{t_0+T} v(t)\cos(n\omega_0 t)dt \qquad n = 1, 2, \cdots \infty \tag{4.16}$$

$$b_n = \frac{2}{T}\int_{t_0}^{t_0+T} v(t)\sin(n\omega_0 t)dt \qquad n = 1, 2, \cdots \infty \tag{4.17}$$

where T is the period of the fundamental component of the signal. Considering that the measured signal is represented as discrete, real numbers, the real and imaginary parts of the phasor representing the sampled signal are obtained as:

$$V_{Re}[k] = \frac{2}{N}\sum_{n=0}^{N-1} v[k-n]\cos\left(\frac{2\pi n}{N}\right) \tag{4.18}$$

$$V_{Im}[k] = \frac{2}{N}\sum_{n=0}^{N-1} v[k-n]\sin\left(\frac{2\pi n}{N}\right) \tag{4.19}$$

The previous equations represent the convolution of the input signal $v[k]$ with the filter described by the coefficients:

$$h_{Re}[n] = \frac{2}{N}\cos\left(\frac{2\pi n}{N}\right) \qquad n = 0, \cdots, N-1 \tag{4.20}$$

$$h_{Im}[n] = \frac{2}{N}\sin\left(\frac{2\pi n}{N}\right) \qquad n = 0, \cdots, N-1 \tag{4.21}$$

where $h_{Re}[n]$ and $h_{Im}[n]$ are the real- and imaginary part filter coefficients, respectively.

The magnitude of the frequency responses $|H_{Re}(\omega)|$ and $|H_{Im}(\omega)|$ of a Full-cycle

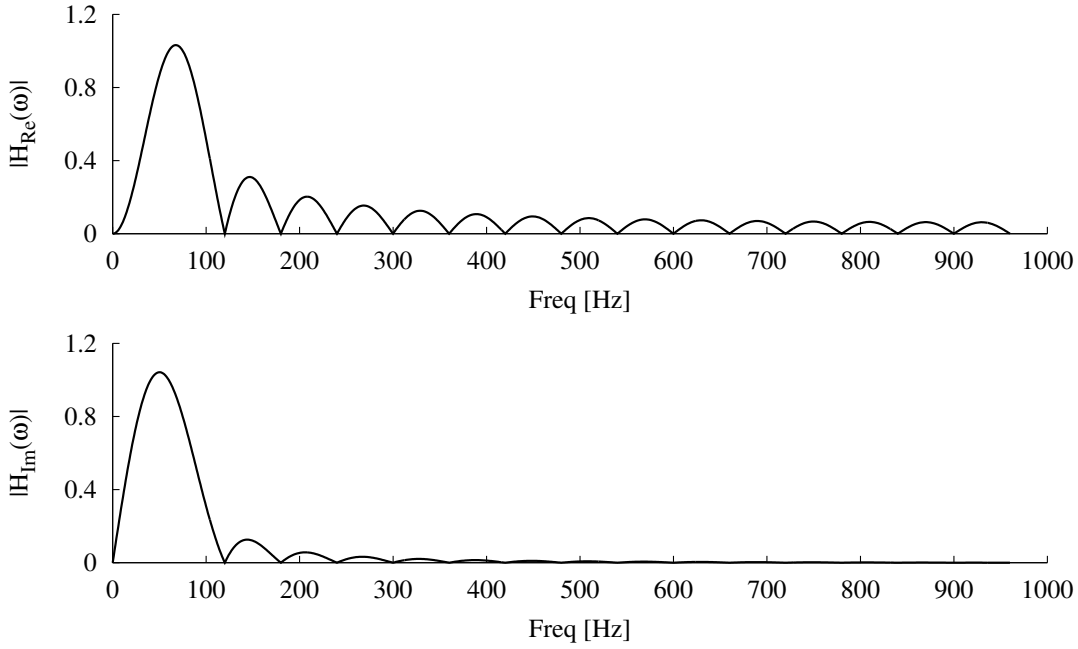

Figure 4.1: Frequency response of a FF algorithm with 32 samples per cycle

Fourier algorithm with coefficients centred over one period of the fundamental frequency are shown in Figs.(4.1) and (4.2) for N equal to 32 and 8 samples per cycle, respectively.

Using the real and imaginary components, the signal amplitude is obtained as:

$$V[k] = \sqrt{(V_{Re}[k])^2 + (V_{Im}[k])^2} \tag{4.22}$$

while the phase is expressed by:

$$\phi[k] = \arctan\left(\frac{V_{Im}[k]}{V_{Re}[k]}\right) \tag{4.23}$$

The performance of the Fourier algorithm when receiving data samples across an Ethernet communications channel has been investigated for both fast- and slow networks. The results are shown in Figs.(4.3) to (4.6). Tests show that reduced

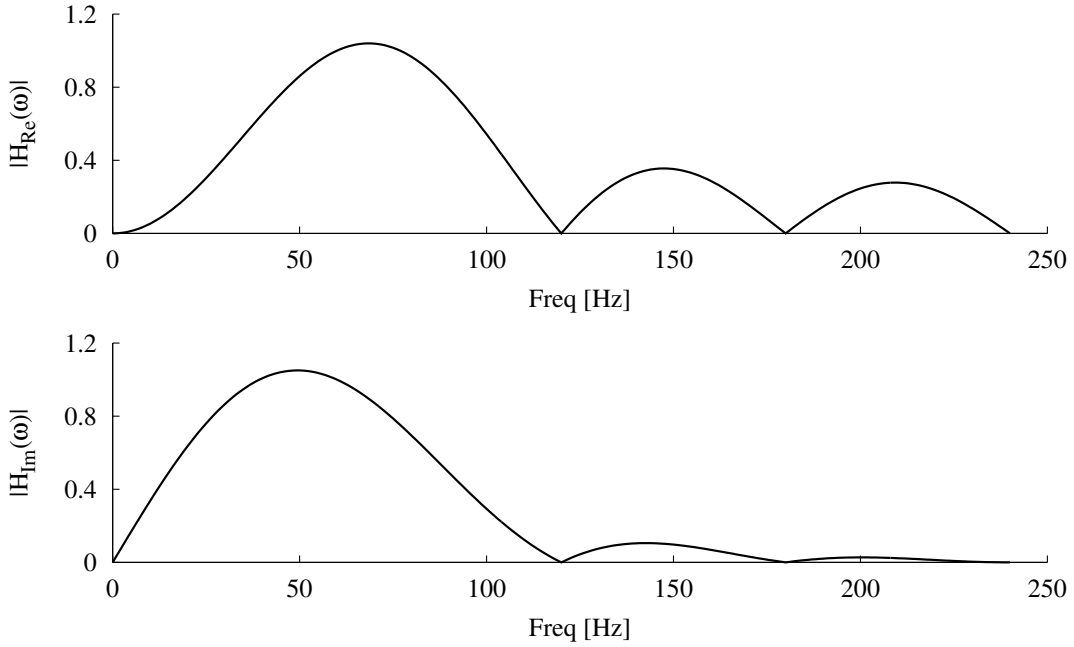

Figure 4.2: Frequency response of a FF algorithm with 8 samples per cycle

sampling rate and fast networks can provide tolerance for the delayed data frames, but only as long as the delay is within the sampling time interval. This is consistent with the network speed requirements outlined by other researchers [87].

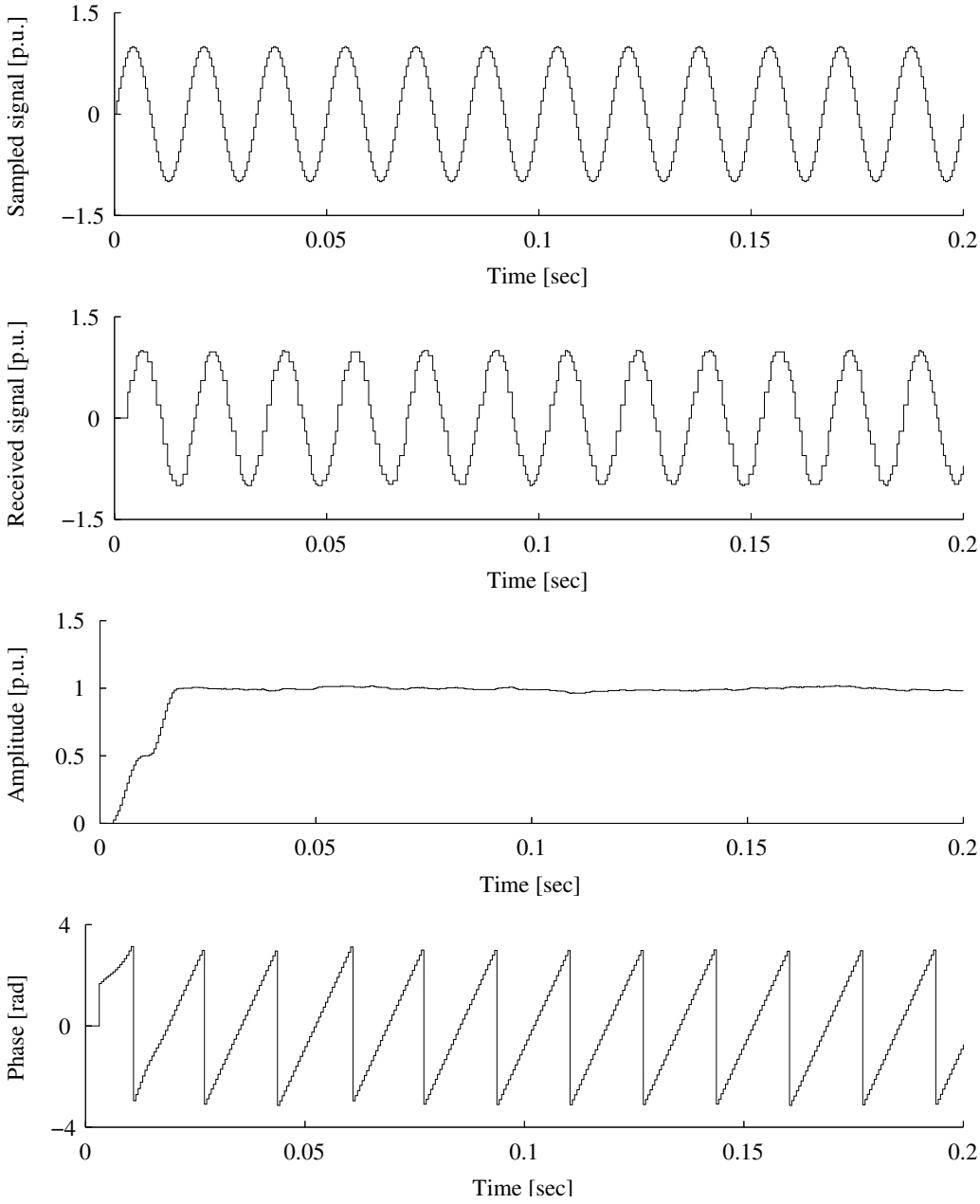

Figure 4.3: Full-cycle Fourier algorithm performance with 32 samples per cycle over fast network

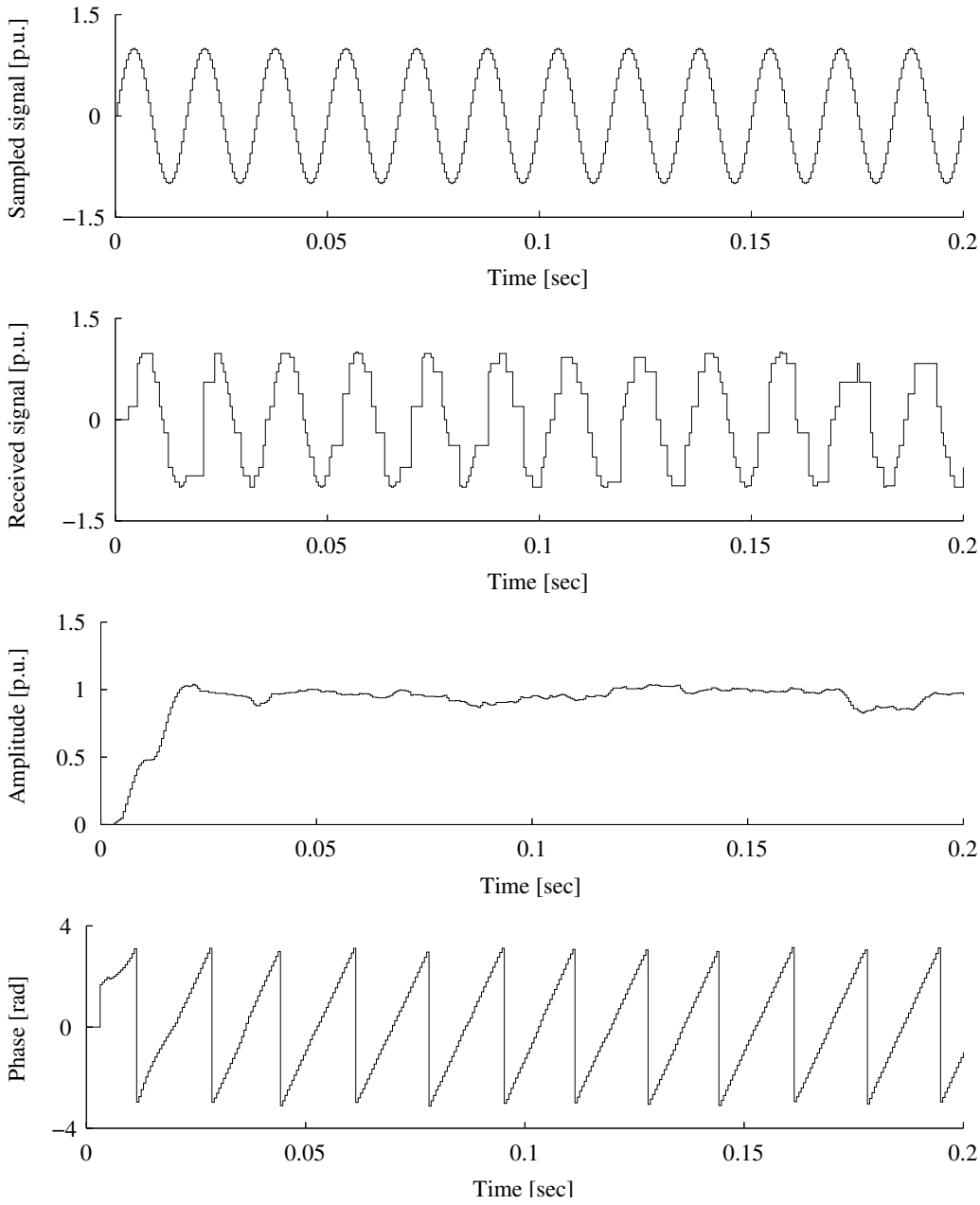

Figure 4.4: Full-cycle Fourier algorithm performance with 32 samples per cycle over slow network

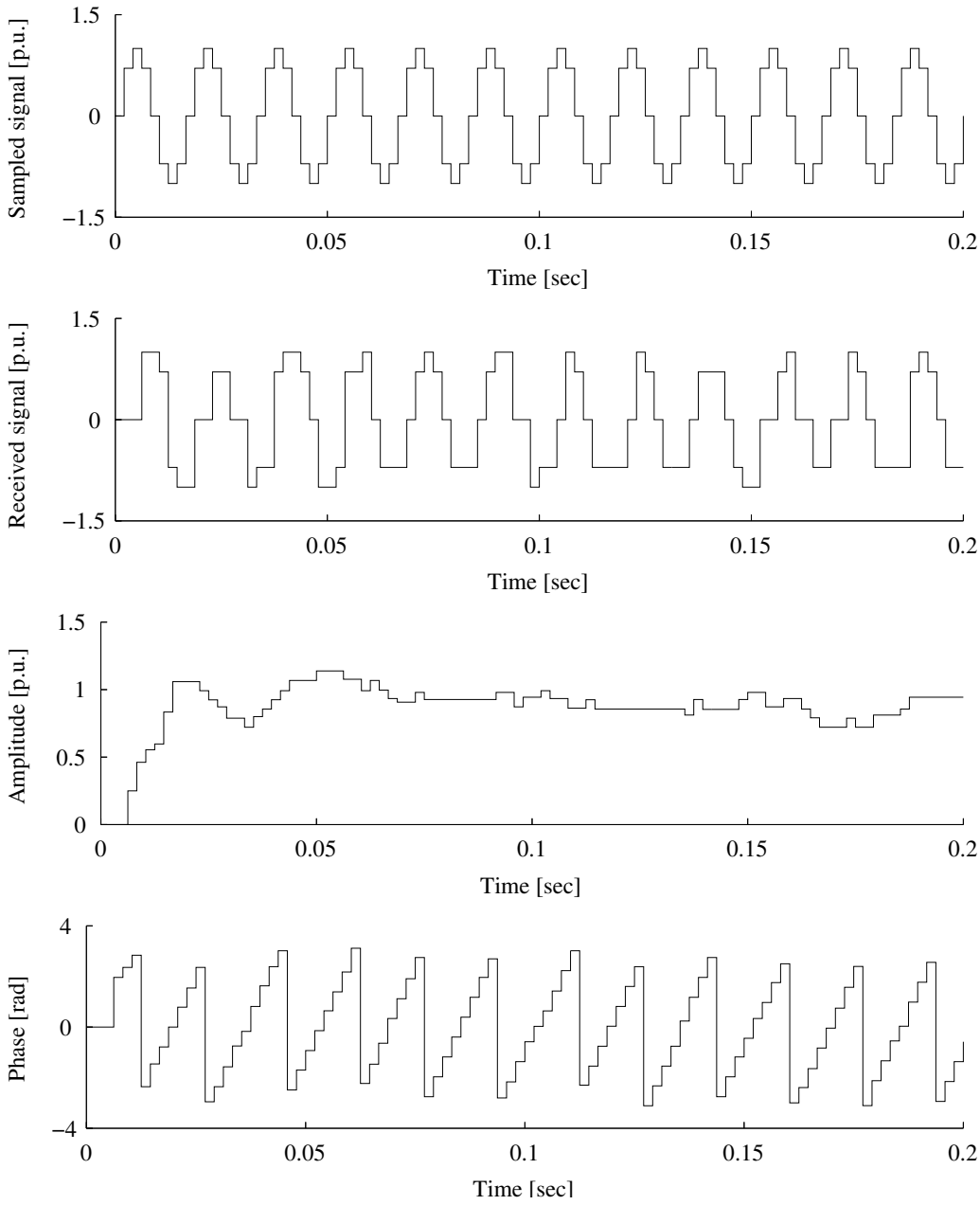

Figure 4.5: Full-cycle Fourier algorithm performance with 8 samples per cycle over fast network

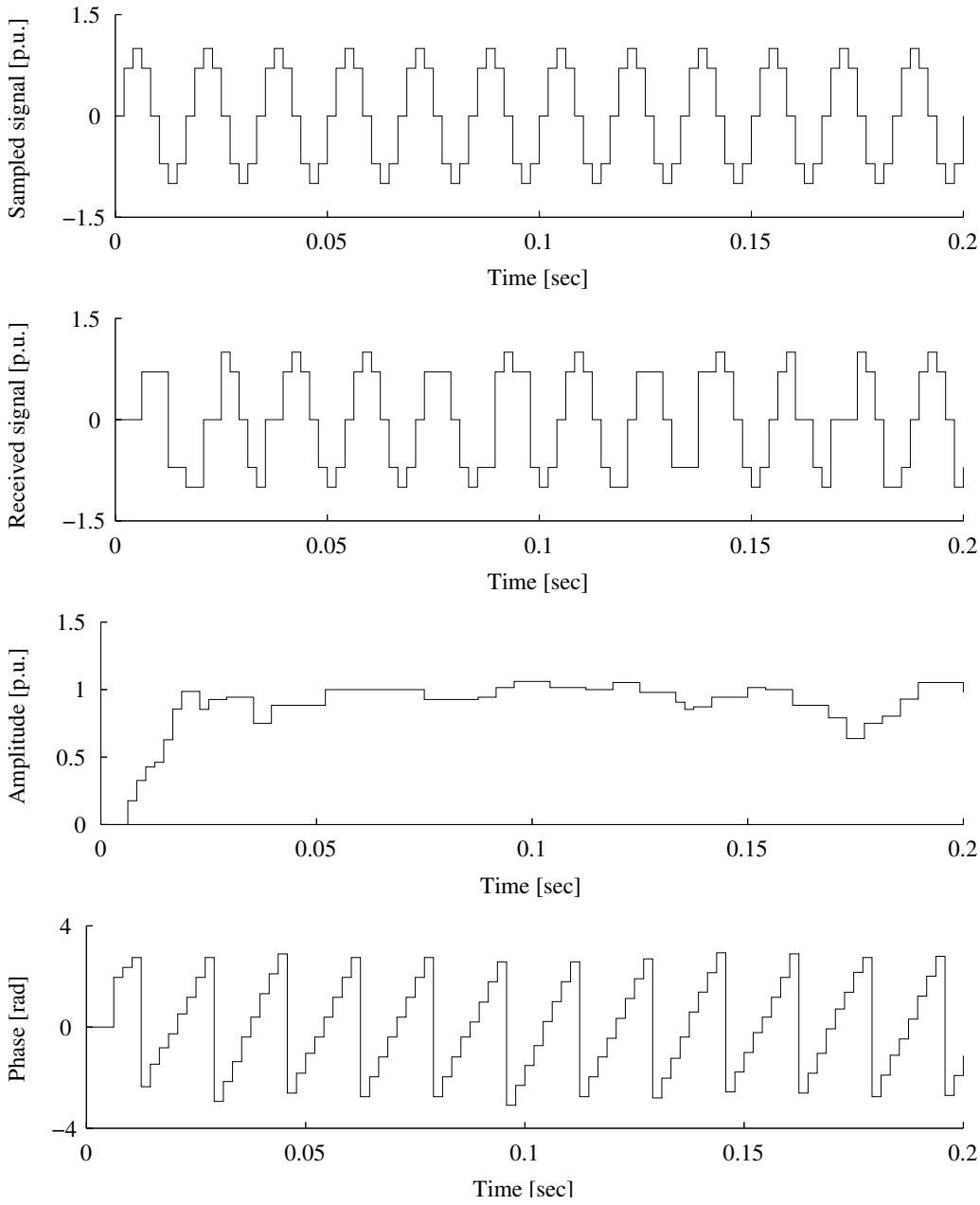

Figure 4.6: Full-cycle Fourier algorithm performance with 8 samples per cycle over slow network

4.4 Half-cycle Fourier algorithm

By using samples taken during half cycle of the fundamental component, the response time of the algorithm can be cut in half. The coefficients of the series expansion can be obtained as:

$$a_0 = \frac{1}{T/2}\int_{t_0}^{t_0+T/2} v(t)dt \tag{4.24}$$

$$a_n = \frac{2}{T/2}\int_{t_0}^{t_0+T/2} v(t)\cos(n\omega_0 t)dt \qquad n = 1, 2, \cdots \infty \tag{4.25}$$

$$b_n = \frac{2}{T/2}\int_{t_0}^{t_0+T/2} v(t)\sin(n\omega_0 t)dt \qquad n = 1, 2, \cdots \infty \tag{4.26}$$

where T is the period of the fundamental component of the signal.

Using the same approach as for the Full-cycle Fourier algorithm, the coefficients of the real- and imaginary part filters can be determined as:

$$h_{Re}[n] = \frac{4}{N}\cos\left(\frac{2\pi n}{N}\right) \qquad n = 0, \cdots, \frac{N}{2} - 1 \tag{4.27}$$

$$h_{Im}[n] = \frac{4}{N}\sin\left(\frac{2\pi n}{N}\right) \qquad n = 0, \cdots, \frac{N}{2} - 1 \tag{4.28}$$

where $h_{Re}[n]$ and $h_{Im}[n]$ are the real- and imaginary part filter coefficients, respectively. The magnitude of the frequency responses $|H_{Re}(\omega)|$ and $|H_{Im}(\omega)|$ of a Half-cycle Fourier (HF) algorithm are shown in Figs.(4.7) and (4.8), respectively. As it can be seen in the figures, the Half-cycle Fourier algorithm is not able to filter out

the DC component or the even harmonics from the signal.

The results shown in Figs.(4.9) to (4.12), lead to the same conclusion: the half-cycle implementation of the Fourier algorithm is not able to overcome the delay in receiving data samples. The amplitude and phase angle of the sampled signal cannot be obtained using the received data.

For the short window algorithms, such as the Half-cycle Fourier, missing samples can have significant effect on the output. In Fig.(4.10), due to the short filter window and missing samples in the data stream, a significant dip can be noticed in the amplitude of the signal. The system responded as if the amplitude reduced, since the missing samples were from the peak of the sinusoid, and the filter window covered only half cycle of the signal.

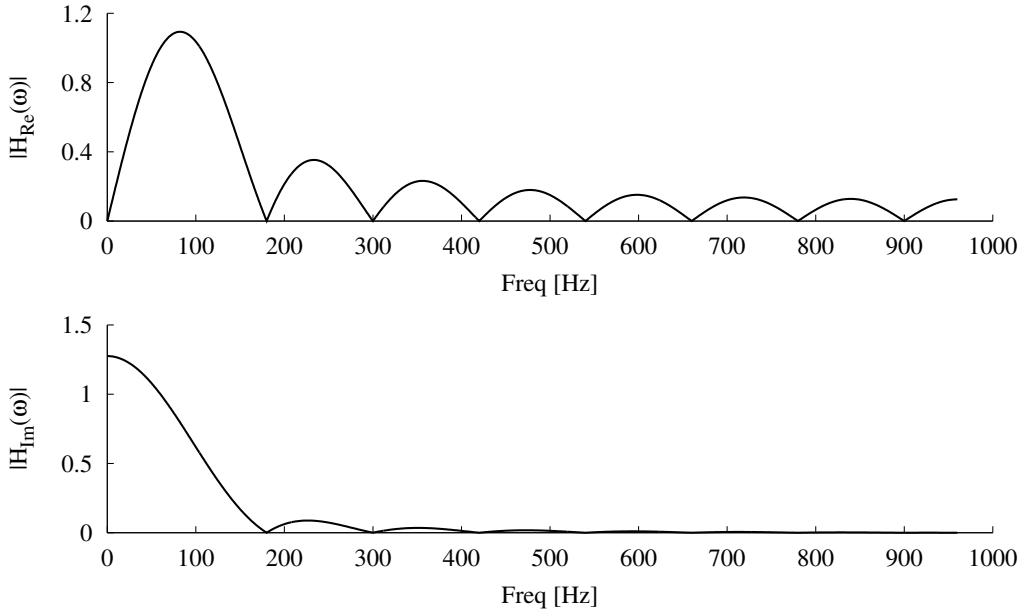

Figure 4.7: Frequency response of a HF algorithm with 32 samples per cycle

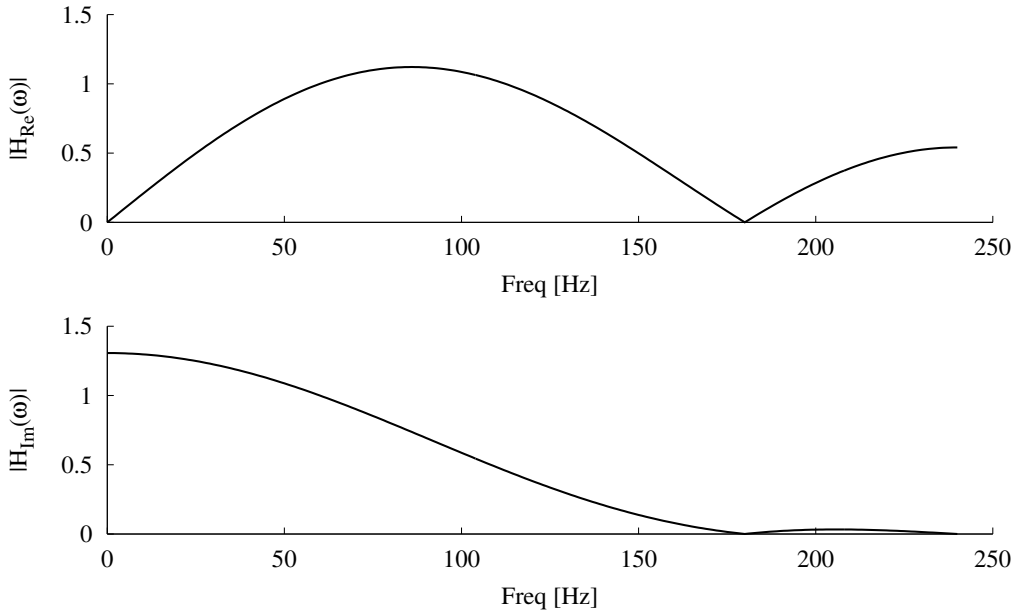

Figure 4.8: Frequency response of a HF algorithm with 8 samples per cycle

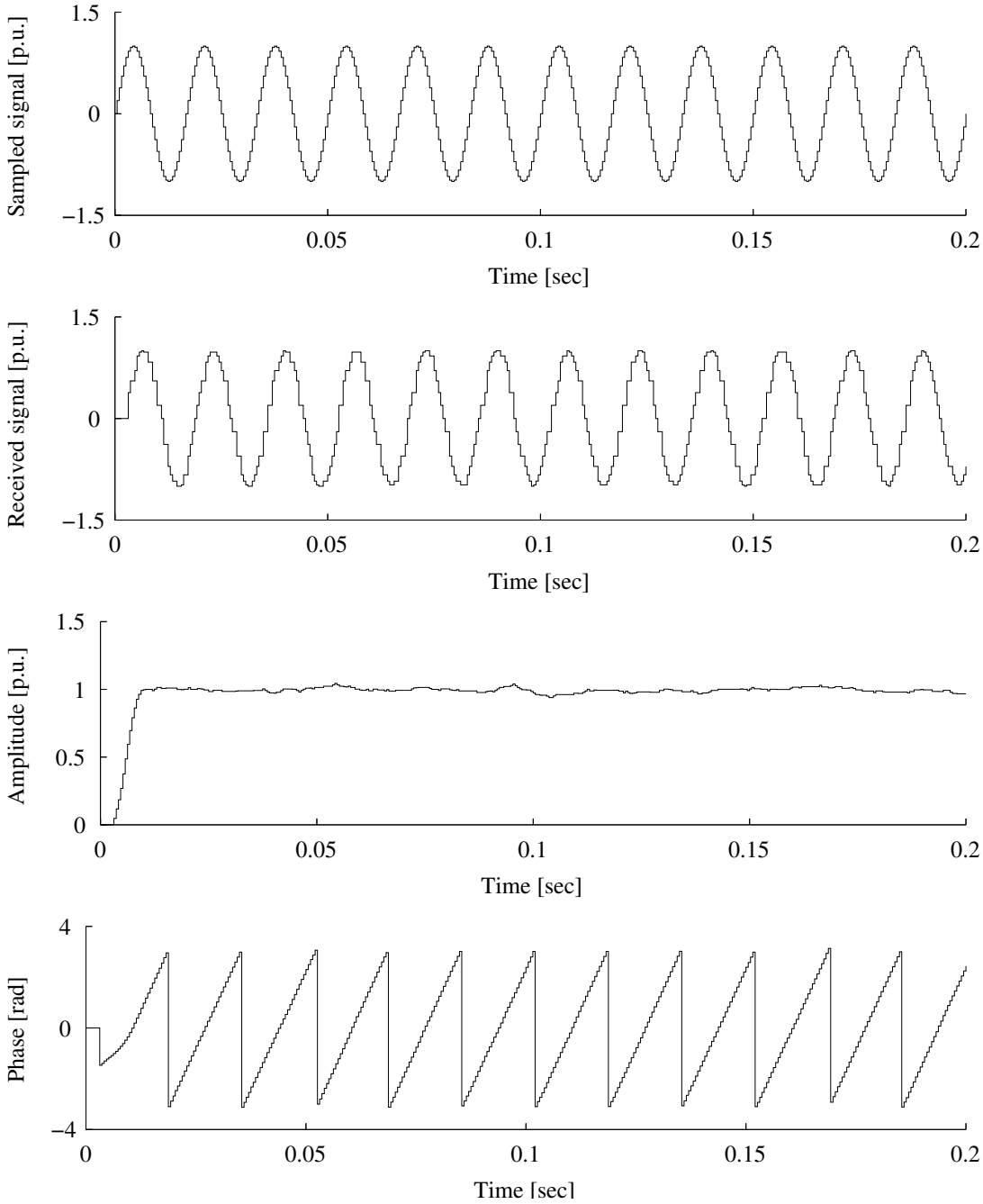

Figure 4.9: Half-cycle Fourier algorithm performance with 32 samples per cycle over fast network

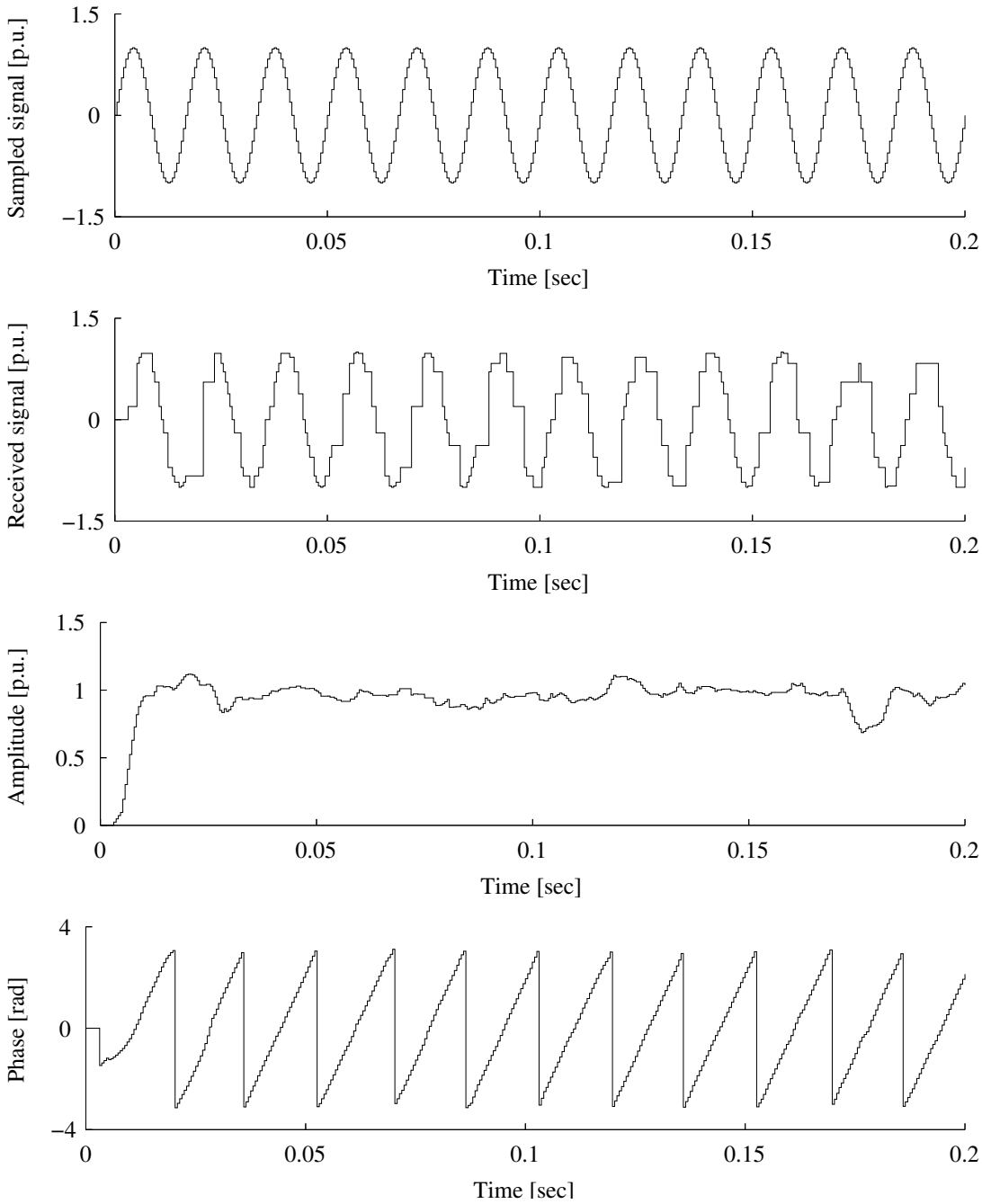

Figure 4.10: Half-cycle Fourier algorithm performance with 32 samples per cycle over slow network

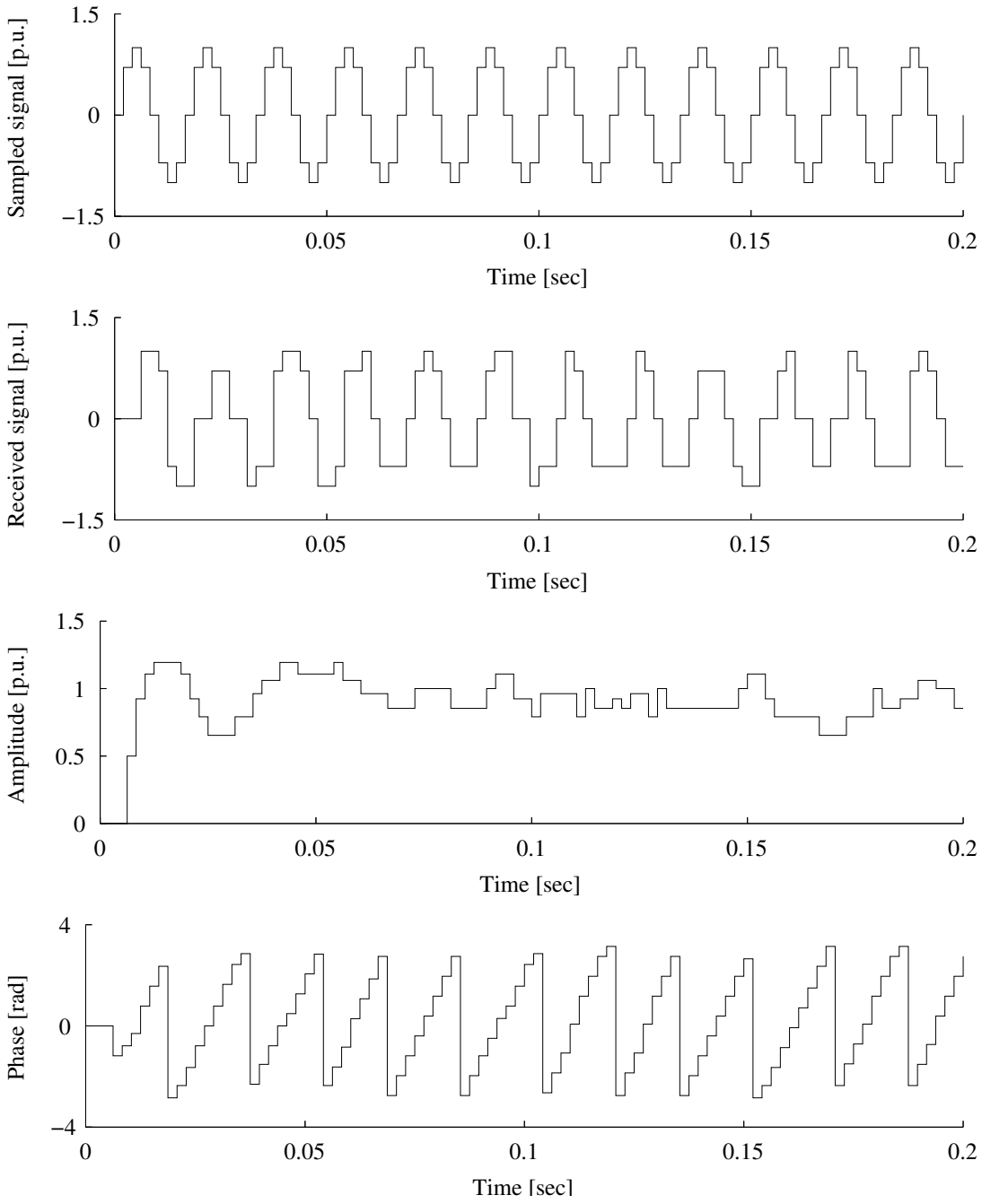

Figure 4.11: Half-cycle Fourier algorithm performance with 8 samples per cycle over fast network

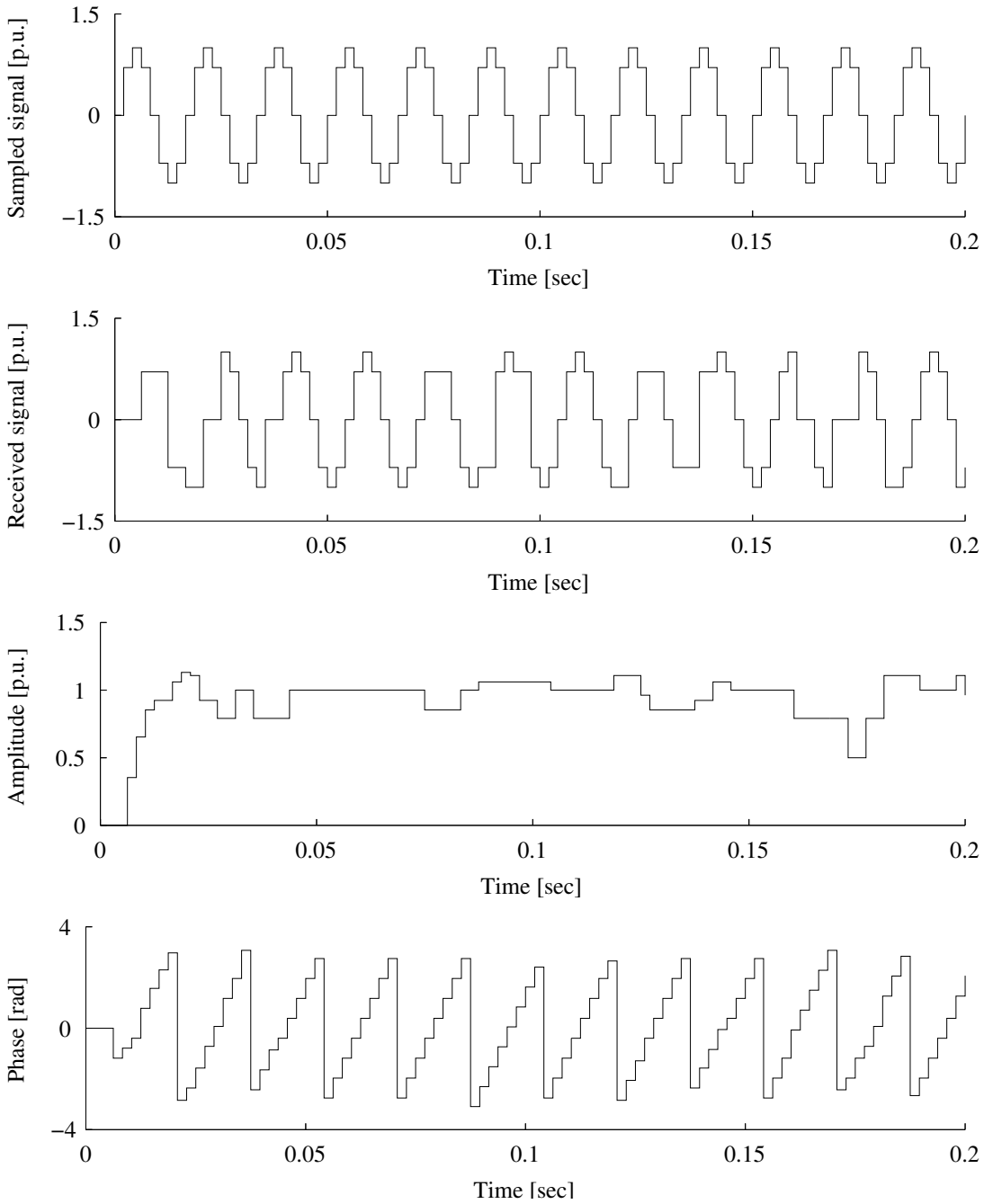

Figure 4.12: Half-cycle Fourier algorithm performance with 8 samples per cycle over slow network

4.5 Least Square Error algorithm

Sachdev and Baribeau proposed the Least Square Error (LSE) digital relaying algorithm that can be implemented for multiple variables [88]. The assumption is made that the sampled signal contains only odd harmonics, and previous filtering has reduced the frequency content of the signal to fundamental and third harmonic. If the signal also contains a decaying DC component, it can be expressed as:

$$v(t) = K_0 e^{-\frac{t}{\tau}} + K_1 \sin(\omega_1 t + \theta_1) + K_3 \sin(\omega_3 t + \theta_3) \tag{4.29}$$

where τ is the time constant describing the decaying exponential.

Using the first three elements of the Taylor series expansion of the DC component, the previous equation can be written as:

$$v(t) = K_0 - K_0 \frac{t}{\tau} + K_0 \frac{t^2}{2\tau^2} + K_1 \sin(\omega_1 t + \theta_1) + K_3 \sin(\omega_3 t + \theta_3) \tag{4.30}$$

Using the fact that:

$$\sin(\omega t + \theta) = \sin(\omega t)\cos(\theta) + \cos(\omega t)\sin(\theta) \tag{4.31}$$

Eq.(4.30) can be written as:

$$\begin{aligned} v(t) \;\; = \;\; & K_0 - K_0 \frac{t}{\tau} + K_0 \frac{t^2}{2\tau^2} + K_1 \sin(\omega_1 t)\cos(\theta_1) + K_1 \cos(\omega_1 t)\sin(\theta_1) \\ & + K_3 \sin(\omega_3 t)\cos(\theta_3) + K_3 \cos(\omega_3 t)\sin(\theta_3) \end{aligned} \tag{4.32}$$

The above equation is valid for any value of t. With the following notations:

$$
\begin{aligned}
a_{k1} &= 1 \\
a_{k2} &= \sin(\omega_1 t_k) \\
a_{k3} &= \cos(\omega_1 t_k) \\
a_{k4} &= \sin(\omega_3 t_k) \\
a_{k5} &= \cos(\omega_3 t_k) \\
a_{k6} &= t_k \\
a_{k7} &= t_k^2
\end{aligned} \tag{4.33}
$$

and

$$
\begin{aligned}
x_1 &= K_0 \\
x_2 &= K_1 \cos(\theta_1) \\
x_3 &= K_1 \sin(\theta_1) \\
x_4 &= K_3 \cos(\theta_3) \\
x_5 &= K_3 \sin(\theta_3) \\
x_6 &= -\frac{K_0}{\tau} \\
x_7 &= \frac{K_0}{2\tau^2}
\end{aligned} \tag{4.34}
$$

Eq.(4.32) can be written for consecutive values $t_1, t_2, \cdots, t_m$ as:

$$
\begin{aligned}
S_1 &= \sum_{n=1}^{7} a_{1n}x_n \\
S_2 &= \sum_{n=1}^{7} a_{2n}x_n \\
&\vdots \\
S_m &= \sum_{n=1}^{7} a_{mn}x_n
\end{aligned} \tag{4.35}
$$

The values of x_j can be obtained using the pseudo-inverse of matrix $A = [a_{ij}]$, where $i = 1, 2, \cdots m$ and $j = 1, 2, \cdots 7$. The matrix format of Eq.(4.35) is:

$$S = AX \tag{4.36}$$

where $X = [x_j]$, with $j = 1, 2, \cdots 7$. It can be subsequently written that:

$$A^T S = A^T AX \tag{4.37}$$

$$(A^T A)^{-1} A^T S = (A^T A)^{-1} A^T AX \tag{4.38}$$

As a result:

$$X = (A^T A)^{-1} A^T S \tag{4.39}$$

Using the values of X, the DC component, the amplitude and phase angle of the fundamental and the third harmonic can be obtained.

The frequency responses of the full-cycle LSE algorithm with 32 and 8 samples per cycle are shown in Figs.(4.13) to (4.16). The performance of the LSE algorithm

to accommodate data samples transmitted over an Ethernet channel has been investigated with results presented in Figs.(4.17) to (4.20). The conclusion that can be drawn from these results is that, similarly to the previous algorithms, the LSE algorithm is not able to overcome the delays and fluctuations in the performance of the communication channel.

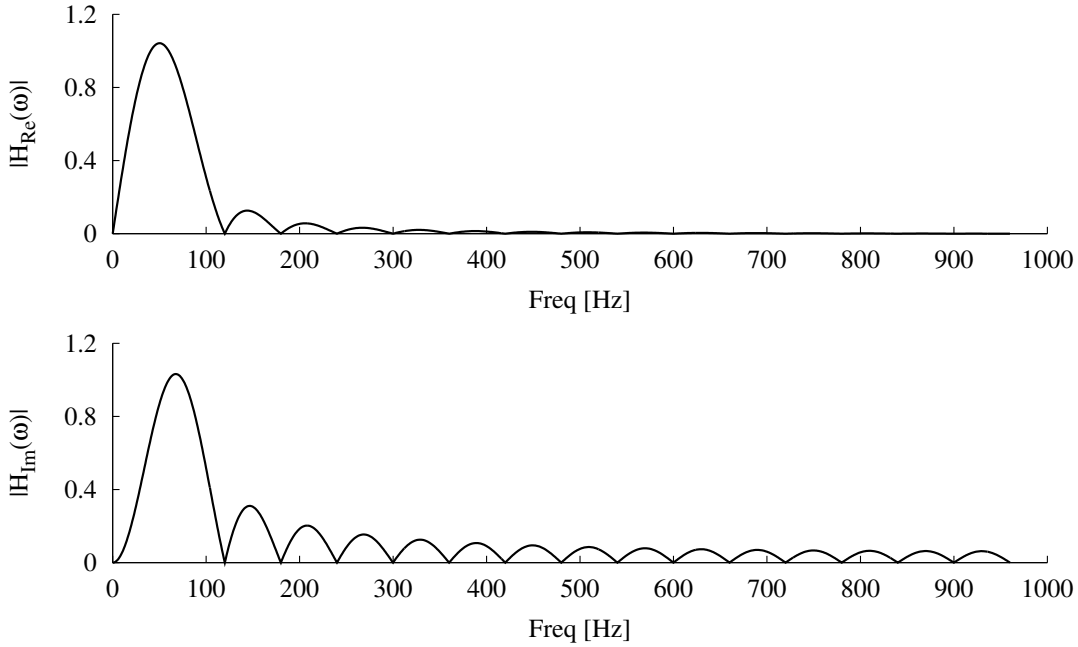

Figure 4.13: Frequency response of the full-cycle LSE algorithm with 32 samples per cycle

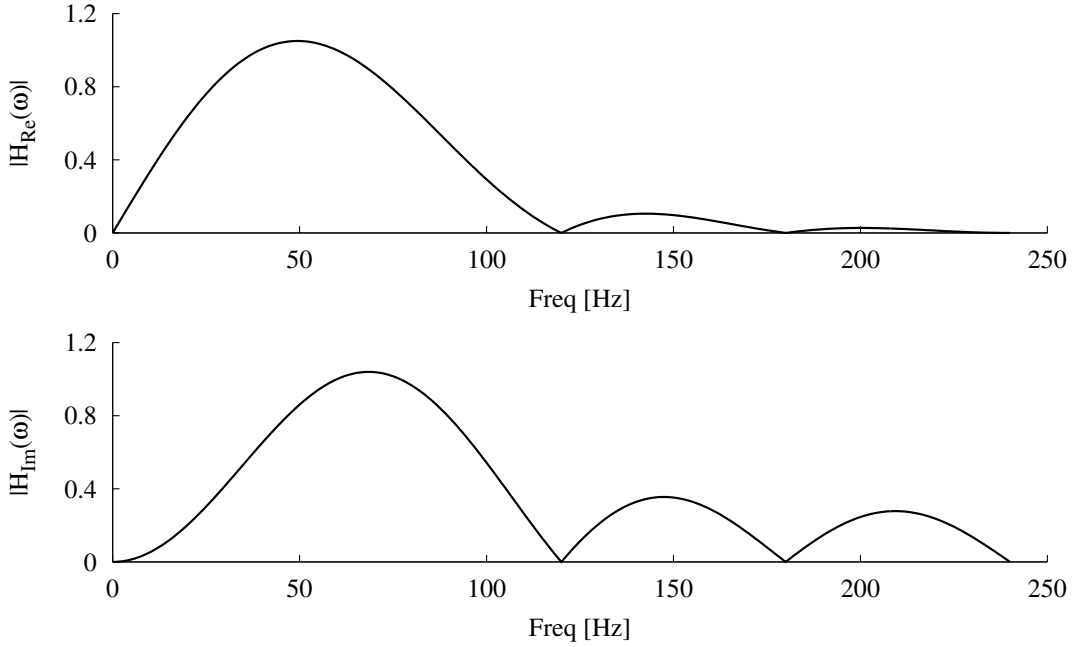

Figure 4.14: Frequency response of the full-cycle LSE algorithm with 8 samples per cycle

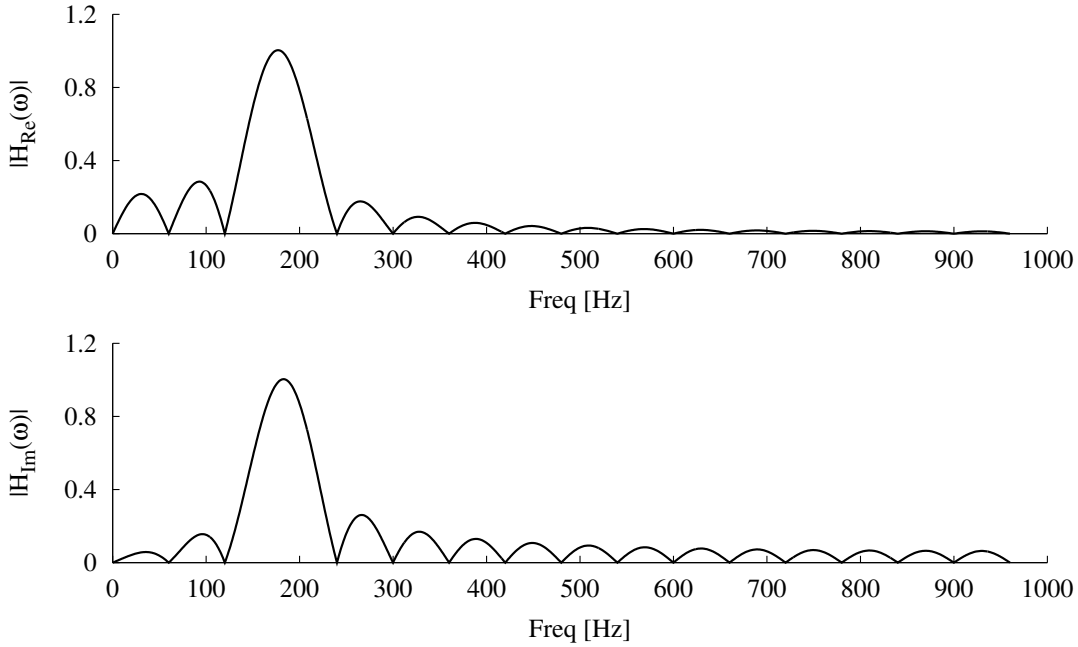

Figure 4.15: Frequency response of the full-cycle, 3rd harmonic LSE algorithm with 32 samples per cycle

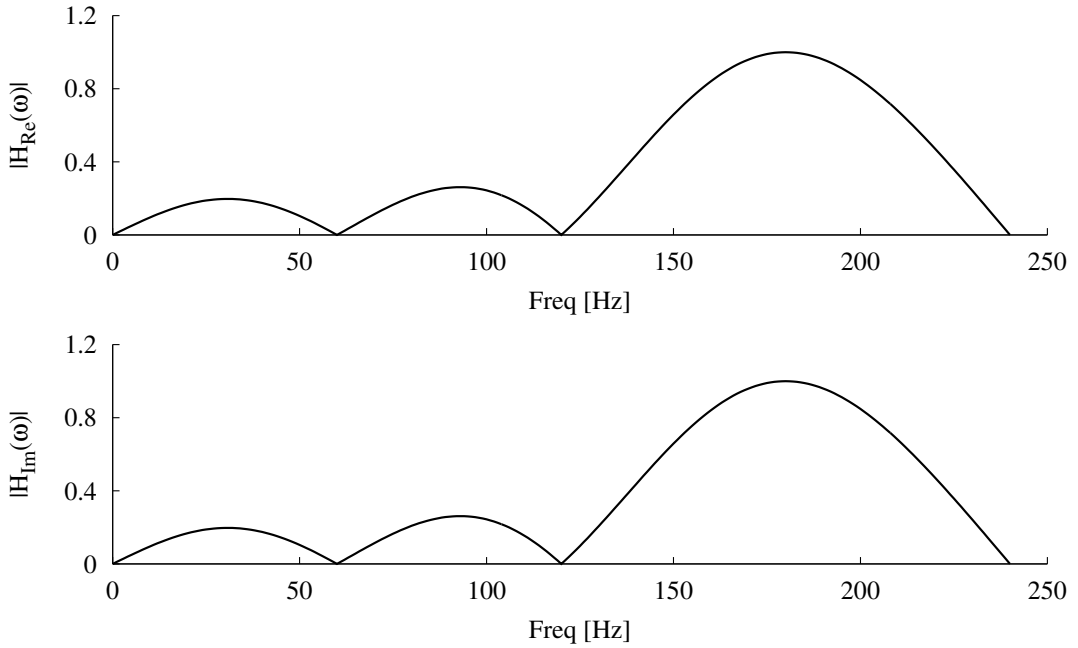

Figure 4.16: Frequency response of the full-cycle, 3rd harmonic LSE algorithm with 8 samples per cycle

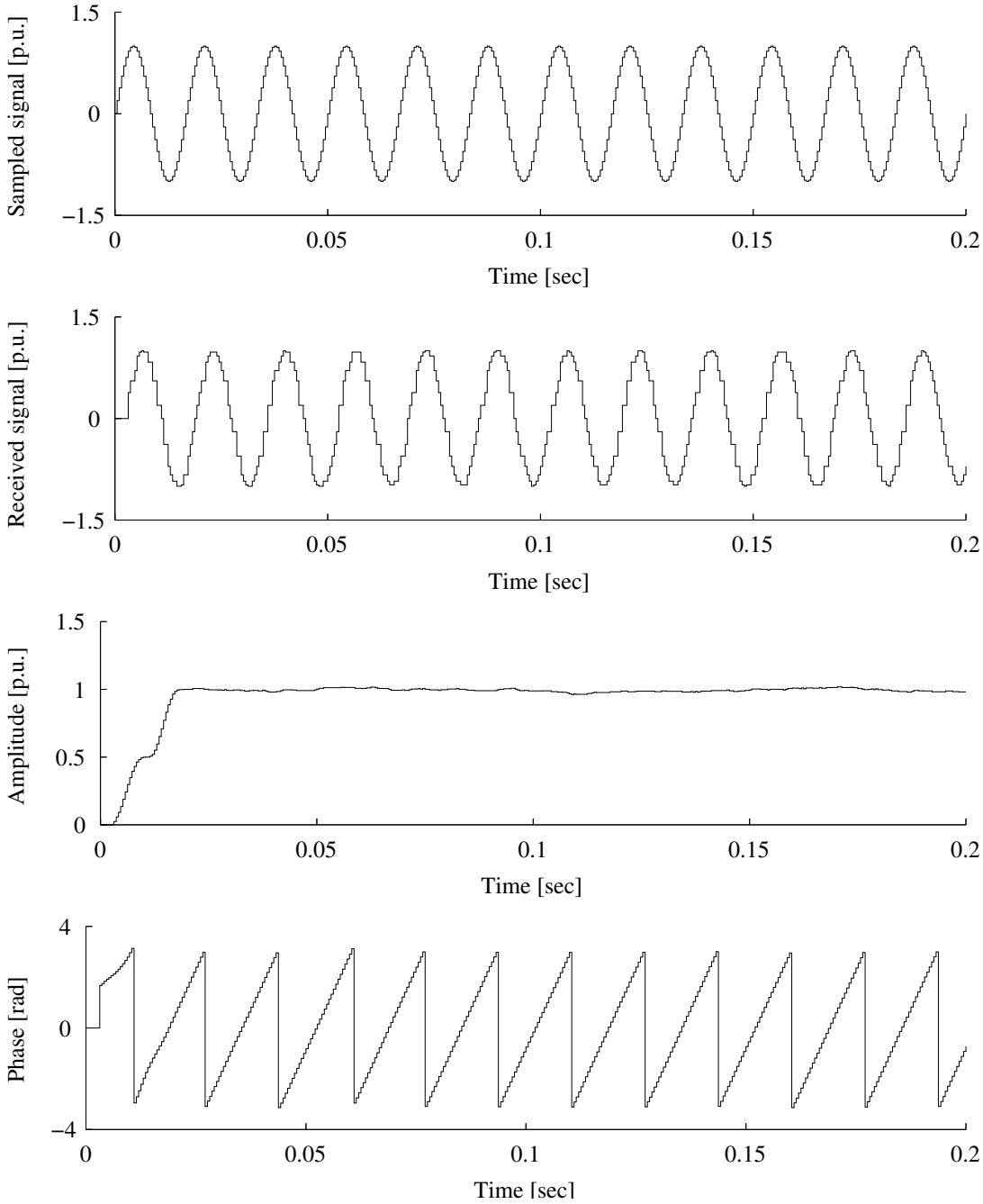

Figure 4.17: Full-cycle LSE algorithm performance with 32 samples per cycle over fast network

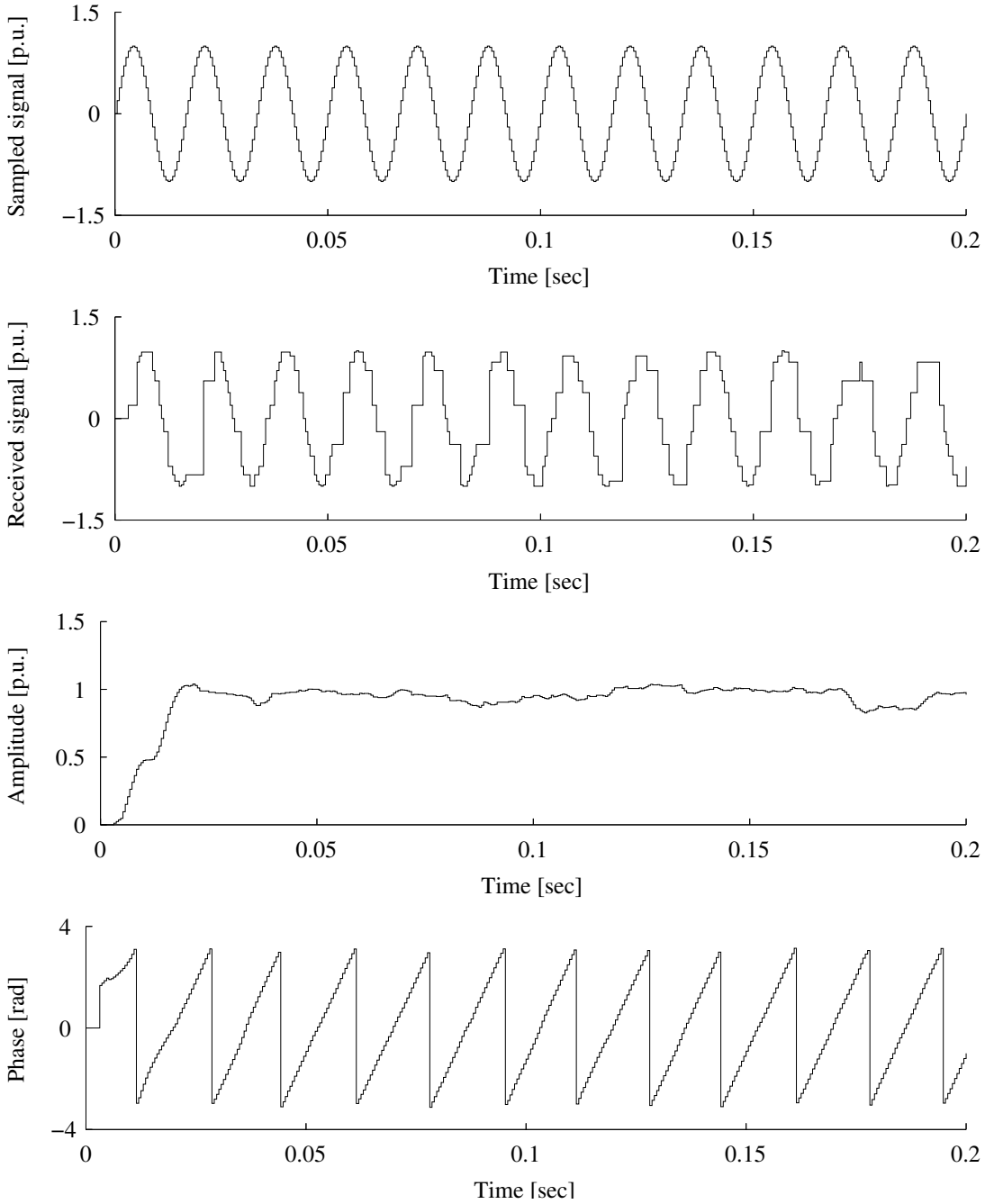

Figure 4.18: Full-cycle LSE algorithm performance with 32 samples per cycle over slow network

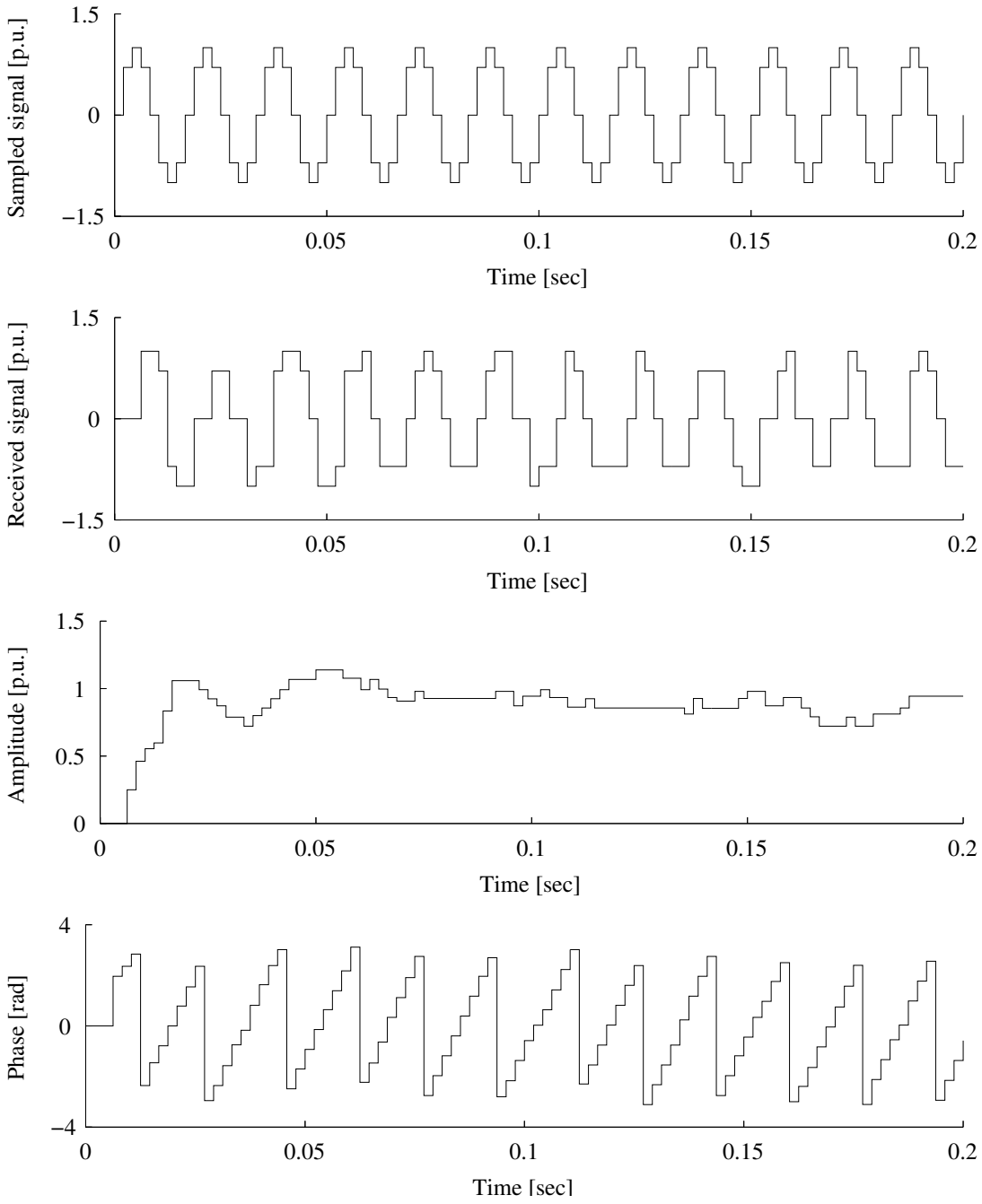

Figure 4.19: Full-cycle LSE algorithm performance with 8 samples per cycle over fast network

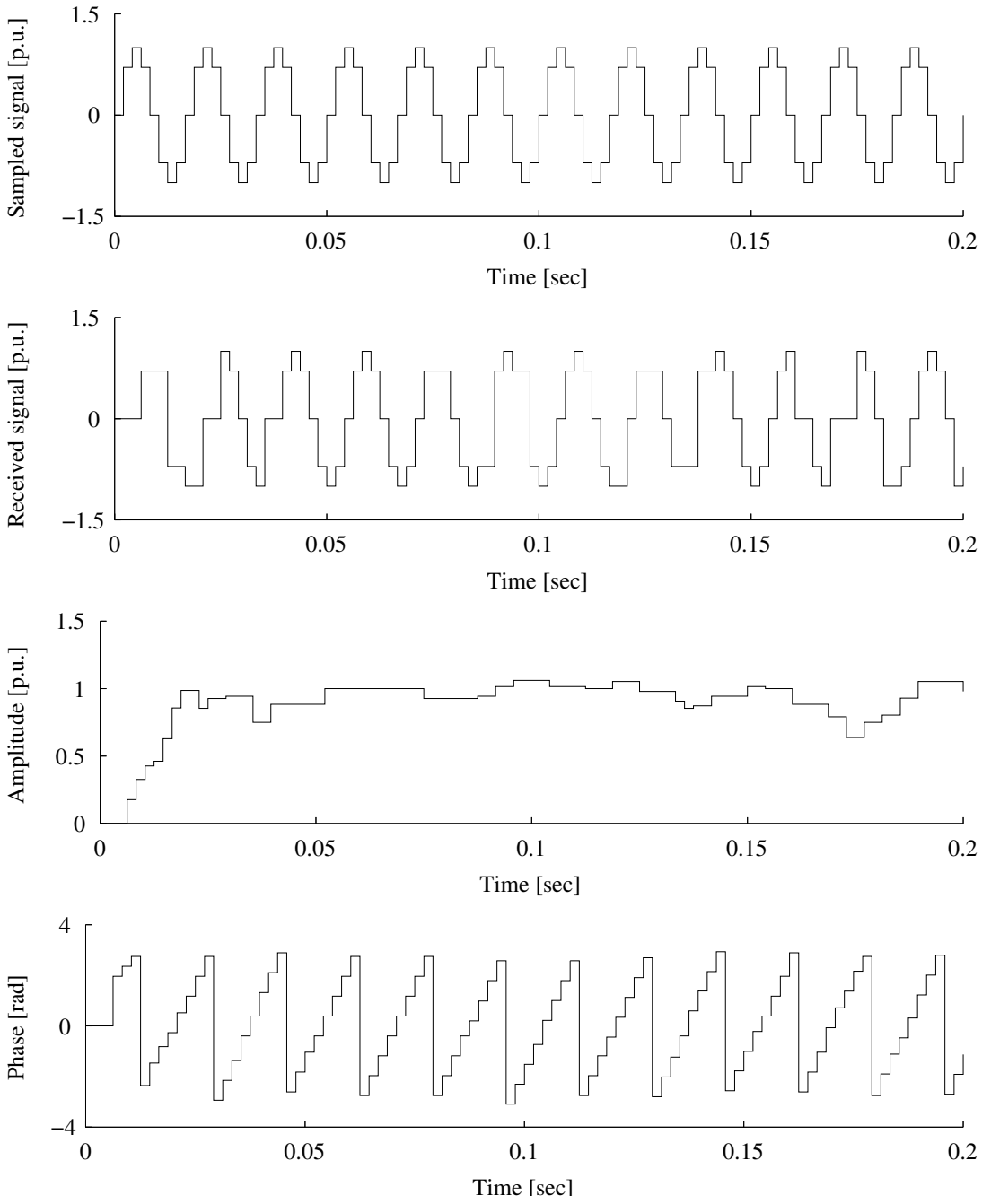

Figure 4.20: Full-cycle LSE algorithm performance with 8 samples per cycle over slow network

4.6 Performance evaluation and requirements

The previous section presented some of the most widely used digital relaying algorithms. Their performance in processing data that was transferred using a non-deterministic, best-effort communications media was tested. The results show that the only way these algorithms can be used to process samples that were transmitted across Ethernet networks, is to place strict performance requirements on the network. When the delay encountered is less than the time interval between two consecutive samples, the performance of the algorithms improved significantly. Similar conclusions can be found in recommendations that address the usage of the Ethernet in the substation.

Using a connection-less UDP protocol would reduce the time required to transfer the samples across the same infrastructure, as compared to the TCP protocol. On the other hand, the presented digital algorithms cannot accommodate missing samples in the data stream. When using the UDP protocol, the delivery of the packets is not monitored, and the missing sample in the stream cannot be identified at the source. The application layer at the destination would have to recognize that there is a missing sample, and send back to the source application a request to resend the missing frame. Using this approach, the output of the protective algorithm is basically put on hold until the missing sample is replaced with a new transmission.

At a level lower than the application layer, the TCP protocol has been suggested in the literature to monitor the packet delivery at destination. Using this approach,

the overall performance of the transmission system is reduced, since the delivery of every frame is checked and confirmed. The use of the TCP protocol would also result in an increase of data traffic on the network, with a negative impact on the system performance, when large quantity of data is streamed from digital instrumentation.

Considering the above characteristics of the digital algorithms, and the protocols used to transmit data packets across the Ethernet network, it is clear that there is no existing single solution that would have all the benefits. Standards and recommendations have taken the route of determining network performance benchmarks that have to be met in order to make the Ethernet usable for protective and other substation applications.

A digital algorithm that would be tolerant to data packets that are delayed beyond the sampling interval, would offer greater flexibility in setting up networking resources. Showing flexibility to out-of-sequence data samples is another feature that would provide extra reliability to mission critical protective equipment using Ethernet-type networking for data transfer. As part of the research presented in this thesis, a digital relaying algorithm has been developed that has these features, and is introduced in the next chapter.

CHAPTER 5

A NEW DIGITAL RELAYING ALGORITHM

A digital relaying algorithm capable of synchronized phasor measurements using data samples received across Ethernet-based networks is introduced in this chapter. During the data transfer, because of the deterministic data delivery, some data packets will arrive late, displaced from their normal position in the data stream. The proposed algorithm offers a solution for overcoming this characteristic of the Ethernet networks [89,90]. The proposed solution can be applied for remote data acquisition applications in the protection, monitoring and control of power systems [91, 92].

5.1 Adaptive filtering

Adaptive filtering has received considerable attention as a possible solution to changing system conditions [93–108]. To account for the variable jitter of the Ethernet transmission, the digital relaying algorithm will have to be capable of adaptive filtering, based on the available samples.

Let the sampled data stream at the source of sampling be represented by $x(n)$, with $-\infty < n < +\infty$. Each sample will get a time tag that will uniquely identify

it by the time instance when it was taken. It can be considered that n identifies mathematically the position of the sample in the data stream.

In case that the data stream arrives in proper sequence to the relay location, as seen in Fig.(5.1), the response of the applied filter can be represented as in Eq.(5.1).

$$y(n) = \sum_{k=0}^{M-1} b_k x(n-k) \tag{5.1}$$

where b_k are the coefficients and M is the length of the digital filter. The output can also be written as the convolution of the input signal with the unit sample impulse response $h(n)$ of the filter, as seen in Eq.(5.2).

$$y(n) = \sum_{k=0}^{M-1} h(k) x(n-k) \tag{5.2}$$

Therefore, $h(k) = b_k$ for $k = 0, \ldots, M-1$. The filter can also be described by its system function:

$$H(z) = \sum_{k=0}^{M-1} h(k) z^{-k} \tag{5.3}$$

which represents a polynomial in z^{-1}, with the coefficients $h(k)$.

In case that a sample does not arrive when it is expected, the first element of the filter, as seen in Fig.(5.2), will be undefined, therefore, the output will yield incorrect results. On the other hand, due to the time stamps embedded in the data packets, the system knows that a sample is missing. Using an adaptive filtering scheme, the system will replace the filter coefficients with a new set, so that the first coefficient

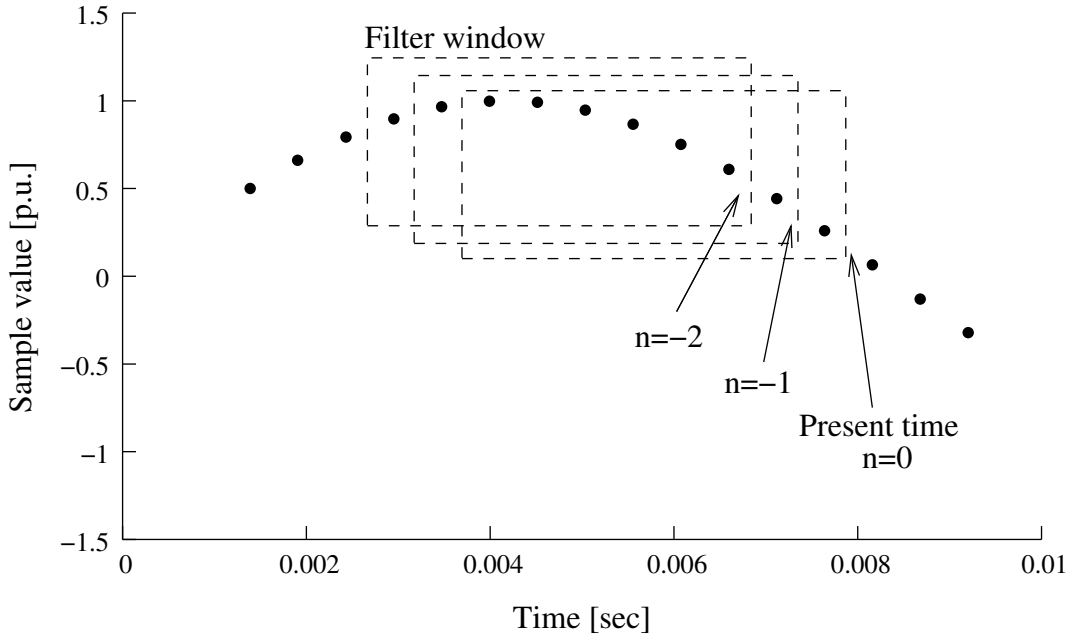

Figure 5.1: Filter window and signal samples

of the polynomial representing the system function is zero: $h(0) = 0$.

$$H(z) = h(0)z^{-0} + \sum_{k=1}^{M-1} h(k)z^{-k}$$

$$= \sum_{k=1}^{M-1} h(k)z^{-k} \tag{5.4}$$

When the filter window shifts to get the new sample during the convolution, the missing value would be multiplied with $h(1)$. In case that the sample has not arrived, new set of filter coefficients for which $h(1) = 0$ are employed to obtain the correct result. The system function of the new filter is represented in Eq.(5.5).

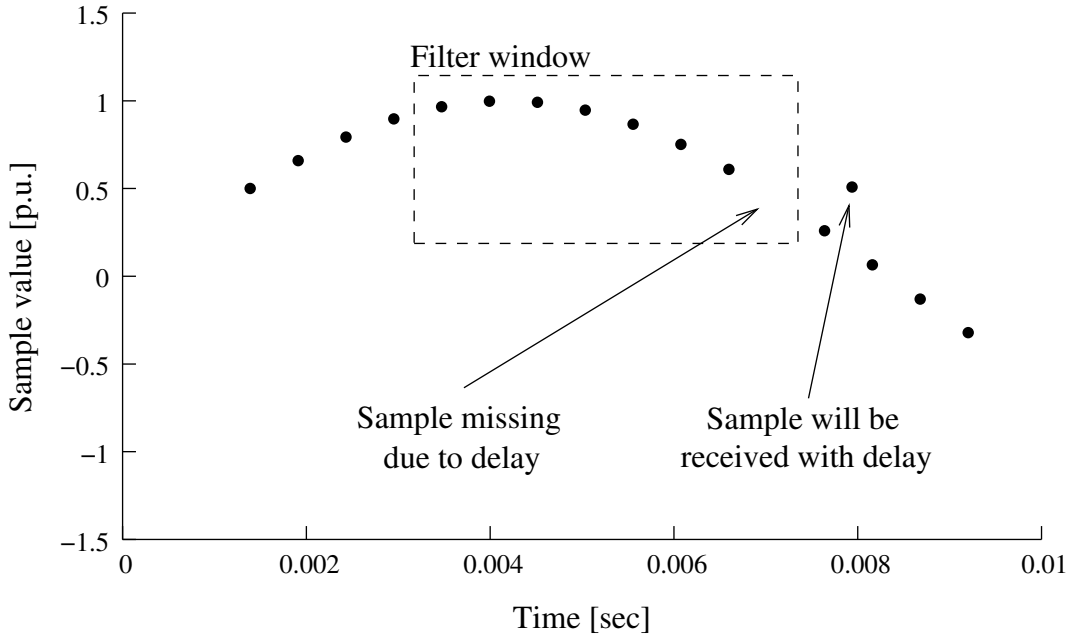

Figure 5.2: Filter window with missing sample

$$
\begin{aligned}
H(z) &= h(0)z^{-0} + h(1)z^{-1} + \sum_{k=2}^{M-1} h(k)z^{-k} \\
&= h(0)z^{-0} + \sum_{k=2}^{M-1} h(k)z^{-k} \qquad (5.5)
\end{aligned}
$$

By applying the above steps, a new set of coefficients can be obtained for each position of the missing sample inside the filter window. Once the sample arrives and is recognized by the system as being covered by the filter window, the sample is inserted into its proper position in the convolution sum, and the original coefficients are reloaded.

The above rationale can be applied for multiple delayed or missing samples, by selecting filters that have $h(k) = 0$ for the unknown samples. The phase characteristics of these filters are such that the resulting phase angle is properly aligned with $n = 0$ for each sample.

It should be noted that with a properly designed system, delayed packets are rare, and are mainly the result of failing communication media. Inside a network segment, data transmitted in broadcast mode is available to all listening devices simultaneously, therefore, with digital instrumentation in place, the sampled values of currents and voltages can be made simultaneously available to any field device on the network segment.

The procedure is general in nature, and is applicable to digital filtering techniques that allow pre-setting of various order filter coefficients. With the proposed algorithm, a set of filters can be developed that can be utilized to solve the problem of possible non-sequential and missing data samples.

5.2 Implementation

In order to test the procedure described in the previous section, the Least Square Error algorithm is used to develop the required set of filters.

Decaying DC components and a reasonable number of harmonics can be calculated using this algorithm. Same as for the general form of the LSE algorithm, the sinusoidal

signal that has a decaying DC component can be written as:

$$y(t) = A_0 e^{-\frac{t}{\tau}} + \sum_{m=1}^{p} A_m \sin(\omega_m t + \phi_m) \tag{5.6}$$

where: A_m is the amplitude of the harmonic m.

The Taylor series expansion of a complex function around a number z_0 is defined by:

$$f(z) = \sum_{m=0}^{\infty} \frac{f^{(m)}(z_0)}{m!}(z - z_0)^m \tag{5.7}$$

where $f^{(m)}$ is the m-th order derivative of $f(z)$.

Starting from Eq.(5.7) and using as centre $z_0 = 0$, the Maclaurin series expansion of the complex function e^z can be written as:

$$e^z = \sum_{n=0}^{\infty} \frac{z^n}{n!} = 1 + \frac{z}{1!} + \frac{z^2}{2!} + \cdots \tag{5.8}$$

For properly filtered signals, in power systems relaying applications, the two term approximation of the previous series is considered sufficient, therefore, Eq.(5.6) can be written as:

$$y(t) = A_0 - A_0 \frac{t}{\tau} + \sum_{m=1}^{p} A_m \sin(\omega_m t + \phi_m) \tag{5.9}$$

When the data stream delay is within the acceptable limits and no samples are missing from the filter window, each of the samples will satisfy Eq.(5.9).

It can be considered that $n = 0$ for $t = 0$. If the sampling rate is set, then the previous sample before the instant $t = 0$ was taken at $t = -\Delta t$, where

$$\Delta t = \frac{1}{f_s} \tag{5.10}$$

with f_s being the sampling frequency.

For each sample that is covered by the filter window, it can be successively written:

$$\begin{aligned}
y_0 &= A_0 - A_0\frac{-0\Delta t}{\tau} + \sum_{m=1}^{p} A_m \sin\left[\omega_m(-0\Delta t) + \phi_m\right] \\
y_1 &= A_0 - A_0\frac{-1\Delta t}{\tau} + \sum_{m=1}^{p} A_m \sin\left[\omega_m(-1\Delta t) + \phi_m\right] \\
&\vdots \\
y_{M-1} &= A_0 - A_0\frac{-(M-1)\Delta t}{\tau} + \sum_{m=1}^{p} A_m \sin\left[\omega_m(1-M)\Delta t + \phi_m\right]
\end{aligned} \tag{5.11}$$

The set of equations represented in (5.11) can be written in matrix form as:

$$Y = HX \tag{5.12}$$

where:

$$Y = \begin{bmatrix} y_0 \\ y_1 \\ y_2 \\ \vdots \\ y_{M-1} \end{bmatrix} \tag{5.13}$$

$$X = \begin{bmatrix} x_1 \\ x_2 \\ \vdots \\ x_{2p+2} \end{bmatrix} = \begin{bmatrix} A_0 \\ -\frac{A_0}{\tau} \\ A_1 \cos(\phi_1) \\ \vdots \\ A_p \sin(\phi_p) \end{bmatrix} \tag{5.14}$$

The matrix H is:

$$H = \begin{bmatrix} 1 & (-0)\Delta t & \sin(-0\Delta t\ \omega_1) & \dots & \cos(-0\Delta t\ \omega_p) \\ 1 & (-1)\Delta t & \sin(-1\Delta t\ \omega_1) & \dots & \cos(-1\Delta t\ \omega_p) \\ & \vdots & & & \\ 1 & (1-M)\Delta t & \sin((1-M)\Delta t\ \omega_1) & \dots & \cos((1-M)\Delta t\ \omega_p) \end{bmatrix} \tag{5.15}$$

The above relationships can be written for any value of t. The equation in (5.12) can be solved for X using the pseudo-inverse of the matrix H to minimize the errors.

Multiplying both sides of Eq.(5.12) with H^T, the transpose of H, it can be subsequently written:

$$\begin{aligned} H^T Y &= H^T H X \\ (H^T H)^{-1} H^T Y &= (H^T H)^{-1}(H^T H) X \\ X &= (H^T H)^{-1} H^T Y \end{aligned} \tag{5.16}$$

Once the values of X are obtained, the elements describing Eq.(5.9) can be cal-

culated. For example, the two elements of matrix X that will give information on the real and imaginary parts of the fundamental frequency signal are x_3 and x_4. Therefore, it can be written that:

$$A_1 = \sqrt{x_3^2 + x_4^2} \tag{5.17}$$

and

$$\phi_1 = \tan^{-1}\left(\frac{x_4}{x_3}\right) \tag{5.18}$$

Using a similar procedure, the values of the amplitude and phase angle of the harmonics included in Eq.(5.9) can be obtained using the corresponding elements of matrix X.

The above described algorithm can be applied for a complete set of samples, that is when all samples are present as it can be seen in Fig.(5.1). When one of the samples is late, the filters obtained in Eq.(5.16) would yield incorrect results. For the situation presented in Fig.(5.2), where a sample is late due to traffic delays, or because its value is not acceptable due to the TLQ (Tags, Limits, Quality) information embedded in the packet used to transmit it, a new set of filter coefficients is required. This new set of filter coefficients can be obtained by ignoring the line representing the missing sample in the previously described algorithm.

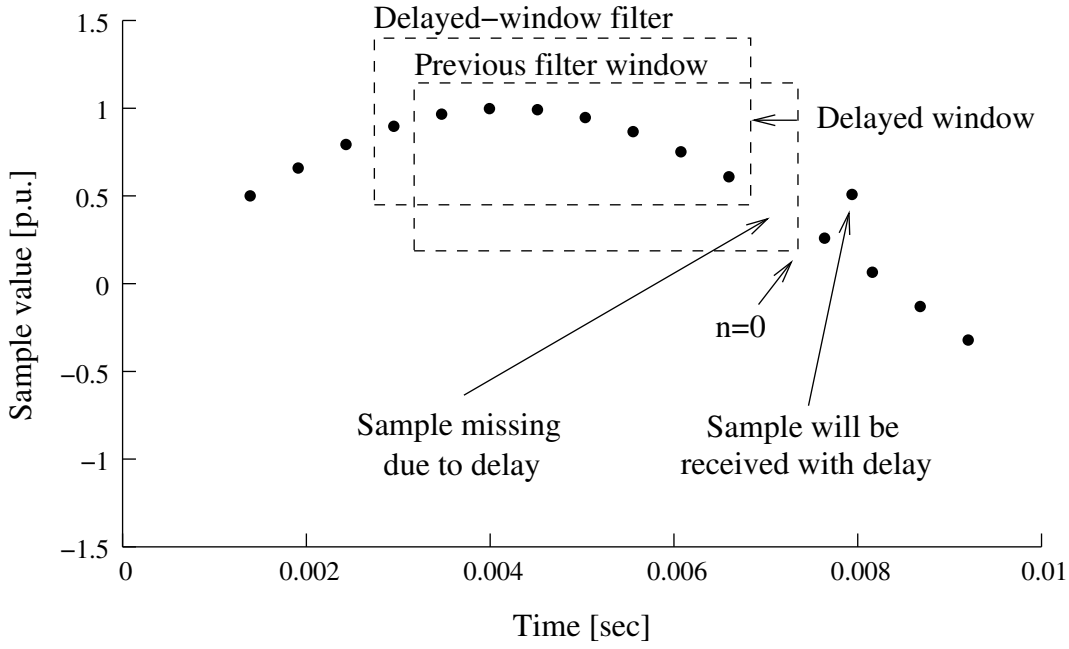

Figure 5.3: Reduced size filter window

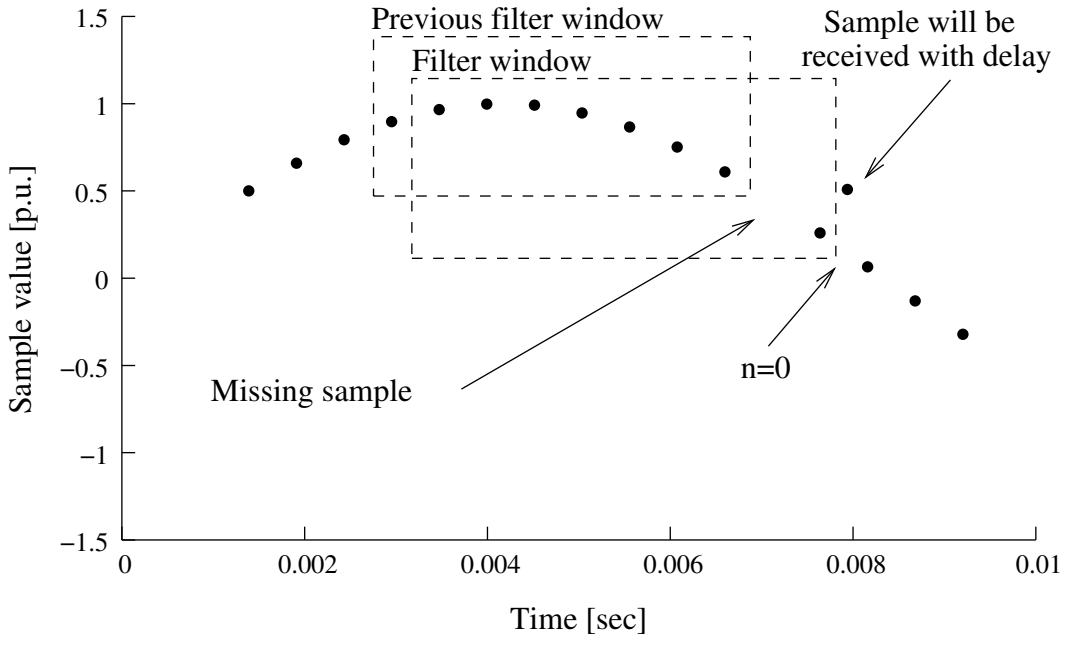

Figure 5.4: Missing sample inside filter window

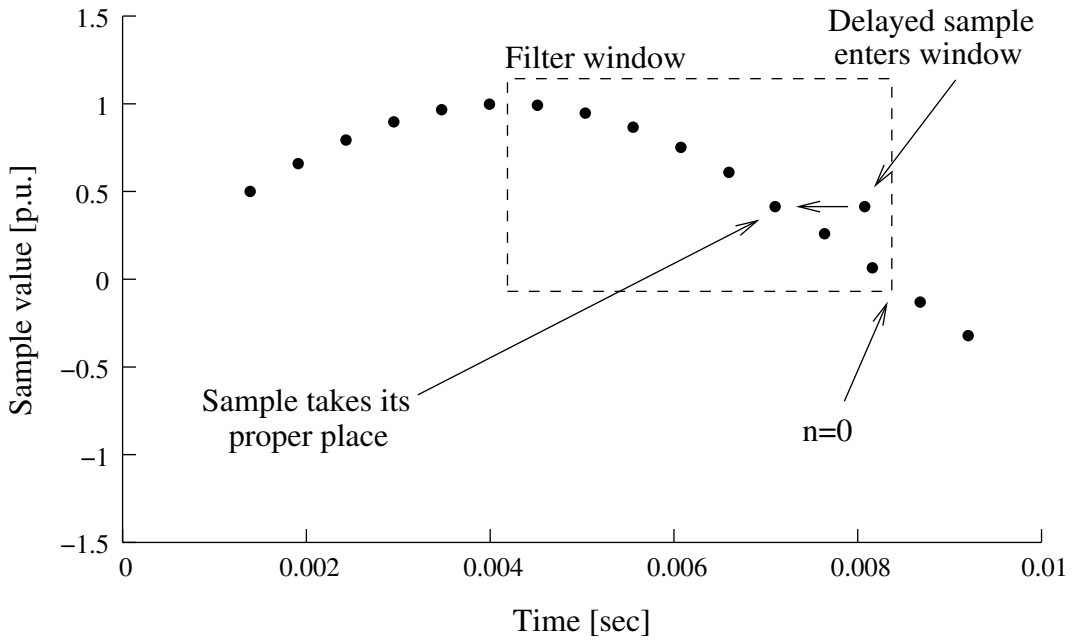

Figure 5.5: Sample moved to proper position

With y_0 sample missing, Y will become:

$$Y = \begin{bmatrix} y_1 \\ y_2 \\ y_3 \\ \vdots \\ y_{M-1} \end{bmatrix} \tag{5.19}$$

The corresponding first row will be dropped from matrix H, and the new filter coefficients can be calculated using the procedure described in Eq.(5.16). The window of samples covered by the new filter in reference to the full window is represented in Fig.(5.3). Once a new sample arrives at the relay location, the filter window can be extended back to the original length, as exemplified in Figs.(5.4) and (5.5).

The location of a missing sample can pass through the filter window if the sample does not arrive to the relay during the time frame covered by the window. Different sets of filters can be obtained for every position the missing sample would have inside the filter window. If k represents the position of the missing sample relative to $n = 0$, the new set of filter coefficients is obtained using the matrix H with the row k removed, as seen in Eq.(5.20).

$$H_k = \begin{bmatrix} 1 & (-0)\Delta t & \sin(-0\Delta t\ \omega_1) & \dots & \cos(-0\Delta t\ \omega_p) \\ 1 & (-1)\Delta t & \sin(-1\Delta t\ \omega_1) & \dots & \cos(-1\Delta t\ \omega_p) \\ & \vdots & & & \\ 1 & -(k-1)\Delta t & \sin(-(k-1)\Delta t\ \omega_1) & \dots & \cos(-(k-1)\Delta t\ \omega_p) \\ 1 & -(k+1)\Delta t & \sin(-(k+1)\Delta t\ \omega_1) & \dots & \cos(-(k+1)\Delta t\ \omega_p) \\ & \vdots & & & \\ 1 & (1-M)\Delta t & \sin((1-M)\Delta t\ \omega_1) & \dots & \cos((1-M)\Delta t\ \omega_p) \end{bmatrix} \quad (5.20)$$

Using the same approach, any combination of missing samples can be assigned a set of filter coefficients. It is up to the system designer to consider a margin or a percentage of delayed packets after which the communication link can be labelled failed. The matrix H can be calculated off-line for a number and combination of samples for which the communication channel is still considered operational, or obtained on-line using a Gram-Schmidt orthogonalization algorithm [109]. The length of the designed filters can vary depending on the performance expected from them.

With proper analogue filtering and antialiasing in place at the location where

the samples are taken, the length of the filter can be reduced for faster response, or the number of filter sets increased, to accommodate less performant communication channels.

5.3 Performance limits

The algorithm presented in the previous section is able to accommodate delayed and missing samples. The described procedure does not include operating limits on the flexibility of the adaptive algorithm. Since the algorithm follows closely the communications system performance, it is important to have predetermined boundaries in which the relaying algorithm can operate.

A possible solution to setting performance limits can be obtained if the target length of the filter is considered fixed to a predetermined number of samples. For example, for a sampling rate of 32 samples per cycle of the fundamental frequency, 16 samples can be considered as the target length of the filter. So as long as the adaptive filter has less than 16 samples in the data window, the oldest sample in the window will not be dropped. When the incoming samples fill up the data window to 16 samples, the 17th will cause the algorithm to drop the oldest, keeping the filter window at the target number of 16 samples. This approach has the disadvantage that when the network has very poor performance, the length of the filter, expressed in time, can grow beyond the length of a period of the fundamental frequency. In fact, it will grow until all the 16 samples have arrived. Setting a time limit on the size of

the filter window puts a performance requirement on the network. In the considered example, a network performance that would result in a filter data window longer than 1 cycle of the fundamental frequency would mean that the communications system has failed.

A different solution can be obtained if the filter length is considered to be fixed at 1 full cycle of the fundamental frequency. In this approach, the samples are dropped from the window as soon as they are "older" than 1 cycle. The performance limit set on the network is that at least a minimum number of samples be present in the filter window at all times, for example 8 samples, at a sampling rate of 32 samples per cycle. The 8 samples can be from any point that is covered by the fixed size filter window. This approach has the disadvantage that a relatively small number of samples can result in the filter window during poor communications performance. The response time of the algorithm is fixed at one full cycle. When the number of samples in the window drops below the minimum acceptable (could be 8 samples for the considered example), the communication media can be considered failed.

The third example to setting limits on the performance of the networking system is a combination between the previously presented solutions. It partly eliminates the disadvantages identified above, by finding a balance between the two. Considering the same sampling rate of 32 samples per cycle of the fundamental frequency component, the length of the filter will be allowed to vary between half and full cycle, while any number of samples between a minimum of 8, and the full complement of 32 would be

considered acceptable. The communications media can be considered failed when the full-cycle filter has less then 8 samples in the data window. The advantage over the previous solution is that during normal communications performance, the filter will respond twice as fast, since it needs only 8 samples in half cycle of the fundamental to process a valid output.

The digital relaying algorithm introduced in this chapter is able to overcome the deterministic data delivery constraint placed on previous digital relaying solutions. Its performance when applied to a wide range of protective solutions is investigated in the next chapter, confirming its applicability to an integrated power system protection and control solution.

CHAPTER 6

APPLICATION AND TESTING OF THE NEW DIGITAL RELAYING ALGORITHM

6.1 The infrastructure

The testing of the proposed GPS-based LSE algorithm (GPS-LSE) is done on a number of functions applied to power system protective applications with increasing complexity. The protective functions are described in the corresponding sections.

The composite system shown in Fig.(6.1) is used to test the new process-bus digital relaying solution. The system has a radial line, similar to structures used to supply large industrial loads on dedicated feeders. There are numerous installations in Saskatchewan that use radial sub-transmission systems to supply large industrial loads. Operation of these dedicated sub-transmission lines is done at medium voltage, usually between 69 and 138 kV. Due to the large load, the system needs to be relatively strong to avoid the voltage flickers during sudden load changes. The resulting separations between fault and load currents make these lines good candidates for overcurrent protection. The radial line structure is also well suited for impedance protection. The operating voltage of the radial line in the test system is 138 kV,

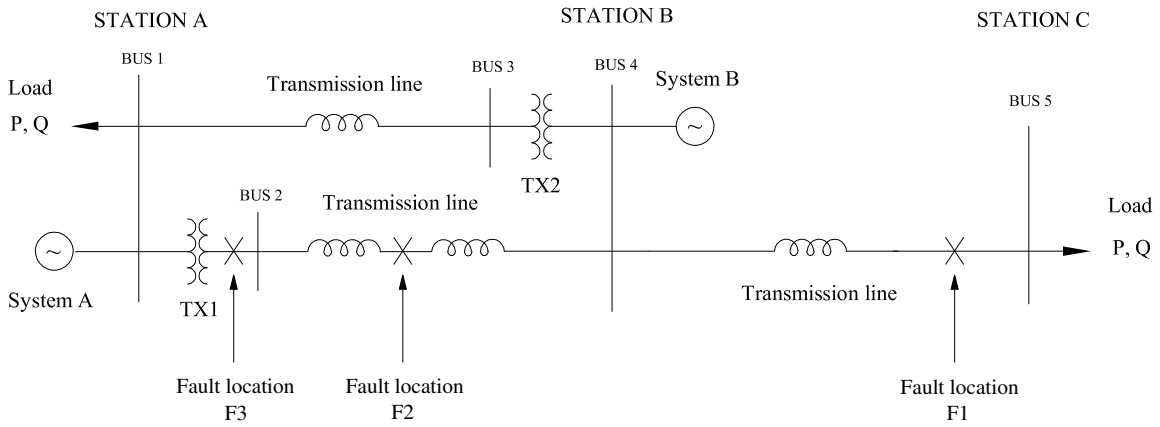

Figure 6.1: Test system and the fault locations

and the fault location is marked with F1. The first set of tests are conducted using the new algorithm in overcurrent and impedance protective solutions applied to the radial sub-transmission line.

The composite power system in Fig.(6.1) has two equivalent power sources connected by two transmission lines operated at different voltage levels. The resulting parallel transmission system is characteristic to power grids that were developed by reinforcing existing transmission corridors at higher voltage levels. The transmission lines are operated at 138 and 230 kV. Due to the two opposite equivalent systems that result in significant current infeeds during transmission line faults, the differential protection of the lines is used. The fault location on the transmission line is marked with F2.

The second set of tests will show the performance of the GPS-LSE algorithm while performing transmission line protection using percentage and alpha-plane differential applications. The percentage and alpha-plane differential protection solutions are

described in the respective sections.

The third set of tests are done using the process-bus solution applied to the differential protection of a transformer. The location of the transformer faults is marked F3 on the test system shown in Fig.(6.1).

The last set of tests are done on the protection of a transmission line that has a Unified Power Flow Controller (UPFC) installation in the middle of the line. The benefits of the open-system protection approach are emphasized, while effective protection is provided to the entire zone, building on the new digital relaying algorithm.

The effect of the data transmission system on the new digital relaying algorithm is investigated by considering two states of the data transmission, marked slow and fast. During fast networking conditions, the equivalent time delay fluctuates with an average of 2 milliseconds, similar to the performance shown in Fig.(2.16), while up to 5 network interface cards (NIC) compete for access on the single collision domain. During slow networking conditions, the average delay can increase up to 4 milliseconds, as shown in Fig.(2.17), while up to 10 NICs compete for network resources in the respective single collision domain. The performance of the new digital relaying algorithm has been considered at sampling frequencies of 8 and 32 samples per cycle.

The complete list of tests are shown in Table (6.1). The test results obtained for line-to-ground faults (LG) are included in the respective protective function sections, while the results of the line-to-line (LL) and 3-line faults (LLL) are included in the

Table 6.1: List of tests conducted

Location	Type of fault	Function	Algorithm	Samples	Network
F1	LG	51, 21	FF, GPS-LSE	8, 32	fast, slow
	LL	51, 21	FF, GPS-LSE	8, 32	fast, slow
	LLL	51, 21	FF, GPS-LSE	8, 32	fast, slow
F2, F3	LG	87-D, 87-A	FF, GPS-LSE	8, 32	fast, slow
	LL	87-D, 87-A	FF, GPS-LSE	8, 32	fast, slow
	LLL	87-D, 87-A	FF, GPS-LSE	8, 32	fast, slow

Table 6.2: Performance benchmarks

Value	Protective function	Description	Benchmark
Pickup time	51	Time required to reach the value of the pickup current during overcurrent protection	< 24 ms
Trip time	21	Time required to reach the operating zone, and issue the trip command during impedance protection	< 16 ms
Trip time	87-D	Time required to reach the operating zone, and issue the trip command during percentage differential protection	< 24 ms
Trip time	87-A	Time required to reach the operating zone, and issue the trip command during alpha-plane differential protection	< 16 ms

Appendices.

To quantify the performance of the relaying algorithms, several operating time values are monitored. The values are listed in Table (6.2).

To monitor the stability of the new relaying algorithm and help benchmark it

against the Full-cycle Fourier, the following additional values are introduced and measured.

$$s_1 = \sqrt{\frac{1}{n}\sum_{i=1}^{n}(x_i - \bar{x})^2} \tag{6.1}$$

where

$$\bar{x} = \frac{1}{n}\sum_{i=1}^{n} x_i \tag{6.2}$$

is the average value of the samples x_i received during a given period of time. The number representing s_1 gives indication about the stability of the algorithm around its average output value.

The next value monitored is s_2 represented by:

$$s_2 = \sqrt{\frac{1}{n}\sum_{i=1}^{n}(x_i - \tilde{x})^2} \tag{6.3}$$

where $\tilde{x}$ is the reference value of the signal obtained at the source, i.e. the amplitude of the fundamental obtained using Fourier analysis on the original signal before transmission. The value of s_2 is indicative of the performance of the algorithm to maintain the correct output.

Both s_1 and s_2 have the meaning of standard deviations, and are presented as percentage values, normalized to the original target signal, i.e. $\tilde{x}$. Benchmark number for acceptable performance is 1-2 % for each of s_1 and s_2.

6.2 Radial line faults

6.2.1 Overcurrent protection

The overcurrent protection is based on the amplitude of the current that flows at the location of the protective relay. It is a widely used protective function and due to its simplicity and reliability it has been maintained in new digital and microcomputer-based solutions [110–116]. The monitored value could be the RMS or peak value of the measured current. It is usually applied on a per phase basis, which means that at least 3 relays, preferably 4 with the one in the neutral, are needed to provide protection against all types of faults. It is a standard protective function on radial lines when the maximum load and minimum fault current are sufficiently distinct to provide enough margin for the relay to discriminate between load and fault currents. A typical installation of an overcurrent relay is shown in Fig.(6.2).

The operation of the overcurrent protective function can be made instantaneously, as soon as the amplitude was determined to exceed a predefined value. In this case, the protective function is instantaneous overcurrent, and is represented by the IEEE function 50.

On radial lines, the fault current amplitude is inversely proportional to the distance between the location of the relay and that of the fault. Inverse-time overcurrent relays offer a fast response at high current values, and slower, delayed response to more distant fault events that result in smaller fault currents. The inverse-time characteristic of these relays permit the time coordination between protective devices

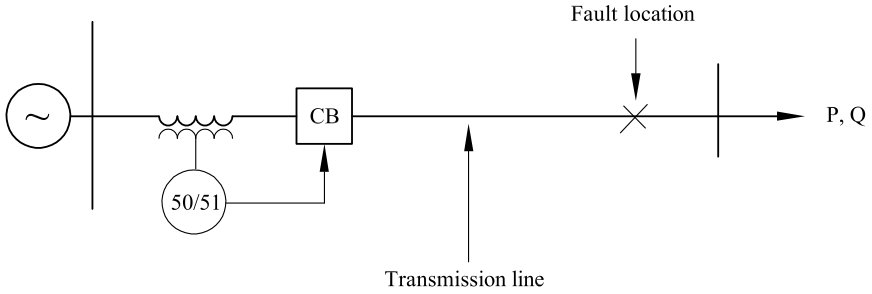

Figure 6.2: Installation of overcurrent relays on radial feeders

along the radial lines. The inverse-time overcurrent characteristic is represented by the IEEE protective function 51.

Standard curves describe the current versus tripping time of inverse-time overcurrent relays. Equation (6.4) describes the IEC inverse-, while Eq.(6.5) describes the IEEE very inverse-time sets of curves. The value of TD represents the time-dial setting, while M is the multiple of pickup current.

$$t = TD\frac{0.014}{M^{0.02} - 1} \tag{6.4}$$

$$t = TD\left(\frac{3.922}{M^2 - 1} + 0.0982\right) \tag{6.5}$$

Depending on the time-dial setting TD, sets of curves are available, as seen in Figs.(6.3) and (6.4) for the curves given in Eqs.(6.4) and (6.5).

6.2.2 Distance protection

Distance protection is applied on radial and transmission lines to identify and discriminate faults along the protected segment of the line, and provide system protection by isolating the faulted segment.

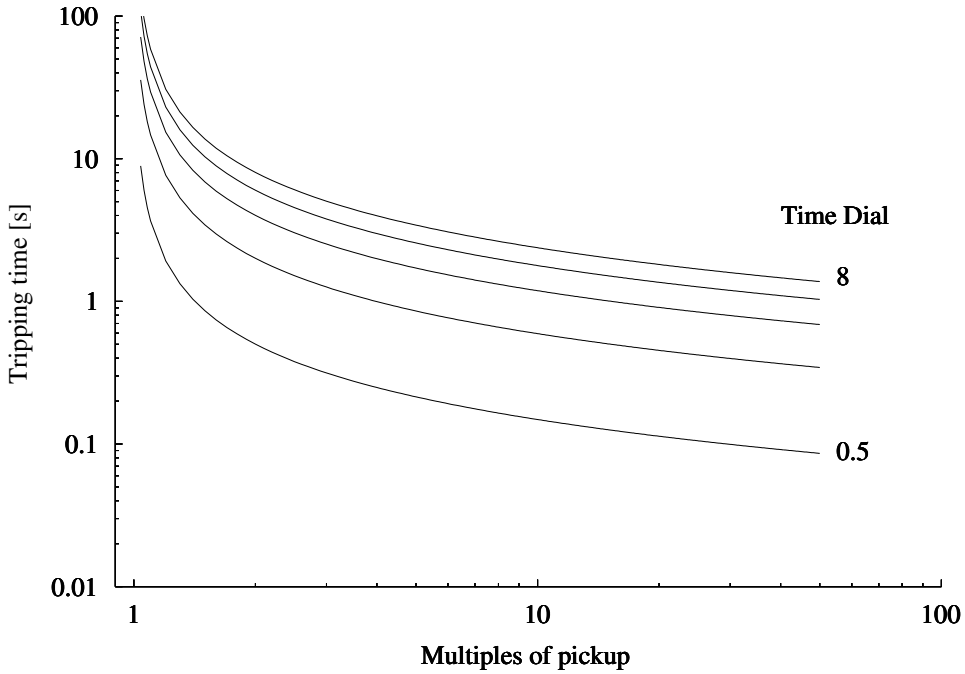

Figure 6.3: IEC inverse-time overcurrent curves

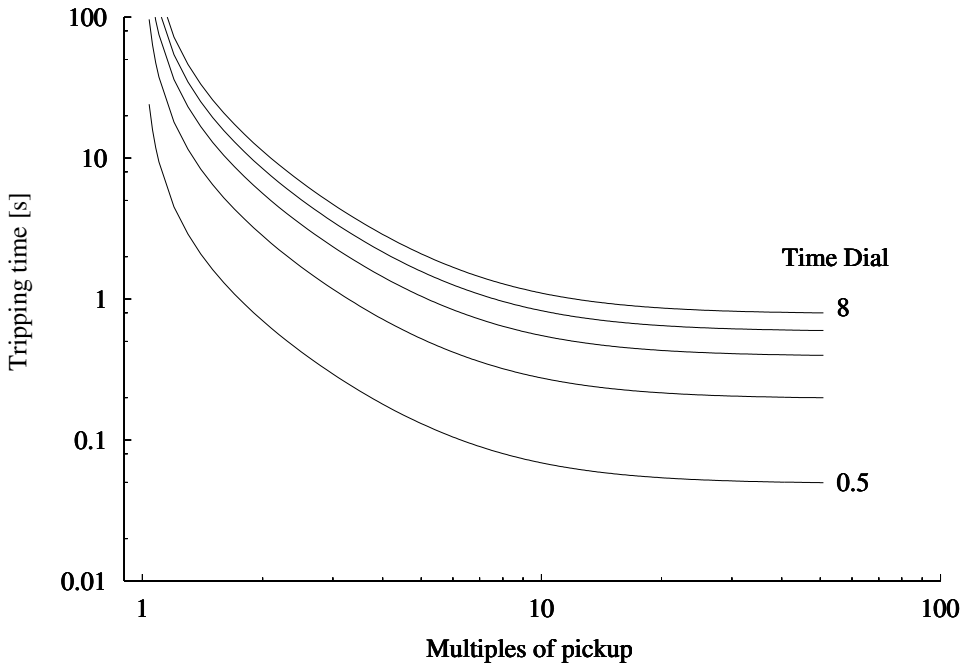

Figure 6.4: IEEE very inverse-time overcurrent curves

The distance to the location of the fault along the line can be expressed as a percentage m of the total length of the line. It has been shown that the length of the line between the location where measurements are taken and the location of the fault is measurable using voltages and currents obtained at the beginning of the line [82]. For a line-to-line fault between phases A and B, the distance to the fault can be determined as:

$$Z_m = mZ_1 = \frac{V_A - V_B}{I_A - I_B} \tag{6.6}$$

where Z_1 is the positive-sequence impedance of the line.

Using a similar approach, the impedance of the line to the location of the fault during a line-to-ground fault on phase A can be expressed as:

$$Z_m = mZ_1 = \frac{V_A}{I_A - kI_0} \tag{6.7}$$

with:

$$k = \frac{Z_0 - Z_1}{Z_0} \tag{6.8}$$

where I_0 and Z_0 are the zero-sequence current and impedance, respectively.

A distance relay that uses the above equations to determine the location of a fault is called a self-polarized impedance relay. The accuracy of the self-polarized distance relay is affected by infeeds and by the resistance of the fault. Therefore, its application is recommended to transmission lines with limited infeed or to radial lines. The effect of the fault resistance R_F on the measured impedance Z_m at the relay location is shown in Fig.(6.5).

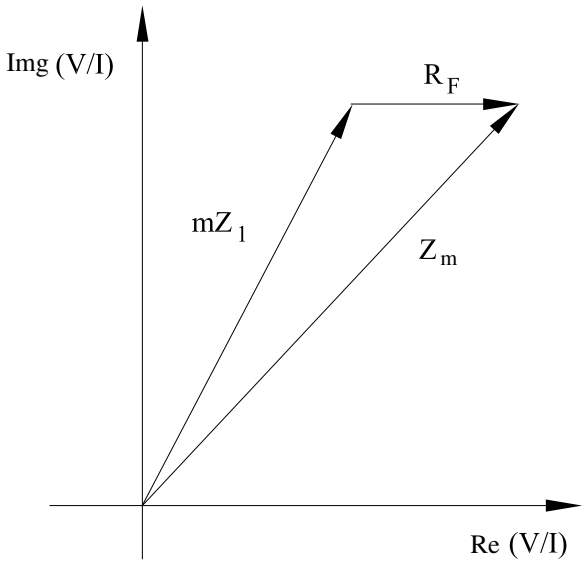

Figure 6.5: Effect of fault resistance on the measured impedance

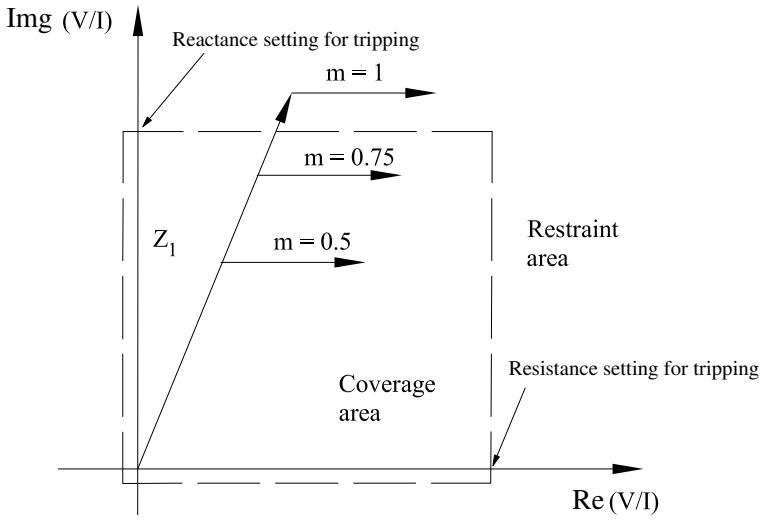

Figure 6.6: Distance protection settings for self-polarized impedance relays

Depending on the measured impedance, different zones of protection can be set up by comparing the value of Z_m to predefined numbers. A rectangular operating characteristic for a distance relay is shown in Fig.(6.6).

As seen from the equations representing the measured apparent impedance to the

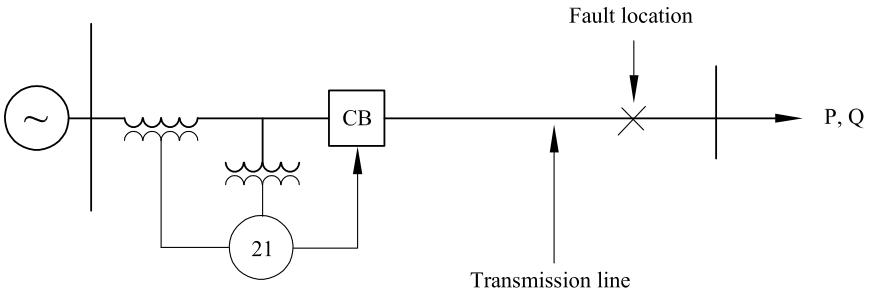

Figure 6.7: Application of distance protection to radial lines

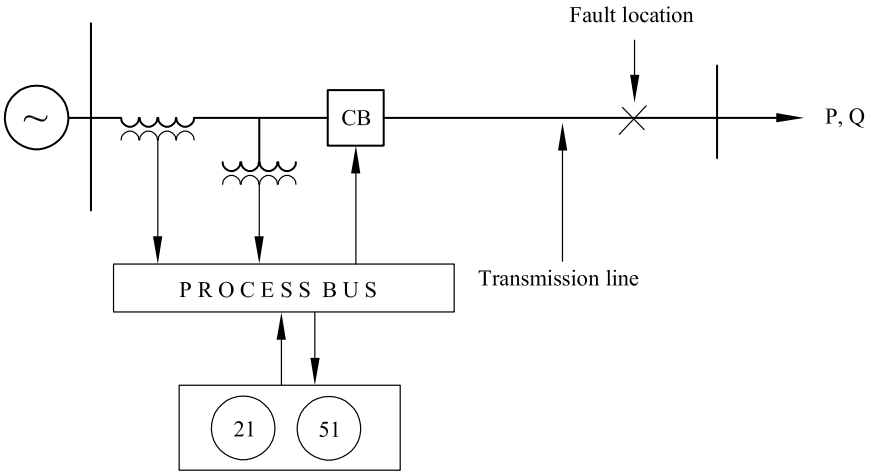

Figure 6.8: Radial line protection over process bus with distance and overcurrent functions

fault, both currents and voltages are required. The connection of the impedance relay to the power line instrumentation is shown in Fig.(6.7).

Using the open-system protection and control approach, both the overcurrent and distance elements can be done by the same clustered relaying installation. The connection of the digital instrumentation to the local process bus is shown in Fig.(6.8). The circuit breaker operation is achieved by the same unified process communications.

The radial line fault tests are conducted on the system shown in Fig.(6.9), implemented in the Matlab environment with the system values listed in Appendix A.

In the figures showing the results obtained for overcurrent and distance protection, the operation of the respective element is depicted by its IEEE function: 21 for the distance- and 51 for the inverse-time overcurrent element. The protective functions 21 and 51 are represented connected to the breaker they operate. To underline the performance of the algorithm and that of the open-system protection philosophy, the protective functions' output are shown, without the time delays required to operate the breaker.

The overcurrent tests are done using the equation:

$$t = TD\frac{0.014}{M^2 - 1} \tag{6.9}$$

with a pickup current $I_p = 2$ [p.u.] and $TD = 0.5$. The exponential of M is set equal to 2 in order to obtain a very fast response from the relay.

Signal curves obtained during line-to-ground faults are shown in Figs.(6.10) to (6.13). The inverse-time overcurrent characteristic curves are shown in Figs.(6.14) to (6.17), while the impedance plane curves during line-to-ground faults are shown in

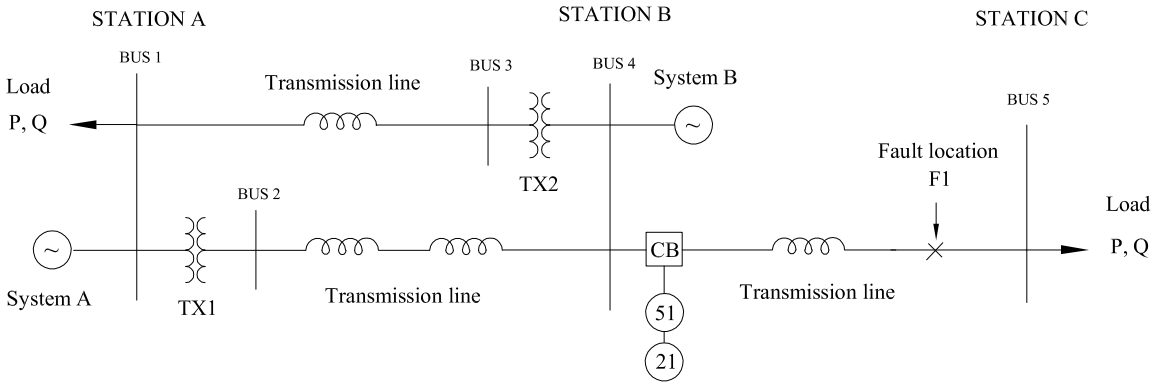

Figure 6.9: Test system for radial line faults

Figs.(6.18) to (6.21).

Results for line-to-line and 3-line faults are shown in the Appendices. A complete list of figures showing radial line test results is given in Table (6.3).

Table 6.3: List of figures showing radial line test results

Type of fault	Function	Algorithm	Samples	Figure
LG	51	FF	8	(6.14)
		GPS-LSE	8	(6.15)
		FF	32	(6.16)
		GPS-LSE	32	(6.17)
	21	FF	8	(6.18)
		GPS-LSE	8	(6.19)
		FF	32	(6.20)
		GPS-LSE	32	(6.21)
LL	51	FF	8	(B.5)
		GPS-LSE	8	(B.6)
		FF	32	(B.7)
		GPS-LSE	32	(B.8)
	21	FF	8	(B.9)
		GPS-LSE	8	(B.10)
		FF	32	(B.11)
		GPS-LSE	32	(B.12)
LLL	51	FF	8	(B.17)
		GPS-LSE	8	(B.18)
		FF	32	(B.19)
		GPS-LSE	32	(B.20)
	21	FF	8	(B.21)
		GPS-LSE	8	(B.22)
		FF	32	(B.23)
		GPS-LSE	32	(B.24)

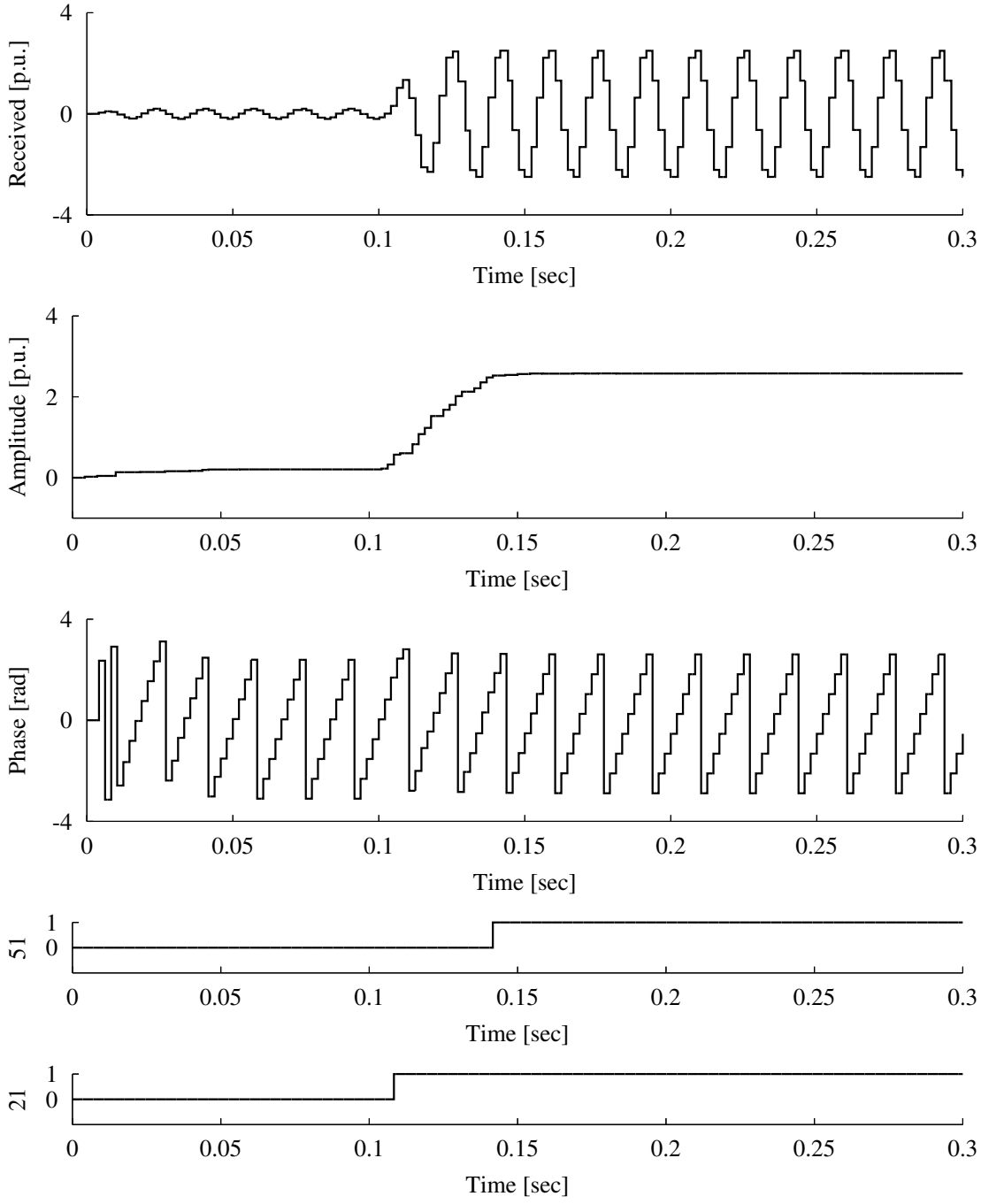

Figure 6.10: GPS-LSE algorithm performance with 8 samples per cycle over slow network during a line-to-ground fault at location F1

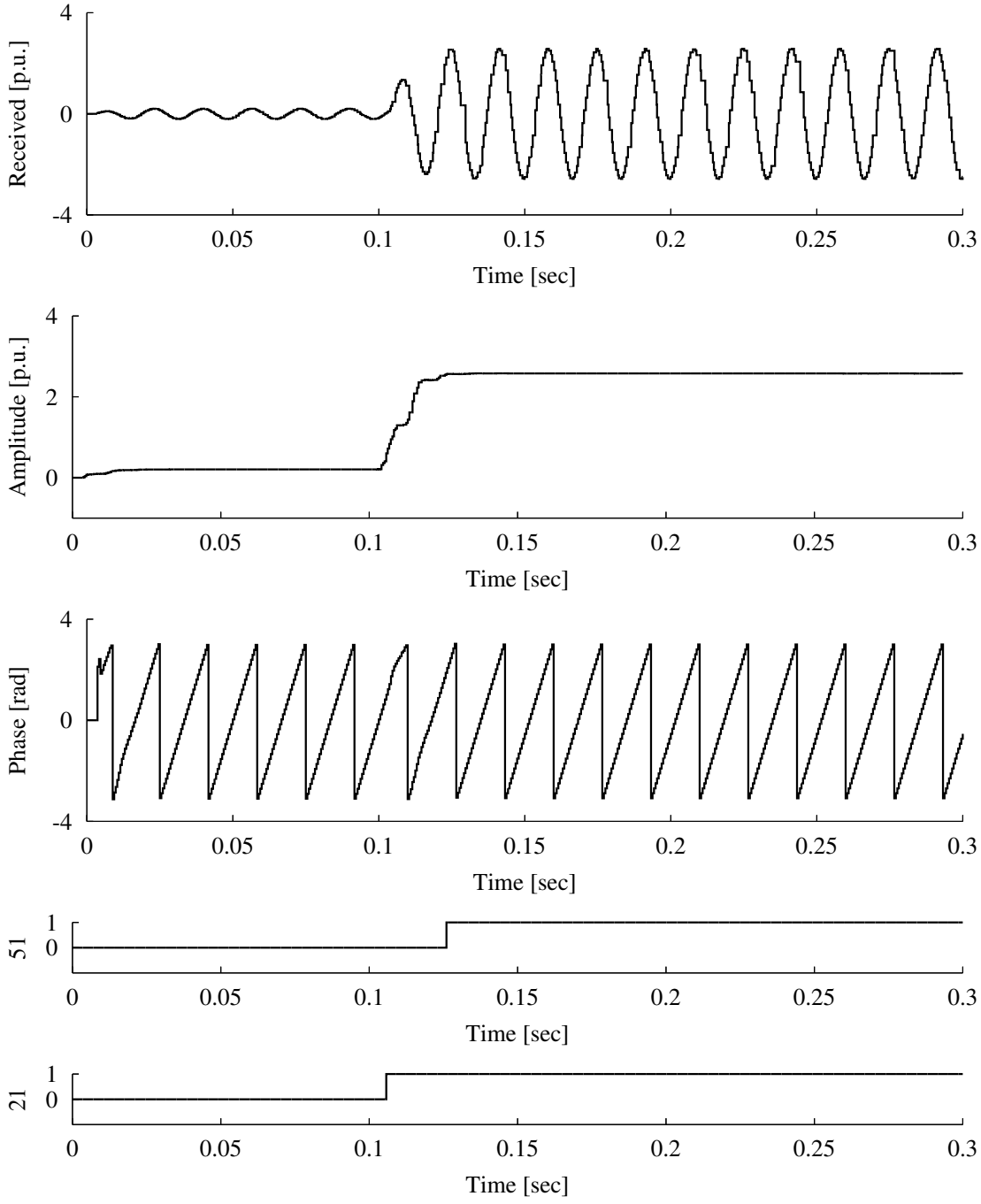

Figure 6.11: GPS-LSE algorithm performance with 32 samples per cycle over slow network during a line-to-ground fault at location F1

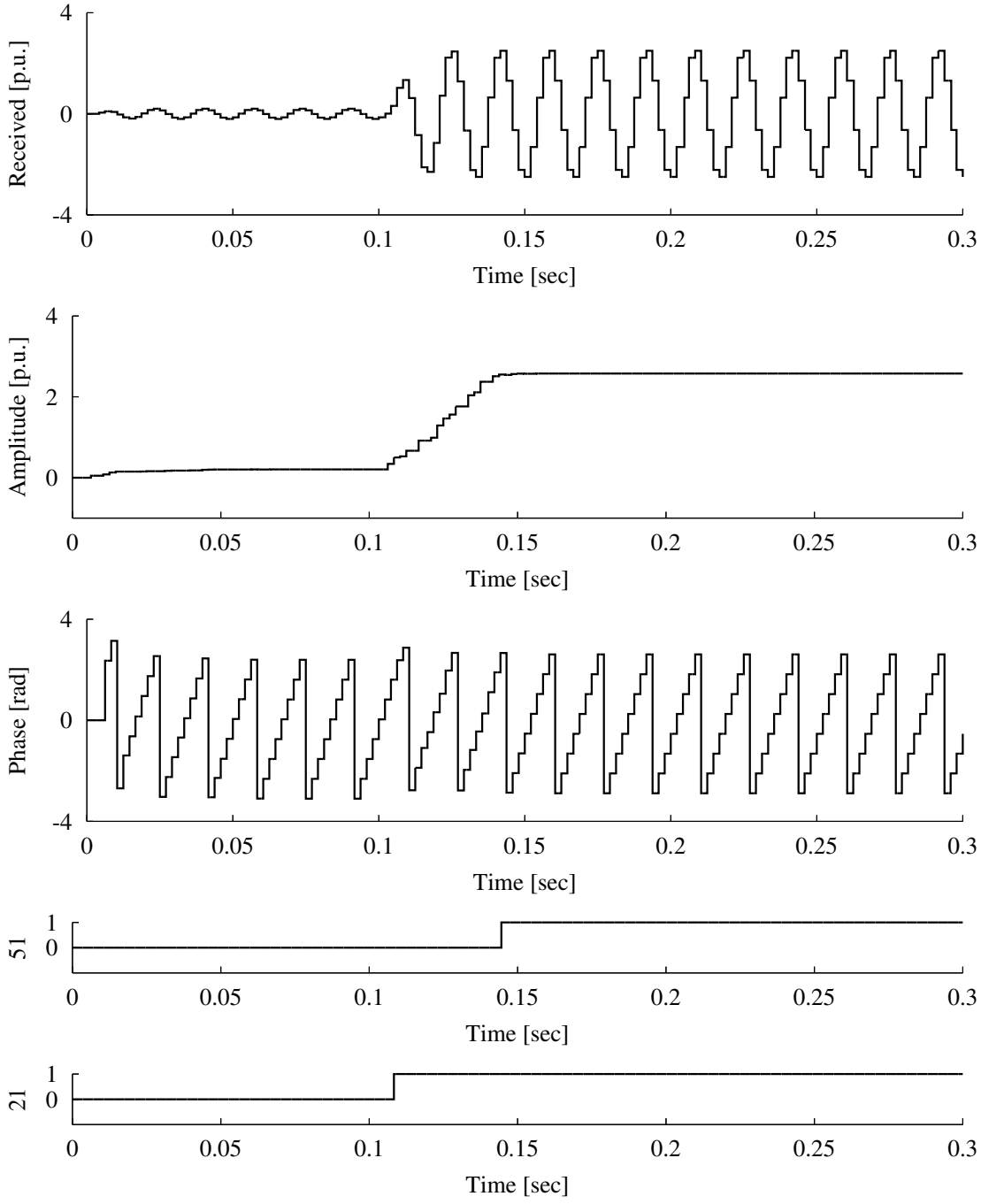

Figure 6.12: GPS-LSE algorithm performance with 8 samples per cycle over fast network during a line-to-ground fault at location F1

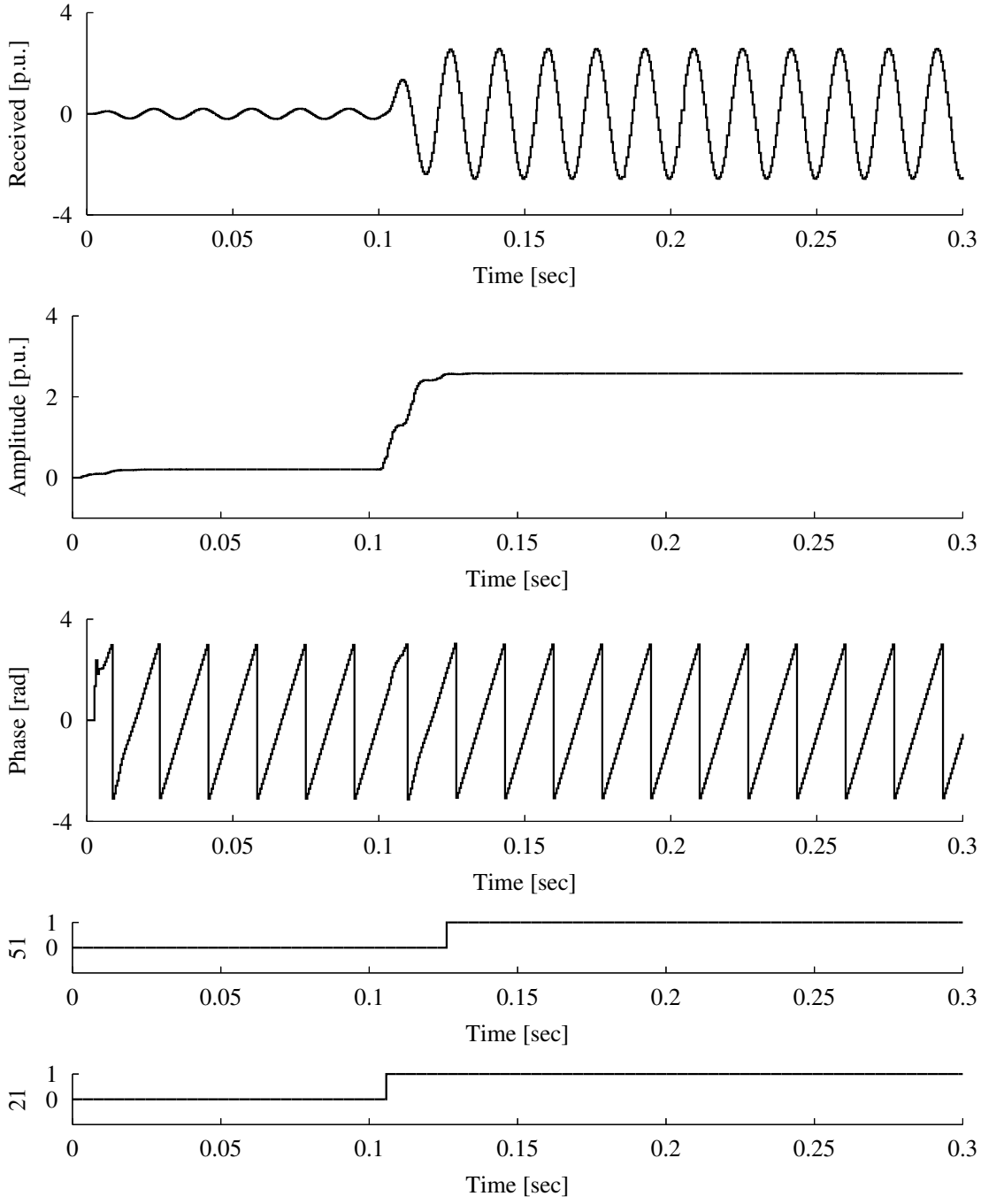

Figure 6.13: GPS-LSE algorithm performance with 32 samples per cycle over fast network during a line-to-ground fault at location F1

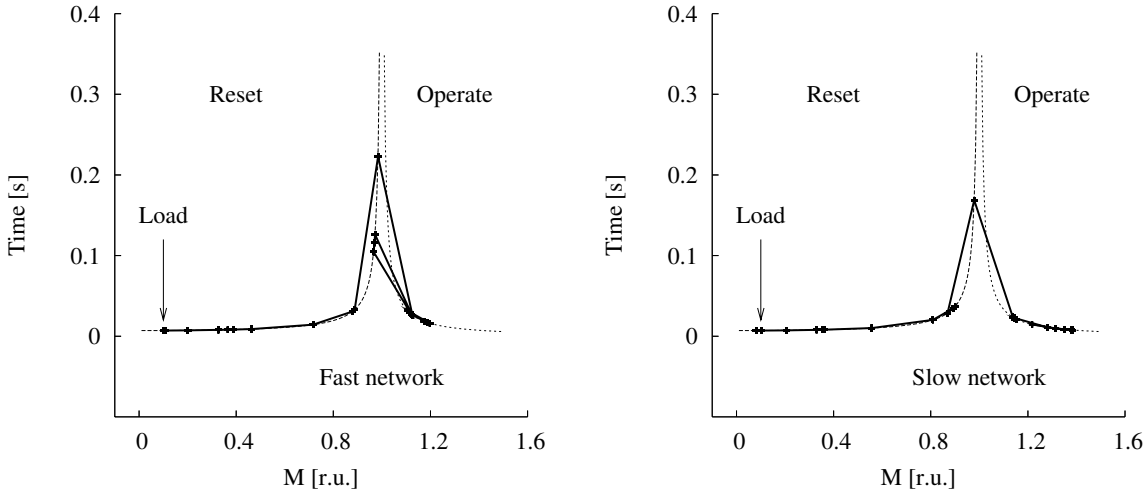

Figure 6.14: Overcurrent protection performance of the FF algorithm with 8 samples per cycle during a line-to-ground fault at location F1

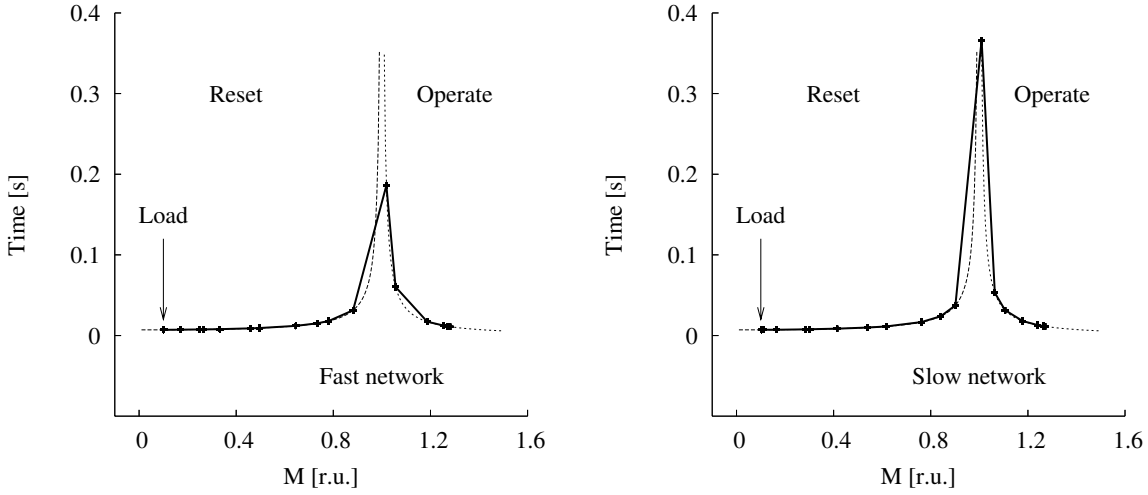

Figure 6.15: Overcurrent protection performance of the GPS-LSE algorithm with 8 samples per cycle during a line-to-ground fault at location F1

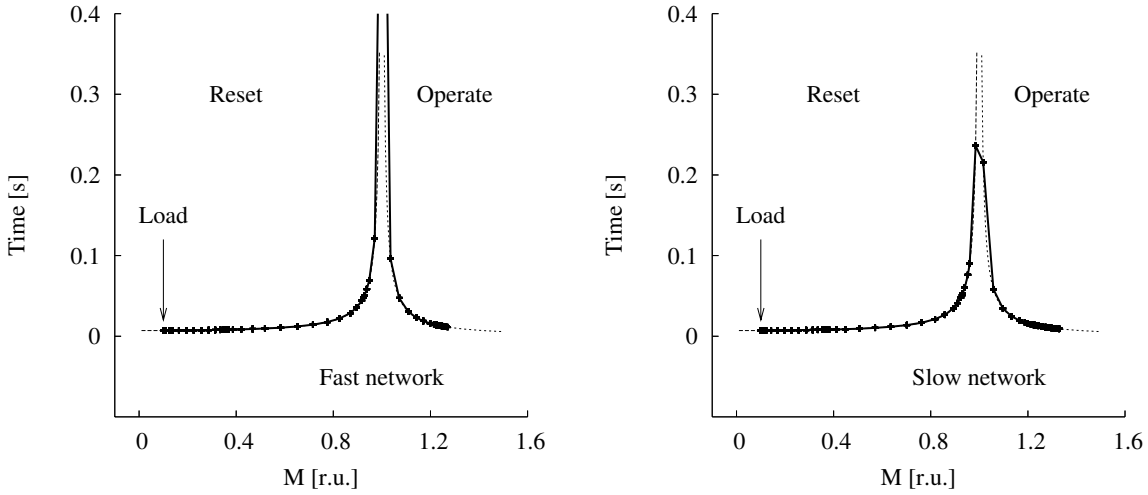

Figure 6.16: Overcurrent protection performance of the FF algorithm with 32 samples per cycle during a line-to-ground fault at location F1

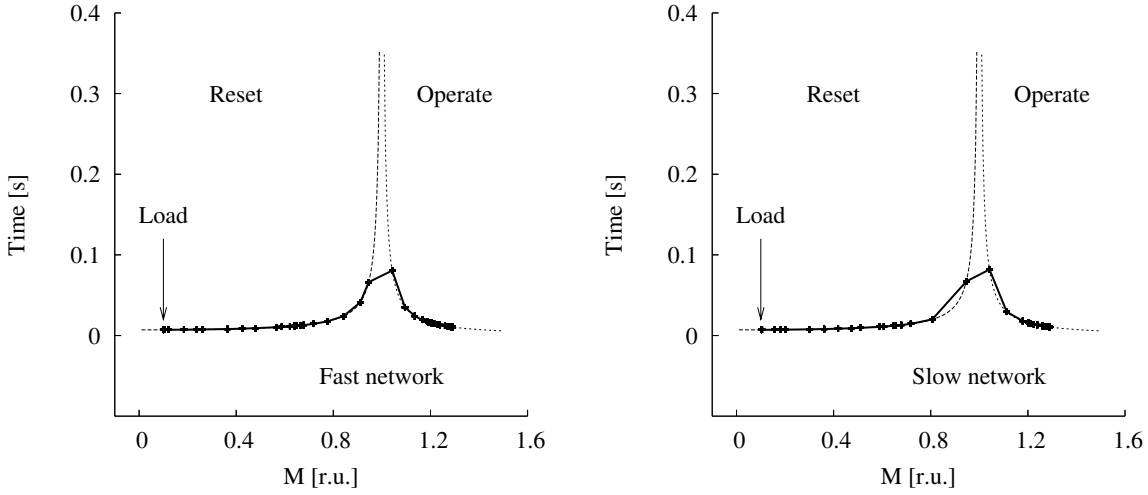

Figure 6.17: Overcurrent protection performance of the GPS-LSE algorithm with 32 samples per cycle during a line-to-ground fault at location F1

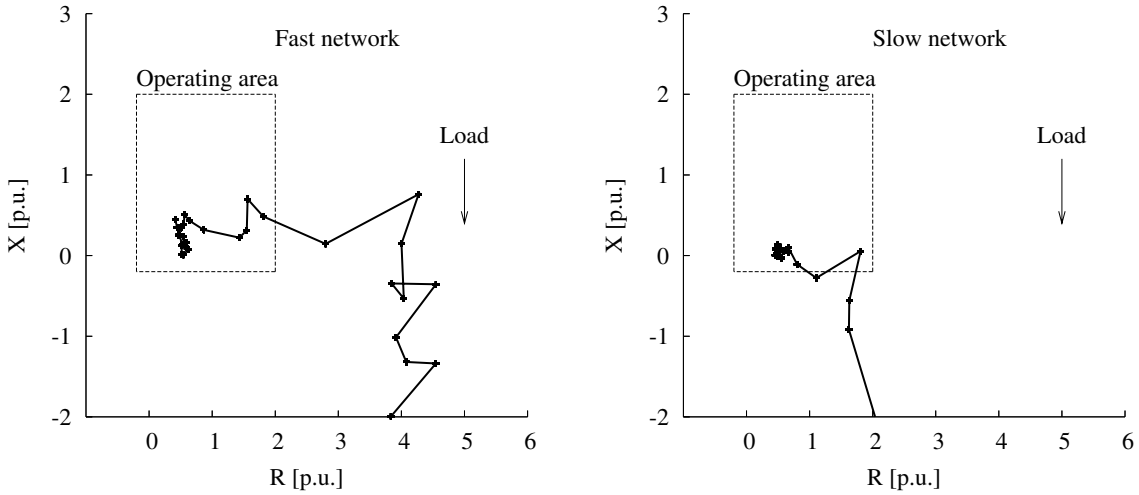

Figure 6.18: Impedance protection performance of the FF algorithm with 8 samples per cycle during a line-to-ground fault at location F1

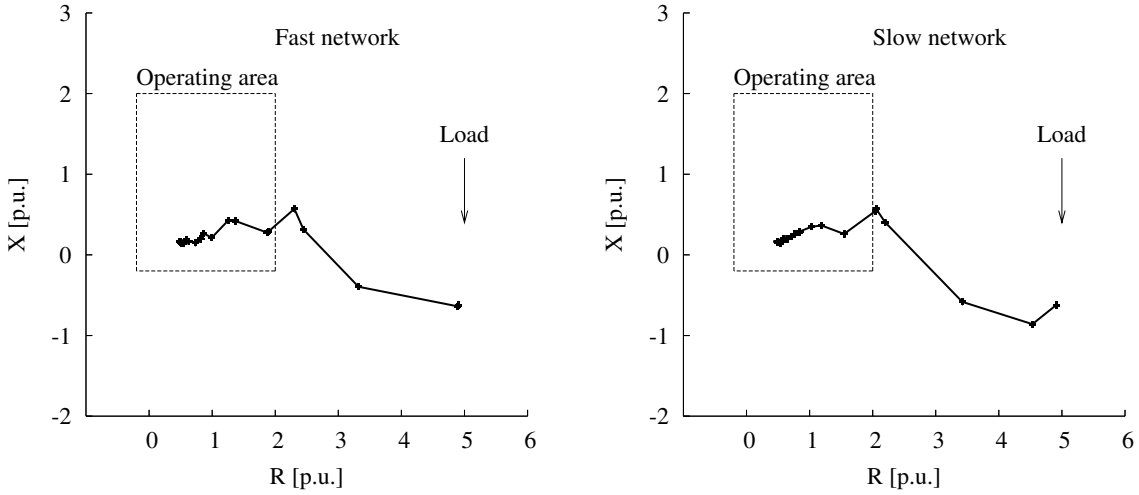

Figure 6.19: Impedance protection performance of the GPS-LSE algorithm with 8 samples per cycle during a line-to-ground fault at location F1

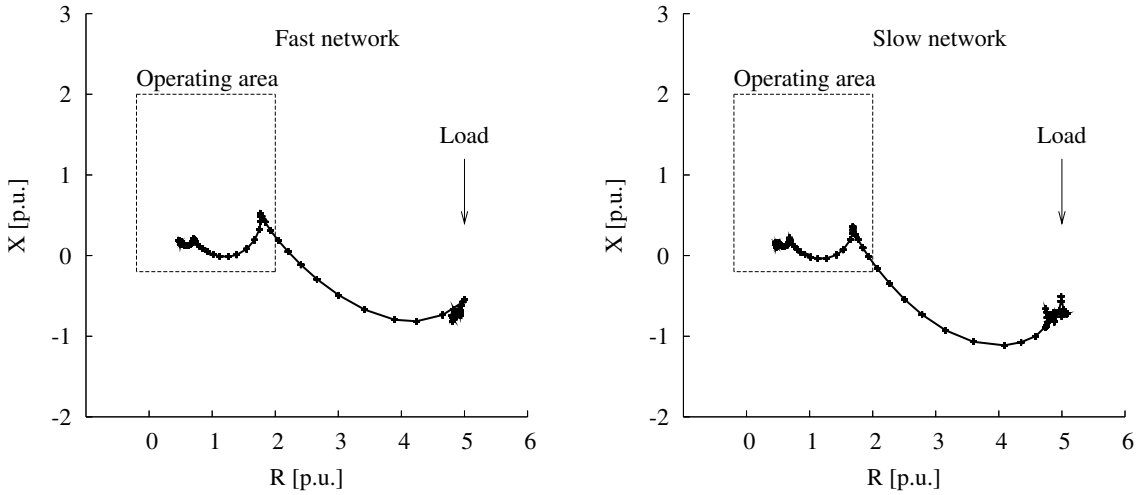

Figure 6.20: Impedance protection performance of the FF algorithm with 32 samples per cycle during a line-to-ground fault at location F1

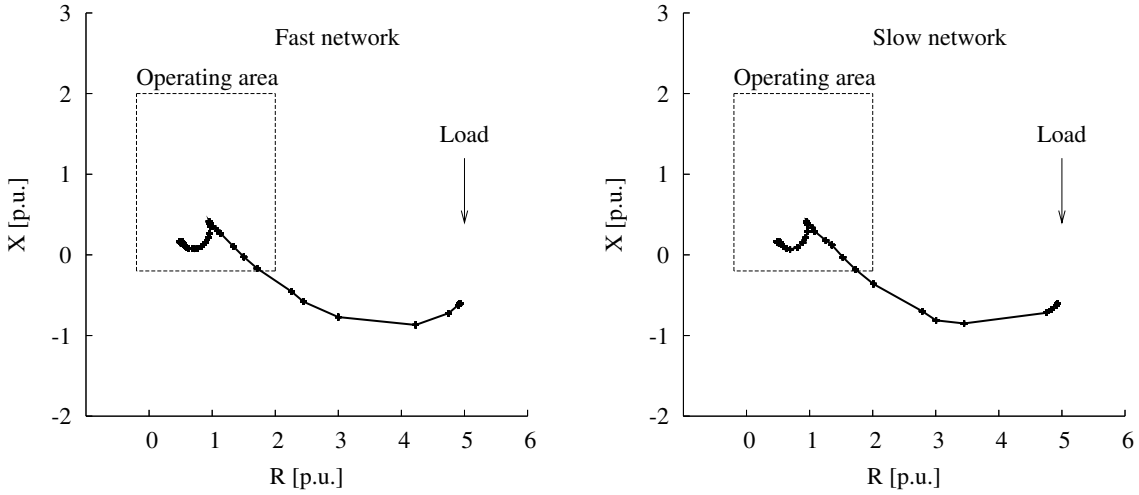

Figure 6.21: Impedance protection performance of the GPS-LSE algorithm with 32 samples per cycle during a line-to-ground fault at location F1

Table 6.4: Test results for radial line protection

Algorithm	Fault type	Network	Samples	Pickup time 51	Trip time 21	Voltage s1	Voltage s2	Current s1	Current s2
GPS-LSE	LG	Slow	8	0.0292	0.0146	0.0206	0.0287	0.3626	0.4059
		Fast	8	0.0333	0.0125	0.1053	0.1208	0.1483	0.1442
		Slow	32	0.0151	0.0063	0.0133	0.0137	0.0193	0.0193
		Fast	32	0.0151	0.0063	0.0061	0.0146	0.0110	0.0223
	LL	Slow	8	0.0292	0.0083	0.0164	0.0252	0.2565	0.3135
		Fast	8	0.0292	0.0083	0.0482	0.0665	0.1258	0.1212
		Slow	32	0.0135	0.0042	0.0137	0.0134	0.0207	0.0199
		Fast	32	0.0130	0.0042	0.0053	0.0175	0.0098	0.0231
	LLL	Slow	8	0.0250	0.0083	0.0183	0.0264	0.3358	0.4068
		Fast	8	0.0292	0.0083	0.0697	0.0861	0.1589	0.1552
		Slow	32	0.0135	0.0052	0.0141	0.0144	0.0192	0.0193
		Fast	32	0.0135	0.0052	0.0063	0.0150	0.0105	0.0210
FF	LG	Slow	8	0.0271	0.0083	8.0943	10.8890	7.4783	12.9065
		Fast	8	0.0250	0.0083	3.8311	8.6395	4.1814	16.3744
		Slow	32	0.0234	0.0089	1.0481	3.0886	1.4826	1.4754
		Fast	32	0.0229	0.0094	0.7587	0.7366	0.7126	0.8467
	LL	Slow	8	0.0229	0.0042	5.9295	8.1847	4.8869	10.4488
		Fast	8	0.0229	0.0063	6.9228	11.3912	7.5381	17.0437
		Slow	32	0.0203	0.0057	1.8993	3.5607	0.8134	0.8100
		Fast	32	0.0203	0.0063	0.5116	0.5460	0.4232	0.4129
	LLL	Slow	8	0.0188	0.0063	8.0960	10.8641	7.4386	13.0166
		Fast	8	0.0188	0.0063	3.7204	8.5448	4.7430	18.4631
		Slow	32	0.0172	0.0068	1.0923	3.0731	1.5179	1.5071
		Fast	32	0.0172	0.0073	0.7580	0.7341	0.6500	0.7256

Based on the results shown in Figs.(6.10) to (6.21) and those listed in Table (6.4), the following conclusions can be drawn.

- Pickup times for the 51 function (overcurrent) are under the benchmark values for the 32 samples per cycle GPS-LSE algorithm for all three types of faults. The 8 samples per cycle algorithm is above the 24 ms benchmark mainly due to the fact that the number of samples required to produce stable output exceeded the length of one cycle.

- Trip times for the 21 function (distance) are all under the 16 ms benchmark,

confirming the performance of both the 32 and 8 samples per cycle algorithms.

- The values of s_1 and s_2, listed as percentages, obtained 3 cycles after fault, show that the deviations from the desired values are smaller than the 2 percent benchmark. The same stability performance has been obtained for both the voltage and current measurements.

- It is interesting to notice that the Fourier algorithm met the benchmark on the trip times for both the 51 and 21 functions, but did not meet the stability requirements. The 3-line fault results for s_2 were above 18 % for the 8 samples per cycle solution.

- Overall, the 32 samples per cycle solution outperformed the 8 samples per cycle solution. This observation is valid for both operating times and stability indices.

The Fourier algorithm had oscillated between reset and operate regions of the overcurrent curve, as seen in Fig.(6.14). The instability of the Fourier solution is further exemplified by Fig.(6.18), where the load is not correctly identified in the impedance plane. This is also shown by the large values of s_1 and s_2 for the respective tests using post fault data.

On the other hand, the results shown confirm that the GPS-LSE digital relaying algorithm is capable of processing data packets and samples transmitted over the shared communications network of the Ethernet-based process bus. The solution when applied to overcurrent and distance protective functions has been proved stable,

fast, and adaptable to the variable system conditions. The 32 samples per second option worked very well, confirming the flexibility of the proposed relaying algorithm.

The difference between the 8 and the 32 samples options was their response time. The 8 samples per cycle solution required longer time to provide stable output, while the 32 samples per cycle solution was able to reduce its data window to half cycle during good networking performance.

6.3 Transmission line and transformer faults

In case of large infeeds or short transmission lines, one of the frequently used protective solutions is the differential protection. The principle of differential protection of power equipment, lines or other devices, is based on comparing some characteristic of the current that enters the protected zone with the same characteristic of the current that is exiting the monitored zone. This solution requires reliable and high speed communications between the points where current enters and leaves the protected element [117]. Standard configuration of a transmission line differential protection is shown in Fig.(6.22).

6.3.1 Percentage differential protection

The percentage differential protection compares the differential current between the incoming and outgoing currents with a restraining current [118]. The performance of the GPS-LSE algorithm operating in a percentage differential setup was tested to determine its performance in effectively protecting electrical equipment in a process-

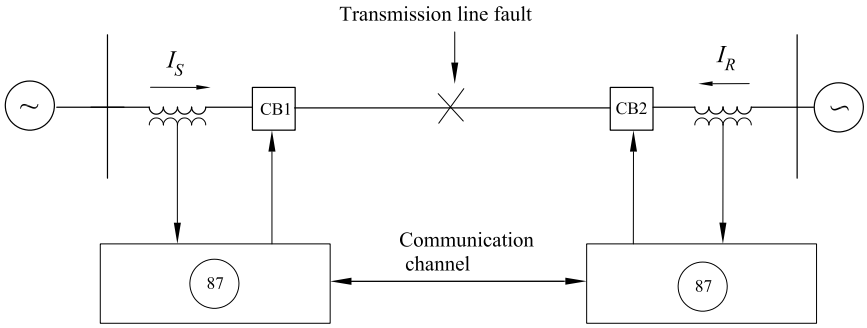

Figure 6.22: Differential protection of a transmission line

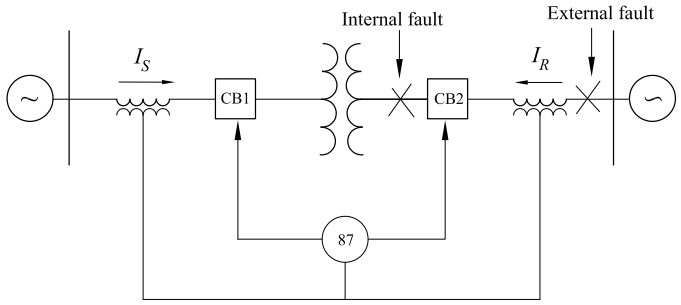

Figure 6.23: Differential protection of a transformer

bus setup.

In the tested algorithm, the operating element is the amplitude of the sum of the sending- and receiving-end currents.

$$I_{OP} = |I_S + I_R| \tag{6.10}$$

The restraining element is determined as:

$$I_{RS} = \frac{1}{2}\left(|I_S| + |I_R|\right) \tag{6.11}$$

The trip decision is reached by comparing the operating current with the restraining element. When the operating current is bigger than a predefined number, the relay will trip. The minimal pickup current is K_0, while the slope K provides margin for error caused by CT saturation during high current conditions.

$$I_{OP} \geq K_0 + KI_{RS} \tag{6.12}$$

The operating characteristic of the percentage differential protection is shown in Fig.(6.24). The performance of the GPS-LSE algorithm in a percentage differential scheme is shown as $87-D$ in the figures depicting transmission line and transformer faults.

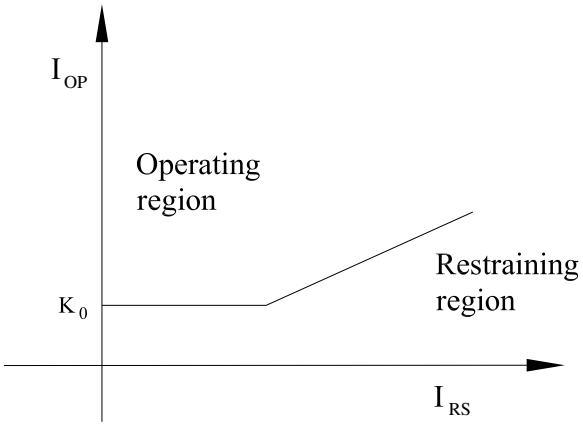

Figure 6.24: Operating characteristic of the percentage differential protection

6.3.2 Alpha-plane differential protection

The alpha-plane differential protection is based on the development of a complex-plane representation of the ratio between the sending-end current phasor I_S and the receiving-end current phasor I_R.

$$\frac{I_S}{I_R} = a + jb = re^{j\theta} \tag{6.13}$$

For normal operating conditions, if the line charging current is neglected, the receiving- and sending-end currents are equal, and out of phase by 180 degrees.

$$\frac{I_S}{I_R} = 1\angle 180 = -1 \tag{6.14}$$

When shown in the alpha-plane, under normal conditions, and for through faults, the sending- and receiving-end currents ratio is located at $a = -1$. For faults internal to the protected area, the sending- and receiving-end currents phasors are dependent on the location of the fault on the line and on the system impedance behind each end of the protected zone. The complex number representing the currents ratio during

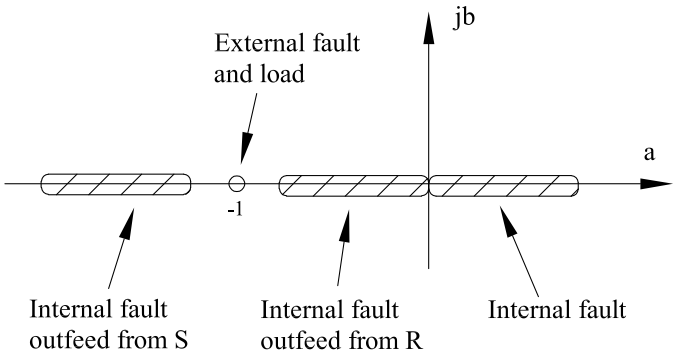

Figure 6.25: Operating characteristic of the alpha-plane differential protection

fault moves from the $a = -1$ position. An algorithm that calculates the ratio of the two currents can detect internal fault conditions by monitoring the ratio's complex number representation in the alpha-plane versus geometrical shapes that take into account system conditions [118]. The shape in Fig.(6.26) accounts for infeeds, outfeeds and different system impedances during internal fault condition on the protected zone. The shape in Fig.(6.27) provides tolerance to excessive outfeeds, while the communication channel asymmetry can be compensated by an operating characteristic similar to the one shown in Fig.(6.28).

The open-system solution using the process-bus communications providing differential protection is shown in Figs.(6.29) and (6.30). It can be seen that other protective functions can be implemented using the same hardware. The multi-function protective device shown provides differential, distance and overcurrent elements.

The test system used for evaluating the transmission line differential element is shown in Fig.(6.31), while the transformer differential element was tested using the system in Fig.(6.32).

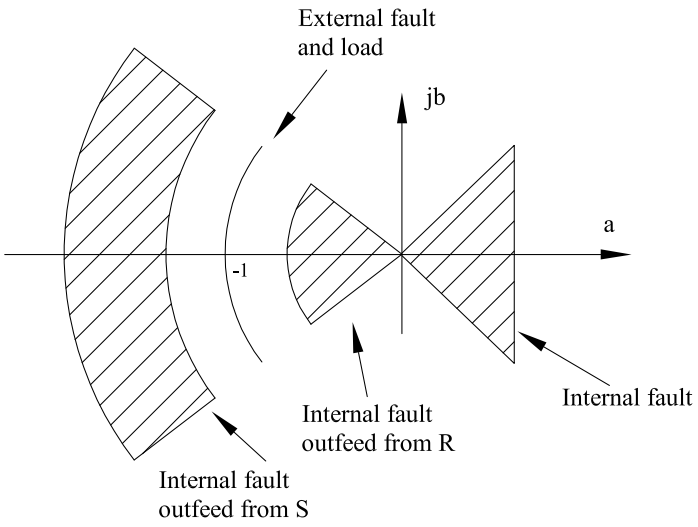

Figure 6.26: Practical application for alpha-plane differential protection

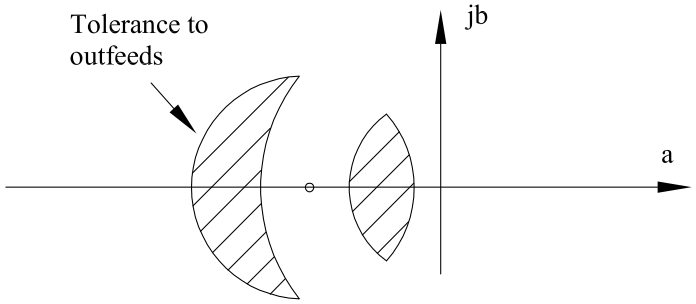

Figure 6.27: Settings with tolerance to outfeeds for alpha-plane differential protection

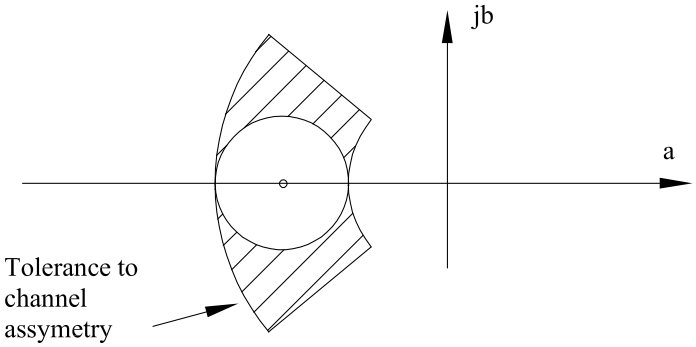

Figure 6.28: Settings with tolerance to channel asymmetry for alpha-plane differential protection

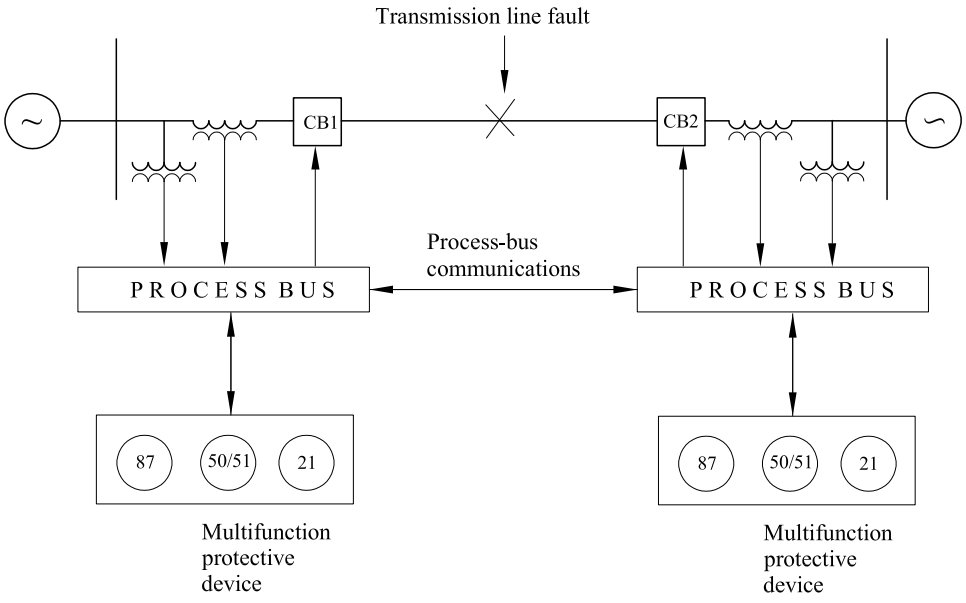

Figure 6.29: Process-bus differential protection of a transmission line

Line-to-ground fault results for the transmission line tests are shown in Figs.(6.33) to (6.44). Line-to-ground fault results for the transformer tests are shown in Figs.(6.45) to (6.56).

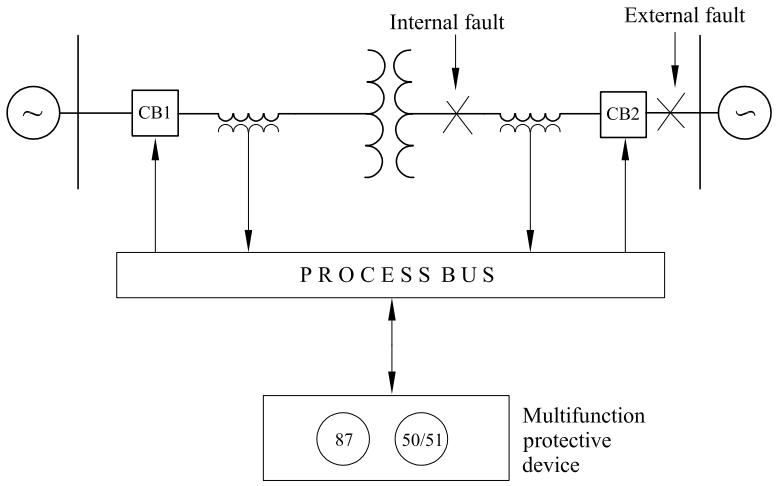

Figure 6.30: Process-bus differential protection of a transformer

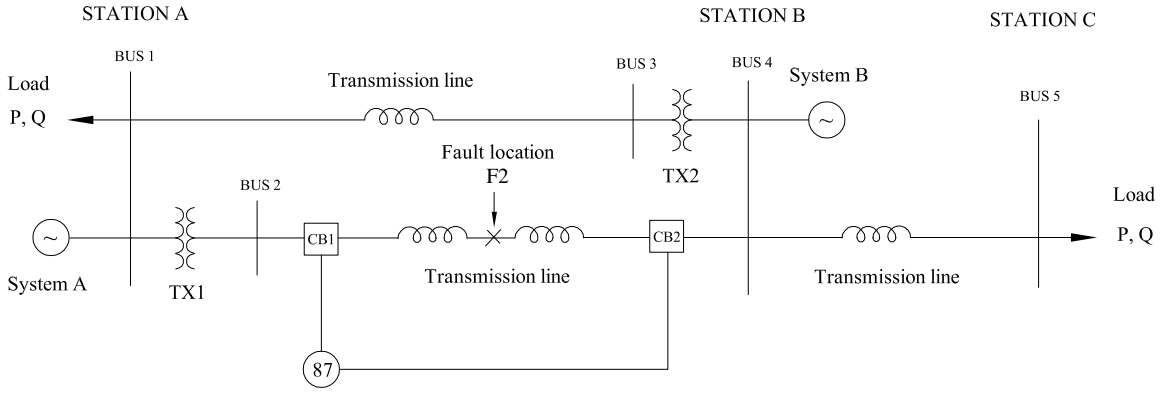

Figure 6.31: Test system for transmission line faults

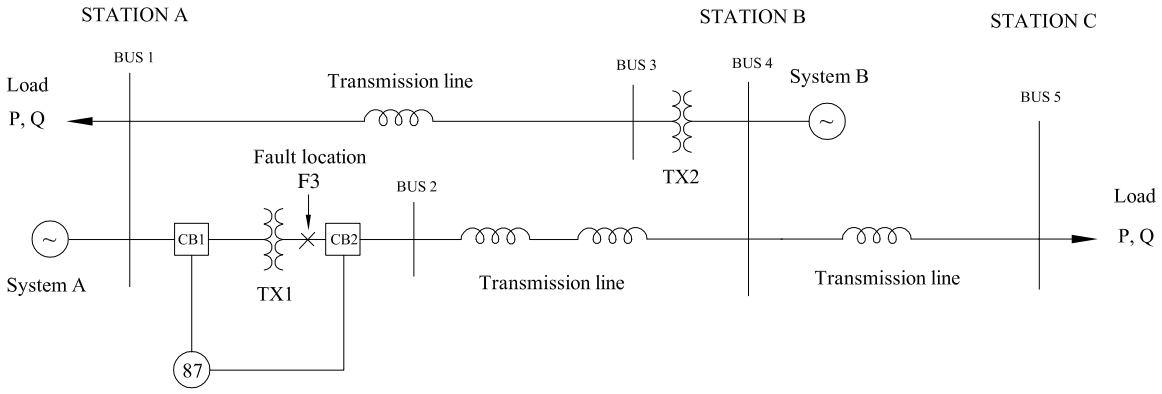

Figure 6.32: Test system for transformer faults

The list of figures showing transmission line and transformer test results are given in Tables (6.5) and (6.6). Numerical results obtained for the transmission line and transformer tests are listed in Tables (6.7) and (6.8), respectively.

Table 6.5: List of figures showing transmission line test results

Type of fault	Function	Algorithm	Samples	Figure
LG	87-D	FF	8	(6.37)
		GPS-LSE	8	(6.38)
		FF	32	(6.39)
		GPS-LSE	32	(6.40)
	87-A	FF	8	(6.41)
		GPS-LSE	8	(6.42)
		FF	32	(6.43)
		GPS-LSE	32	(6.44)
LL	87-D	FF	8	(B.29)
		GPS-LSE	8	(B.30)
		FF	32	(B.31)
		GPS-LSE	32	(B.32)
	87-A	FF	8	(B.33)
		GPS-LSE	8	(B.34)
		FF	32	(B.35)
		GPS-LSE	32	(B.36)
LLL	87-D	FF	8	(B.41)
		GPS-LSE	8	(B.42)
		FF	32	(B.43)
		GPS-LSE	32	(B.44)
	87-A	FF	8	(B.45)
		GPS-LSE	8	(B.46)
		FF	32	(B.47)
		GPS-LSE	32	(B.48)

Table 6.6: List of figures showing transformer test results

Type of fault	Function	Algorithm	Samples	Figure
LG	87-D	FF	8	(6.49)
		GPS-LSE	8	(6.50)
		FF	32	(6.51)
		GPS-LSE	32	(6.52)
	87-A	FF	8	(6.53)
		GPS-LSE	8	(6.54)
		FF	32	(6.55)
		GPS-LSE	32	(6.56)
LL	87-D	FF	8	(B.53)
		GPS-LSE	8	(B.54)
		FF	32	(B.55)
		GPS-LSE	32	(B.56)
	87-A	FF	8	(B.57)
		GPS-LSE	8	(B.58)
		FF	32	(B.59)
		GPS-LSE	32	(B.60)
LLL	87-D	FF	8	(B.65)
		GPS-LSE	8	(B.66)
		FF	32	(B.67)
		GPS-LSE	32	(B.68)
	87-A	FF	8	(B.69)
		GPS-LSE	8	(B.70)
		FF	32	(B.71)
		GPS-LSE	32	(B.72)

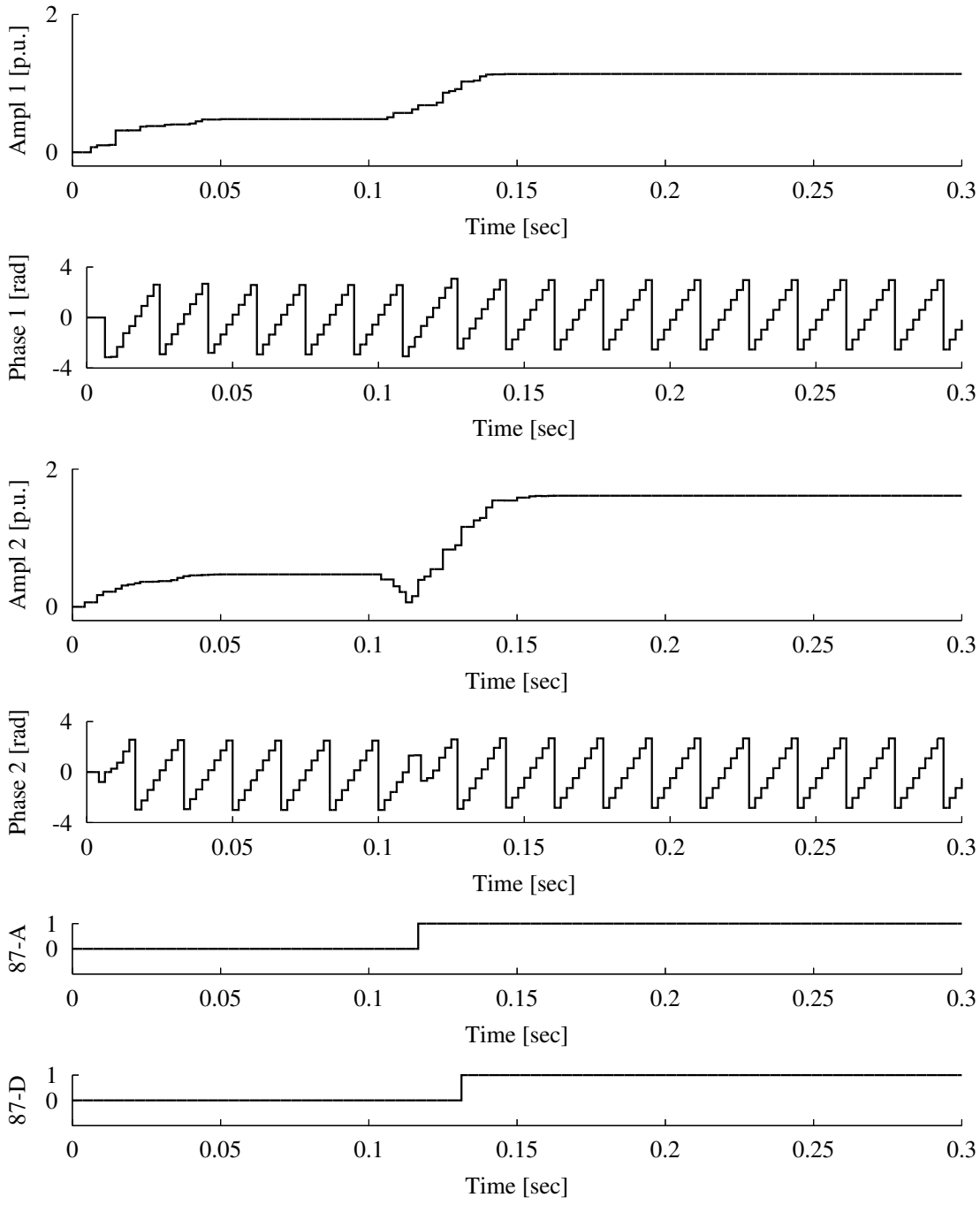

Figure 6.33: GPS-LSE algorithm performance with 8 samples per cycle over slow network during a line-to-ground fault at location F2

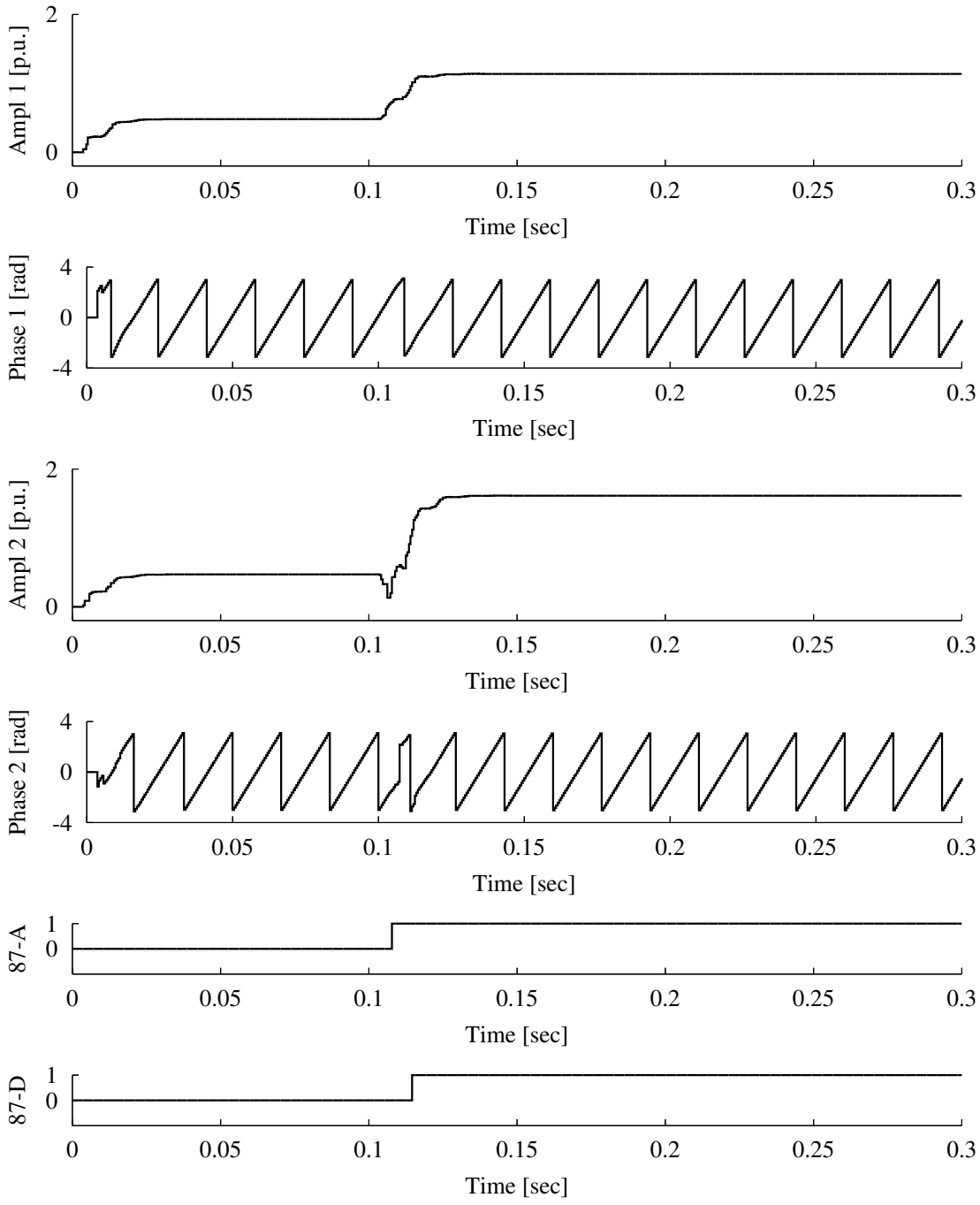

Figure 6.34: GPS-LSE algorithm performance with 32 samples per cycle over slow network during a line-to-ground fault at location F2

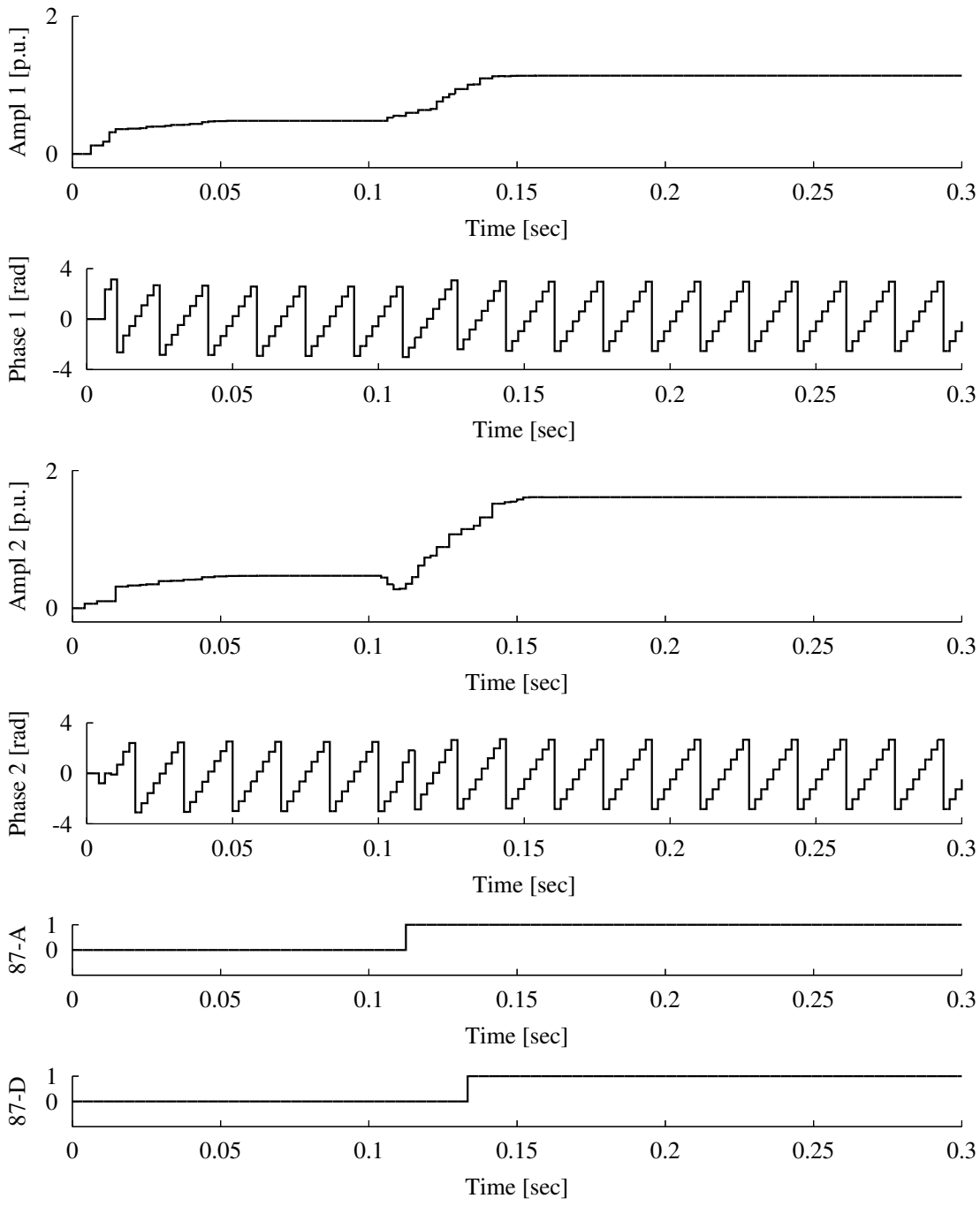

Figure 6.35: GPS-LSE algorithm performance with 8 samples per cycle over fast network during a line-to-ground fault at location F2

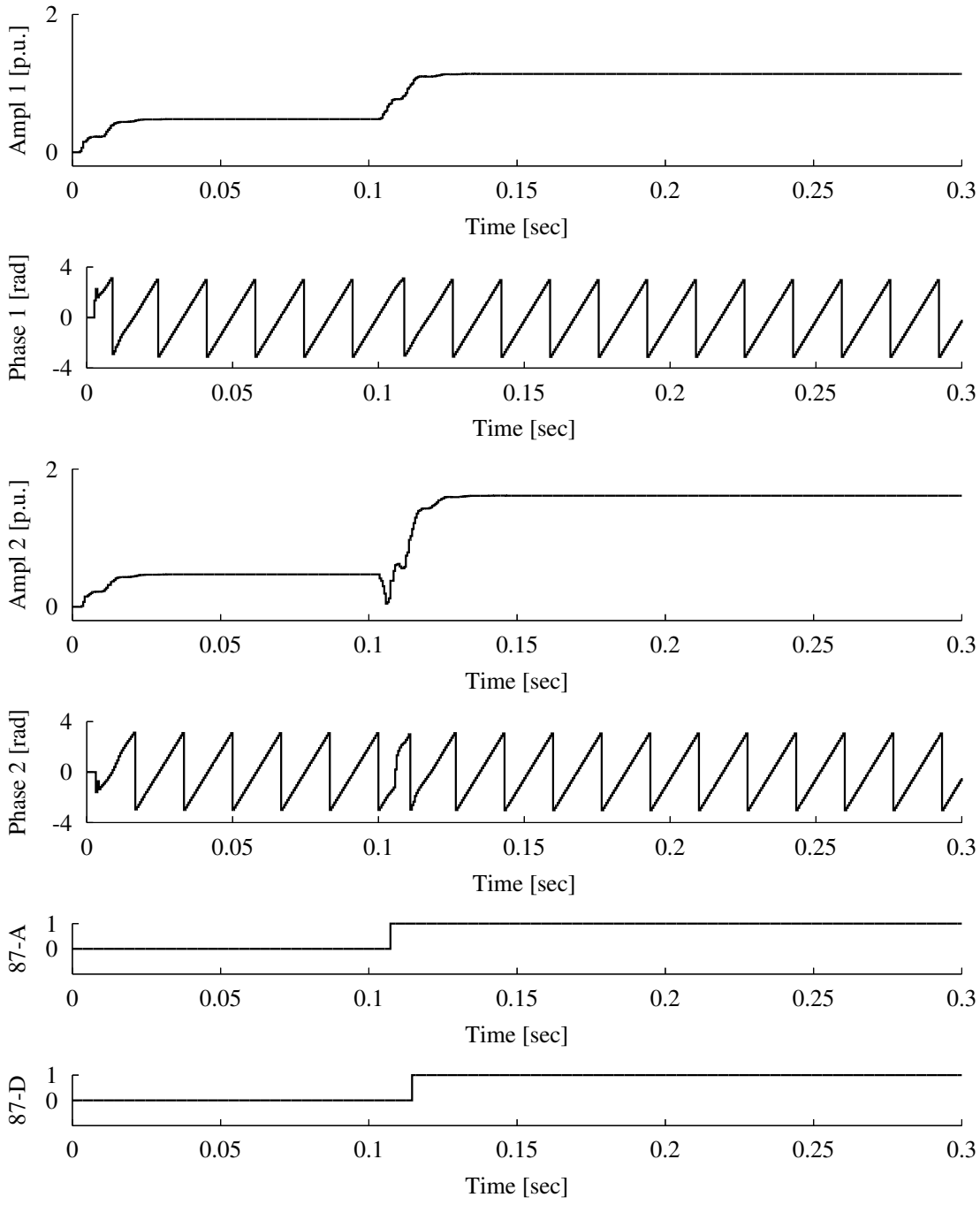

Figure 6.36: GPS-LSE algorithm performance with 32 samples per cycle over fast network during a line-to-ground fault at location F2

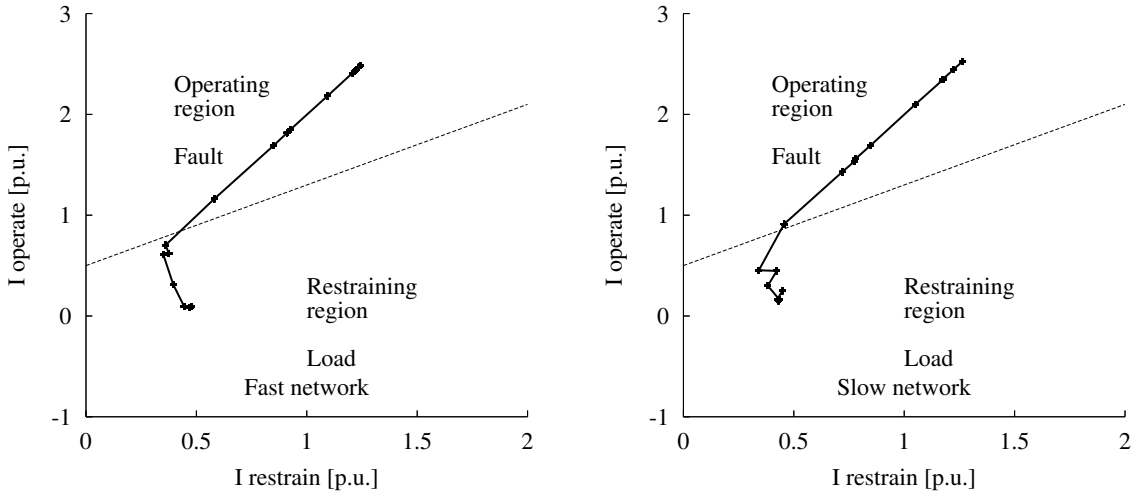

Figure 6.37: Percentage differential protection performance of the FF algorithm with 8 samples per cycle during a line-to-ground fault at location F2

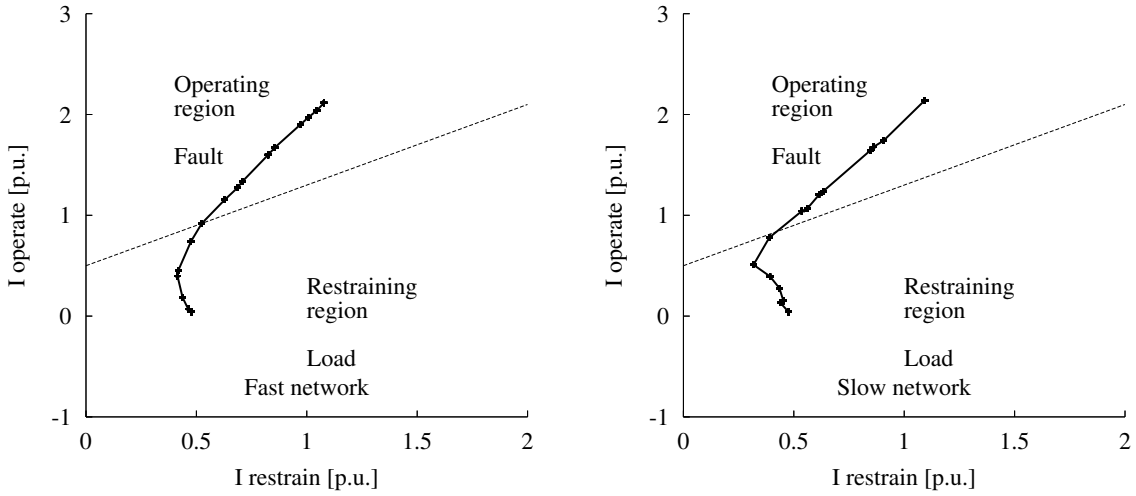

Figure 6.38: Percentage differential protection performance of the GPS-LSE algorithm with 8 samples per cycle during a line-to-ground fault at location F2

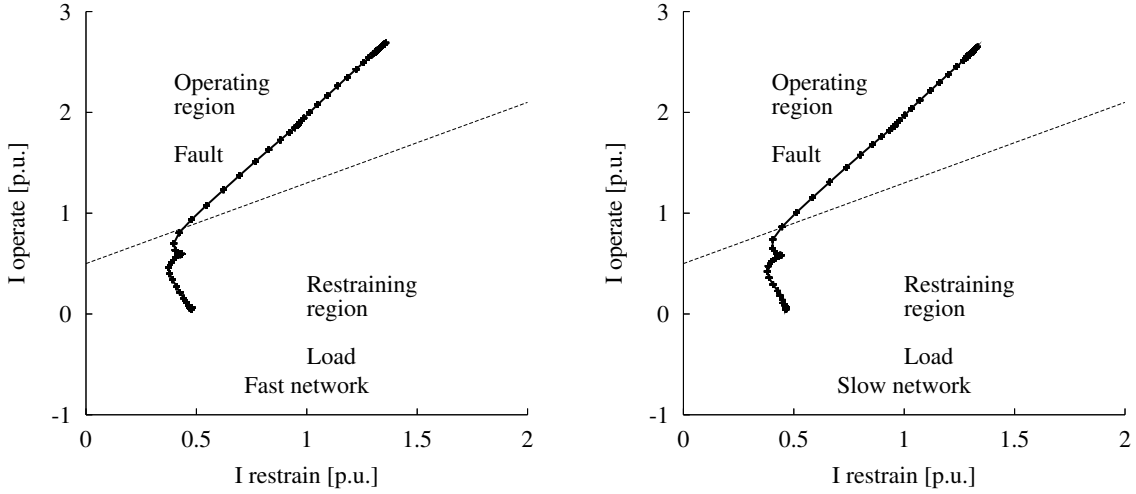

Figure 6.39: Percentage differential protection performance of the FF algorithm with 32 samples per cycle during a line-to-ground fault at location F2

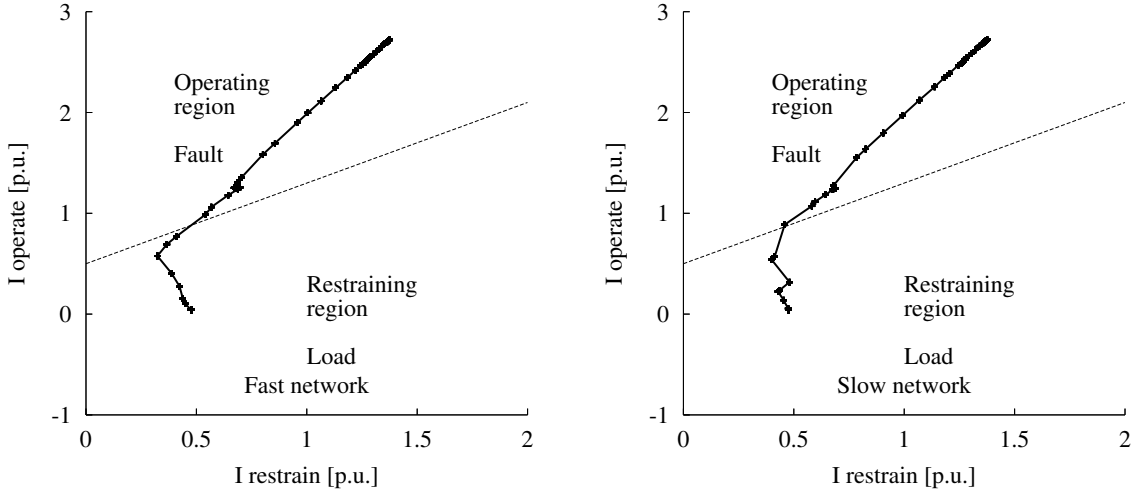

Figure 6.40: Percentage differential protection performance of the GPS-LSE algorithm with 32 samples per cycle during a line-to-ground fault at location F2

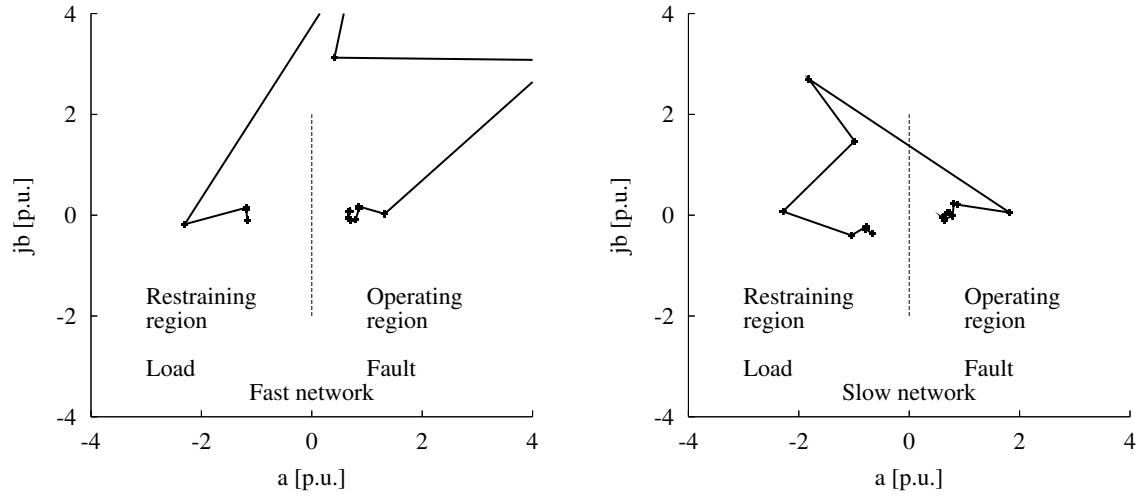

Figure 6.41: Alpha-plane differential protection performance of the FF algorithm with 8 samples per cycle during a line-to-ground fault at location F2

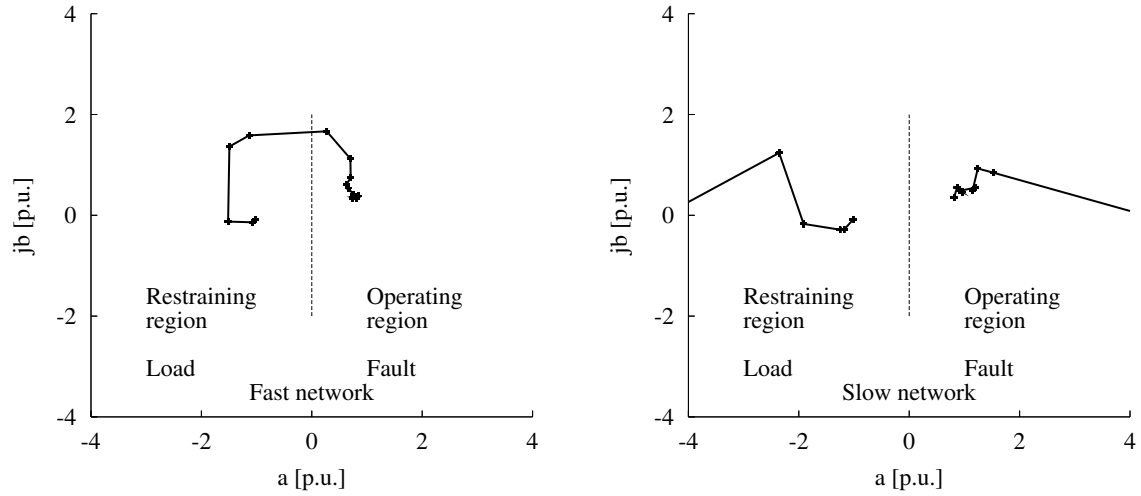

Figure 6.42: Alpha-plane differential protection performance of the GPS-LSE algorithm with 8 samples per cycle during a line-to-ground fault at location F2

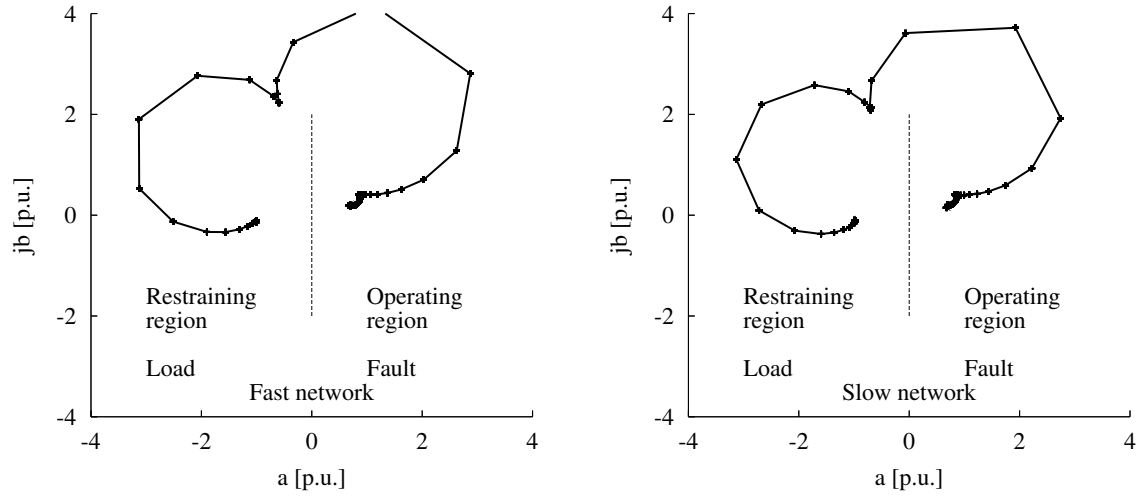

Figure 6.43: Alpha-plane differential protection performance of the FF algorithm with 32 samples per cycle during a line-to-ground fault at location F2

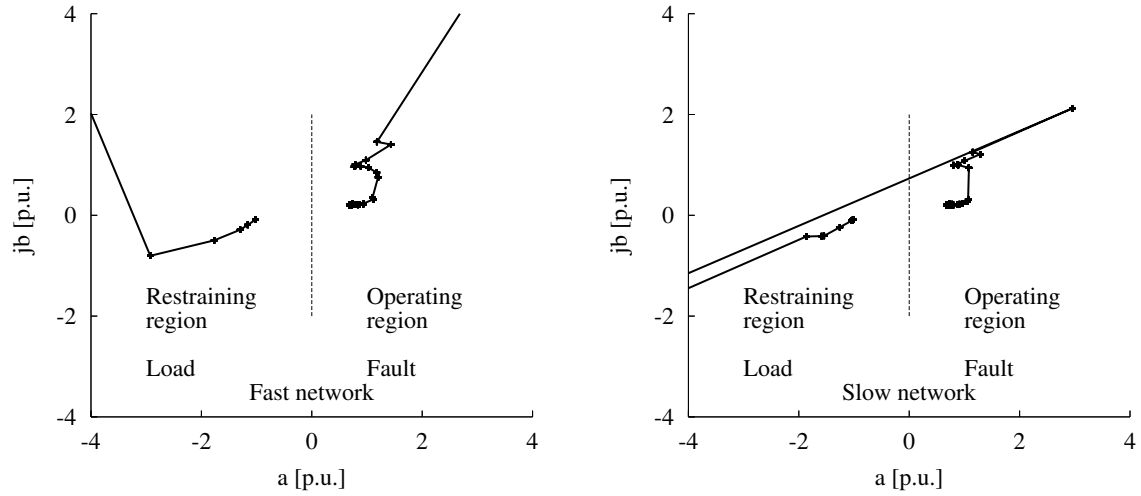

Figure 6.44: Alpha-plane differential protection performance of the GPS-LSE algorithm with 32 samples per cycle during a line-to-ground fault at location F2

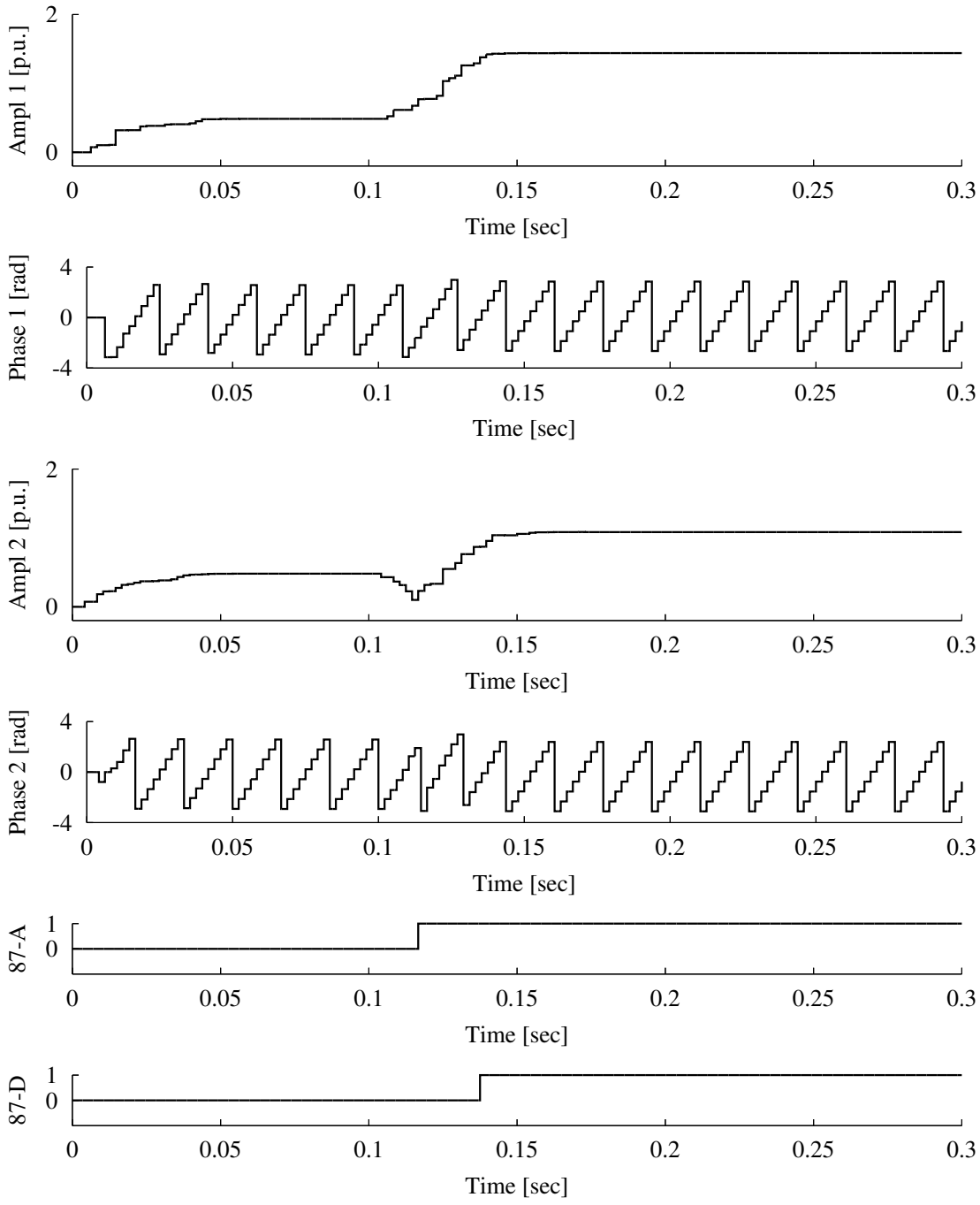

Figure 6.45: GPS-LSE algorithm performance with 8 samples per cycle over slow network during a line-to-ground fault at location F3

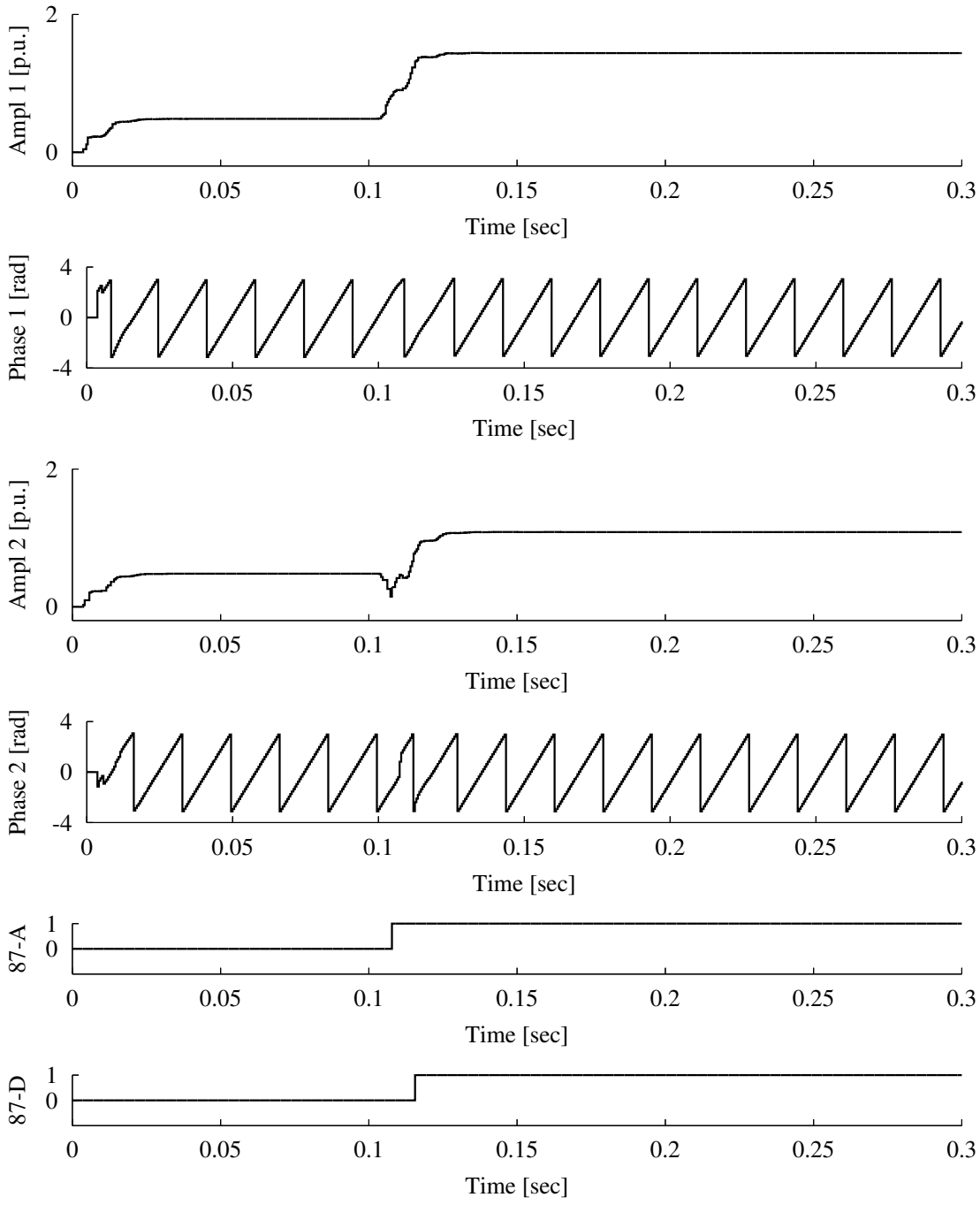

Figure 6.46: GPS-LSE algorithm performance with 32 samples per cycle over slow network during a line-to-ground fault at location F3

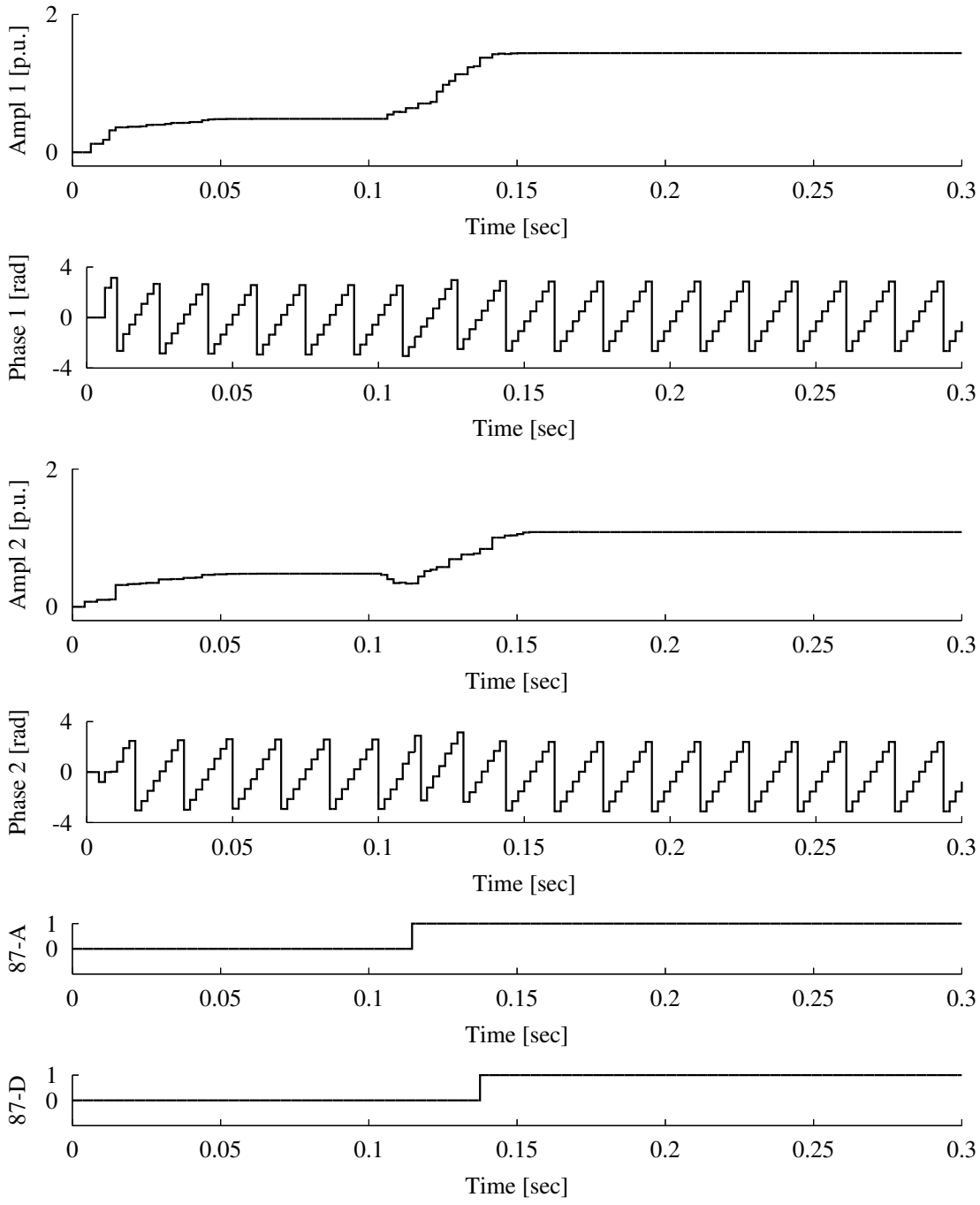

Figure 6.47: GPS-LSE algorithm performance with 8 samples per cycle over fast network during a line-to-ground fault at location F3

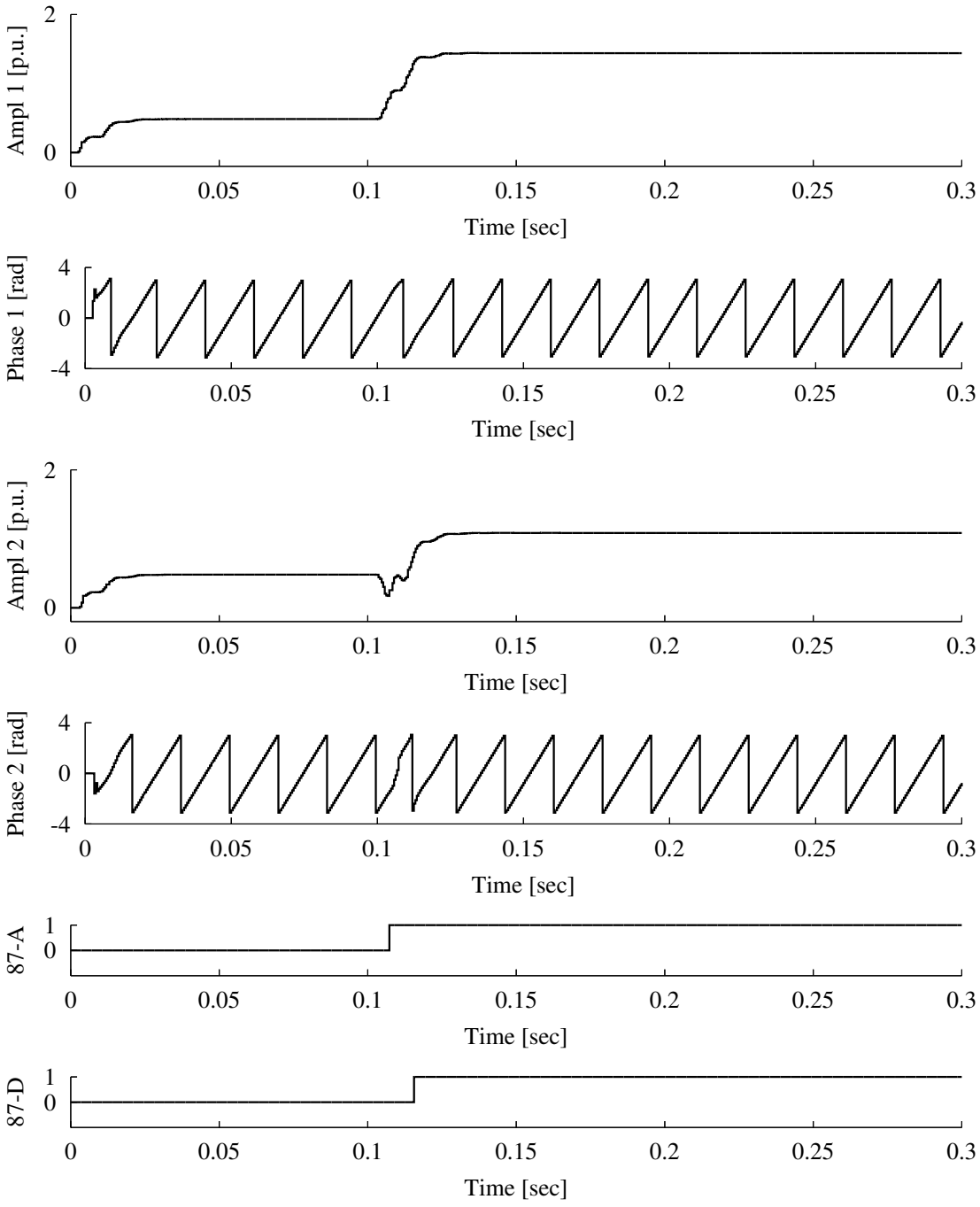

Figure 6.48: GPS-LSE algorithm performance with 32 samples per cycle over fast network during a line-to-ground fault at location F3

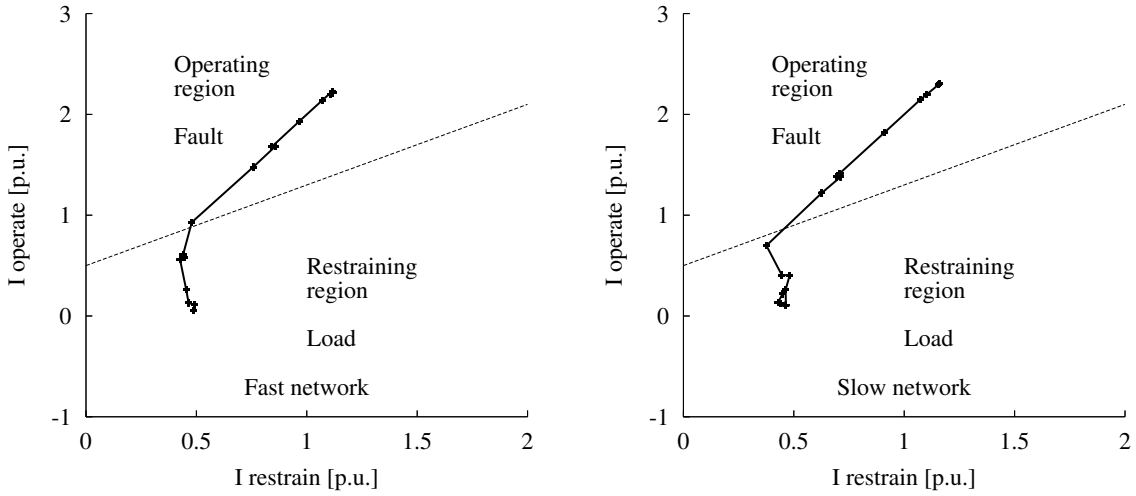

Figure 6.49: Percentage differential protection performance of the FF algorithm with 8 samples per cycle during a line-to-ground fault at location F3

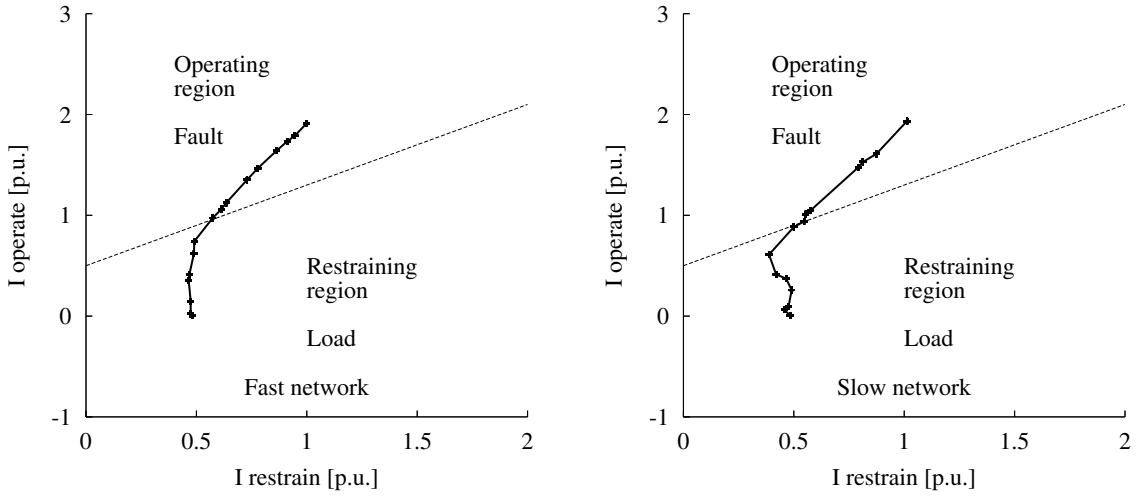

Figure 6.50: Percentage differential protection performance of the GPS-LSE algorithm with 8 samples per cycle during a line-to-ground fault at location F3

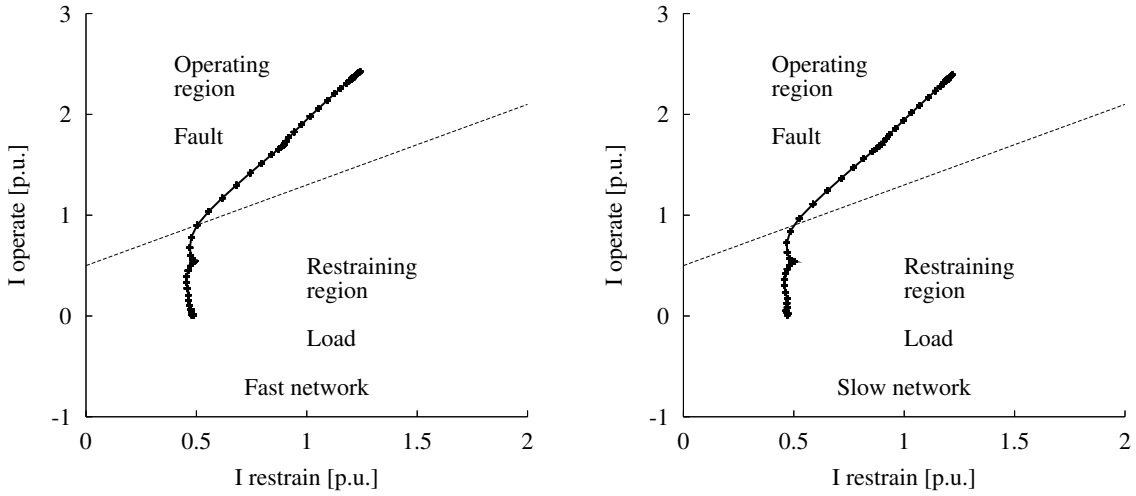

Figure 6.51: Percentage differential protection performance of the FF algorithm with 32 samples per cycle during a line-to-ground fault at location F3

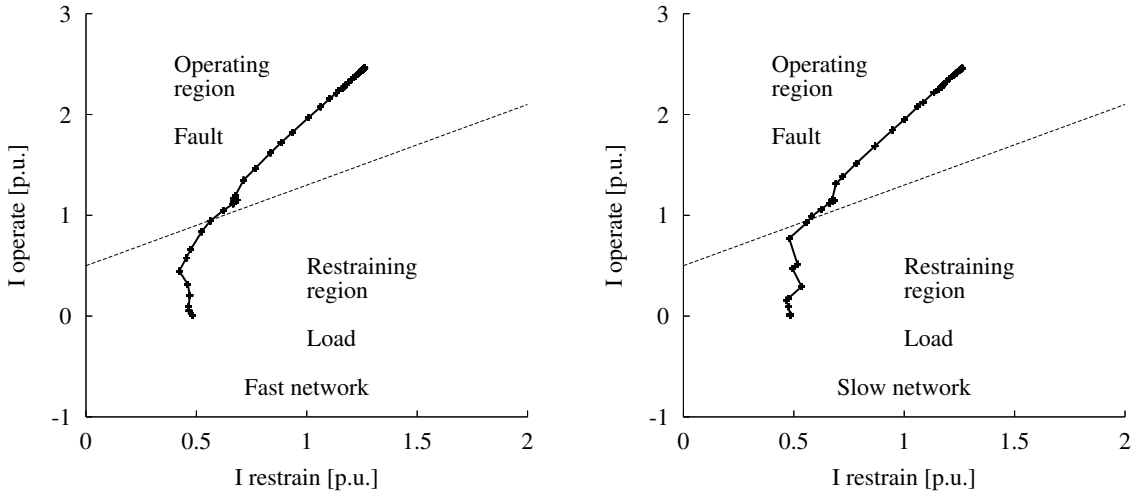

Figure 6.52: Percentage differential protection performance of the GPS-LSE algorithm with 32 samples per cycle during a line-to-ground fault at location F3

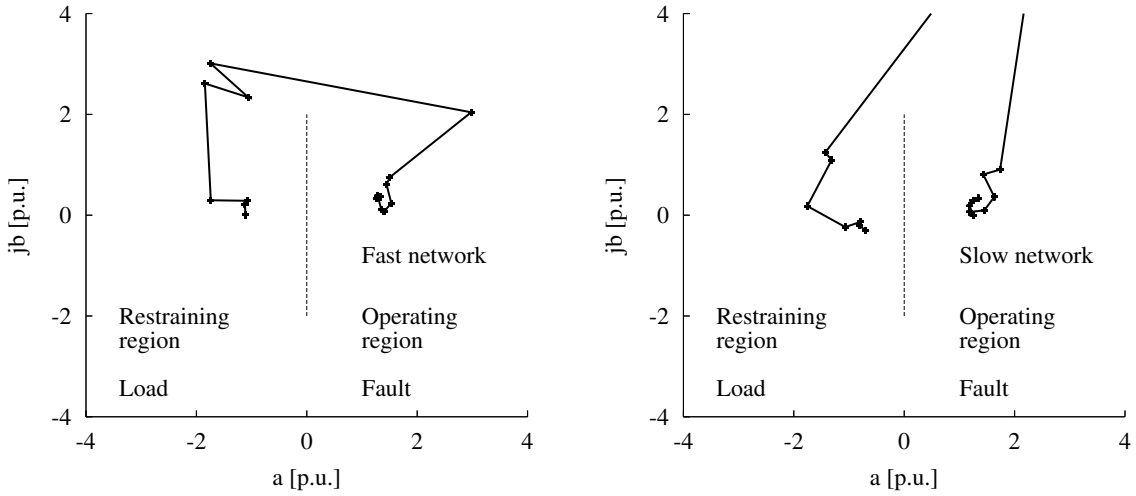

Figure 6.53: Alpha-plane differential protection performance of the FF algorithm with 8 samples per cycle during a line-to-ground fault at location F3

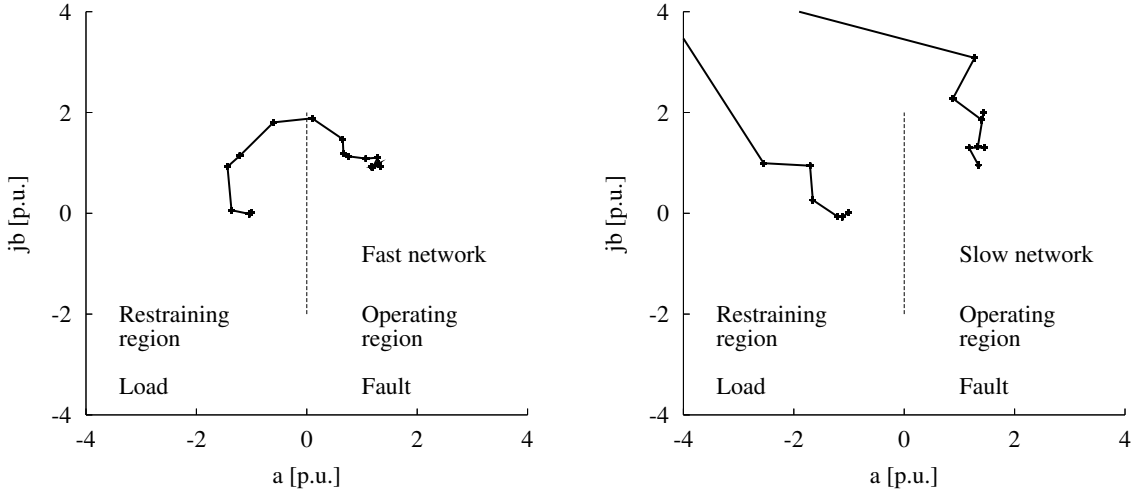

Figure 6.54: Alpha-plane differential protection performance of the GPS-LSE algorithm with 8 samples per cycle during a line-to-ground fault at location F3

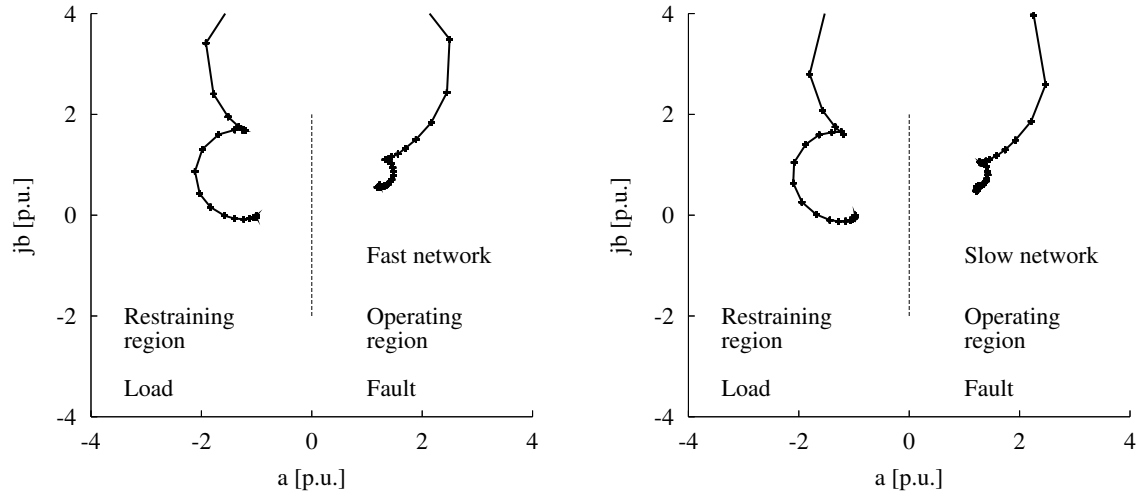

Figure 6.55: Alpha-plane differential protection performance of the FF algorithm with 32 samples per cycle during a line-to-ground fault at location F3

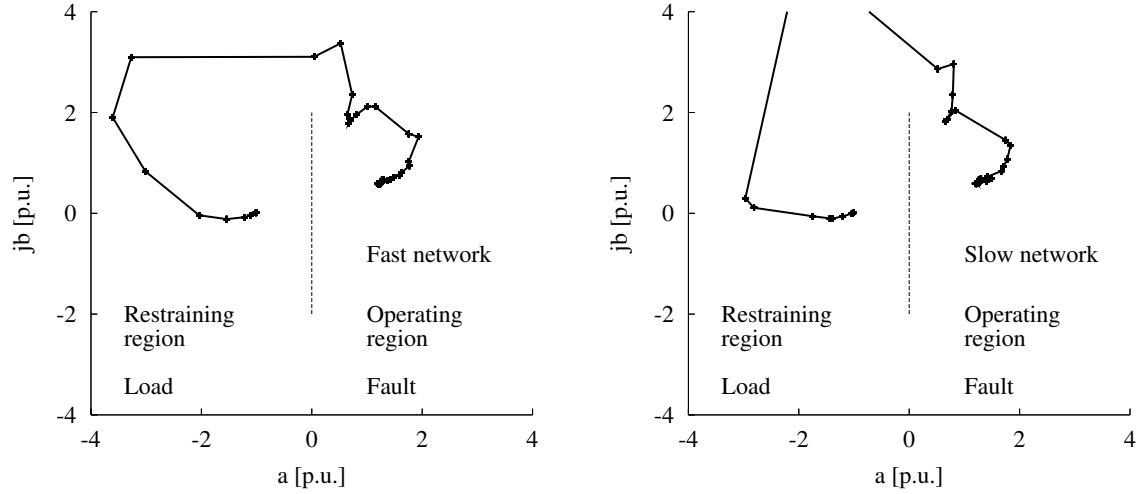

Figure 6.56: Alpha-plane differential protection performance of the GPS-LSE algorithm with 32 samples per cycle during a line-to-ground fault at location F3

Table 6.7: Test results for transmission line protection

Algorithm	Fault type	Network	Samples	Trip time 87-D	Trip time 87-A	Sending s1	Sending s2	Receiving s1	Receiving s2
GPS-LSE	LG	Slow	8	0.03125	0.01667	0.07248	0.07170	1.22497	1.24942
		Fast	8	0.03333	0.01250	0.07493	0.07210	1.15639	1.16122
		Slow	32	0.01458	0.00781	0.01270	0.01322	0.00408	0.00534
		Fast	32	0.01458	0.00729	0.01286	0.01300	0.00379	0.00510
	LL	Slow	8	0.03125	0.01250	0.13507	0.14230	0.81869	0.83317
		Fast	8	0.02708	0.01667	0.09729	0.09645	0.64928	0.65420
		Slow	32	0.01250	0.00729	0.01012	0.01018	0.00605	0.00697
		Fast	32	0.01250	0.00729	0.01016	0.01015	0.00550	0.00654
	LLL	Slow	8	0.03125	0.01667	0.11967	0.12015	1.23908	1.26430
		Fast	8	0.02708	0.01250	0.10816	0.10581	1.10770	1.12598
		Slow	32	0.01354	0.00781	0.01346	0.01398	0.00556	0.00593
		Fast	32	0.01302	0.00729	0.01365	0.01374	0.00560	0.00597
FF	LG	Slow	8	0.02500	0.01458	5.05296	10.33137	3.03304	7.09718
		Fast	8	0.02292	0.01458	6.23458	19.55629	0.54578	5.94448
		Slow	32	0.02240	0.01406	2.65059	2.45151	2.16298	2.46983
		Fast	32	0.02240	0.01406	0.50195	0.50185	0.51405	0.51196
	LL	Slow	8	0.02292	0.01458	6.88545	10.50499	8.39087	10.17900
		Fast	8	0.02292	0.01250	7.55474	14.72280	6.76979	11.26435
		Slow	32	0.02135	0.01302	1.24331	1.43506	0.80863	1.78906
		Fast	32	0.02083	0.01250	0.56197	0.54567	0.39017	0.39030
	LLL	Slow	8	0.02500	0.01458	5.22254	10.40758	3.62388	7.47541
		Fast	8	0.01875	0.01458	6.41971	19.51424	2.74383	7.74143
		Slow	32	0.01771	0.01458	2.55793	2.38607	2.18485	2.63894
		Fast	32	0.01719	0.01406	0.47858	0.47729	0.51932	0.46722

Based on the results shown in Tables (6.7) and (6.8), the following conclusions can be drawn.

- Both the 8 and 32 samples per second options confirmed the flexibility of the proposed relaying algorithm. The 8 samples per cycle algorithms required some additional time to reach tripping outputs, since the minimum number of samples needed was equal to the target length of the algorithm. The response time was significantly improved when the 32 samples per cycle algorithm was able to

Table 6.8: Test results for transformer protection

Algorithm	Fault type	Network	Samples	Trip time 87-D	Trip time 87-A	Sending s1	Sending s2	Receiving s1	Receiving s2
GPS-LSE	LG	Slow	8	0.03750	0.01667	0.07921	0.07503	1.36899	1.40572
		Fast	8	0.03750	0.01667	0.07988	0.07631	1.29654	1.32997
		Slow	32	0.01563	0.00781	0.01132	0.01204	0.00563	0.00638
		Fast	32	0.01563	0.00781	0.01144	0.01177	0.00524	0.00604
	LL	Slow	8	0.03125	0.02083	0.11869	0.11822	1.06686	1.11758
		Fast	8	0.02917	0.02083	0.08140	0.07883	0.92093	0.96428
		Slow	32	0.01354	0.00729	0.00987	0.01011	0.01169	0.01181
		Fast	32	0.01302	0.00729	0.00997	0.01022	0.01162	0.01161
	LLL	Slow	8	0.03125	0.01667	0.13430	0.13527	1.63508	1.68164
		Fast	8	0.02708	0.01667	0.12064	0.11868	1.47270	1.51193
		Slow	32	0.01354	0.00781	0.01060	0.01099	0.01522	0.01466
		Fast	32	0.01302	0.00781	0.01054	0.01090	0.01500	0.01493
FF	LG	Slow	8	0.02708	0.01667	4.35334	9.94609	4.58441	7.57998
		Fast	8	0.02500	0.01458	5.37075	19.24371	2.79112	4.65136
		Slow	32	0.02448	0.01458	2.76842	2.66786	1.63467	1.76174
		Fast	32	0.02396	0.01458	0.61884	0.63528	0.52058	0.61622
	LL	Slow	8	0.02500	0.01458	6.86254	9.24683	4.93682	8.20421
		Fast	8	0.02292	0.01458	6.52119	8.45154	4.38071	9.12919
		Slow	32	0.02135	0.01406	1.26539	1.85960	1.96936	2.57356
		Fast	32	0.02135	0.01354	0.82784	0.82112	0.51223	0.43899
	LLL	Slow	8	0.02500	0.01667	5.28234	10.43272	3.03575	7.16749
		Fast	8	0.01875	0.01667	6.48584	19.48720	1.42631	6.69424
		Slow	32	0.01771	0.01563	2.52497	2.36309	2.23039	2.58805
		Fast	32	0.01771	0.01563	0.46916	0.46912	0.51550	0.49105

reduce its size for fast response. The conclusion is that the target length of the algorithm and the sampling rate should be different to reduce even further the time required for the same stable output.

- All stability benchmarks for the GPS-LSE algorithms, for both 8 and 32 samples options, have been met, proving the stability of the proposed solution.

- The Fourier algorithms were able to produce tripping times that are propor-

tional to the length of the data window, but the stability indices indicate that the source target values have not been met. Standard deviations beyond 19 percent have been experienced with the 8 samples per cycle solution during fast networking. As a result, the algorithm cannot provide reliable output using data samples transmitted over Ethernet networks.

Tests on the differential protective function confirm the previous findings. Regardless of the networking performance, the 8 and 32 samples per cycle Fourier algorithms are not able to overcome delayed or missing packets in the sample stream received from the remote end.

The results confirm that the GPS-LSE digital relaying algorithm is capable of processing sample streams with delayed and missing data packets. The solution when applied to differential protective functions has been proven stable.

The last set of tests, presented in the next section, were done on the protection of a transmission line that has a Unified Power Flow Controller, using the new digital relaying algorithm.

6.4 Transmission line with a UPFC installation

The process-bus integration is not limited to local protective applications. It provides the benefits of extensive data availability for any application that requires remote monitoring, protection and control. The Unified Power Flow Controller (UPFC), by combining a shunt and series device, is one of the most complex applications of power systems control [119–127]. It can effectively regulate both real and reactive power flow in the line. Figure (6.57) shows the two functional parts of the UPFC: the shunt and series converters.

The series device is able to inject the voltage V_S into the line, as seen in Fig.(6.58), effectively controlling the power flow. The shunt device is required to compensate for any real power drawn or injected by the series device, and also to cover losses.

Applications of the UPFC can range from load flow control to reactive power compensation. The shunt and the series installations can be controlled separately. The shunt converter can be operated in reactive power (VAR) control mode, or in voltage control mode.

The operation of the series converter can be done in direct injection mode, bus voltage regulation and control mode, line impedance control mode, phase angle regulation mode and automatic power flow control mode.

Due to its versatility, the UPFC can be used to reconfigure power flows in transmission corridors, depending on system conditions measured at remote locations. With the help of the process bus and the GPS-LSE algorithm, the information required can

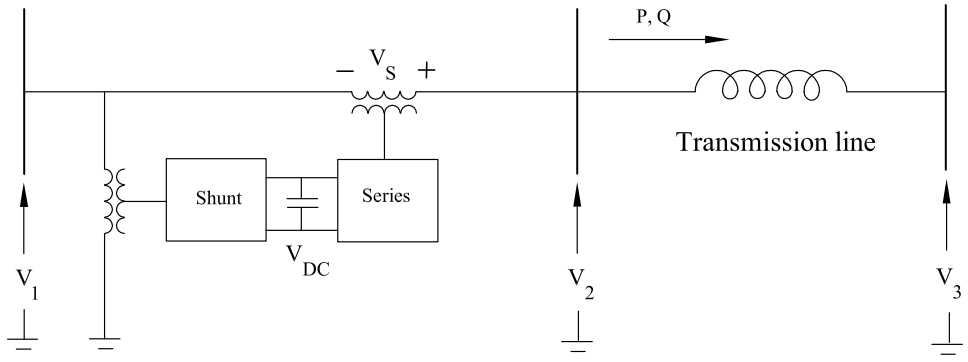

Figure 6.57: Unified Power Flow Controller functional representation

be transferred to- and from the UPFC installation for real-time control and system protection.

The performance of the proposed digital relaying algorithm is tested as part of a protection system of a transmission line with a UPFC installation. The test system implemented is shown in Fig.(6.59).

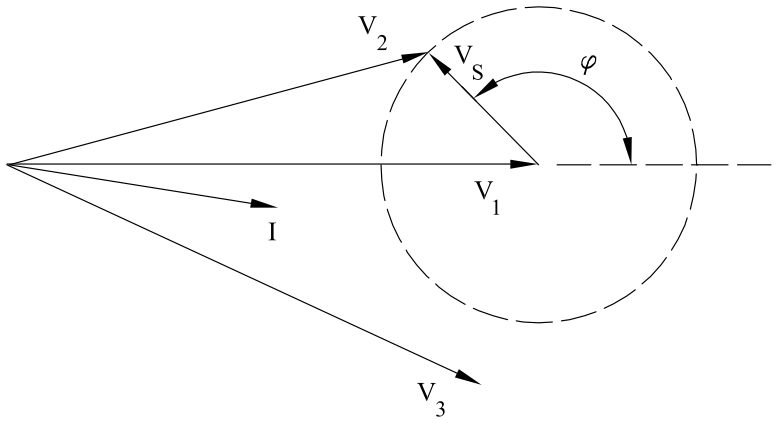

Figure 6.58: Phasor representation of the UPFC operation

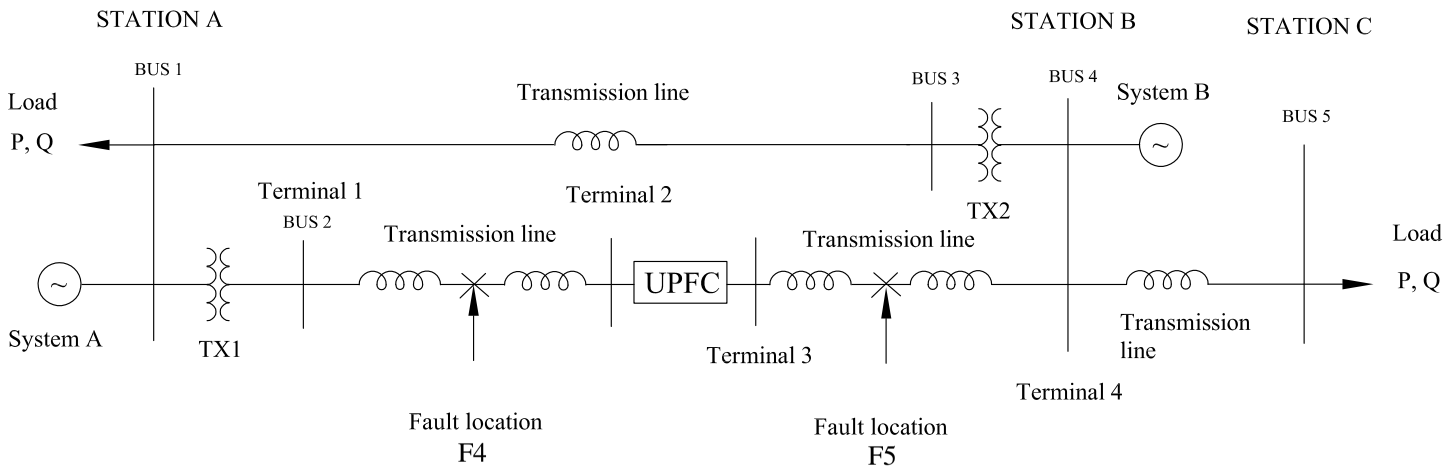

Figure 6.59: Test system for protecting transmission line with UPFC

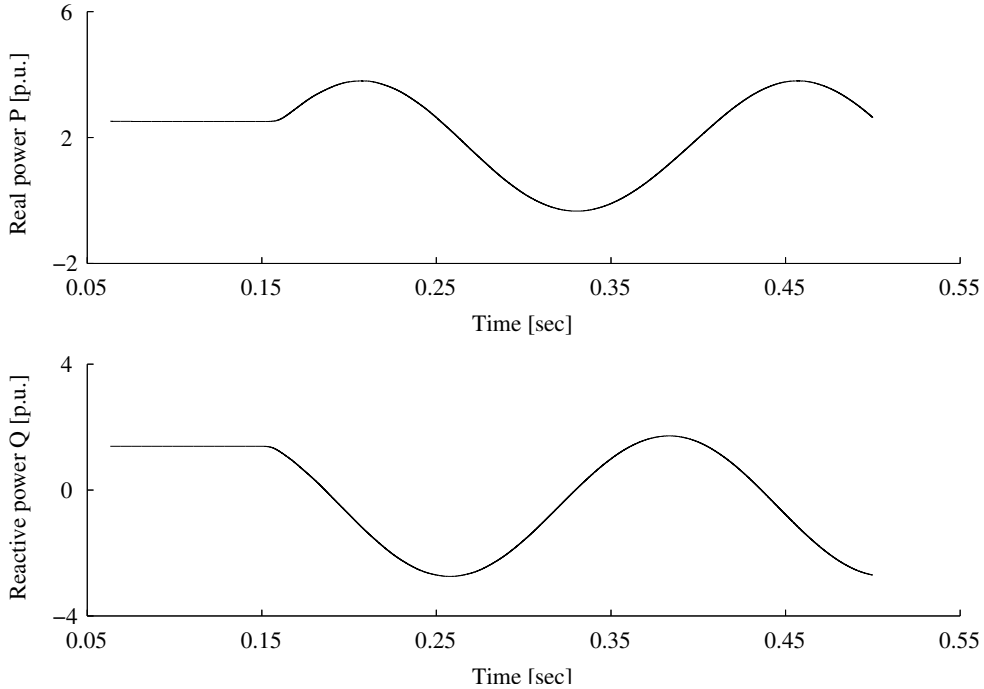

Figure 6.60: Real and reactive power flow control on the line

To cover the entire operating range of the series converter, the injected voltage amplitude $|V_S|$ has been kept constant at 0.05 [pu], while the phase angle of the same voltage was varied between 0 and 2π. As a result, the power flow in the line was modified over a wide range, effectively controlling the load flow distribution between the two parallel lines. The controllable area, as measured at Station A during the test, is shown in Figs.(6.60) and (6.61).

During the operation of the UPFC, the protection of the transmission line is made difficult by the fact that the apparent impedances measured at line ends can have wide excursions across the entire impedance plane, as shown in Fig.(6.62). The response time of the UPFC is under one cycle, which makes standard rate-of-change blocking

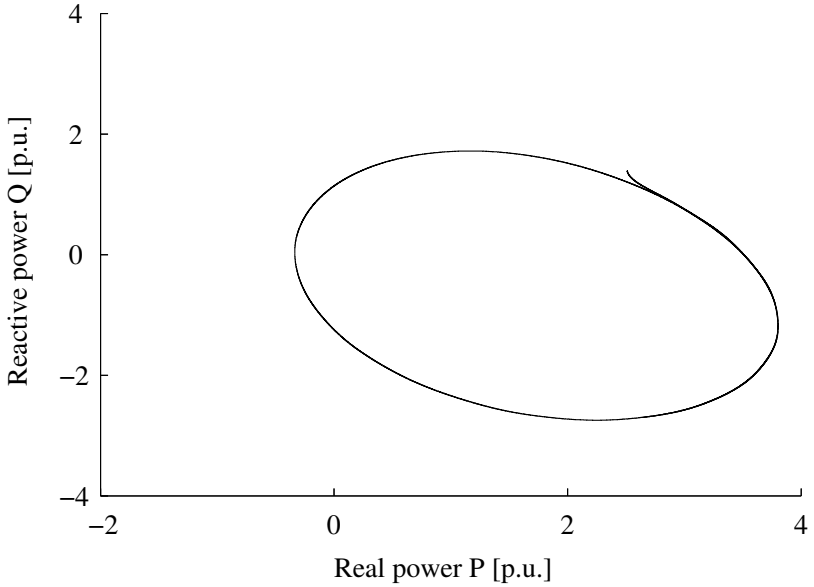

Figure 6.61: Load flow controllable area

solutions of distance protective relays unreliable.

The current differential protection is a solution that is immune to the rapid modifications of the apparent characteristics of the line. With the help of a process-bus application, the line can be protected as two separate segments. At Station A, the first line segment is protected with an 87 element. In case that a fault is determined between Station A and the UPFC installation, a direct transfer trip can be initiated to Station B. The second segment of the line can be protected in a similar fashion from Station B.

In the process-bus configuration, the samples taken from both ends of the UPFC installation are available at each station connected to the system. The 87 function can operate at Stations A and B, with both line segments being monitored at each

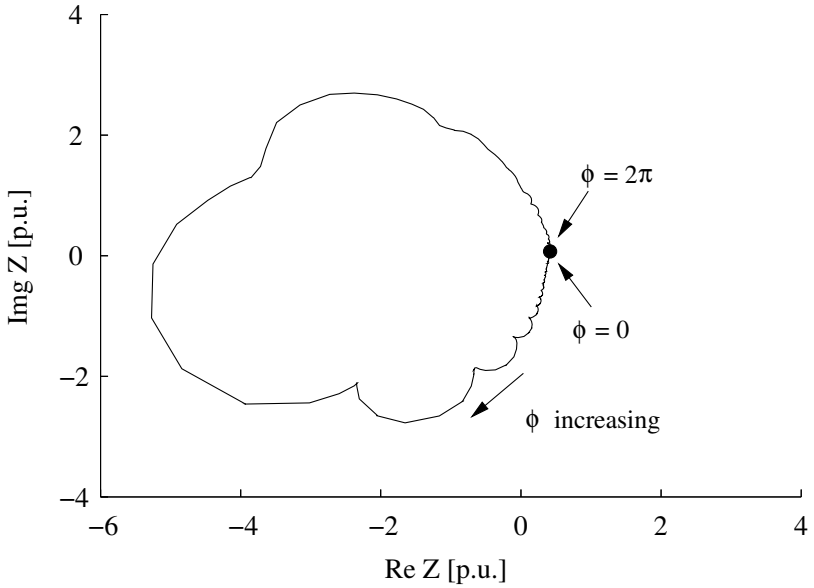

Figure 6.62: Apparent impedance seen at Bus 2 during real and reactive power flow control

line-end location. The breaker operation in this case is not dependent on a transfer trip signal, and the trip/no-trip decision is made based on the samples received from all 4 terminals, as shown in Fig.(6.59).

Tests have been conducted to determine the proposed system's performance. For fault events at F4 and F5, in Fig.(6.63), the amplitude and phase angle of the measured signals are presented in Figs.(6.64) to (6.75), together with the trip signal output of the 87 protective function, at both stations A and B.

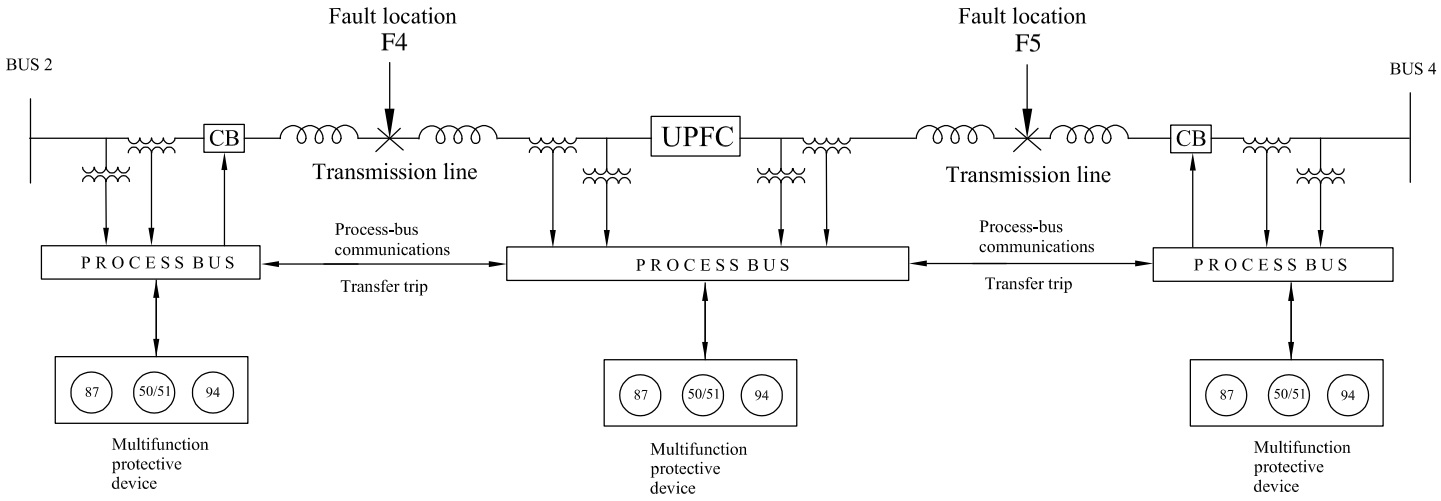

Figure 6.63: Process-bus protection of the transmission line that has a UPFC installation

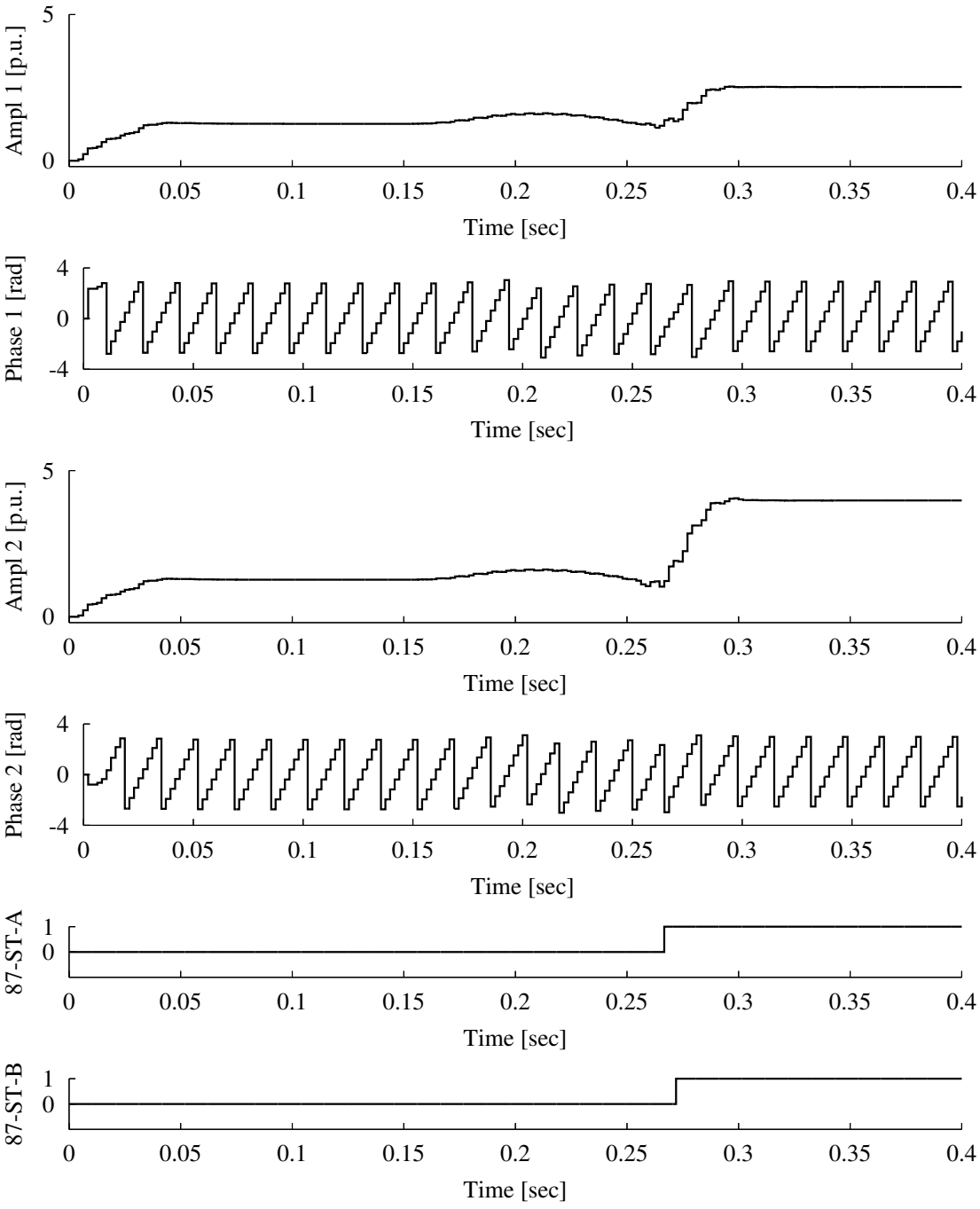

Figure 6.64: Line-to-ground fault on phase A at location F4 with 8 samples per cycle GPS-LSE algorithm

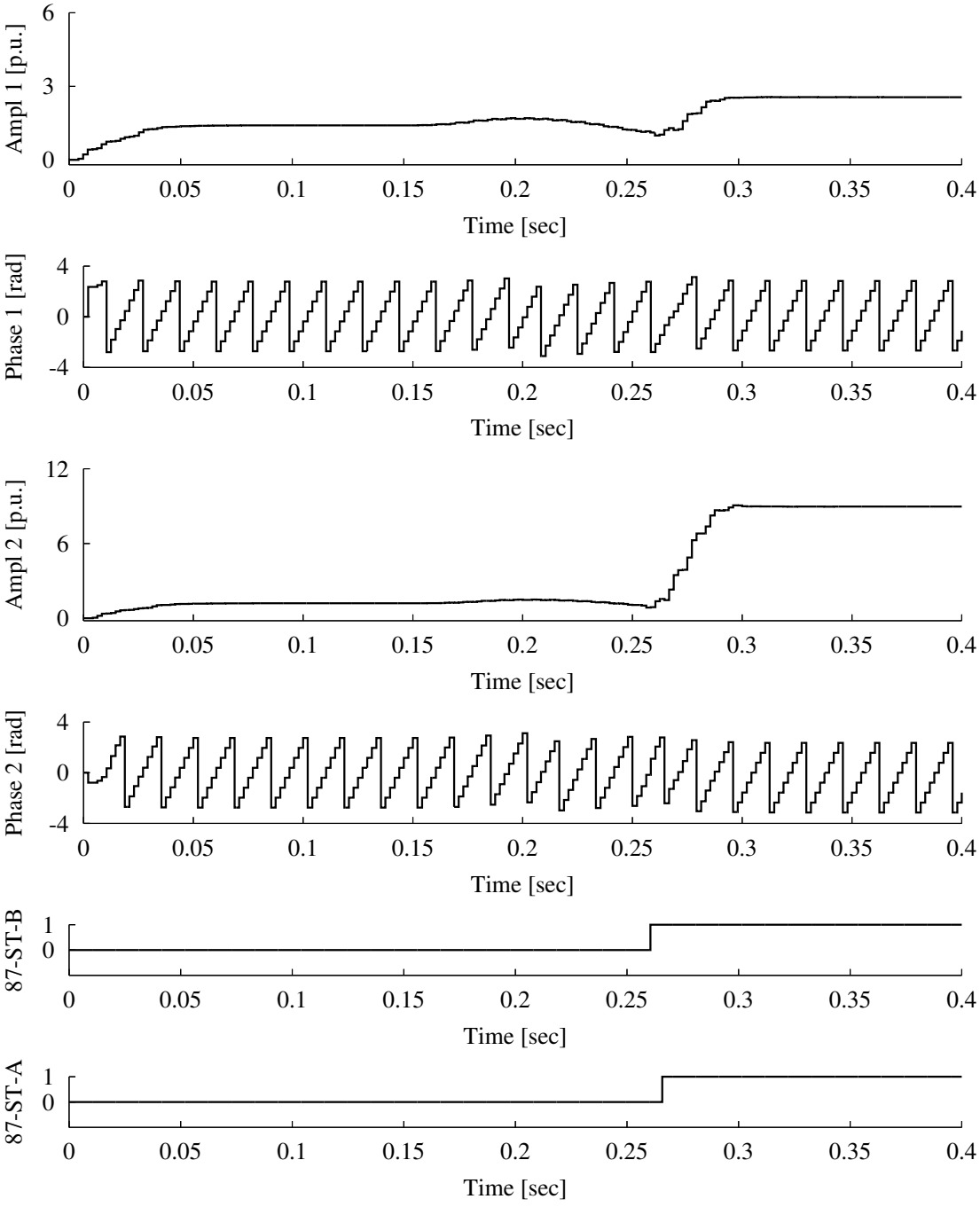

Figure 6.65: Line-to-ground fault on phase A at location F5 with 8 samples per cycle GPS-LSE algorithm

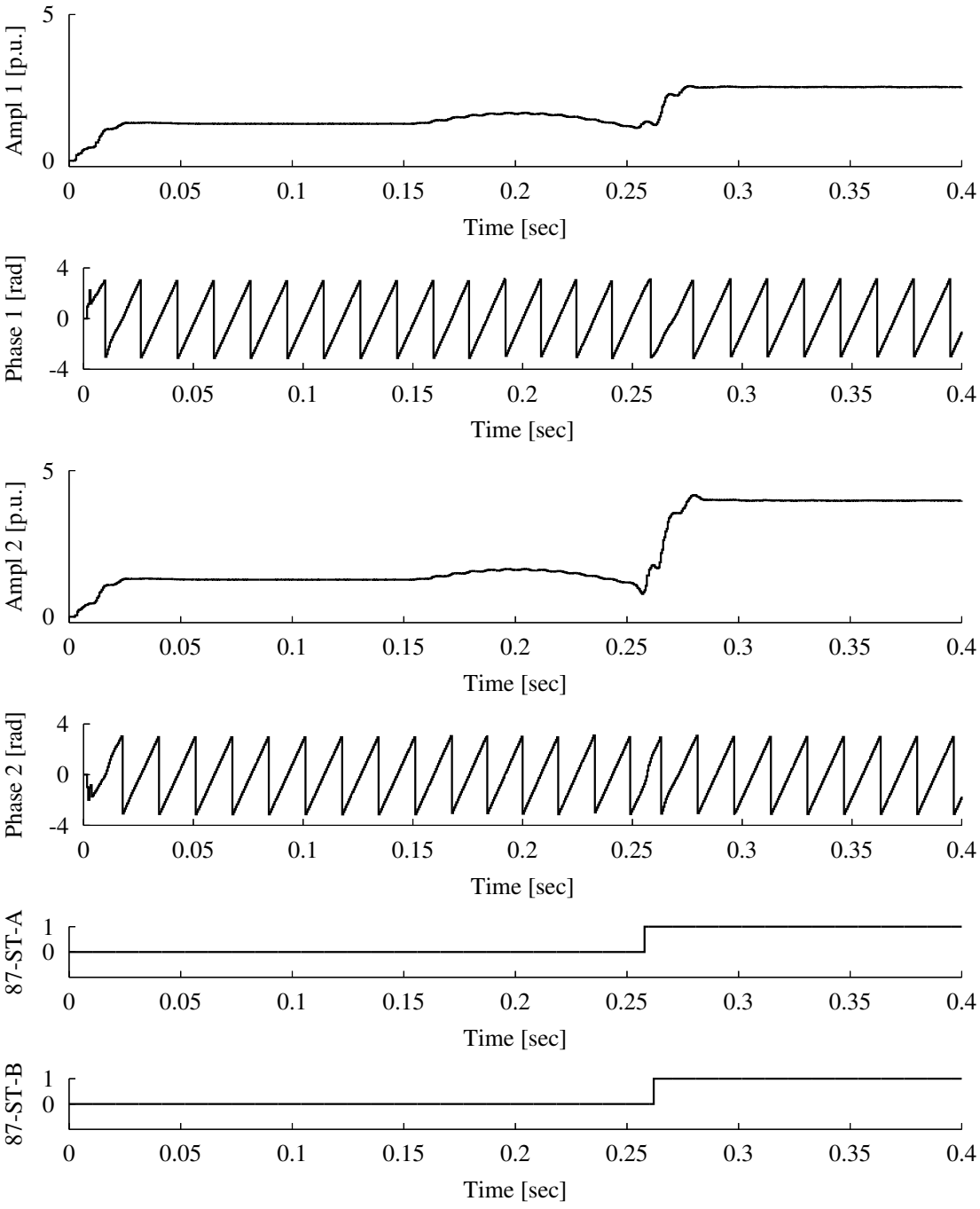

Figure 6.66: Line-to-ground fault on phase A at location F4 with 32 samples per cycle GPS-LSE algorithm

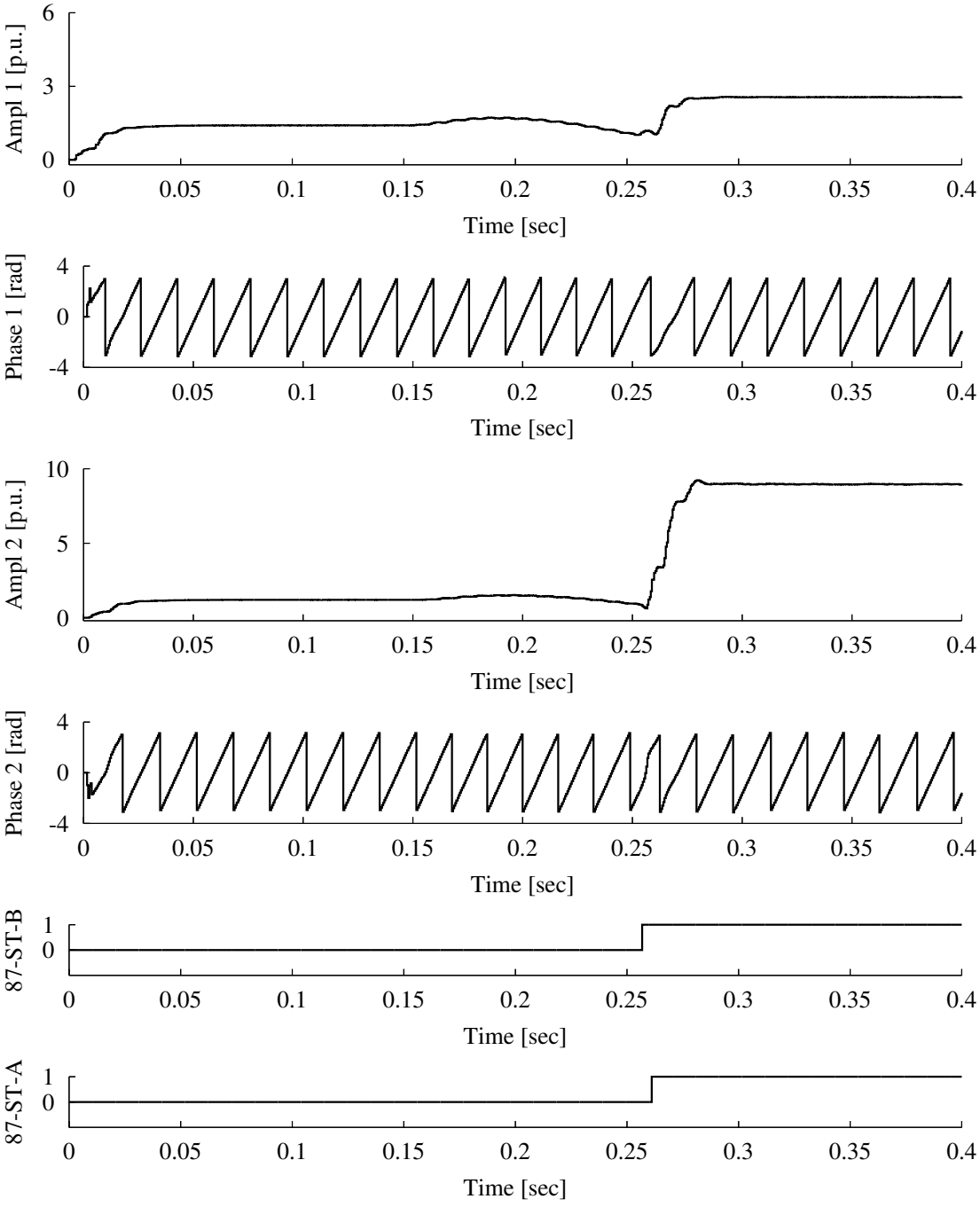

Figure 6.67: Line-to-ground fault on phase A at location F5 with 32 samples per cycle GPS-LSE algorithm

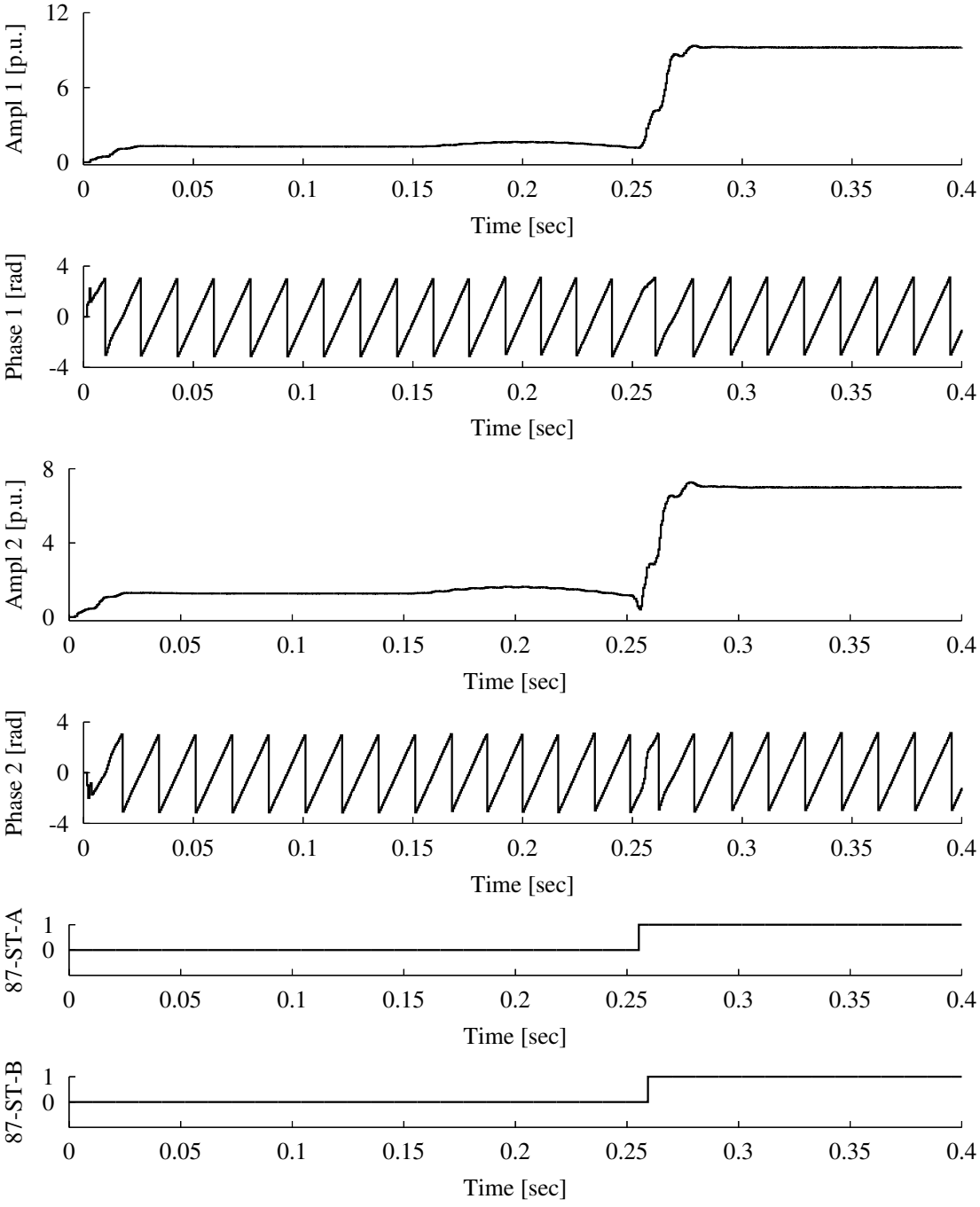

Figure 6.68: Line-to-line fault at location F4 with 32 samples per cycle GPS-LSE algorithm, phase A

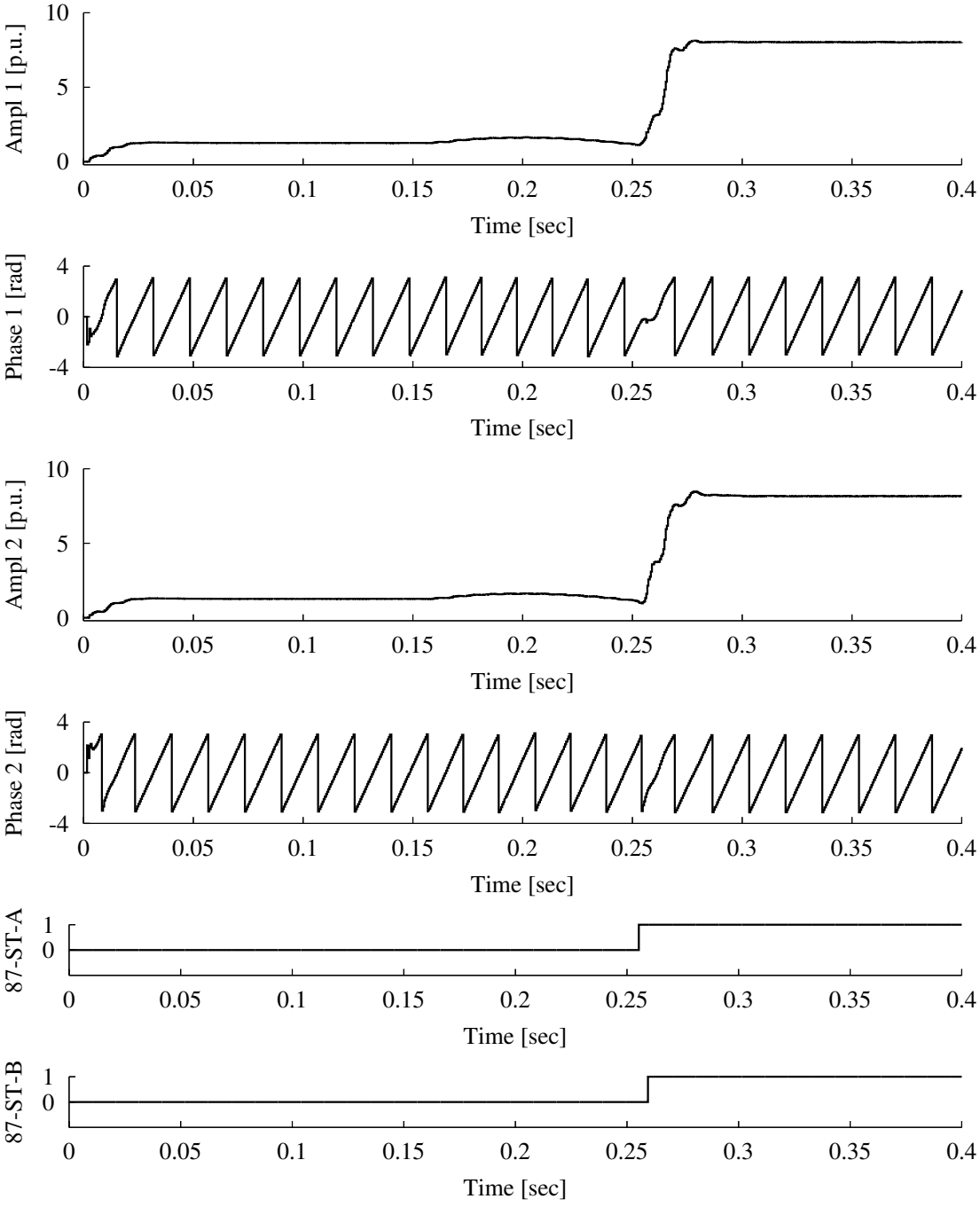

Figure 6.69: Line-to-line fault at location F4 with 32 samples per cycle GPS-LSE algorithm, phase B

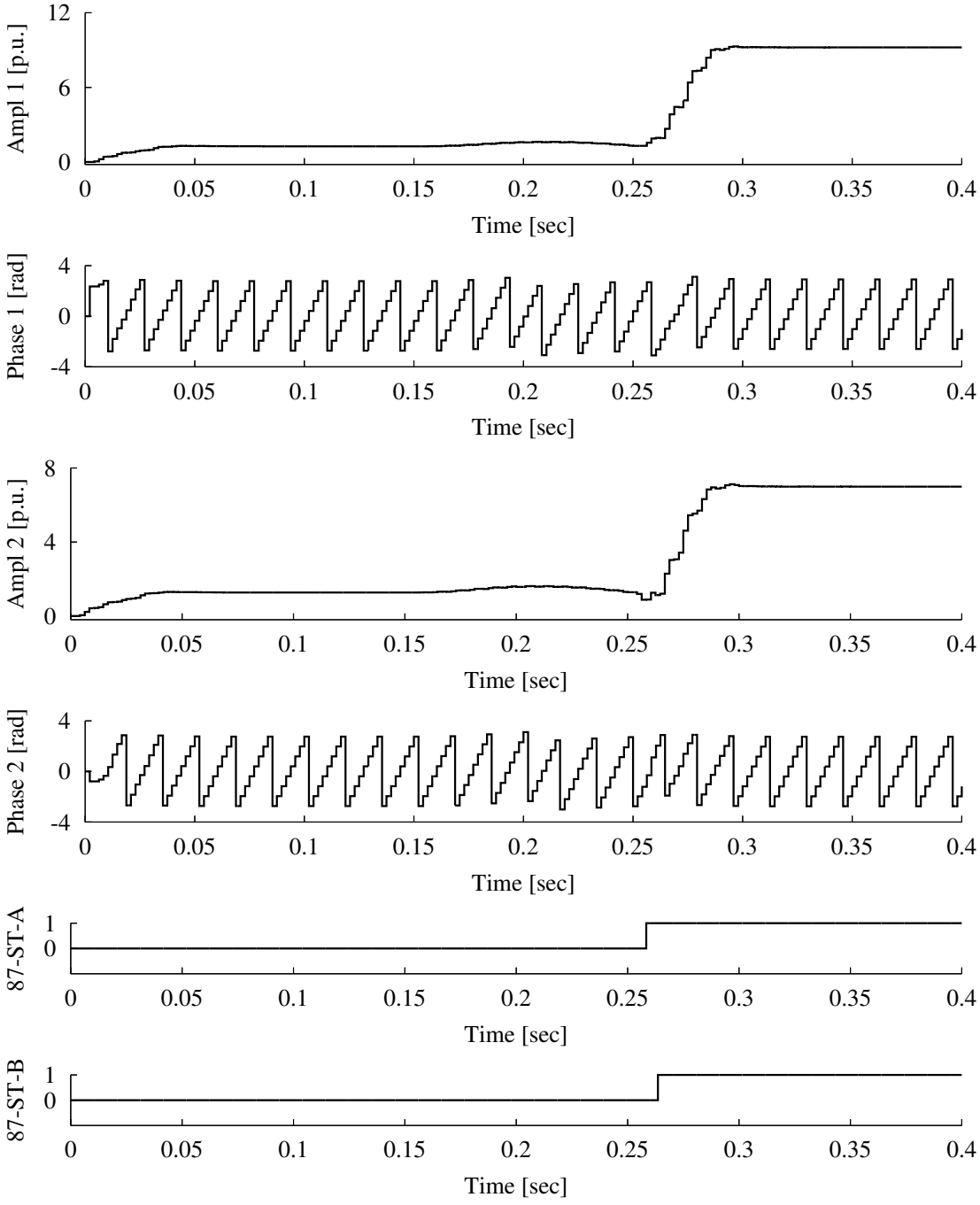

Figure 6.70: Line-to-line fault at location F4 with 8 samples per cycle GPS-LSE algorithm, phase A

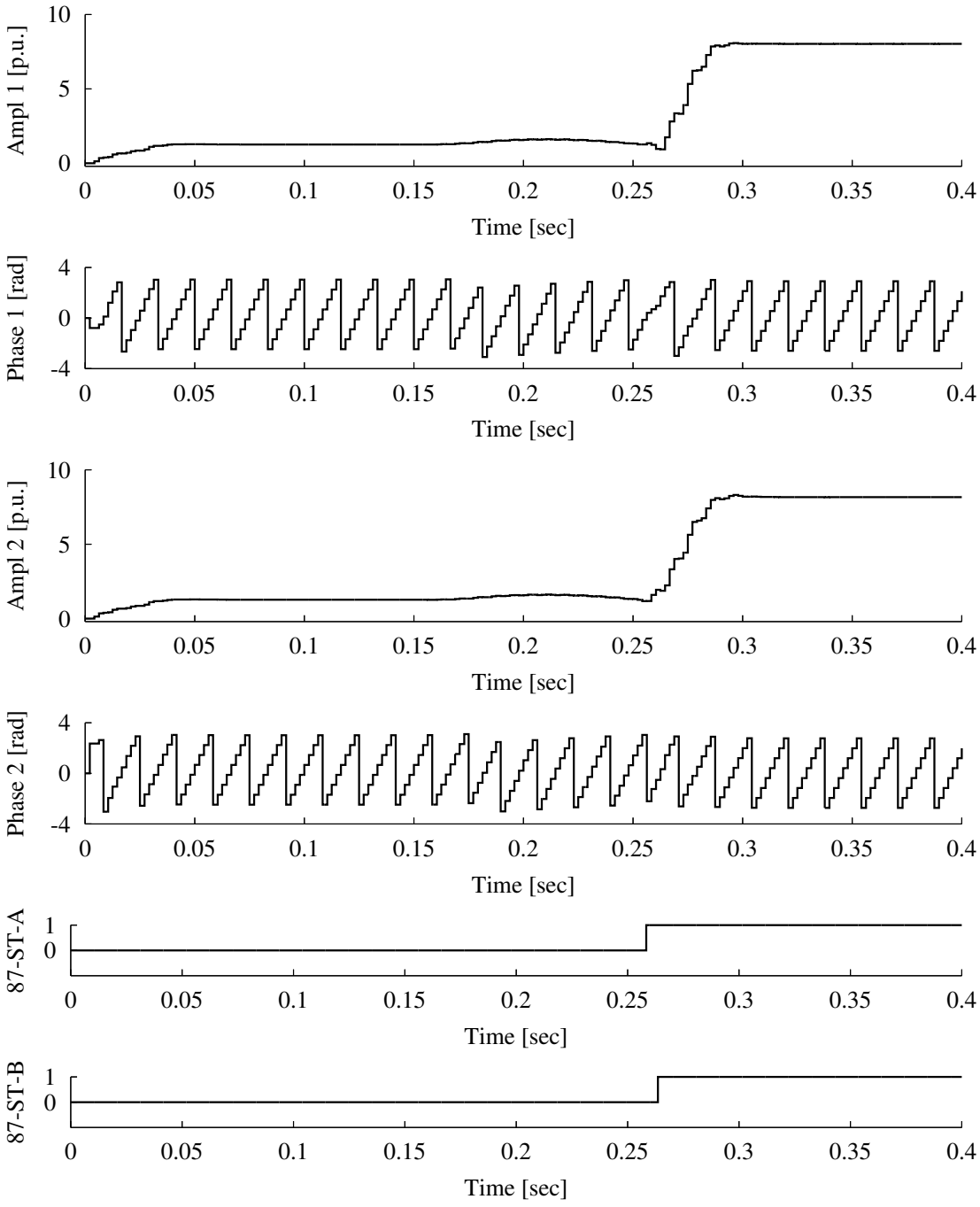

Figure 6.71: Line-to-line fault at location F4 with 8 samples per cycle GPS-LSE algorithm, phase B

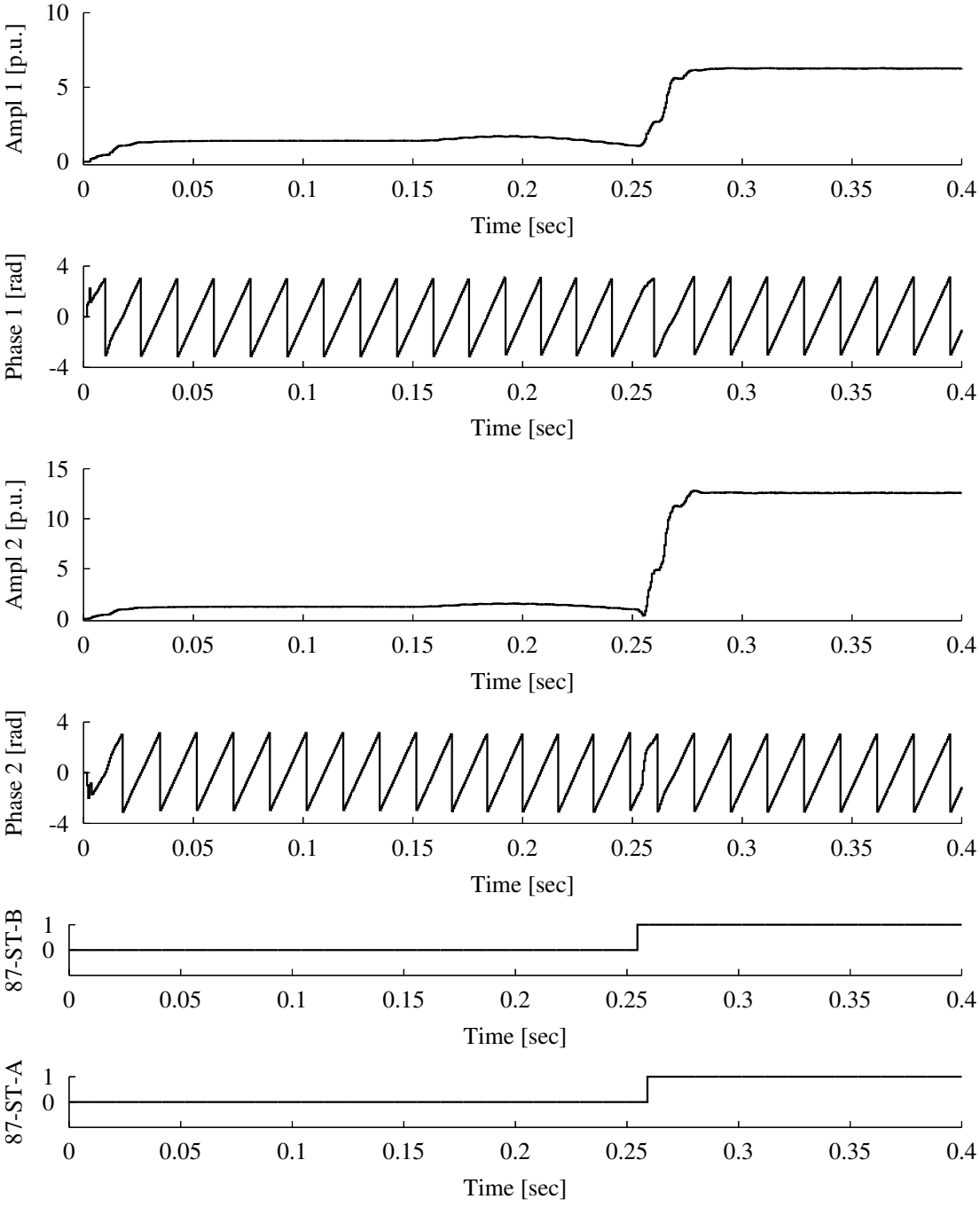

Figure 6.72: Line-to-line fault at location F5 with 32 samples per cycle GPS-LSE algorithm, phase A

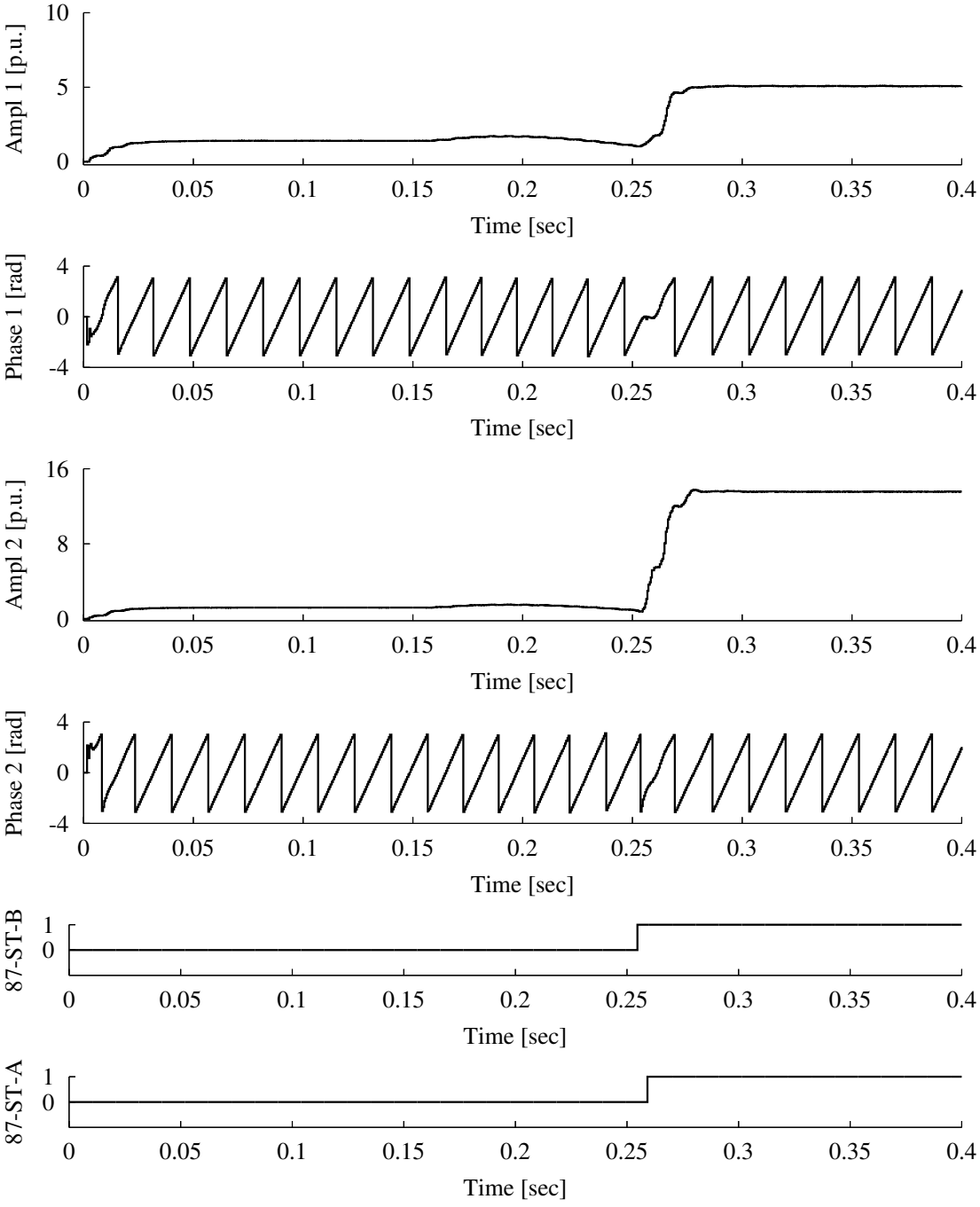

Figure 6.73: Line-to-line fault at location F5 with 32 samples per cycle GPS-LSE algorithm, phase B

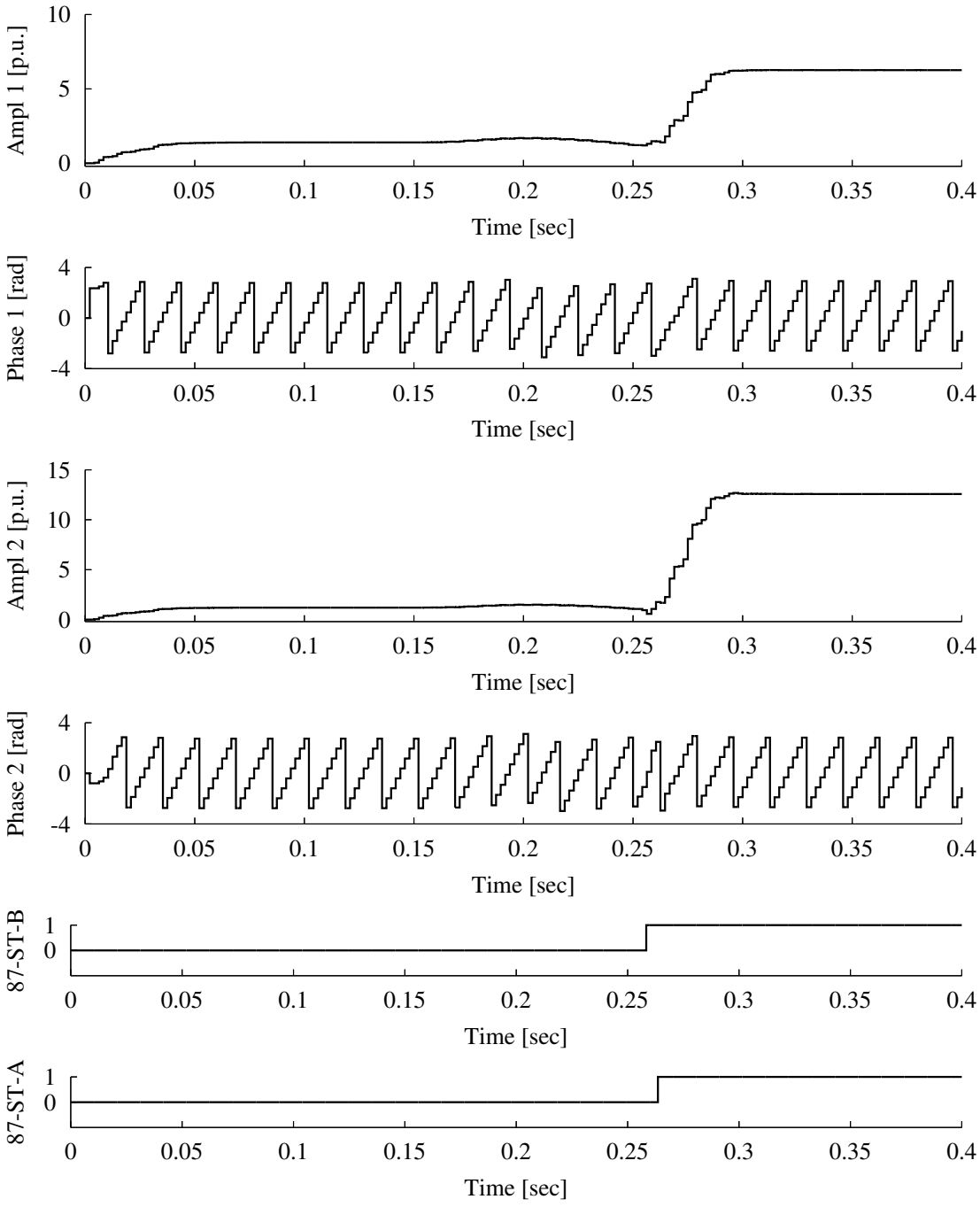

Figure 6.74: Line-to-line fault at location F5 with 8 samples per cycle GPS-LSE algorithm, phase A

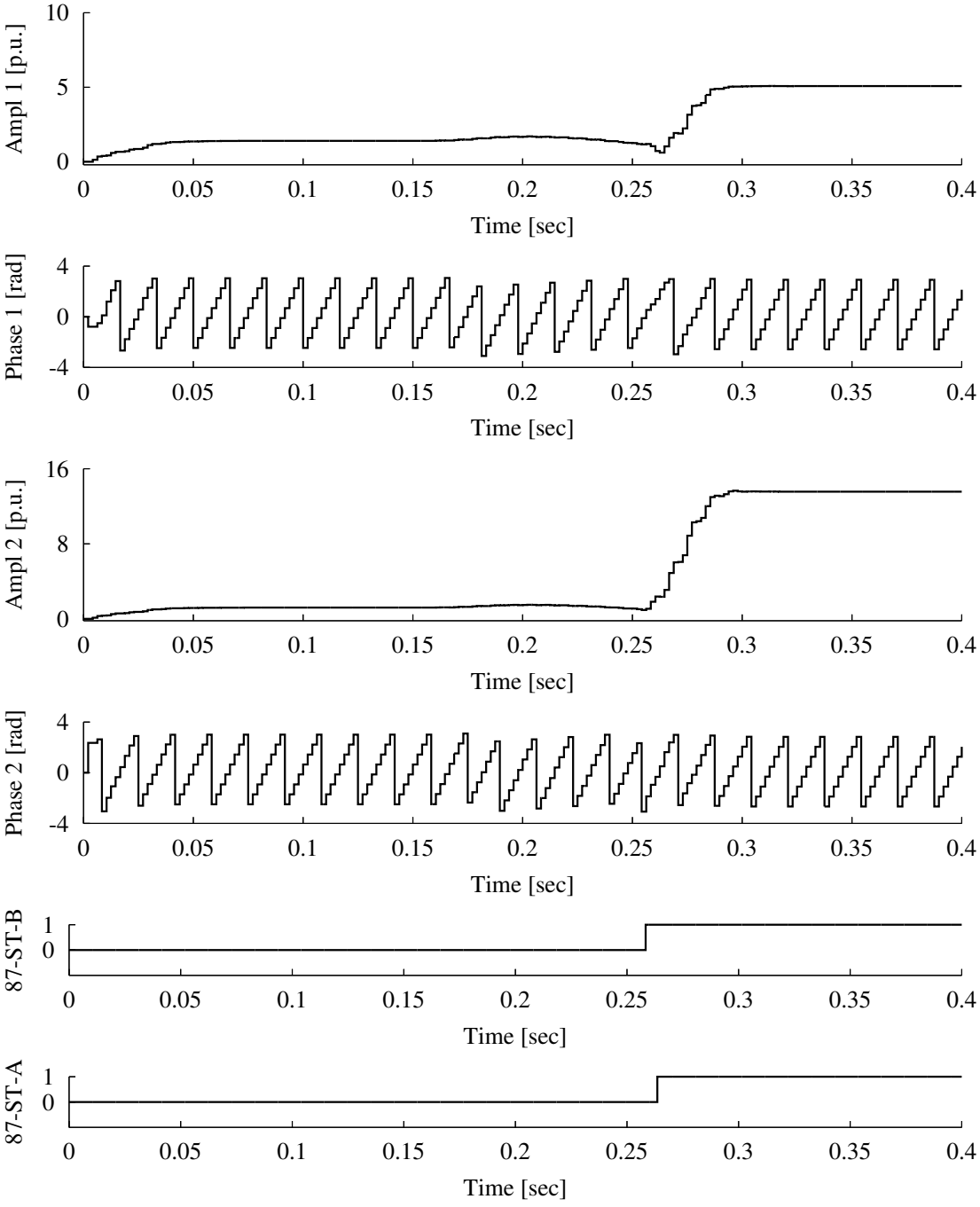

Figure 6.75: Line-to-line fault at location F5 with 8 samples per cycle GPS-LSE algorithm, phase B

The results shown in Figs.(6.64) to (6.67) confirm that the proposed solution performs well during single line-to-ground faults on both line segments. Similar conclusions can be reached for the line-to-line faults depicted in Figs.(6.68) to (6.75). Variations in the network performance are well compensated by both the 32 and 8 samples per cycle algorithms.

The performance of the solution proposed in this section for the protection of a transmission line that has a UPFC installation confirms that the system level process-bus concept is effective in providing protection and monitoring across multiple stations using the new digital relaying algorithm.

6.5 Application to control systems

Intelligent Electronic Devices (IED) are capable of performing a multitude of protective, monitoring, metering and controlling functions. The proposed integrated open-system application is not limited to processing data for protective functions only.

Having information technology type equipment as hardware, and running high level software applications, control functions can also be part of the integrated solution. With the help of the proposed digital relaying algorithm, measurements taken at remote locations can be transferred and used for voltage regulation, generated power and load flow control at key locations on the power system.

CHAPTER 7

SUMMARY AND CONCLUSIONS

During recent years, the energy crisis in the United States and Canada has taken various forms. Shortage of generating facilities, transmission grid bottlenecks, forced load shedding to avoid catastrophic failures have become commonplace in many locations across North America. As the severity of these events increases, there are few reasons to believe that new generation and transmission capacity will be available to fuel the ever increasing demand for electrical energy.

To avoid catastrophic failures, power systems monitoring has to be performed with an increasing detail [128–133]. Investigations conducted after catastrophic power system failures have recognized that they all have common characteristics. An overloaded and stressed power system where transmission lines are loaded close to operating limits, reactive power supply limited, generation reserve not sufficient for significant contingencies are the signs of a system that will have difficulty recovering even from limited disturbances.

Due to the characteristics of the existing monitoring facilities, system operators could have very limited or no information about the developing instability of the

system. A significant local disturbance can quickly cascade through transmission lines, creating load and generation islands that can result in a total blackout.

In a possible sequence of events, protective applications that are monitoring individual power system apparatus will do their job, and remove their respective protected unit from service when the system condition is such that it poses an unacceptable risk. In such a scenario, everything in the protective solution works as planned, yet, a blackout is the outcome.

In order to avoid having the system spiral into a cascading blackout, advanced system-wide management and protection solutions would have to recognize the developing system condition, take or suggest preventive measures, and at the onset of cascading operations, minimize damage by isolating parts of the system that have maximum chance of surviving as an island [133–135]. The experience of the August 2003 blackout in the U.S. and Canada has shown that generation islands that survived the catastrophic event were vital as starting points to restore service to the affected areas.

Historically, power systems protection efforts were focused primarily on unit protection, with applications designed to identify local faults. The reach of protection was increased beyond the primary equipment by defining multiple and larger zones of protection. New challenges and increasing load have pushed system use beyond previously seen limits. There are cases where overcurrent protection is not able to detect system faults, while distance protection applications include only limited fea-

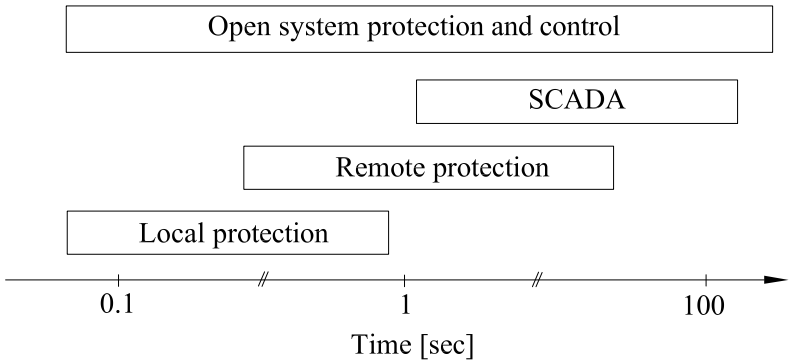

Figure 7.1: Open system operating times

tures to identify system level disturbances. These and similar challenges are changing the way electrical power systems protection is performed.

The solution proposed in this thesis can provide the basis for the integration of the local protective functions performed on individual power apparatus with wide-area protective functions. This is possible by making available to remote locations samples taken from voltages and currents, in a wide-area process-bus configuration. The area of applicability based on the response time of the proposed system is shown in Fig.(7.1).

Having voltage and current measurement values available at remote locations allows for a real-time, adaptive protection of the system, based on specific system conditions and events. By utilizing dynamic protection and control approaches, transmission lines can be protected with flexible protection and control solutions.

The previously discussed clustered hardware is well suited to perform wide-area protection, based on functions that can span across multiple stations and regions. Monitoring and coordination can be done in a pro-active manner, as opposed to the

present day, mostly reactive SCADA operations. System operation functions can be decentralized, providing security from catastrophic loss of centralized control facilities.

The static nature of the electrical power transmission facilities is a matter of the past. The new and exciting field of system level, or wide-area protection is emerging. Transmission lines are taken out of service, or reconnected on short notice, entire transmission corridors are reconfigured based on spot-market events. The reliable protection of flexible transmission grids becomes a system level necessity and challenge.

Information technology solutions are evolving to a level that permits unprecedented integration into industrial systems automation and control. On the other hand, electrical power systems protection has been an area that was considered too critical to be in the forefront of the acceptance curve of the IT-based solutions at substation level.

The adaptation of existing power systems protection and control applications to the demands and performance of the new technologies was first considered on the basis that the new technology had to meet the requirements of the existing power systems protection and control solutions. It has been recognized that the process of adapting the reliability of previous solutions to the advantages of the new technologies has to be a two way street. New protection and control solutions have been developed that take advantage of the benefits of digital signal processing and digital communications.

Due to its flexibility, scalability and robustness, Ethernet networking has gained

significant ground in utility applications in the substation. Until recently, this type of networking was used mainly to exchange metering information for off-line processing. With the increase in speed and reliability, process-bus applications based on Ethernet networking communications have emerged.

Digital instrumentation in the substation is capable of streaming measured current and voltage values into a process bus. Protection algorithms have to be able to process this type of information that is sent across shared networking infrastructure.

In this thesis, it has been shown that lower sampling frequencies can mask the data transmission performance problems of slower communication networks. During the years, the fact that smaller sampling rates can mask communication problems was considered as a possible solution to solve the data transmission characteristics of the Ethernet communications. Tests show that a wide range of faults can be identified using standard, Full-cycle Fourier algorithms, with low sampling rate and fast responding networks.

The network speed requirements have been found to be very critical to the performance of protective algorithms. When using analogue data streaming, keeping network delays at maximum 2 ms has been found to be critical for protection applications. This is a direct consequence of the fact that the protection algorithms considered were not able to compensate for network jitters causing delayed packets. The challenges of previous solutions are evident from the results shown in this thesis when using slower communication channels.

The work presented identifies the performance requirements of a digital protective algorithm for processing samples that are sent across Ethernet-based communication channels. The shortcomings and unstable performance of widely used protective algorithms in accommodating data samples that are out of step from their proper position due to variable time delays are described.

A new digital protection algorithm was developed that is able to extract the amplitude and phase angle of sampled signals from data samples received across Ethernet networks with variable jitter. The time delay experienced by data samples was obtained by compounding the delays introduced by the various layers of the communications process represented in the Open Systems Interconnection (OSI) networking model.

The performance of the algorithm allows the extraction of source signal phase information as it was at the time of sampling. This is a significant advantage when applied to differential-type relaying, where transmission line asymmetries can negatively affect protective equipment performance, and are still a challenge for the industry. The developed algorithm is also able to compensate for variable time delay during data transmission.

The performance of the algorithm was tested by using the recovered phasor amplitude and phase angle information in different types of protective solutions. These included inverse time overcurrent-, self-polarized distance-, and differential protective functions. The performance and response time of the algorithm is tested on different

types of faults, resulting in different voltage and current signal characteristics. Tests confirm the stability of the algorithm to variable transport delays, signal characteristics and jitters.

The results show that there is significant flexibility in the algorithm that can be used by the protective system designer to facilitate less performant communication channels, or, to take advantage of very fast communication channels by reducing the response time of the protective function.

The results show that the algorithm works well with variable length data windows, and variable sampling frequencies. Higher sampling rates make communication problems more visible, but the presented algorithm is able to compensate for wide variations in network performance, effectively maintaining sampled signal phase and amplitude information during network performance fluctuations.

Results show that the algorithm has sufficient flexibility to be used for both full-cycle and sub-cycle operations. System level events happen during longer periods of time, as compared to substation fault events. The suggested solution is able to recover fundamental component phase and amplitude information based also on slow sampling rates, making long distance transmission of data possible. This can make the proposed algorithm a solution of choice for wide-area protection applications.

As the August 2003 blackout in the U.S. and Canada has shown, reliable electrical power supply is vital to the social and economic fabric of the society. Too often taken for granted, its value to society becomes obvious during system-wide blackouts. The

report and recommendations of the commission that investigated the event recognizes the development of new system level protective solutions an important research area, that can prevent the occurrence of similar magnitude disturbances. Based on the new digital relaying algorithm for integrated power system protection and control, the research reported in this thesis will continue with the development of wide-area protection systems and algorithms.

REFERENCES

[1] C. A. Gross, *Power system analysis.* New York, NY: John Wiley and Sons, 1986.

[2] C. R. Mason, *The art and science of protective relaying.* New York, NY: John Wiley and Sons, 1956.

[3] B. D. Russel and M. E. Council, *Power system control and protection.* New York, NY: Academic Press, 1978.

[4] S. H. Horowitz, *Protective relaying for power systems.* New York, NY: John Wiley and Sons, 1980.

[5] G. Gangadharan and P. Anbalagan, "Microprocessor based three step quadrilateral distance relay for the protection of EHV/UHV transmission lines," *IEEE Transactions on Power Delivery*, vol. 7, no. 0885-8977, pp. 91–97, 1992.

[6] L. Perez and A. Urdaneta, "Optimal computation of distance relays second zone timing in a mixed protection scheme with directional overcurrent relays," *IEEE Transactions on Power Delivery*, vol. 16, no. 0885-8977, pp. 385–388, 2001.

[7] M. Eissa and M. Masoud, "A novel digital distance relaying technique for transmission line protection," *IEEE Transactions on Power Delivery*, vol. 16, no. 0885-8977, pp. 380–384, 2001.

[8] M. Saha, B. Kasztenny, E. Rosolowski, and J. Izykowski, "First zone algorithm for protection of series compensated lines," *IEEE Transactions on Power Delivery*, vol. 16, no. 0885-8977, pp. 200–207, 2001.

[9] T. Segui, P. Bertrand, M. Guillot, P. Hanchin, and P. Bastard, "Fundamental basis for distance relaying with parametrical estimation," *IEEE Transactions on Power Delivery*, vol. 15, no. 0885-8977, pp. 659–664, 2000.

[10] T. Adu, "A new transmission line fault locating system," *IEEE Transactions on Power Delivery*, vol. 16, no. 0885-8977, pp. 498–503, 2001.

[11] M. Sanaye-Pasand and O. Malik, "High speed transmission line directional protection evaluation using field data," *IEEE Transactions on Power Delivery*, vol. 14, no. 0885-8977, pp. 851–856, 1999.

[12] M. Sanaye-Pasand and O. Malik, "Implementation and laboratory test results of an Elman network-based transmission line directional relay," *IEEE Transactions on Power Delivery*, vol. 14, no. 0885-8977, pp. 782–788, 1999.

[13] K. Cho, Y. Kang, S. Kim, J. Park, S. Kang, and K. Kim, "An ANN based approach to improve the speed of a differential equation based distance relaying algorithm," *IEEE Transactions on Power Delivery*, vol. 14, no. 0885-8977, pp. 349–357, 1999.

[14] A. Mechraoui and D. Thomas, "A new blocking principle with phase and earth fault detection during fast power swings for distance protection," *IEEE Transactions on Power Delivery*, vol. 10, no. 0885-8977, pp. 1242–1248, 1995.

[15] P. McLaren, G. Swift, Z. Zhang, E. Dirks, R. Jayasinghe, and I. Fernando, "A new directional element for numerical distance relays," *IEEE Transactions on Power Delivery*, vol. 10, no. 0885-8977, pp. 666–675, 1995.

[16] M. Gilany, O. Malik, and G. Hope, "A laboratory investigation of a digital protection technique for parallel transmission lines," *IEEE Transactions on Power Delivery*, vol. 10, no. 0885-8977, pp. 187–193, 1995.

[17] P. Dutta and P. Gupta, "Microprocessor-based UHS relaying for distance protection using advanced generation signal processing," *IEEE Transactions on Power Delivery*, vol. 7, no. 0885-8977, pp. 1121–1128, 1992.

[18] A. T. Johns and S. K. Salman, *Digital protection for power systems.* London, UK: Institution of Electrical Engineers, 1995.

[19] G. Ziegler, *Numerical distance protection.* Munich, Germany: Siemens, AG, 1999.

[20] M. Yalla, "A digital multifunction protective relay," *IEEE Transactions on Power Delivery*, vol. 7, no. 0885-8977, pp. 193–201, 1992.

[21] R. Aggarwal, A. Husseini, and M. Redfern, "Design and testing of a new microprocessor-based current differential relay for EHV teed feeders," *IEEE Transactions on Power Delivery*, vol. 6, no. 0885-8977, pp. 991–999, 1991.

[22] D. Crameri, K.-P. Brand, H. Hager, and J. Kopainsky, "Digital station protection," *IEEE Transactions on Power Delivery*, vol. 4, no. 0885-8977, pp. 1617–1624, 1989.

[23] O. Youssef, "A fundamental digital approach to impedance relays," *IEEE Transactions on Power Delivery*, vol. 7, no. 0885-8977, pp. 1861–1870, 1992.

[24] M. Kezunovic, P. Spasojevic, and B. Perunicic, "New digital signal processing algorithms for frequency deviation measurement," *IEEE Transactions on Power Delivery*, vol. 7, no. 0885-8977, pp. 1563–1573, 1992.

[25] D. Fischer and R. Madge, "Digital teleprotection units. A technology overview," *IEEE Transactions on Power Delivery*, vol. 7, no. 0885-8977, pp. 1769–1774, 1992.

[26] P. Bastard, P. Bertrand, T. Emura, and M. Meunier, "The technique of finite-impulse-response filtering applied to digital protection and control of medium voltage power system," *IEEE Transactions on Power Delivery*, vol. 7, no. 0885-8977, pp. 620–626, 1992.

[27] M. Kezunovic, E. Soljanin, B. Perunicic, and S. Levi, "New approach to the design of digital algorithms for electric power measurements," *IEEE Transactions on Power Delivery*, vol. 6, no. 0885-8977, pp. 516–523, 1991.

[28] IEEE FACTS Terms and Definitions Task Force, "Proposed terms and definitions for flexible AC transmission system (FACTS)," *IEEE Transactions on Power Delivery*, vol. 12, no. 0885-8977, pp. 1848–1853, 1997.

[29] J. Brochu, F. Beauregard, J. Lemay, G. Morin, P. Pelletier, and R. Thallam, "Application of the interphase power controller technology for transmission line power flow control," *IEEE Transactions on Power Delivery*, vol. 12, no. 0885-8977, pp. 888–894, 1997.

[30] M. Noroozian and G. Andersson, "Power flow control by use of controllable series components," *IEEE Transactions on Power Delivery*, vol. 8, no. 0885-8977, pp. 1420–1429, 1993.

[31] L. Pilotto, W. Ping, A. Carvalho, A. Wey, W. Long, F. Alvarado, and A. Edris, "Determination of needed FACTS controllers that increase asset utilization of power systems," *IEEE Transactions on Power Delivery*, vol. 12, no. 0885-8977, pp. 364–371, 1997.

[32] P. Sensarma, K. Padiyar, and V. Ramanarayanan, "Analysis and performance evaluation of a distribution STATCOM for compensating voltage fluctuations," *IEEE Transactions on Power Delivery*, vol. 16, no. 0885-8977, pp. 259–264, 2001.

[33] M. Noroozian, M. Ghandhari, G. Andersson, J. Gronquist, and I. Hiskens, "A robust control strategy for shunt and series reactive compensators to damp

electromechanical oscillations," *IEEE Transactions on Power Delivery*, vol. 16, no. 0885-8977, pp. 812–817, 2001.

[34] M. Noroozian, L. Angquist, M. Ghandhari, and G. Andersson, "Improving power system dynamics by series-connected FACTS devices," *IEEE Transactions on Power Delivery*, vol. 12, no. 0885-8977, pp. 1635–1641, 1997.

[35] H. Wang and F. Swift, "A unified model for the analysis of FACTS devices in damping power system oscillations. i. single-machine infinite-bus power systems," *IEEE Transactions on Power Delivery*, vol. 12, no. 0885-8977, pp. 941–946, 1997.

[36] L. Gyugyi, C. Schauder, and K. Sen, "Static synchronous series compensator: a solid-state approach to the series compensation of transmission lines," *IEEE Transactions on Power Delivery*, vol. 12, no. 0885-8977, pp. 406–417, 1997.

[37] G. Ericsson, "A holistic approach for analyzing communication utilization in power system control," *IEEE Transactions on Power Delivery*, vol. 13, no. 0885-8977, pp. 979–983, 1998.

[38] A. Patrick, J. Newbury, and S. Gargan, "Two-way communications systems in the electricity supply industry," *IEEE Transactions on Power Delivery*, vol. 13, no. 0885-8977, pp. 53–58, 1998.

[39] G. Ericsson, "Communication utilization in power system control. A state-of-the-practice description," *IEEE Transactions on Power Delivery*, vol. 13, no. 0885-8977, pp. 984–989, 1998.

[40] J. Tengdin, "Development of an IEEE standard for integrated substation automation communication (p1525): specifications for substation applications and key communication performance drivers," *Power Engineering Society Summer Meeting, 2000. IEEE*, vol. 1, pp. 136–137 vol. 1, 2000.

[41] D. Marihart, "Communications technology guidelines for EMS/SCADA systems," *IEEE Transactions on Power Delivery*, vol. 16, no. 0885-8977, pp. 181–188, 2001.

[42] S. Sciacca and W. Block, "Advanced SCADA concepts," *IEEE Computer Applications in Power*, vol. 8, no. 0895-0156, pp. 23–28, 1995.

[43] C. Lu, K. Chen, M. Lin, and Y. Lin, "Performance assessment of an integrated distribution SCADA-AM/FM system," *IEEE Transactions on Power Delivery*, vol. 12, no. 0885-8977, pp. 971–978, 1997.

[44] J. Luque and I. Gomez, "The role of medium access control protocols in SCADA systems," *IEEE Transactions on Power Delivery*, vol. 11, no. 0885-8977, pp. 1195–1200, 1996.

[45] K. Kato and H. Fudeh, "Performance simulation of distributed energy management systems," *IEEE Transactions on Power Systems*, vol. 7, no. 0885-8950, pp. 820–827, 1992.

[46] MODBUS Interface for Distributed Automation. (2004) Modbus application protocol v1.1a. MODBUS-IDA. [Online]. Available: http://www.modbus.org/

[47] OPC Foundation. (1998) OLE for Process Control Overview. OPCF. [Online]. Available: http://www.opcfoundation.org/

[48] H. Falk and J. Robbins. (1995) An explanation of the architecture of the MMS standard. SISCO. [Online]. Available: http://www.sisconet.com

[49] C. Brunner and H. Schubert. (2002, Jan.) The ABB - SIEMENS IEC 61850 interoperability projects. [Online]. Available: http://www.nettedautomation.com/download/KEMA_ABB-SIEMENS_slides_R0-2.pdf

[50] G. Ericsson and A. Johnsson, "Examination of ELCOM-90, TASE.1, and ICCP/TASE.2 for inter-control center communication," *IEEE Transactions on Power Delivery*, vol. 12, no. 0885-8977, pp. 607–615, 1997.

[51] W. Sweet, "Robert N. Metcalfe," *IEEE Spectrum*, vol. 33, no. 0018-9235, pp. 48–49, 52–5, 1996.

[52] G. Kaplan, "Ethernet's winning ways," *IEEE Spectrum*, vol. 38, no. 0018-9235, pp. 113–115, 2001.

[53] D. Clark, "Are ATM, Gigabit Ethernet ready for prime time," *Computer*, vol. 31, no. 0018-9162, pp. 11–13, 1998.

[54] S. Vaughan-Nichols, "Will 10-Gigabit Ethernet have a bright future?" *Computer*, vol. 35, no. 0018-9162, pp. 22–24, 2002.

[55] C. E. Spurgeon, *Ethernet: the Definitive Guide*. Sebastopol, CA: O'Reilly, 2000.

[56] J. Lewis, "Bandwidth utilization of a large local area network," *IEEE Communications Magazine*, vol. 27, no. 0163-6804, pp. 25–30, 1989.

[57] K. Rege, S. Dravida, S. Nanda, S. Narayan, J. Strombosky, M. Tandon, and D. Gupta, "QoS management in trunk-and-branch switched Ethernet networks," *IEEE Communications Magazine*, vol. 40, no. 0163-6804, pp. 30–36, 2002.

[58] J. Angelopoulos, H.-C. Leligou, T. Argyriou, S. Zontos, E. Ringoot, and T. Van Caenegem, "Efficient transport of packets with QoS in an FSAN-aligned GPON," *IEEE Communications Magazine*, vol. 42, no. 0163-6804, pp. 92–98, 2004.

[59] V. Ramamurti, J. Siwko, G. Young, and M. Pepe, "Initial implementations of point-to-point Ethernet over SONET/SDH transport," *IEEE Communications Magazine*, vol. 42, no. 0163-6804, pp. 64–70, 2004.

[60] G. Brunello, R. Smith, and C. Campbell, "An application of a protective relaying scheme over an Ethernet LAN/WAN," *Transmission and Distribution Conference and Exposition*, vol. 1, pp. 522–526, 2001.

[61] "Optimizing Ethernet networks," White Paper, Schneider Electric, Nov. 2001.

[62] "Securing your automation Ethernet network," White Paper, Schneider Electric, Nov. 2001.

[63] L.-Q. Nguyen and B. Paradis, "Installation of Hydro-Quebec's distribution feeder automation system," *IEEE Transactions on Power Delivery*, vol. 3, no. 0885-8977, pp. 1935–1941, 1988.

[64] P. McLaren, G. Swift, A. Neufeld, Z. Zhang, E. Dirks, and R. Haywood, "Open systems relaying," *IEEE Transactions on Power Delivery*, vol. 9, no. 0885-8977, pp. 1316–1324, 1994.

[65] G. Brunello, R. Smith, and C. Campbell, "An application of a protective relaying scheme over an Ethernet LAN/WAN," *Transmission and Distribution Conference and Exposition, 2001 IEEE/PES*, vol. 1, pp. 522–526 vol.1, 2001.

[66] E. Udren and J. Deliyannides, "Integrated system for substation relaying and control shows benefits," *IEEE Computer Applications in Power*, vol. 2, no. 0895-0156, pp. 21–27, 1989.

[67] S. Bricker, T. Gonen, and L. Rubin, "Substation automation technologies and advantages," *IEEE Computer Applications in Power*, vol. 14, no. 0895-0156, pp. 31–37, 2001.

[68] B. Qiu, Y. Liu, E. K. Chan, and L. Cao, "LAN-based control for load shedding," *IEEE Computer Applications in Power*, vol. 14, no. 0895-0156, pp. 38–43, 2001.

[69] P.-H. Hsi and S.-L. Chen, "Distribution automation communication infrastructure," *IEEE Transactions on Power Delivery*, vol. 13, no. 0885-8977, pp. 728–734, 1998.

[70] G. Allen and R. Cheung, "Integration of protection, control and monitoring functions for transmission and distribution substations," *IEEE Transactions on Power Delivery*, vol. 13, no. 0885-8977, pp. 96–101, 1998.

[71] S. Jun-ping, S. Wan-xing, W. Sun-an, and K. Wu, "Substation automation high speed network communication platform based on MMS+TCP/IP+Ethernet," *International Conference on Power System Technology, 2002. Proceedings PowerCon 2002*, vol. 2, pp. 1296–1300 vol.2, 2002.

[72] H. Smith, "Substation automation problems and possibilities," *IEEE Computer Applications in Power*, vol. 9, no. 0895-0156, pp. 33–36, 1996.

[73] Y. Liu, N. Schulz, H.-J. Lee, B.-S. Ahn, and Y.-M. Park, "Discussion of 'A fault diagnosis expert system for distribution substations' [Closure to discussion]," *IEEE Transactions on Power Delivery*, vol. 15, no. 0885-8977, pp. 1350–1351, 2000.

[74] D. Brown, J. Skeen, P. Daryani, and F. Rahimi, "Prospects for distribution automation at Pacific Gas and Electric Company," *IEEE Transactions on Power Delivery*, vol. 6, no. 0885-8977, pp. 1946–1954, 1991.

[75] D. Rizy, J. Lawler, J. Patton, and N. Fortson, "Distribution automation applications software for the Athens Utilities Board," *IEEE Transactions on Power Delivery*, vol. 4, no. 0885-8977, pp. 715–724, 1989.

[76] D. Borowski and R. Seamon, "EPRI project RP 2592, 'Large scale distribution automation and load control', enters test year," *IEEE Transactions on Power Delivery*, vol. 5, no. 0885-8977, pp. 486–492, 1990.

[77] A. Phadke, "Computer relaying: its impact on improved control and operation of power systems," *IEEE Computer Applications in Power*, vol. 1, no. 0895-0156, pp. 5–10, 1988.

[78] M. Kezunovic and B. Russell, "Microprocessor applications to substation control and protection," *IEEE Computer Applications in Power*, vol. 1, no. 0895-0156, pp. 16–20, 1988.

[79] K. Richter, M. Jersak, and R. Ernst, "A formal approach to MpSoC performance verification," *Computer*, vol. 4, no. 0018-9162, pp. 60–67, 2003.

[80] J. Luque, J. Escudero, and F. Perez, "Analytic model of the measurement errors caused by communications delay," *IEEE Transactions on Power Delivery*, vol. 17, no. 0885-8977, pp. 334–337, 2002.

[81] Y. Serizawa, E. Ohba, and A. Tsuboi, "Probabilistic investigations on bit error ratio requirement for digital teleprotection employing digital microwave links," *IEEE Transactions on Power Delivery*, vol. 7, no. 0885-8977, pp. 202–206, 1992.

[82] A. G. Phadke, *Computer relaying for power systems*. New York, NY: John Wiley and Sons, 1988.

[83] K. E. Martin *et al.*, "IEEE standard for synchrophasors for power systems," *IEEE Transactions on Power Delivery*, vol. 13, no. 1, pp. 73–77, 1998.

[84] K. Martin, G. Benmouyal, M. Adamiak, M. Begovic, J. Burnett, R.O., K. Carr, A. Cobb, J. Kusters, S. Horowitz, G. Jensen, G. Michel, R. Murphy, A. Phadke, M. Sachdev, and J. Thorp, "IEEE standard for synchrophasors for power systems," *IEEE Transactions on Power Delivery*, vol. 13, no. 0885-8977, pp. 73–77, 1998.

[85] A. Phadke *et al.*, "Synchronized sampling and phasor measurements for relaying and control," *IEEE Transactions on Power Delivery*, vol. 9, no. 0885-8977, pp. 442–452, 1994.

[86] E. Kreyszig, *Advanced engineering mathematics*. New York, NY: John Wiley and Sons, 1995.

[87] H. Falk. (1997) Test methodologies, setup, and result documentation for EPRI sponsored benchmark of Ethernet for protection control. SISCO. [Online]. Available: ftp://ftp.sisconet.com/EPRI/benchmrk/Ethernet.zIP

[88] M. S. Sachdev and M. A. Baribeau, "A new algorithm for digital impedance relays," *IEEE Transactions on Power Apparatus and Systems*, vol. 98, no. 6, pp. 2232–2240, 1979.

[89] T. S. Sidhu, E. Demeter, and S. O. Faried, "A digital relay algorithm for Ethernet-based data transfer," in *Proc. IEEE PES Transmission and Distribution 2003*, Dallas, TX, Sept. 7–12, 2003.

[90] T. S. Sidhu, E. Demeter, and S. O. Faried, "Power system protection and control integration over Ethernet-based communication channels," in *Proc. IEEE CCECE 2004*, vol. 1, Niagara Falls, ON, May 2004, pp. 225–228.

[91] E. Demeter, T. S. Sidhu, and S. O. Faried, "An open system approach to power system protection and control integration," *IEEE Transactions on Power Delivery - accepted for publication.*

[92] E. Demeter, S. O. Faried, and T. S. Sidhu, "Signal phase shifting during synchrophasor measurements," in *Proc. IEEE CCECE 2005 - accepted for presentation*, Saskatoon, SK, 2005.

[93] G. Rockefeller, C. Wagner, J. Linders, K. Hicks, and D. Rizy, "Adaptive transmission relaying concepts for improved performance," *IEEE Transactions on Power Delivery*, vol. 3, no. 0885-8977, pp. 1446–1458, 1988.

[94] S. Horowitz, A. Phadke, and J. Thorpe, "Adaptive transmission system relaying," *IEEE Transactions on Power Delivery*, vol. 3, no. 0885-8977, pp. 1436–1445, 1988.

[95] G. Benmouyal, "An adaptive sampling-interval generator for digital relaying," *IEEE Transactions on Power Delivery*, vol. 4, no. 0885-8977, pp. 1602–1609, 1989.

[96] Y. Xia, A. David, and K. Li, "High-resistance faults on a multi-terminal line: analysis, simulated studies and an adaptive distance relaying scheme," *IEEE Transactions on Power Delivery*, vol. 9, no. 0885-8977, pp. 492–500, 1994.

[97] Y. Xia, K. Li, and A. David, "Adaptive relay setting for stand-alone digital distance protection," *IEEE Transactions on Power Delivery*, vol. 9, no. 0885-8977, pp. 480–491, 1994.

[98] J. Kumar, S. Venkata, and M. Damborg, "Adaptive transmission protection: concepts and computational issues," *IEEE Transactions on Power Delivery*, vol. 4, no. 0885-8977, pp. 177–185, 1989.

[99] A. Jongepier and L. van der Sluis, "Adaptive distance protection of double-circuit lines using artificial neural networks," *IEEE Transactions on Power Delivery*, vol. 12, no. 0885-8977, pp. 97–105, 1997.

[100] B. Chattopadhyay, M. Sachdev, and T. Sidhu, "An on-line relay coordination algorithm for adaptive protection using linear programming technique," *IEEE Transactions on Power Delivery*, vol. 11, no. 0885-8977, pp. 165–173, 1996.

[101] A. Jongepier and L. van der Sluis, "Adaptive distance protection of a double-circuit line," *IEEE Transactions on Power Delivery*, vol. 9, no. 0885-8977, pp. 1289–1297, 1994.

[102] V. Centeno, A. Phadke, A. Edris, J. Benton, M. Gaudi, and G. Michel, "An adaptive out-of-step relay [for power system protection]," *IEEE Transactions on Power Delivery*, vol. 12, no. 0885-8977, pp. 61–71, 1997.

[103] A. Girgis, A. Sallam, and A. El-Din, "An adaptive protection scheme for advanced series compensated (ASC) transmission lines," *IEEE Transactions on Power Delivery*, vol. 13, no. 0885-8977, pp. 414–420, 1998.

[104] IEEE Power System Relaying Committee, "Feasibility of adaptive protection and control," *IEEE Transactions on Power Delivery*, vol. 8, no. 0885-8977, pp. 975–983, 1993.

[105] A. Girgis, D. Hart, and W. Chang, "An adaptive scheme for digital protection of power transformers," *IEEE Transactions on Power Delivery*, vol. 7, no. 0885-8977, pp. 546–553, 1992.

[106] Z. Zhizhe and C. Deshu, "An adaptive approach in digital distance protection," *IEEE Transactions on Power Delivery*, vol. 6, no. 0885-8977, pp. 135–142, 1991.

[107] Y. Ohura, M. Suzuki, K. Yanagihashi, M. Yamaura, K. Omata, T. Nakamura, S. Mitamura, and H. Watanabe, "A predictive out-of-step protection system based on observation of the phase difference between substations," *IEEE Transactions on Power Delivery*, vol. 5, no. 0885-8977, pp. 1695–1704, 1990.

[108] Y. Hu, D. Novosel, M. Saha, and V. Leitloff, "An adaptive scheme for parallel-line distance protection," *IEEE Transactions on Power Delivery*, vol. 17, no. 0885-8977, pp. 105–110, 2002.

[109] G. H. Golub and C. F. Van Loan, *Matrix Computations*. Baltimore, MD: The Johns Hopkins University Press, 1996.

[110] C. Henville, "Combined use of definite and inverse time overcurrent elements assists in transmission line ground relay coordination," *IEEE Transactions on Power Delivery*, vol. 8, no. 0885-8977, pp. 925–932, 1993.

[111] G. Benmouyal *et al.*, "IEEE standard inverse-time characteristic equations for overcurrent relays," *IEEE Transactions on Power Delivery*, vol. 14, no. 0885-8977, pp. 868–872, 1999.

[112] A. Apostolov *et al.*, "IEEE/PSRC working group report on considerations in setting instantaneous overcurrent relays on transmission lines," *IEEE Transactions on Power Delivery*, vol. 14, no. 0885-8977, pp. 116–125, 1999.

[113] A. Urdaneta, R. Nadira, and L. Perez Jimenez, "Optimal coordination of directional overcurrent relays in interconnected power systems," *IEEE Transactions on Power Delivery*, vol. 3, no. 0885-8977, pp. 903–911, 1988.

[114] G. Benmouyal, "Design of a digital multi-curve time-overcurrent relay," *IEEE Transactions on Power Delivery*, vol. 6, no. 0885-8977, pp. 656–665, 1991.

[115] G. Benmouyal, "Design of a digital multi-curve time-overcurrent relay," *IEEE Transactions on Power Delivery*, vol. 5, no. 0885-8977, pp. 1725–1731, 1990.

[116] IEEE Committee Report, "Computer representation of overcurrent relay characteristics," *IEEE Transactions on Power Delivery*, vol. 4, no. 0885-8977, pp. 1659–1667, 1989.

[117] A. R. van C. Warrington, *Protective relays: their theory and practice*. New York, NY: Chapman and Hall, 1977.

[118] H. Altuve, G. Benmouyal, J. Roberts, and D. Tziouvaras, "Transmission line differential protection with an enhanced characteristic," in *Proc. Eighth IEE International Conference on Developments in Power System Protection, 2004*, 2004, pp. 414 – 419.

[119] L. Gyugyi, C. Schauder, S. Williams, T. Rietman, D. Torgerson, and A. Edris, "The unified power flow controller: a new approach to power transmission control," *IEEE Transactions on Power Delivery*, vol. 10, no. 0885-8977, pp. 1085–1097, 1995.

[120] H. Wang, "A unified model for the analysis of FACTS devices in damping power system oscillations. iii. unified power flow controller," *IEEE Transactions on Power Delivery*, vol. 15, no. 0885-8977, pp. 978–983, 2000.

[121] C. Schauder, E. Stacey, M. Lund, L. Gyugyi, L. Kovalsky, A. Keri, A. Mehraban, and A. Edris, "AEP UPFC project: installation, commissioning and operation of the +160 MVA STATCOM (phase I)," *IEEE Transactions on Power Delivery*, vol. 13, no. 0885-8977, pp. 1530–1535, 1998.

[122] K. Sen and E. Stacey, "UPFC-unified power flow controller: theory, modeling, and applications," *IEEE Transactions on Power Delivery*, vol. 13, no. 0885-8977, pp. 1453–1460, 1998.

[123] H. Wang, F. Swift, and M. Li, "A unified model for the analysis of FACTS devices in damping power system oscillations. ii. multi-machine power systems," *IEEE Transactions on Power Delivery*, vol. 13, no. 0885-8977, pp. 1355–1362, 1998.

[124] C. Schauder, L. Gyugyi, M. Lund, D. Hamai, T. Rietman, D. Torgerson, and A. Edris, "Operation of the unified power flow controller (UPFC) under practical constraints," *IEEE Transactions on Power Delivery*, vol. 13, no. 0885-8977, pp. 630–639, 1998.

[125] A. Keri, A. Mehraban, X. Lombard, A. Eiriachy, and A. Edris, "Unified power flow controller (UPFC): modeling and analysis," *IEEE Transactions on Power Delivery*, vol. 14, no. 0885-8977, pp. 648–654, 1999.

[126] A. Edris, "Facts technology development: an update," *IEEE Power Engineering Review*, vol. 20, no. 3, pp. 4–9, Mar. 2000.

[127] A. Edris, A. Mehraban, M. Rahman, L. Gyugyi, S. Arabi, and T. Reitman, "Controlling the flow of real and reactive power," *IEEE Computer Applications in Power*, vol. 11, no. 1, pp. 20 – 25, Jan. 1998.

[128] J. Tan, P. Crossley, P. McLaren, P. Gale, I. Hall, and J. Farrell, "Application of a wide area backup protection expert system to prevent cascading outages," *IEEE Transactions on Power Delivery*, vol. 17, no. 0885-8977, pp. 375–380, 2002.

[129] C. Leon, M. Mejias, J. Luque, and F. Gonzalo, "Expert system for the integrated management of a power utility's communication system," *IEEE Transactions on Power Delivery*, vol. 14, no. 0885-8977, pp. 1208–1212, 1999.

[130] J. Mitsche, "Stretching the limits of power system analysis," *IEEE Computer Applications in Power*, vol. 6, no. 0895-0156, pp. 16–21, 1993.

[131] I. Roytelman and V. Ganesan, "Coordinated local and centralized control in distribution management systems," *IEEE Transactions on Power Delivery*, vol. 15, no. 0885-8977, pp. 718–724, 2000.

[132] S. Corrigan and J. Linders, "System reliability revisited," *IEEE Computer Applications in Power*, vol. 11, no. 0895-0156, pp. 37–42, 1998.

[133] G. Heydt, C. Liu, A. Phadke, and V. Vittal, "Solution for the crisis in electric power supply," *IEEE Computer Applications in Power*, vol. 14, no. 0895-0156, pp. 22–30, 2001.

[134] K. Vu, M. Begouic, and D. Novosel, "Grids get smart protection and control," *IEEE Computer Applications in Power*, vol. 10, no. 0895-0156, pp. 40–44, 1997.

[135] B. Ingelsson, P.-O. Lindstrom, D. Karlsson, G. Runvik, and J.-O. Sjodin, "Wide-area protection against voltage collapse," *IEEE Computer Applications in Power*, vol. 10, no. 0895-0156, pp. 30–35, 1997.

APPENDIX A

THE TEST SYSTEM

The test system used is shown in Fig.(A.1). The parameters of the system are listed in Tables (A.1) to (A.4).

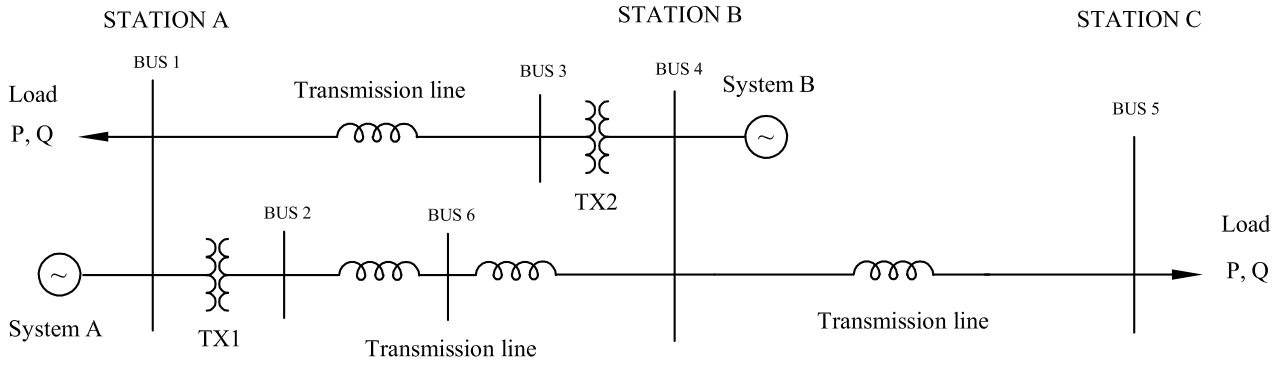

Figure A.1: Test system

Table A.1: Test system transmission lines parameters

Voltage [kV L-L]	From Bus	To Bus	R_1 [Ω]	R_0 [Ω]	L_1 [H]	L_0 [H]	C_1 [F]	C_0 [F]
138	4	5	4.46e-01	1.35e+01	3.27e-02	1.44e-01	4.46e-07	2.71e-07
138	2	6	3.18e-01	9.66e+00	2.33e-02	1.03e-01	3.19e-07	1.94e-07
138	6	4	2.55e-01	7.73e+00	1.87e-02	8.25e-02	2.55e-07	1.55e-07
230	1	3	4.46e-01	1.35e+01	3.27e-02	1.44e-01	4.46e-07	2.71e-07

Table A.2: Equivalent systems parameters

System	Voltage [kV] L-L	Internal connection	Short circuit level [MVA]	X/R ratio	Initial phase angle [deg]
A	230	Yg	10,000	5	0
B	138	Yg	1,500	2	-10

Table A.3: Test system loads parameters

Station	Voltage [kV] L-L	Real load [MW]	Inductive load [MVAR]	Capacitive load [MVAR]
A	230	0	0	0
C	138	20	0.4	0

Table A.4: Test system transformers parameters

Connection TX 1	Yg-Y
Connection TX 2	Y-Yg
Rated power [VA]	2.50E+008
Winding 1 impedance [p.u.]	0.002 + j 0.08
Winding 2 impedance [p.u.]	0.002 + j 0.08
Magnetization resistance [p.u.]	500
Magnetization reactance [p.u.]	500

APPENDIX B

RESULTS FOR LINE-TO-LINE AND 3-LINE FAULTS

This appendix contains the line-to-line and 3-line curves for the radial line, transmission line and transformer tests.

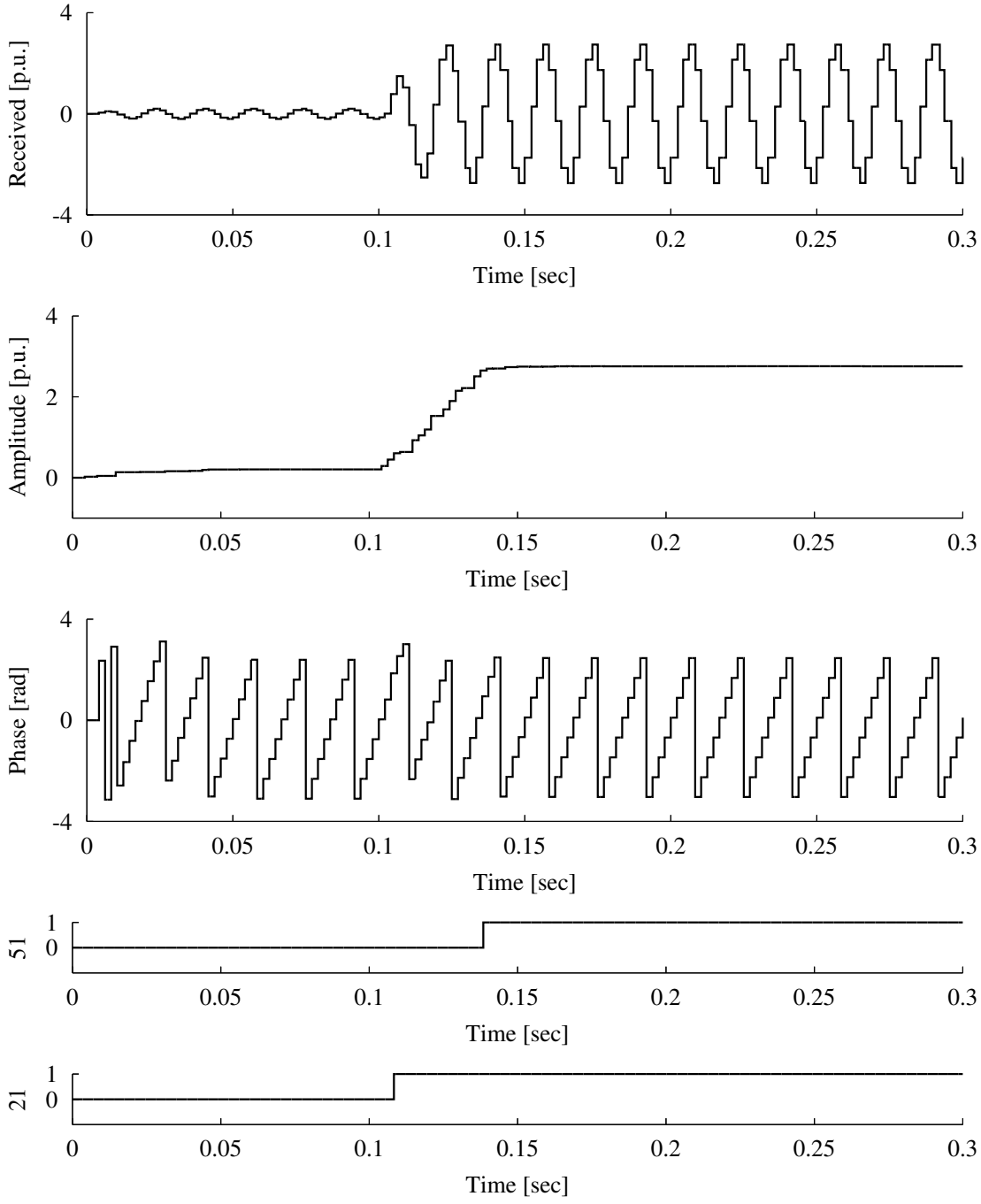

Figure B.1: GPS-LSE algorithm performance with 8 samples per cycle over slow network during a line-to-line fault at location F1

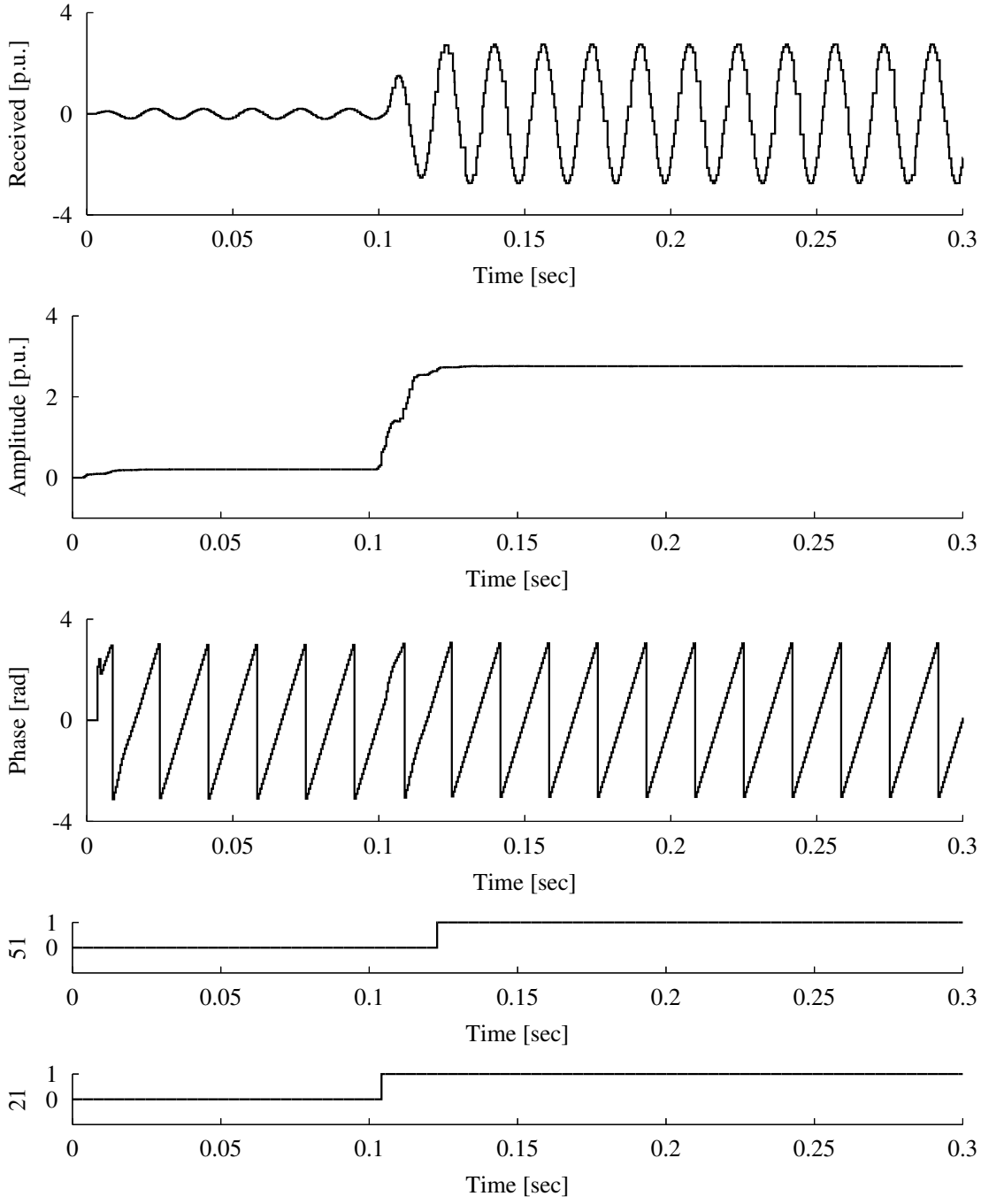

Figure B.2: GPS-LSE algorithm performance with 32 samples per cycle over slow network during a line-to-line fault at location F1

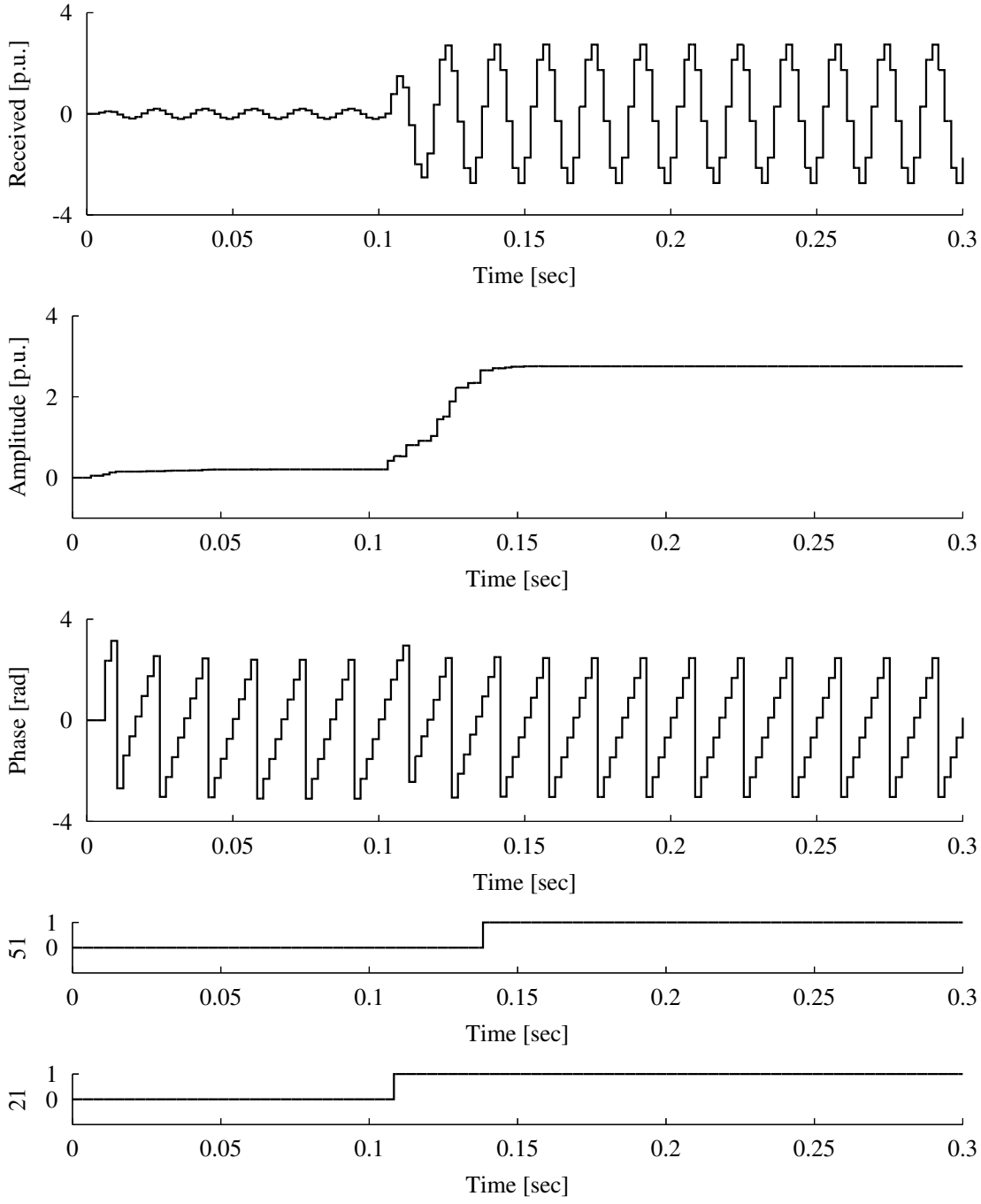

Figure B.3: GPS-LSE algorithm performance with 8 samples per cycle over fast network during a line-to-line fault at location F1

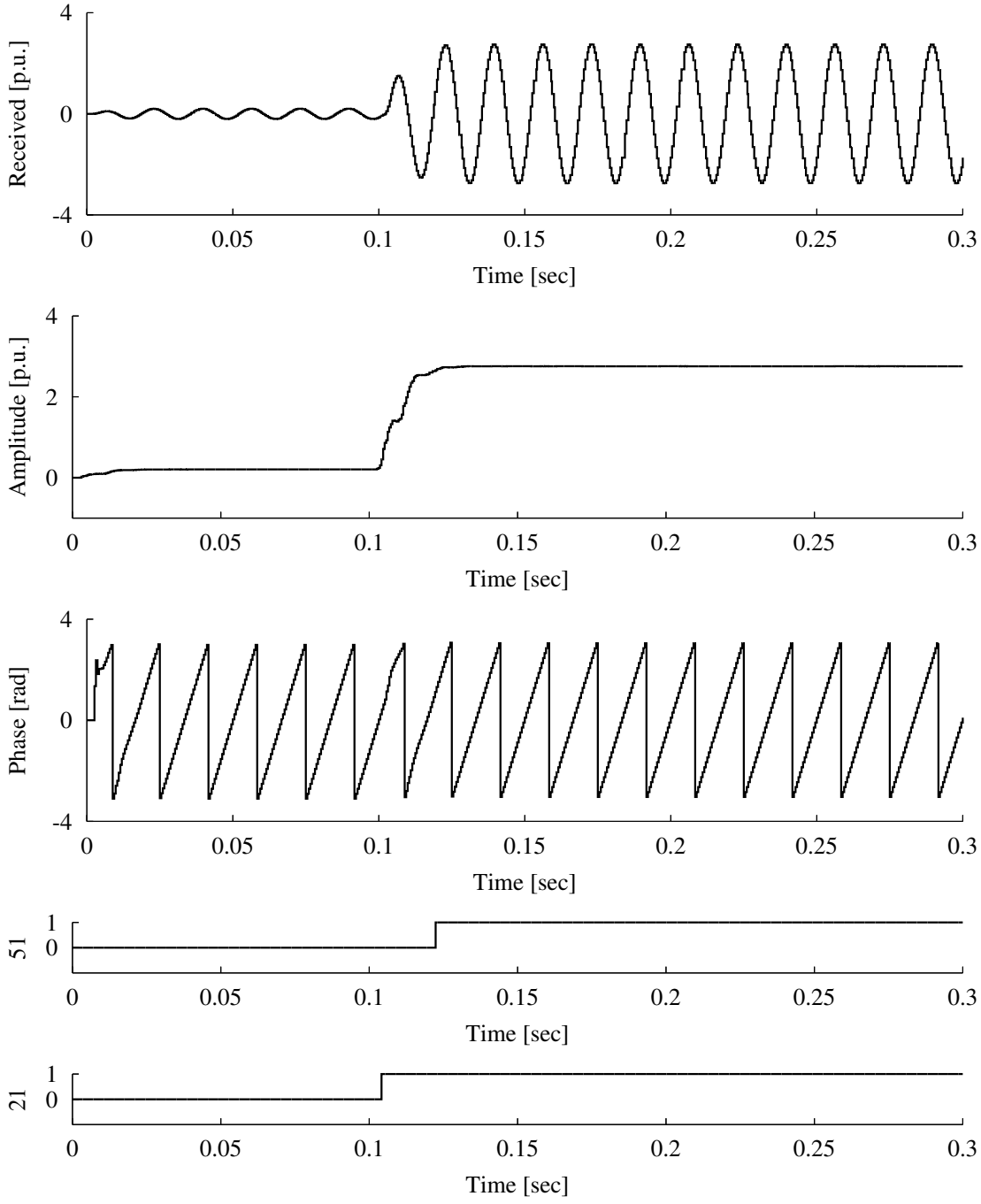

Figure B.4: GPS-LSE algorithm performance with 32 samples per cycle over fast network during a line-to-line fault at location F1

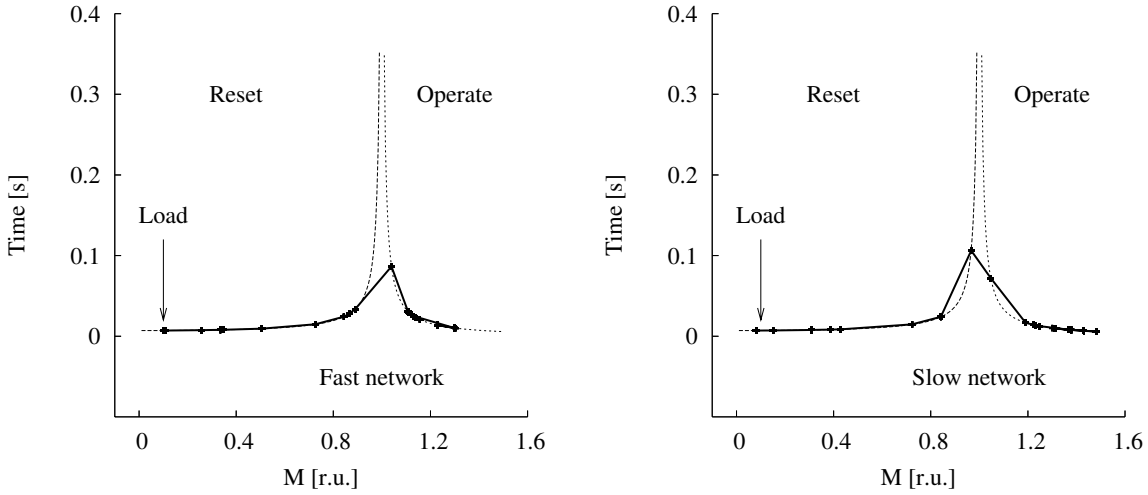

Figure B.5: Overcurrent protection performance of the FF algorithm with 8 samples per cycle during a line-to-line fault at location F1

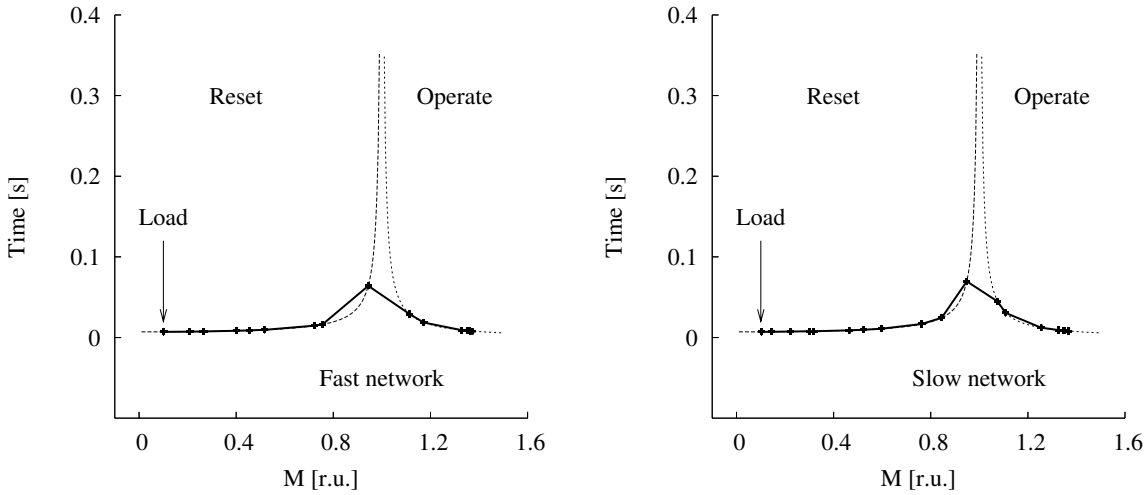

Figure B.6: Overcurrent protection performance of the GPS-LSE algorithm with 8 samples per cycle during a line-to-line fault at location F1

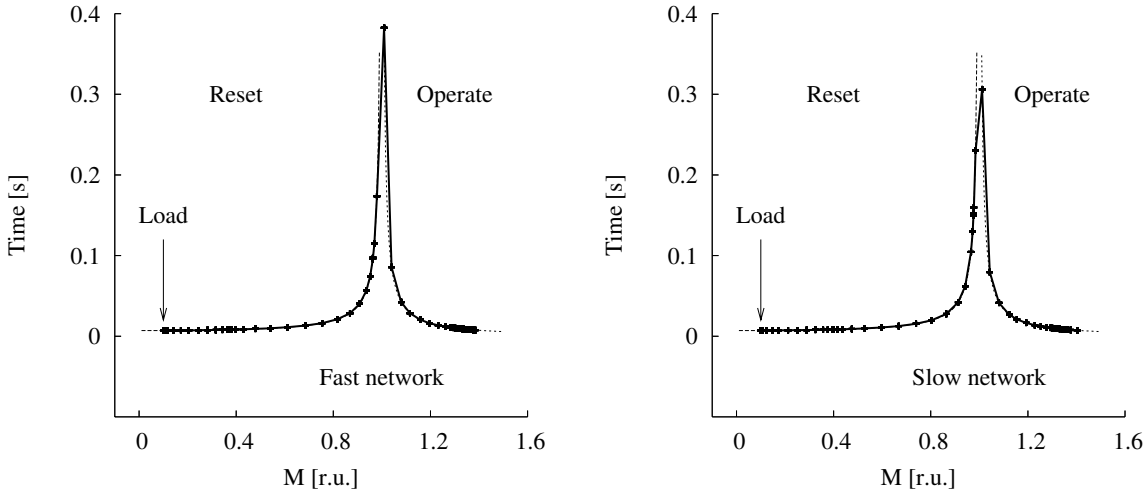

Figure B.7: Overcurrent protection performance of the FF algorithm with 32 samples per cycle during a line-to-line fault at location F1

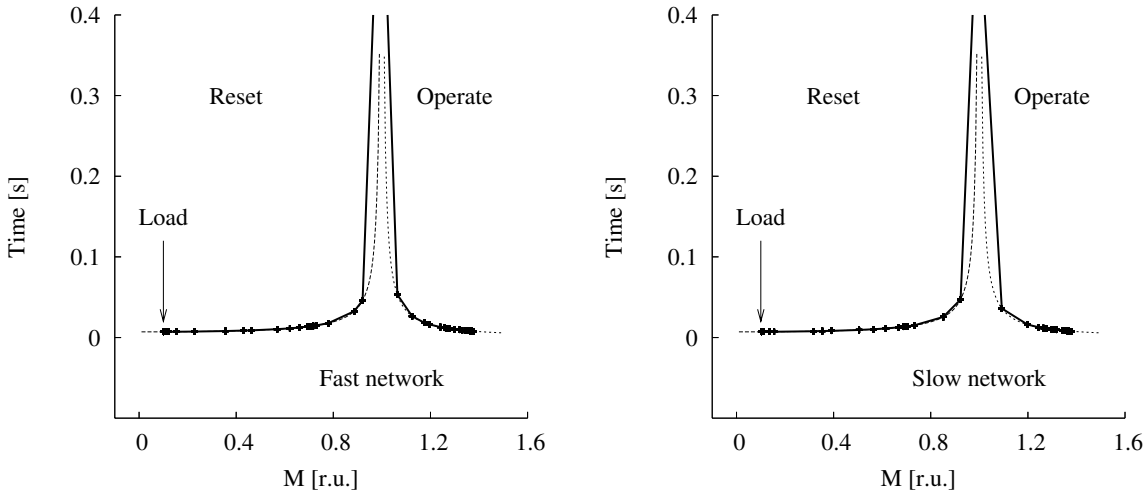

Figure B.8: Overcurrent protection performance of the GPS-LSE algorithm with 32 samples per cycle during a line-to-line fault at location F1

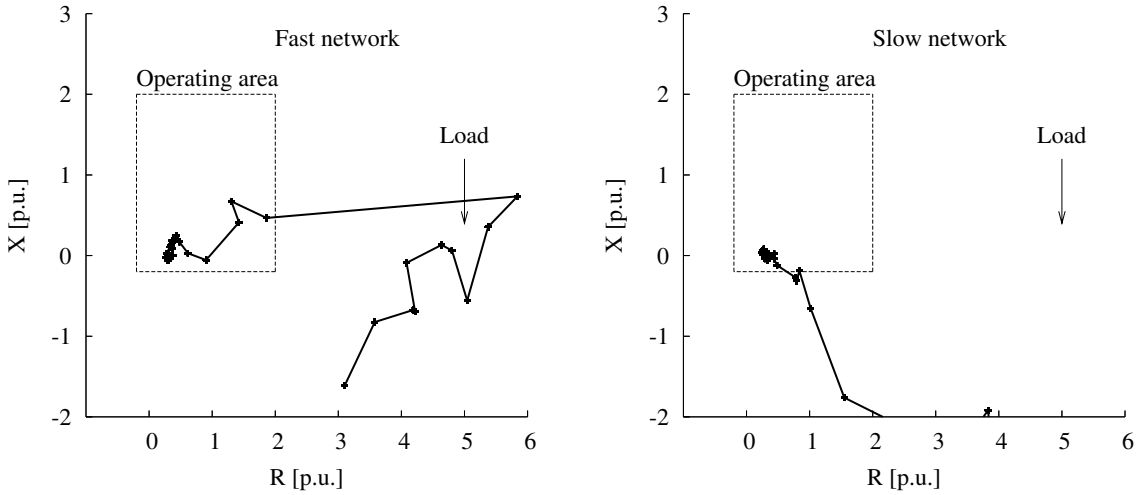

Figure B.9: Impedance protection performance of the FF algorithm with 8 samples per cycle during a line-to-line fault at location F1

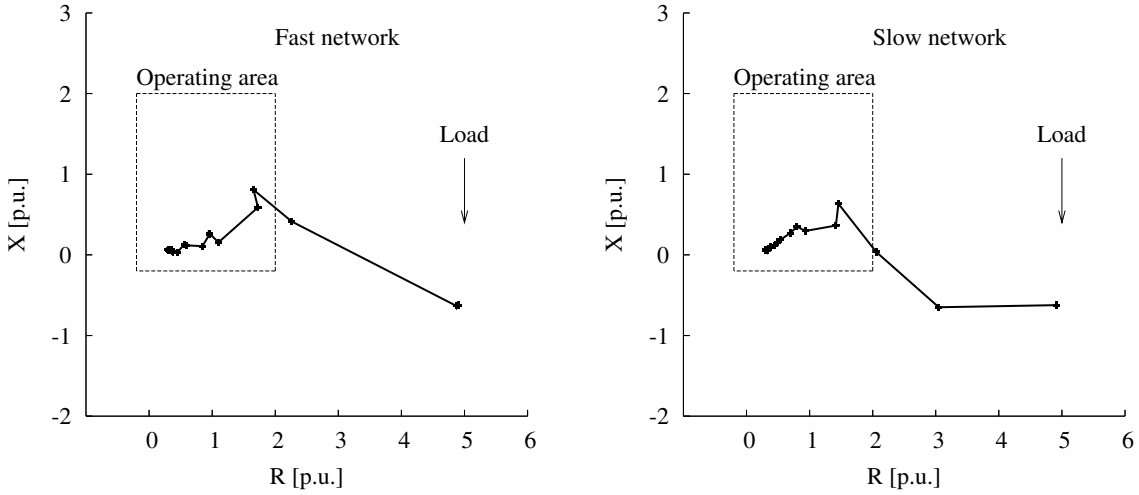

Figure B.10: Impedance protection performance of the GPS-LSE algorithm with 8 samples per cycle during a line-to-line fault at location F1

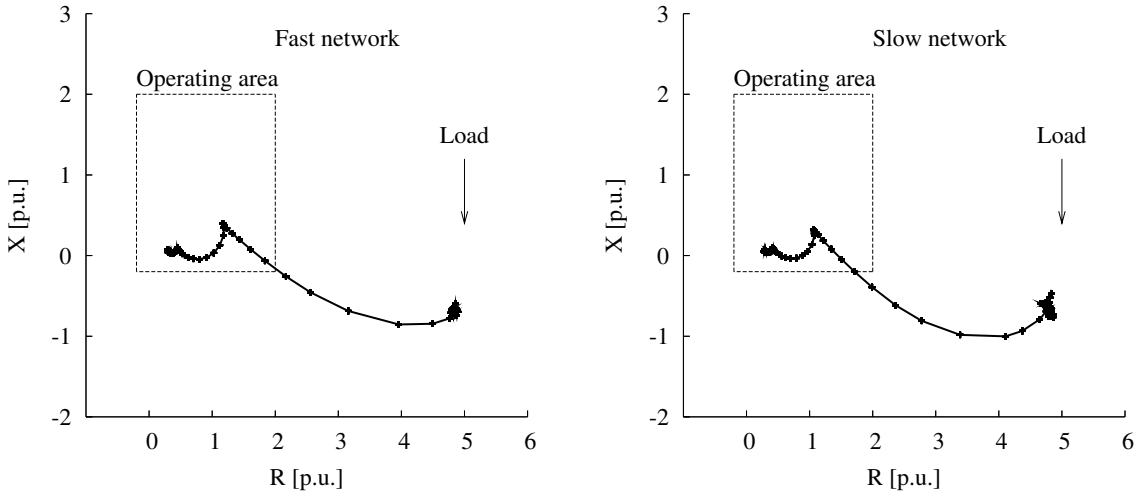

Figure B.11: Impedance protection performance of the FF algorithm with 32 samples per cycle during a line-to-line fault at location F1

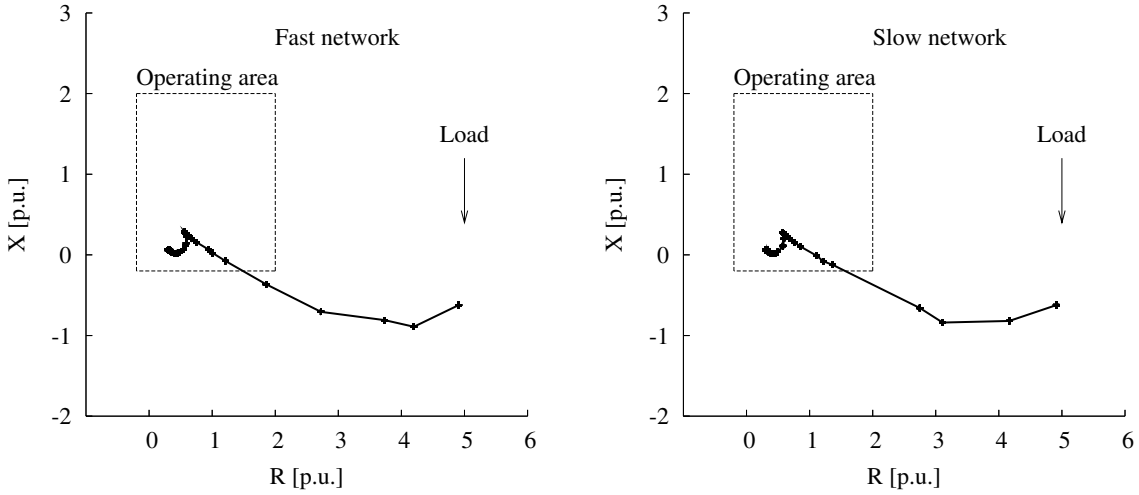

Figure B.12: Impedance protection performance of the GPS-LSE algorithm with 32 samples per cycle during a line-to-line fault at location F1

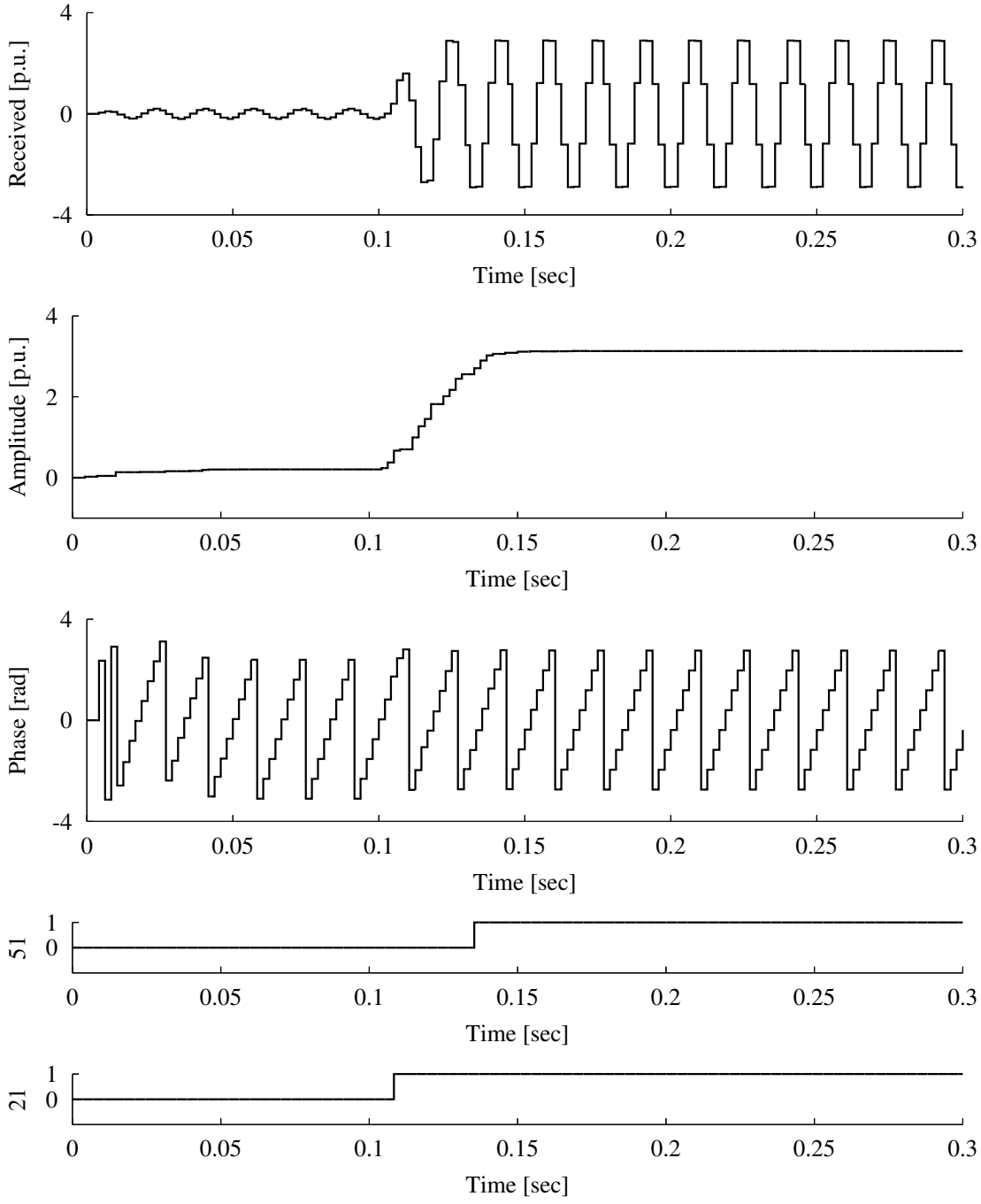

Figure B.13: GPS-LSE algorithm performance with 8 samples per cycle over slow network during a 3-line fault at location F1

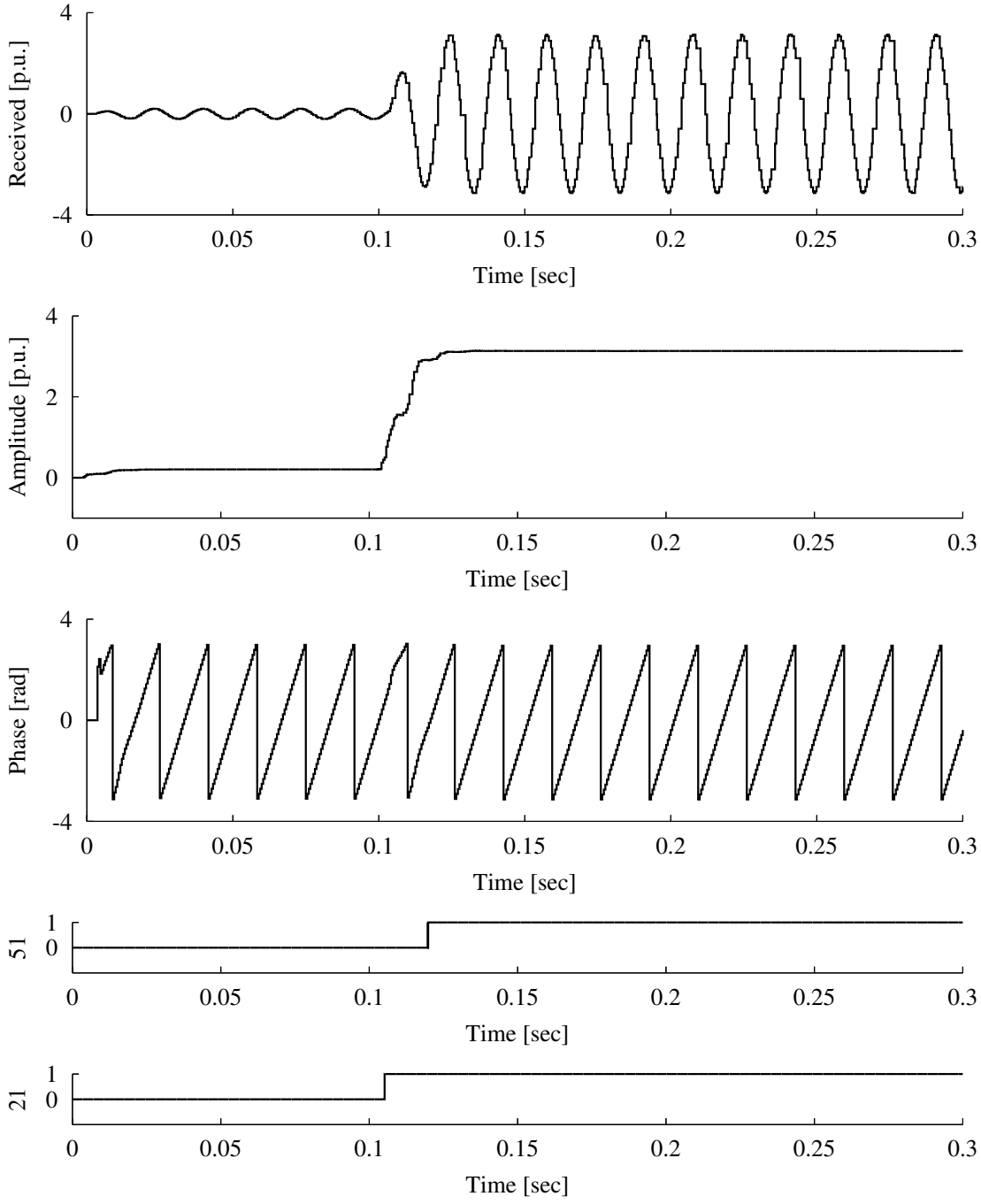

Figure B.14: GPS-LSE algorithm performance with 32 samples per cycle over slow network during a 3-line fault at location F1

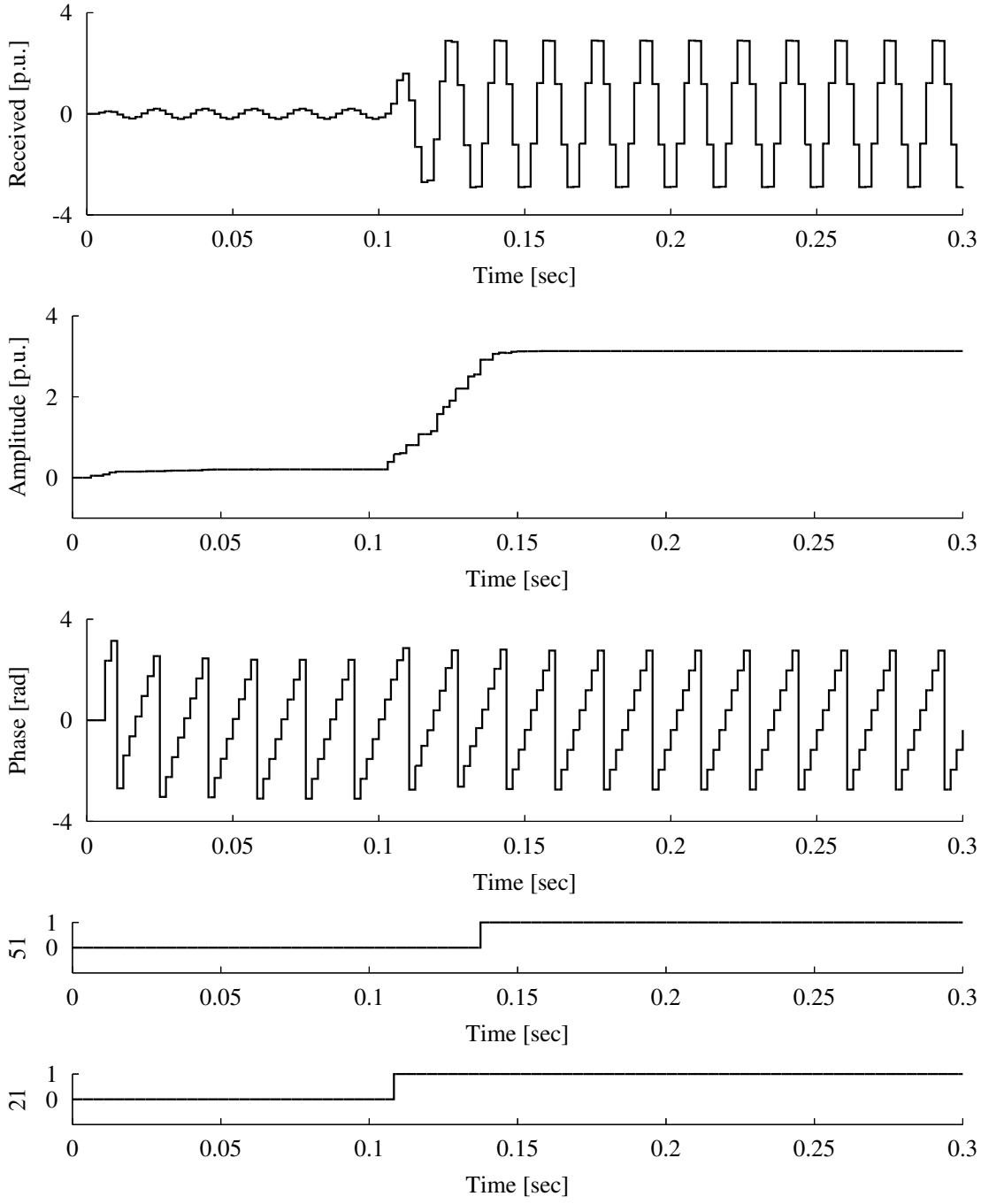

Figure B.15: GPS-LSE algorithm performance with 8 samples per cycle over fast network during a 3-line fault at location F1

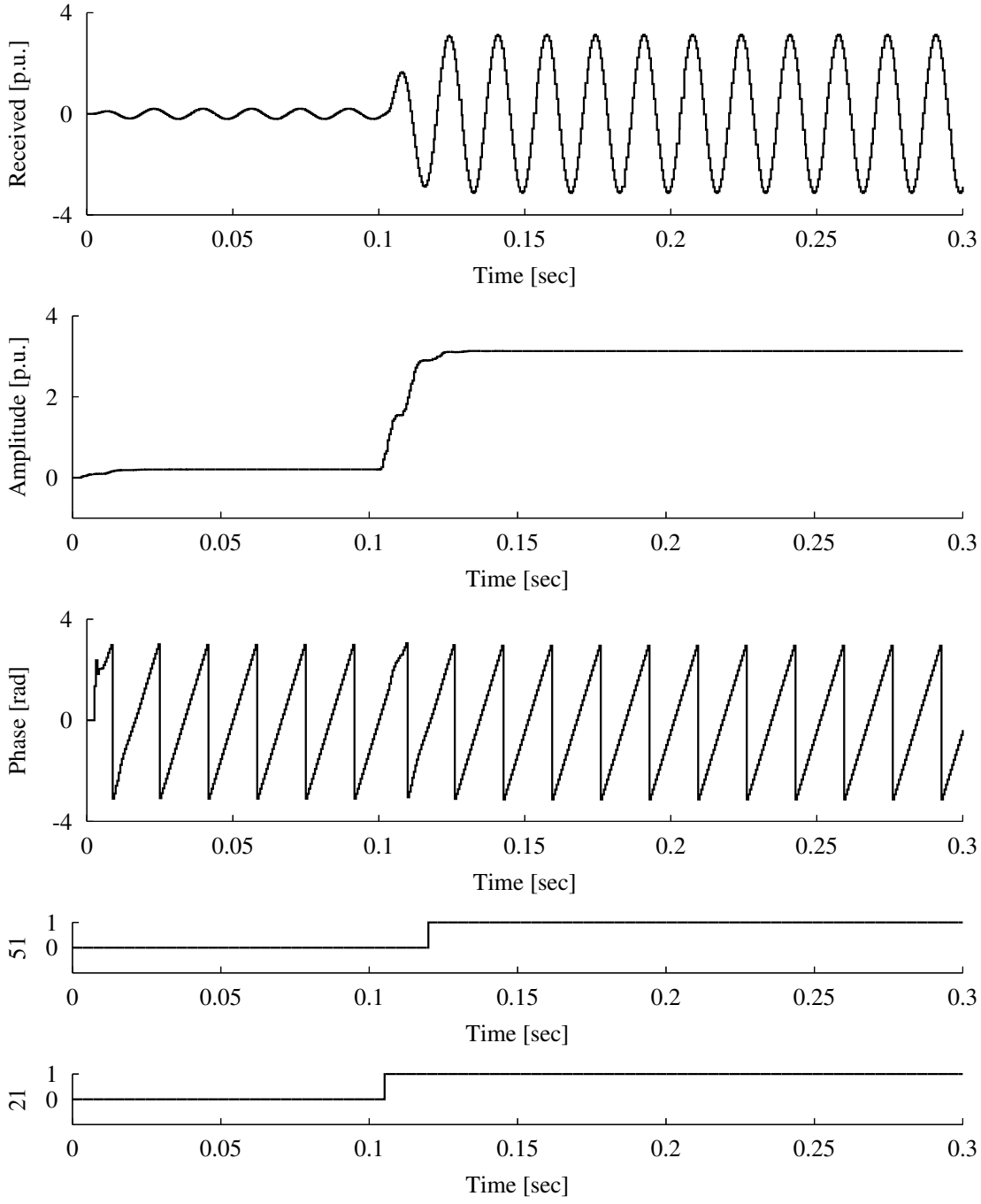

Figure B.16: GPS-LSE algorithm performance with 32 samples per cycle over fast network during a 3-line fault at location F1

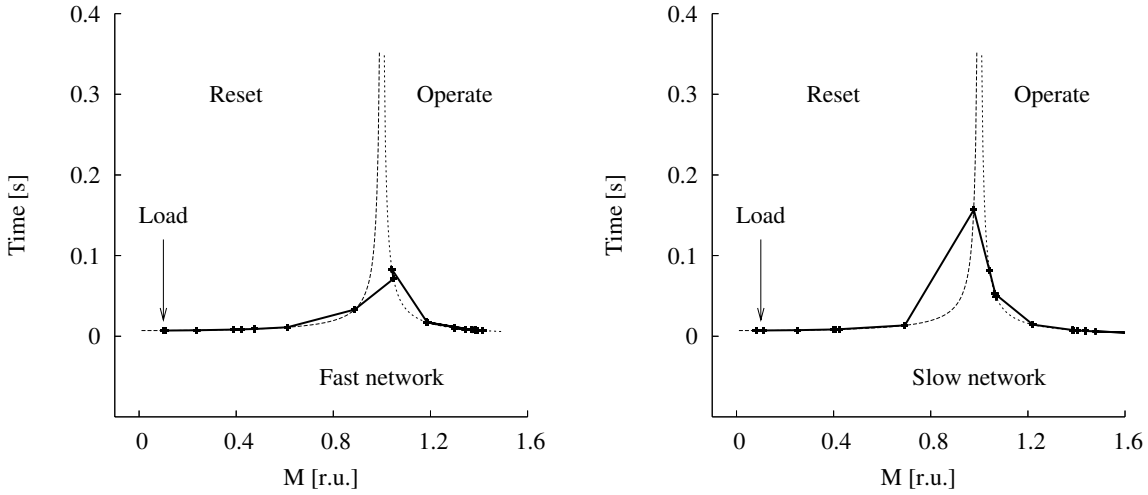

Figure B.17: Overcurrent protection performance of the FF algorithm with 8 samples per cycle during a 3-line fault at location F1

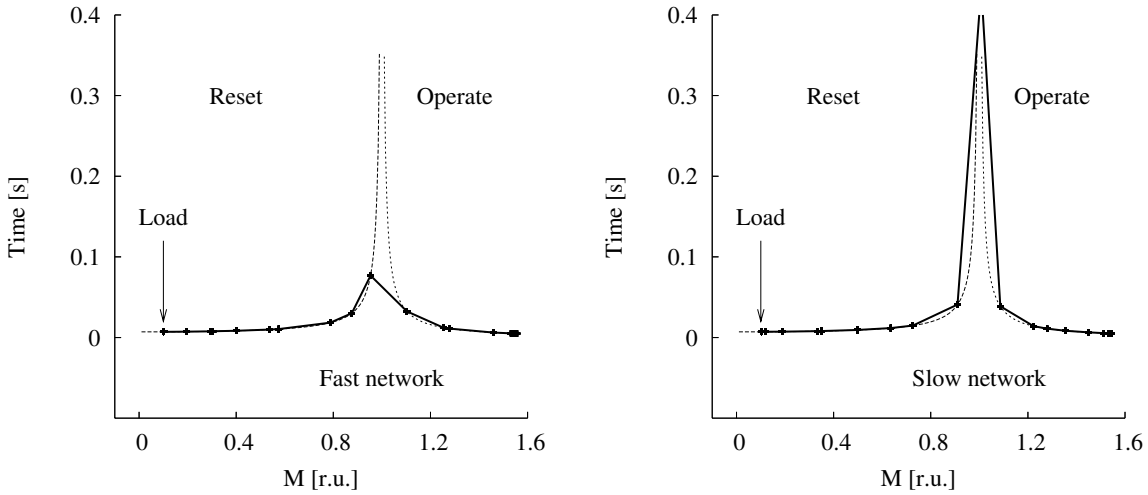

Figure B.18: Overcurrent protection performance of the GPS-LSE algorithm with 8 samples per cycle during a 3-line fault at location F1

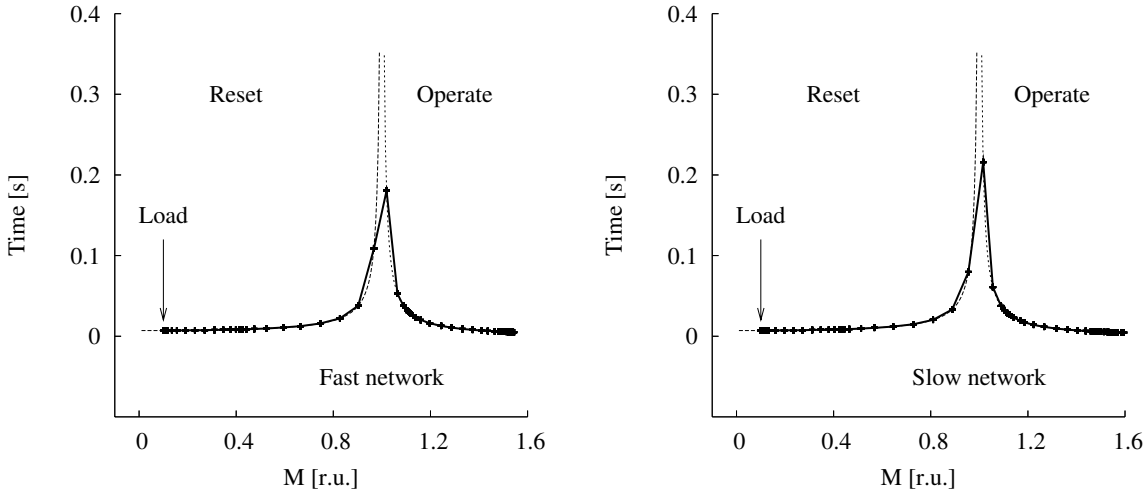

Figure B.19: Overcurrent protection performance of the FF algorithm with 32 samples per cycle during a 3-line fault at location F1

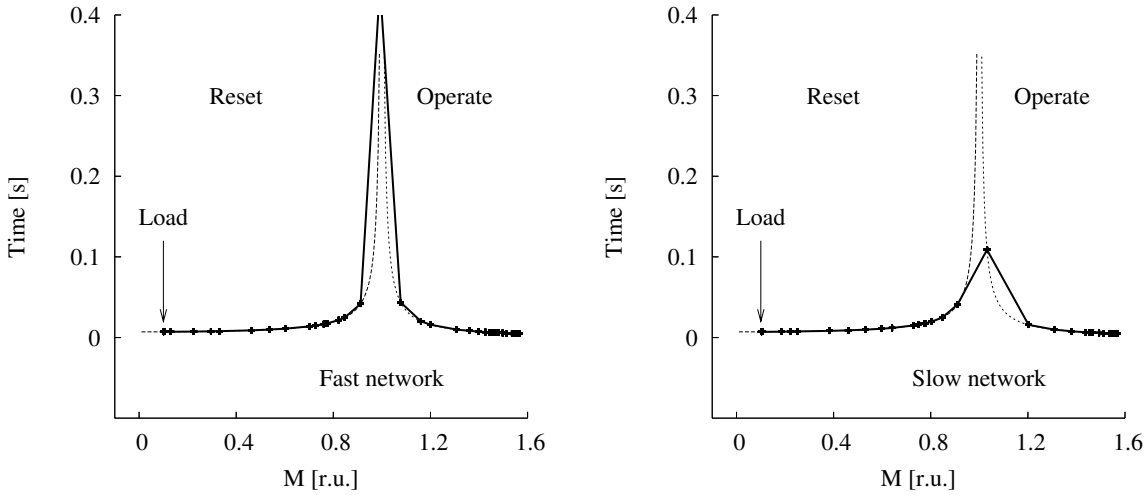

Figure B.20: Overcurrent protection performance of the GPS-LSE algorithm with 32 samples per cycle during a 3-line fault at location F1

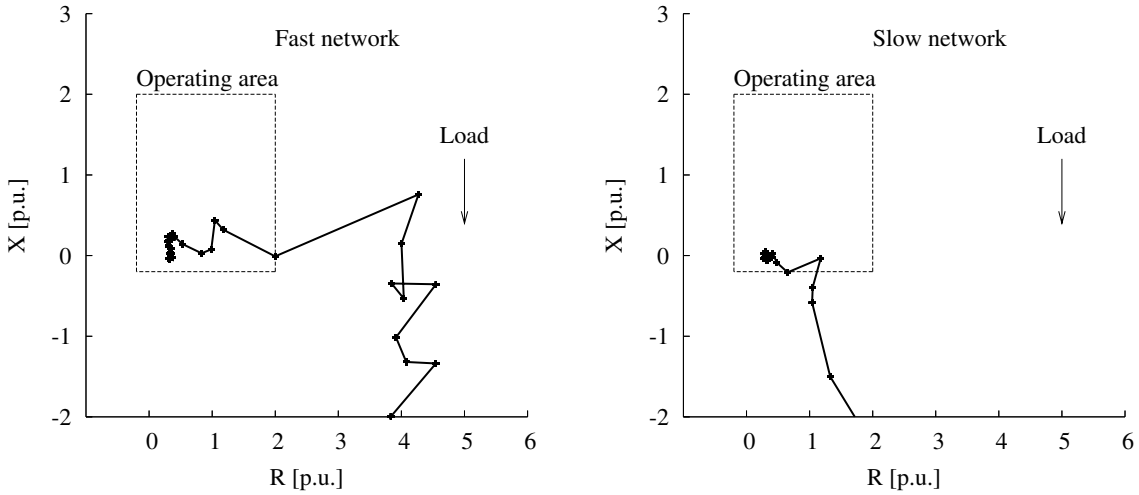

Figure B.21: Impedance protection performance of the FF algorithm with 8 samples per cycle during a 3-line fault at location F1

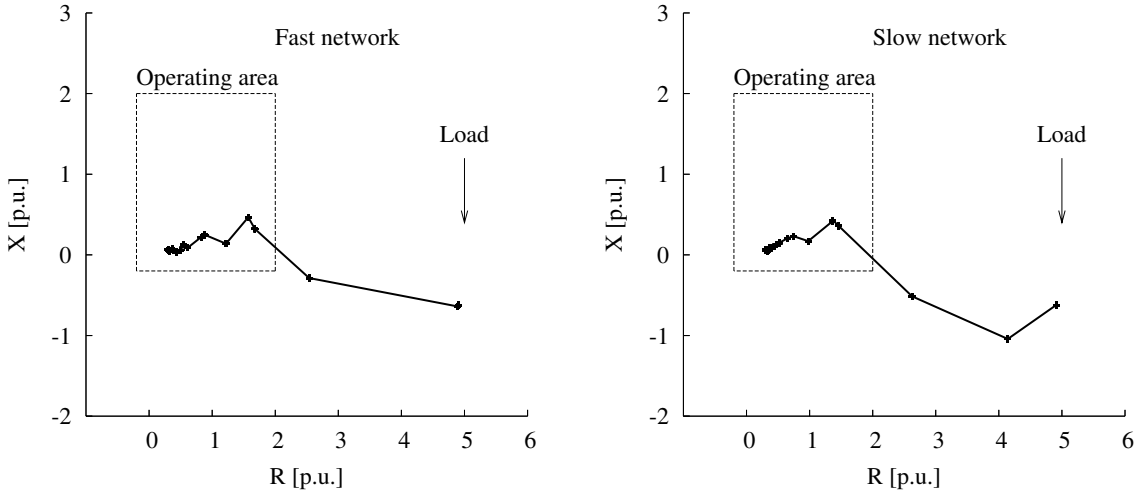

Figure B.22: Impedance protection performance of the GPS-LSE algorithm with 8 samples per cycle during a 3-line fault at location F1

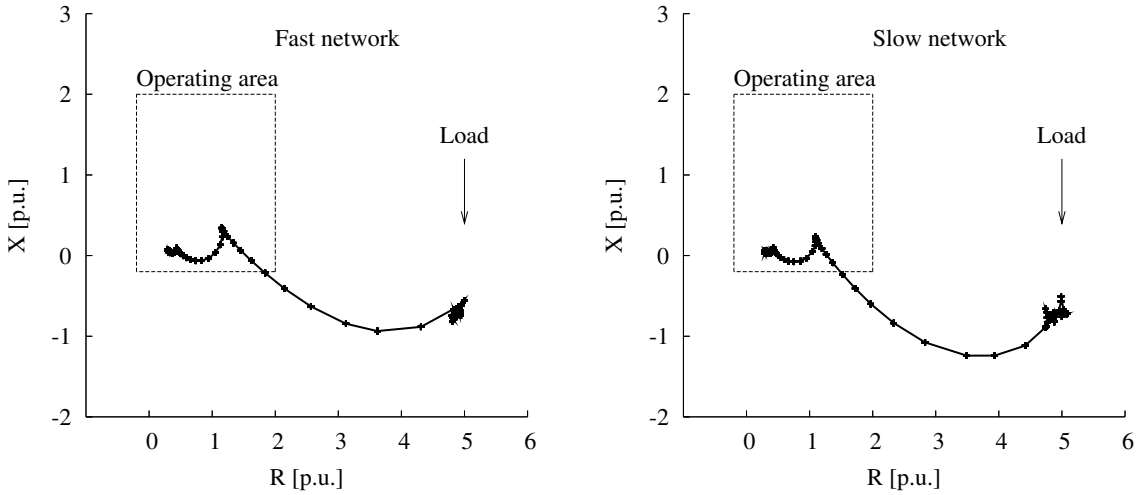

Figure B.23: Impedance protection performance of the FF algorithm with 32 samples per cycle during a 3-line fault at location F1

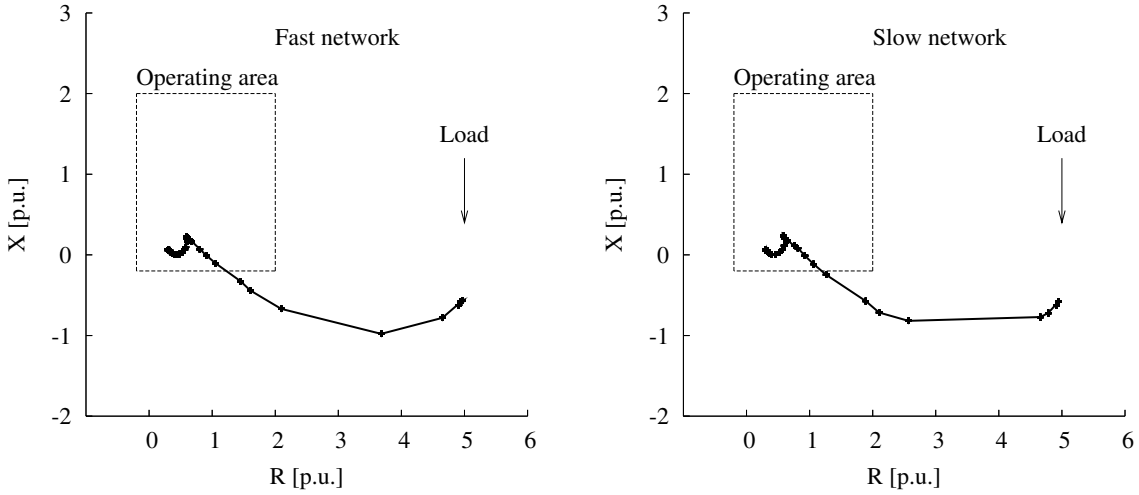

Figure B.24: Impedance protection performance of the GPS-LSE algorithm with 32 samples per cycle during a 3-line fault at location F1

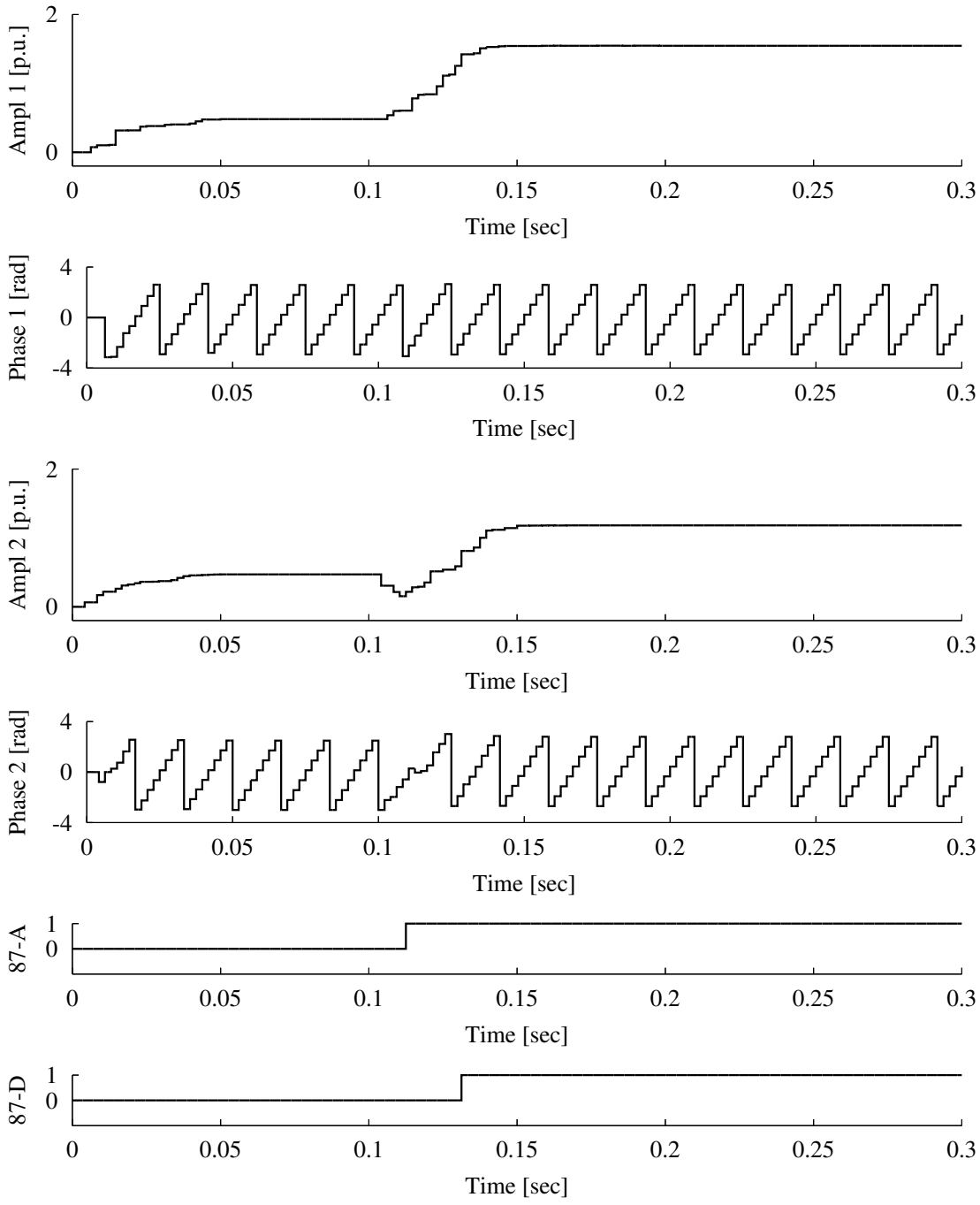

Figure B.25: GPS-LSE algorithm performance with 8 samples per cycle over slow network during a line-to-line fault at location F2

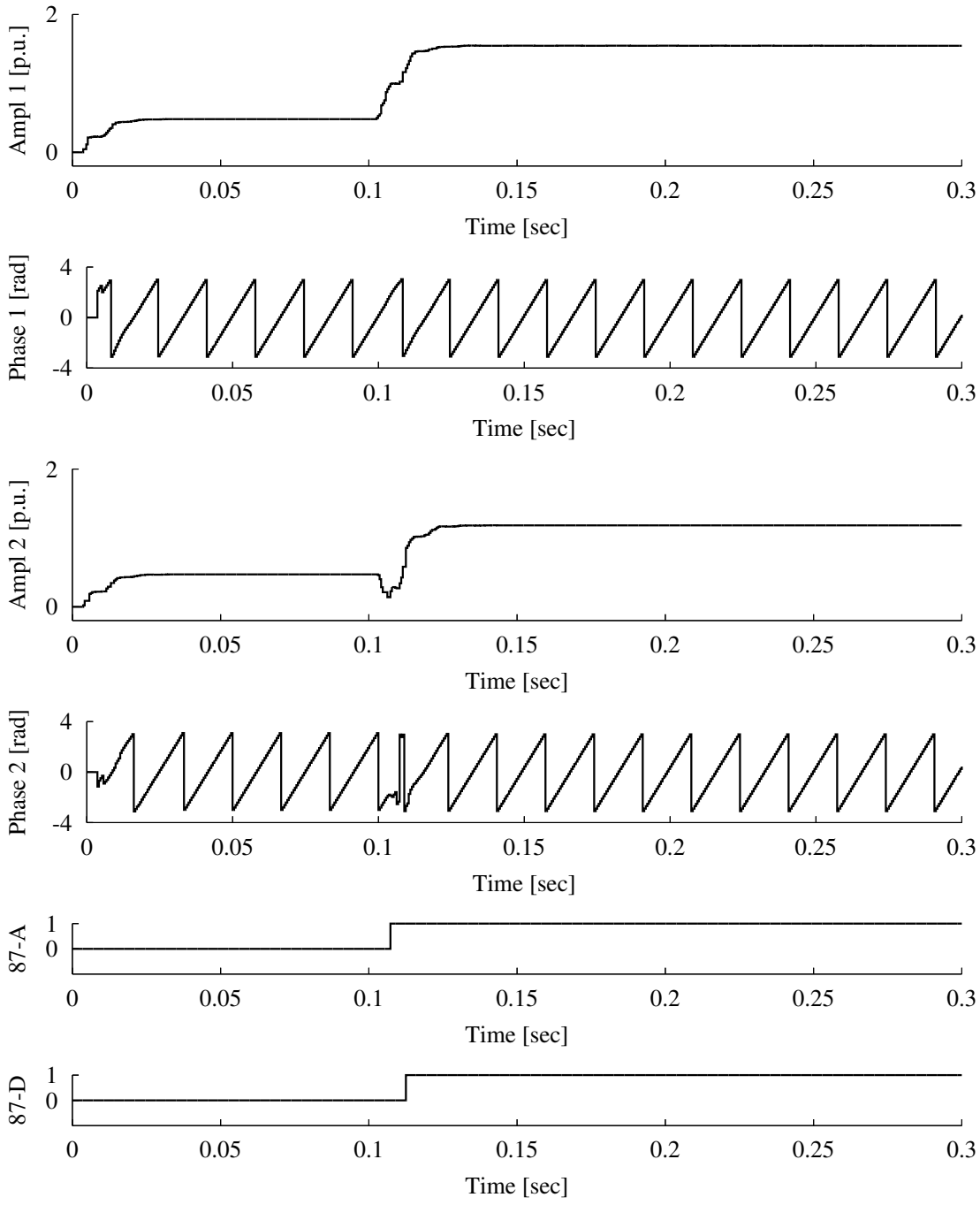

Figure B.26: GPS-LSE algorithm performance with 32 samples per cycle over slow network during a line-to-line fault at location F2

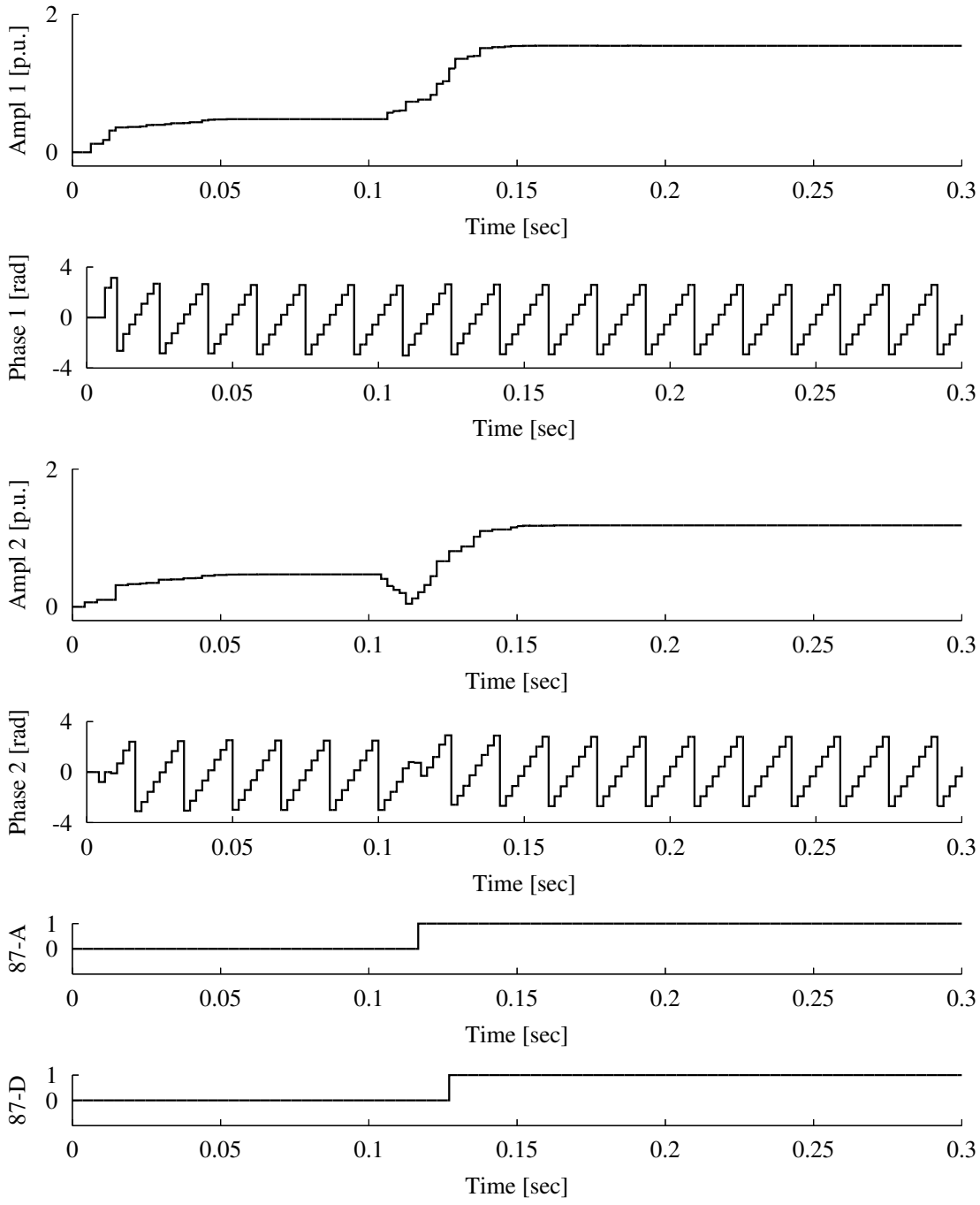

Figure B.27: GPS-LSE algorithm performance with 8 samples per cycle over fast network during a line-to-line fault at location F2

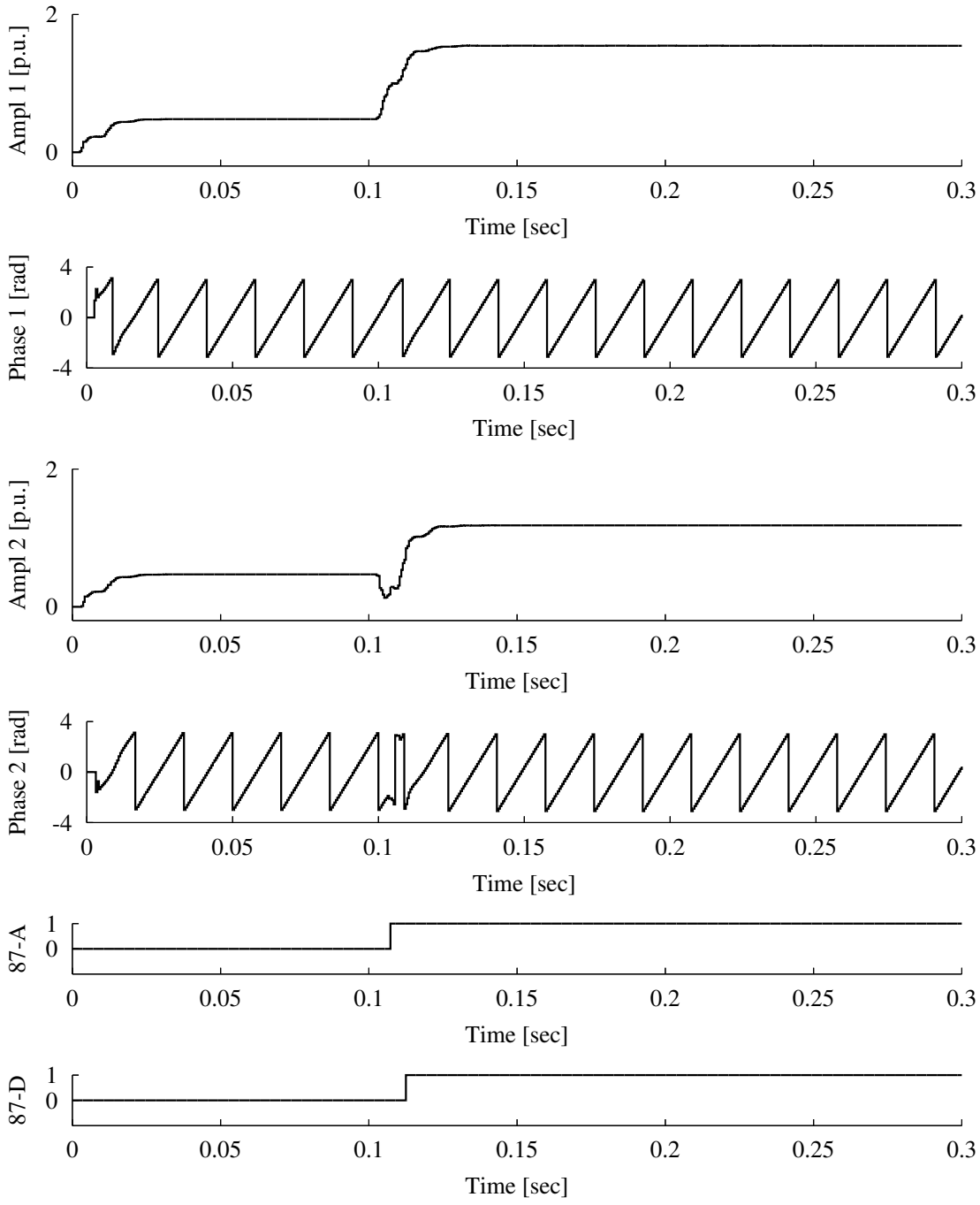

Figure B.28: GPS-LSE algorithm performance with 32 samples per cycle over fast network during a line-to-line fault at location F2

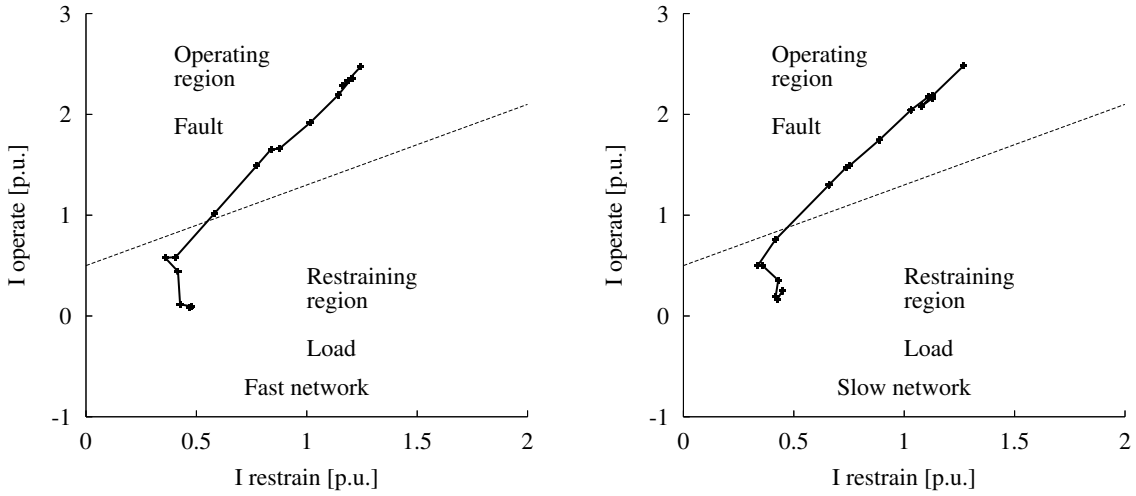

Figure B.29: Percentage differential protection performance of the FF algorithm with 8 samples per cycle during a line-to-line fault at location F2

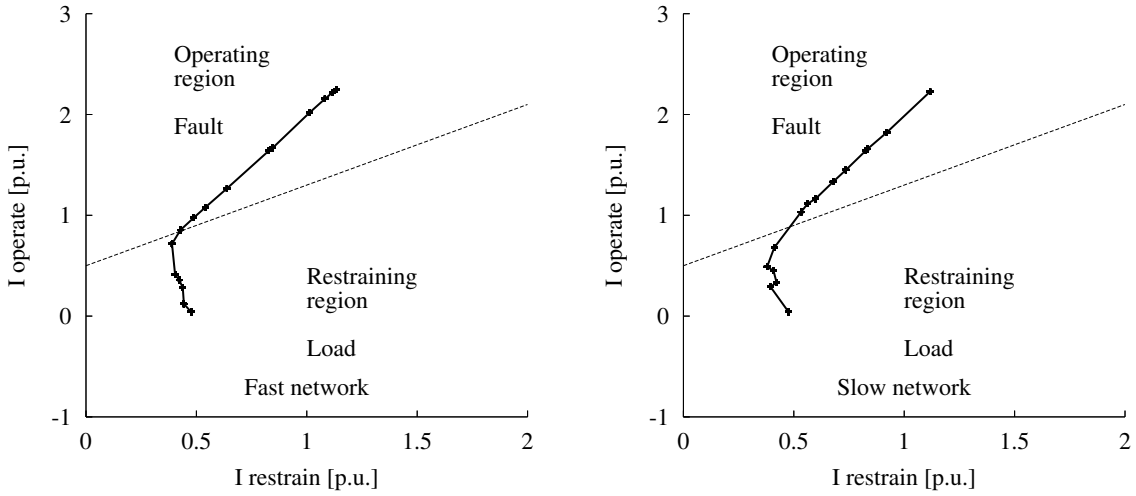

Figure B.30: Percentage differential protection performance of the GPS-LSE algorithm with 8 samples per cycle during a line-to-line fault at location F2

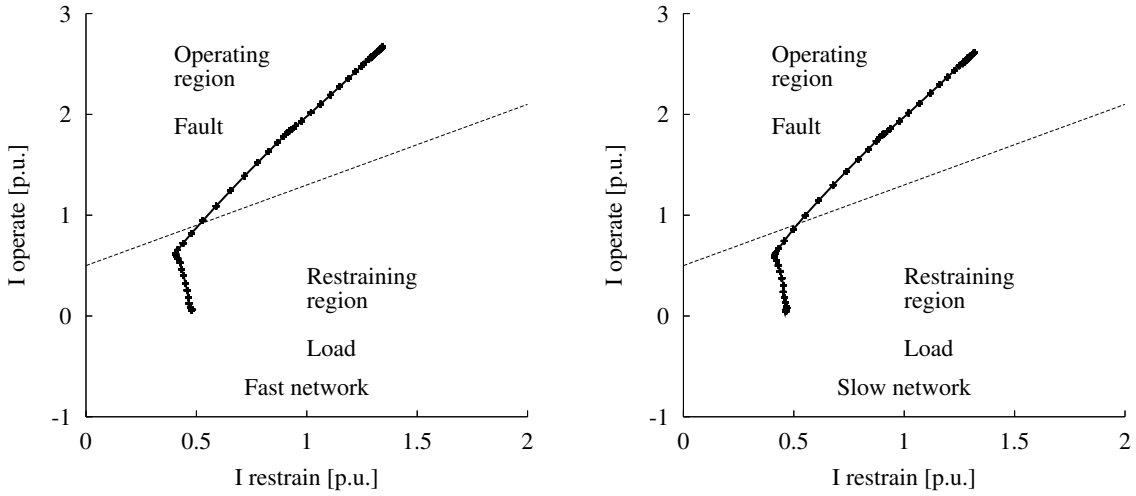

Figure B.31: Percentage differential protection performance of the FF algorithm with 32 samples per cycle during a line-to-line fault at location F2

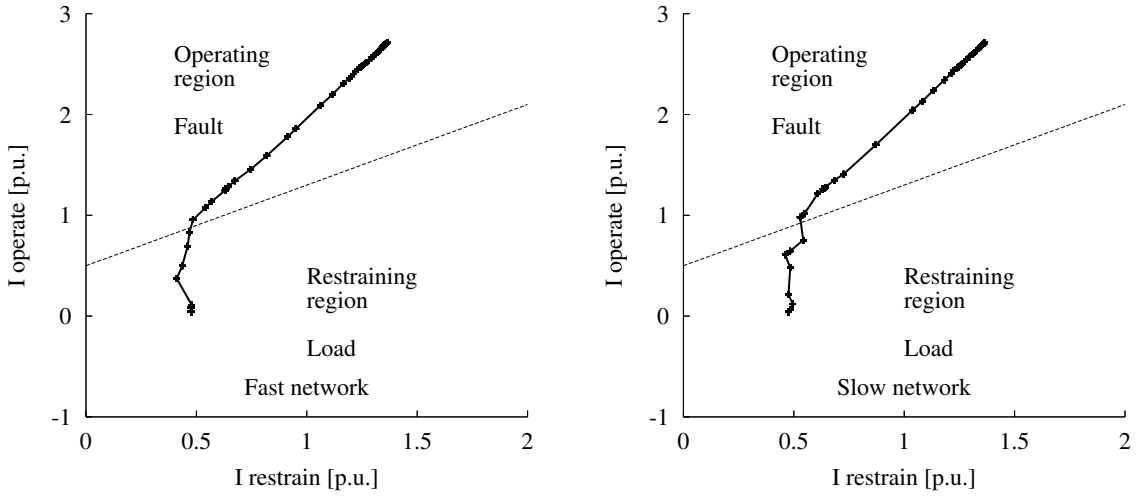

Figure B.32: Percentage differential protection performance of the GPS-LSE algorithm with 32 samples per cycle during a line-to-line fault at location F2

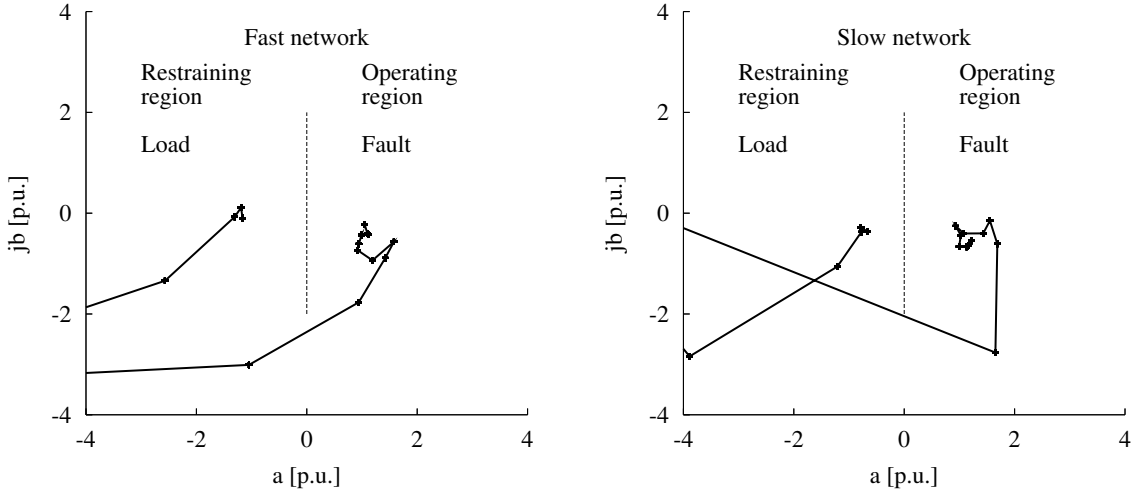

Figure B.33: Alpha-plane differential protection performance of the FF algorithm with 8 samples per cycle during a line-to-line fault at location F2

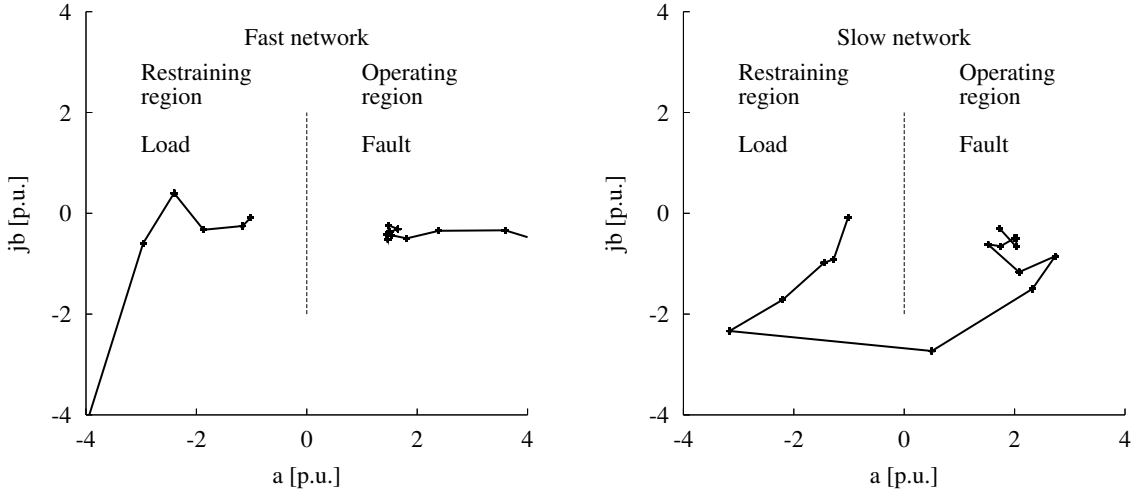

Figure B.34: Alpha-plane differential protection performance of the GPS-LSE algorithm with 8 samples per cycle during a line-to-line fault at location F2

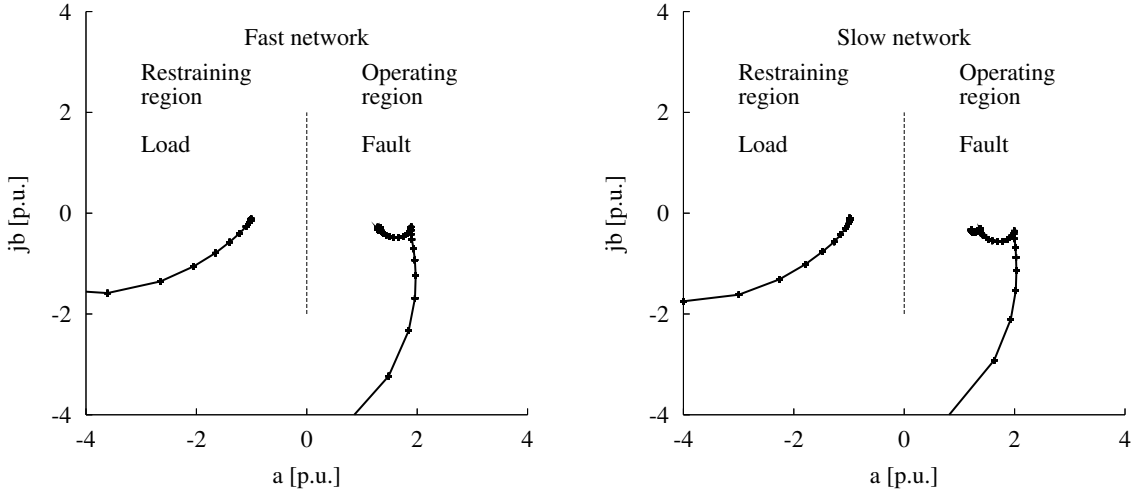

Figure B.35: Alpha-plane differential protection performance of the FF algorithm with 32 samples per cycle during a line-to-line fault at location F2

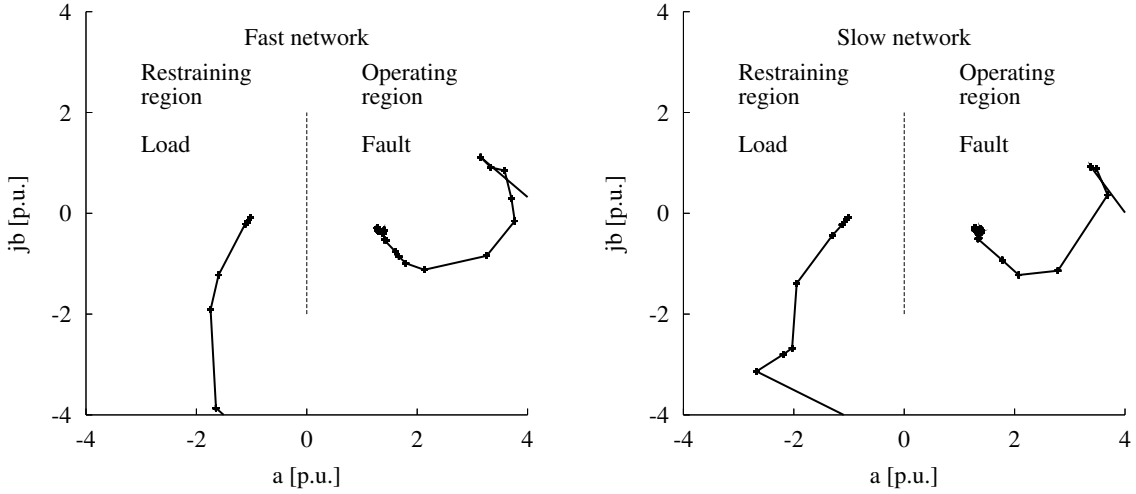

Figure B.36: Alpha-plane differential protection performance of the GPS-LSE algorithm with 32 samples per cycle during a line-to-line fault at location F2

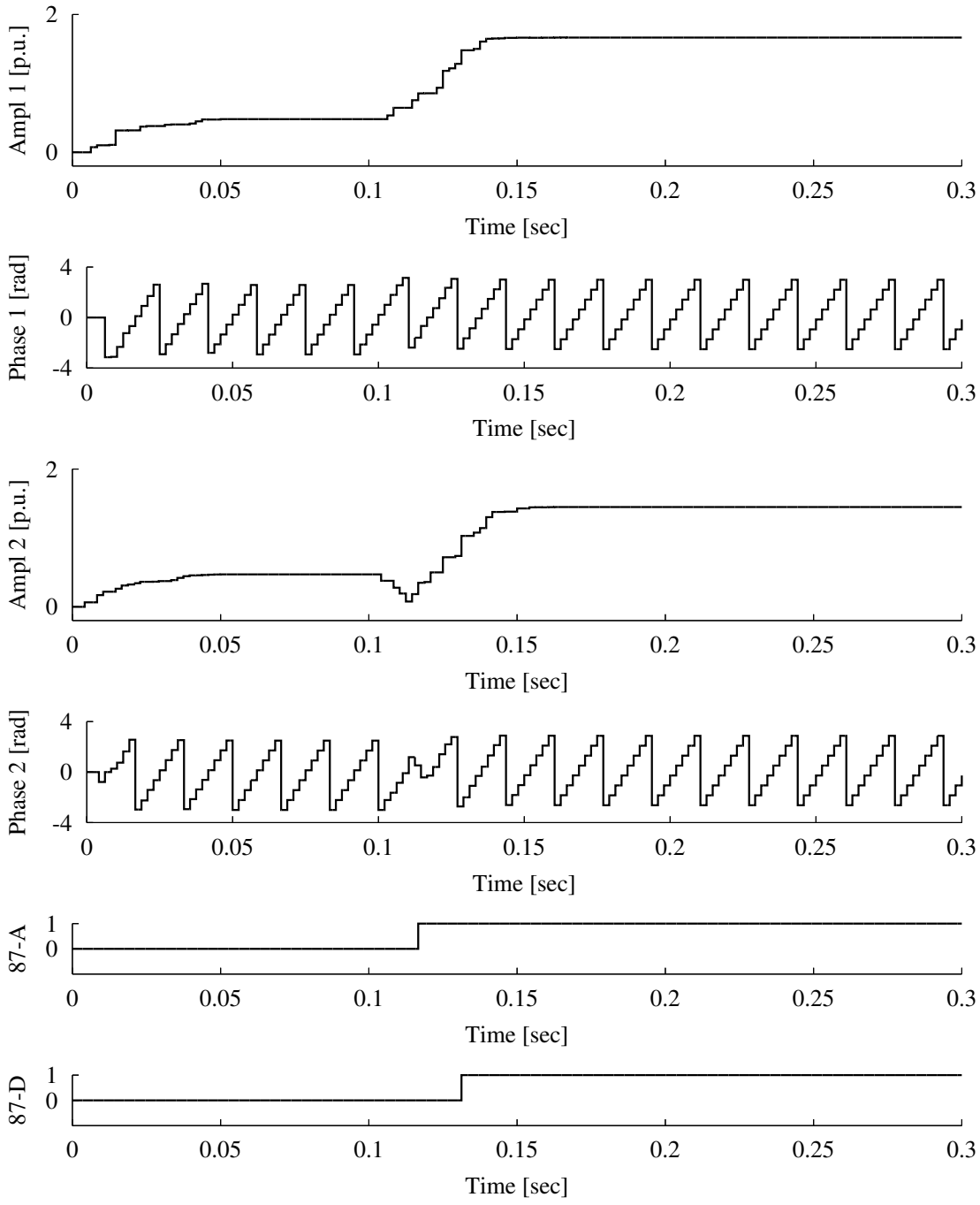

Figure B.37: GPS-LSE algorithm performance with 8 samples per cycle over slow network during a 3-line fault at location F2

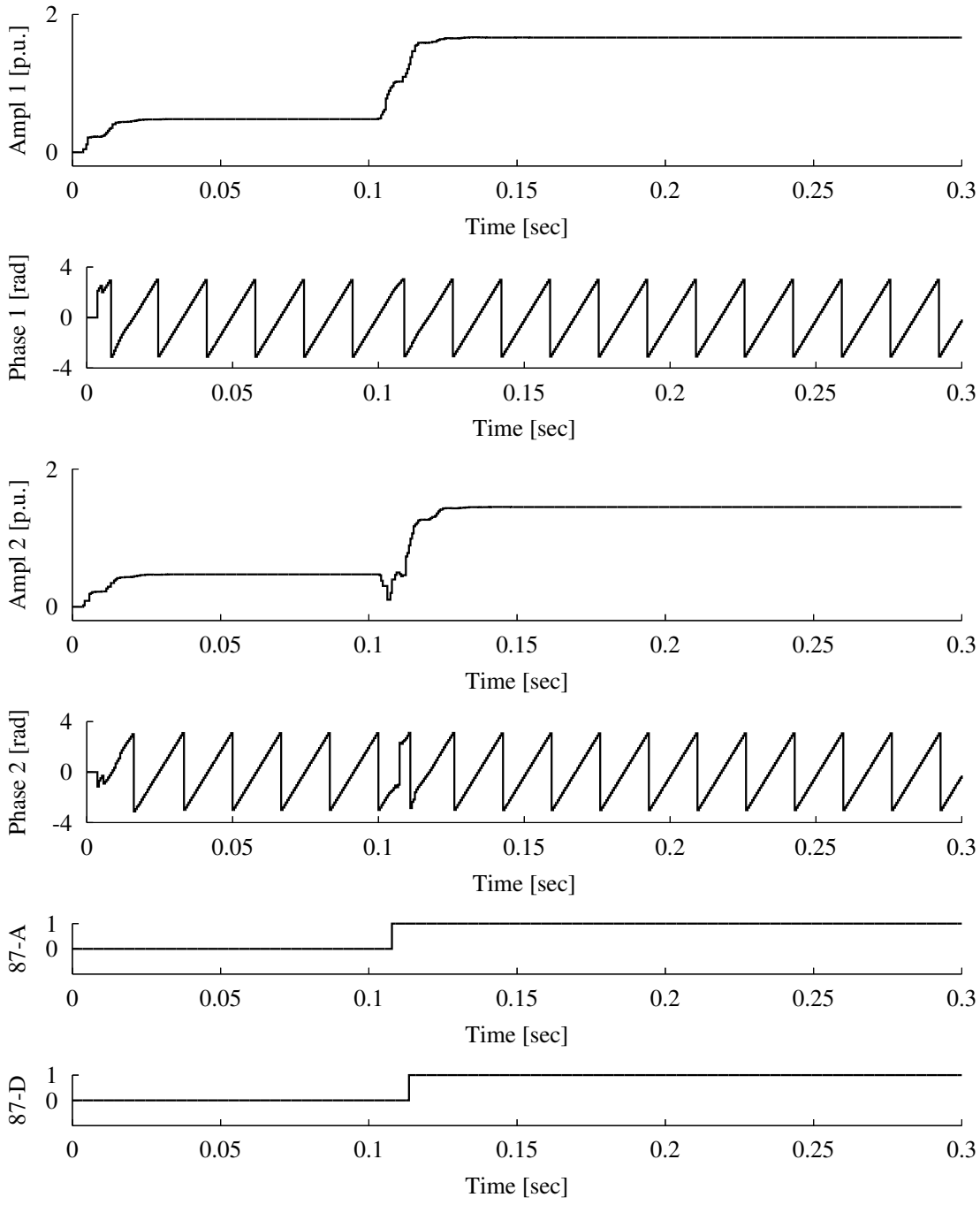

Figure B.38: GPS-LSE algorithm performance with 32 samples per cycle over slow network during a 3-line fault at location F2

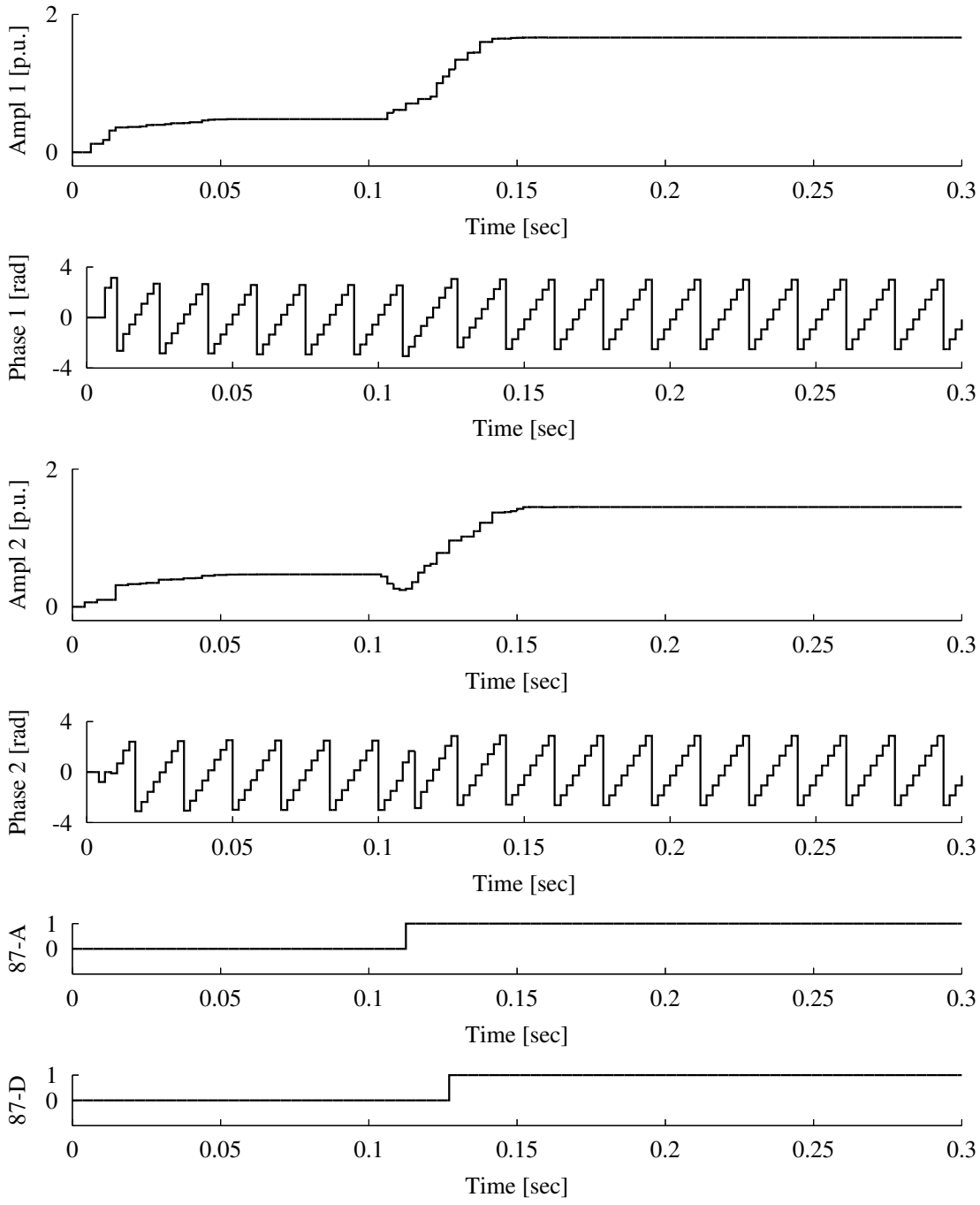

Figure B.39: GPS-LSE algorithm performance with 8 samples per cycle over fast network during a 3-line fault at location F2

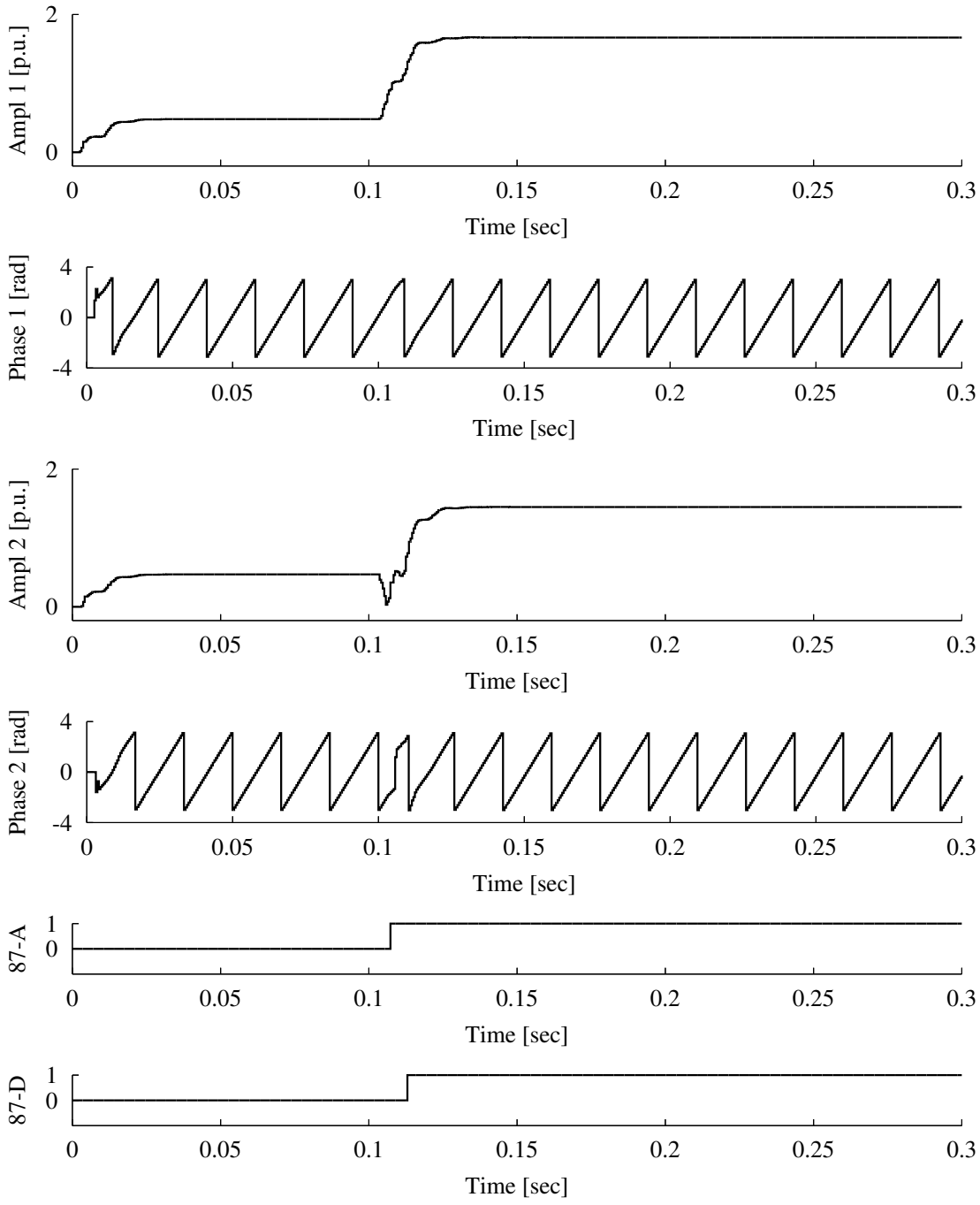

Figure B.40: GPS-LSE algorithm performance with 32 samples per cycle over fast network during a 3-line fault at location F2

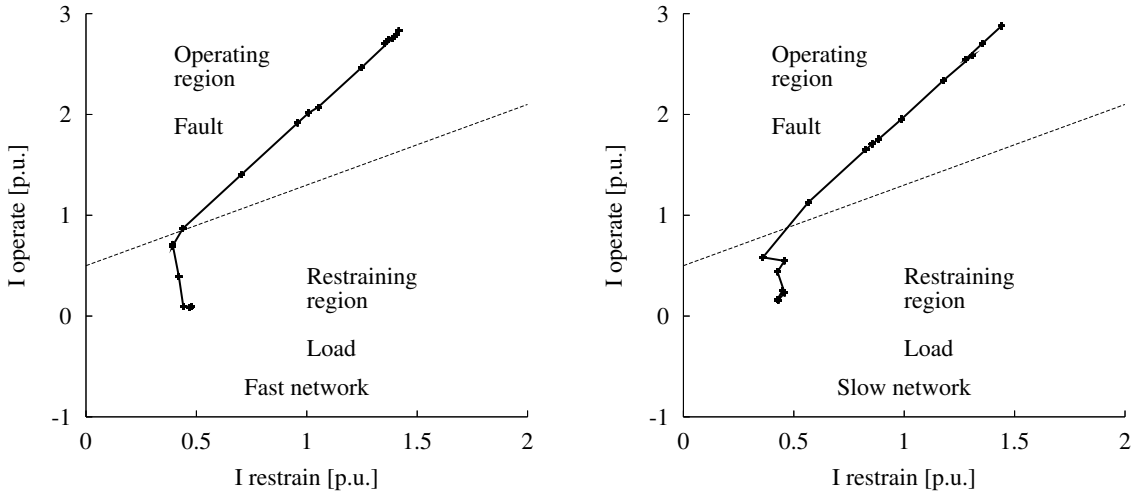

Figure B.41: Percentage differential protection performance of the FF algorithm with 8 samples per cycle during a 3-line fault at location F2

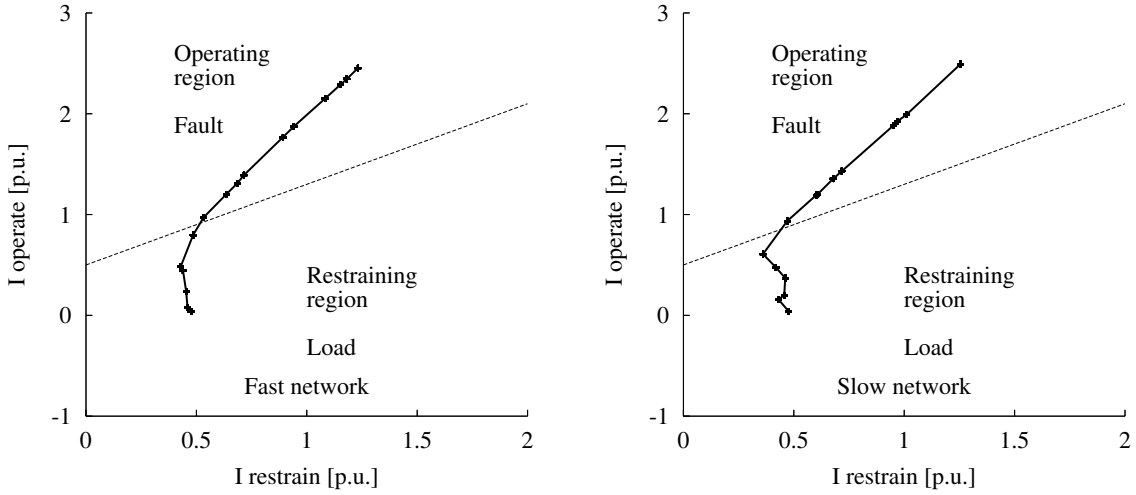

Figure B.42: Percentage differential protection performance of the GPS-LSE algorithm with 8 samples per cycle during a 3-line fault at location F2

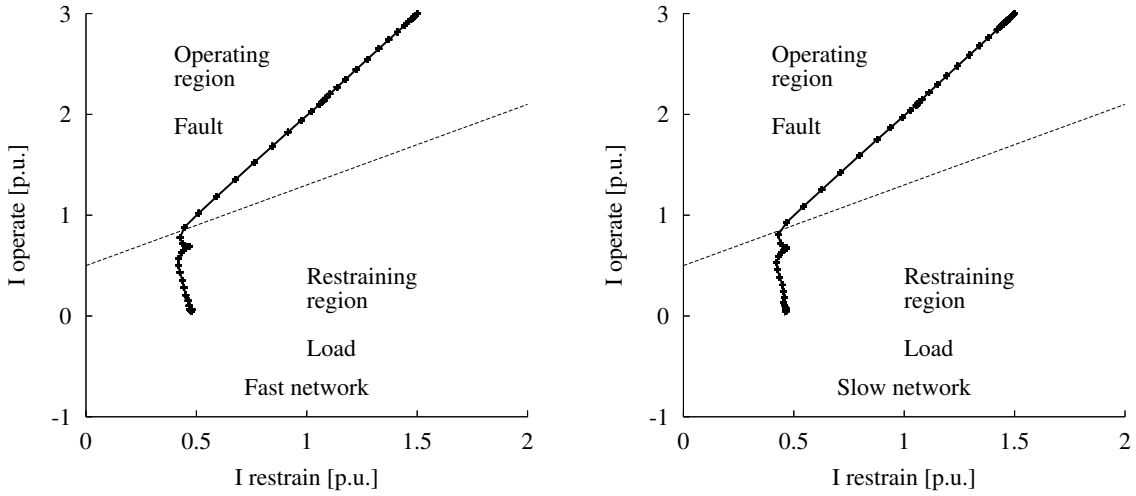

Figure B.43: Percentage differential protection performance of the FF algorithm with 32 samples per cycle during a 3-line fault at location F2

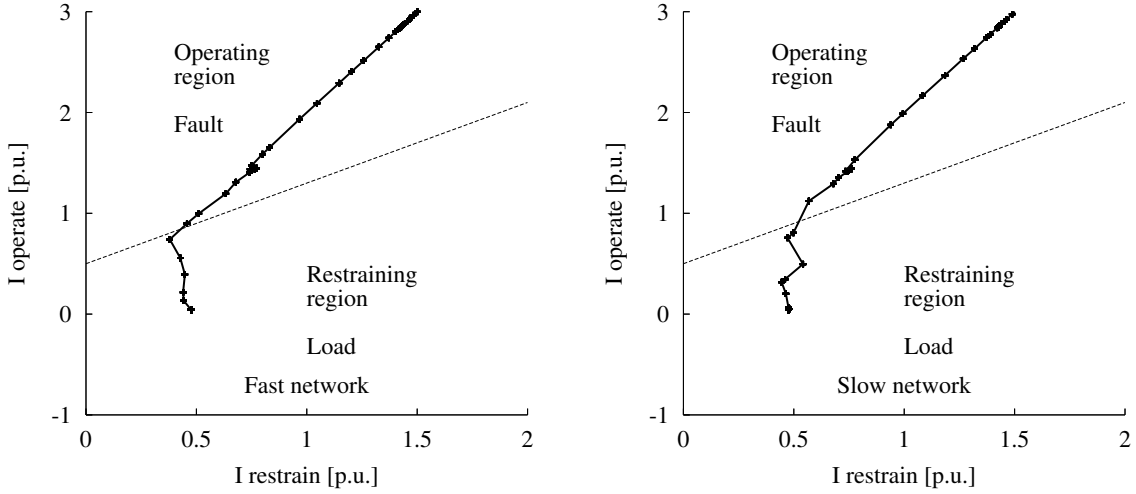

Figure B.44: Percentage differential protection performance of the GPS-LSE algorithm with 32 samples per cycle during a 3-line fault at location F2

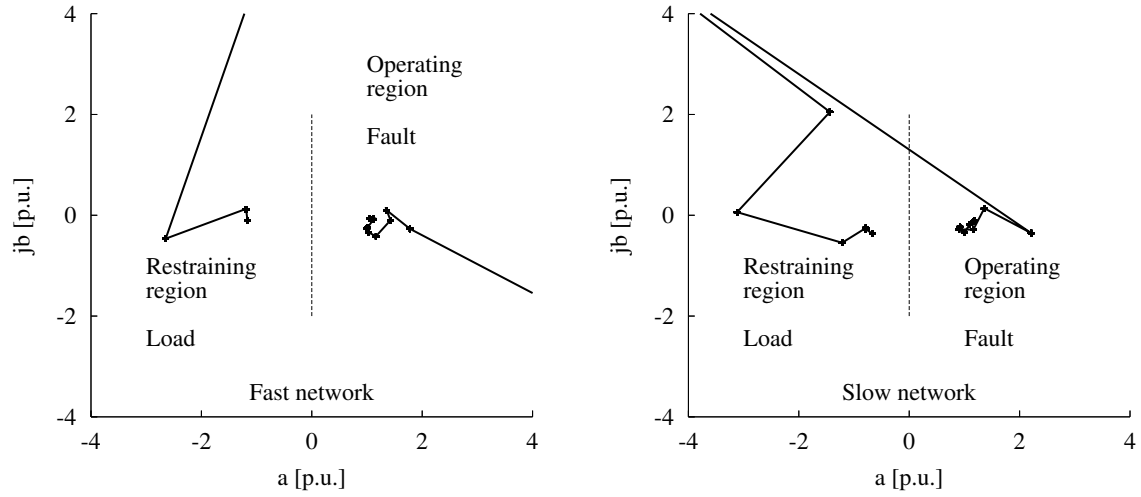

Figure B.45: Alpha-plane differential protection performance of the FF algorithm with 8 samples per cycle during a 3-line fault at location F2

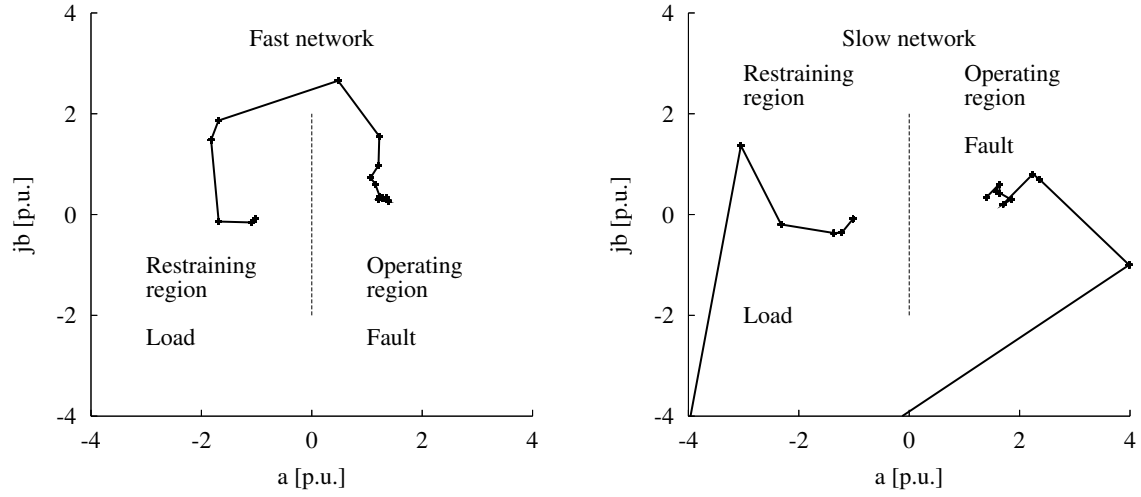

Figure B.46: Alpha-plane differential protection performance of the GPS-LSE algorithm with 8 samples per cycle during a 3-line fault at location F2

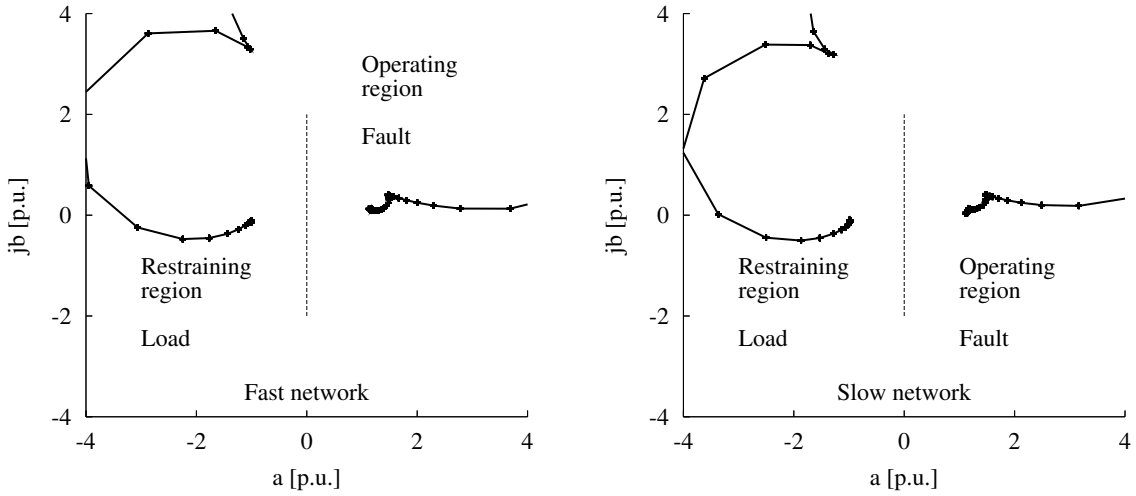

Figure B.47: Alpha-plane differential protection performance of the FF algorithm with 32 samples per cycle during a 3-line fault at location F2

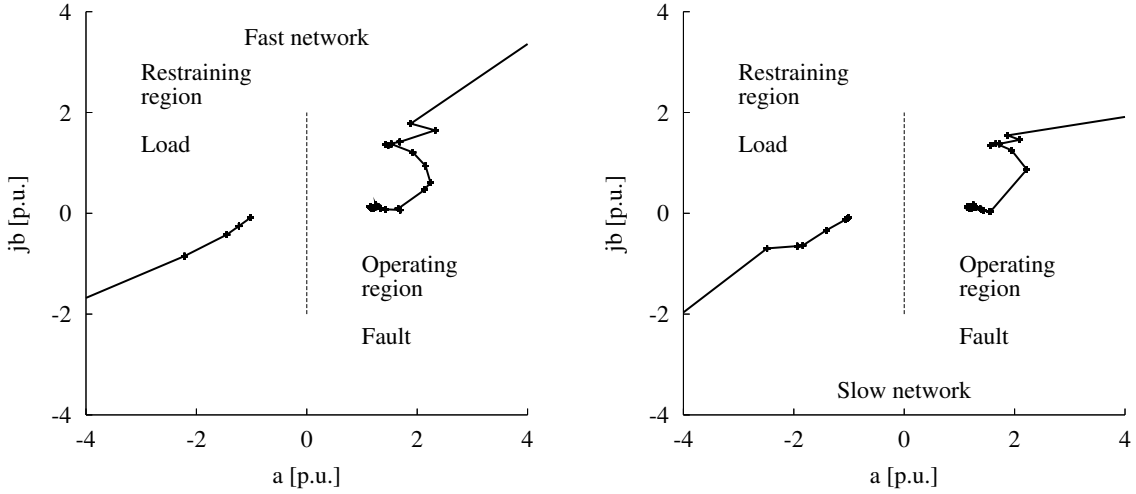

Figure B.48: Alpha-plane differential protection performance of the GPS-LSE algorithm with 32 samples per cycle during a 3-line fault at location F2

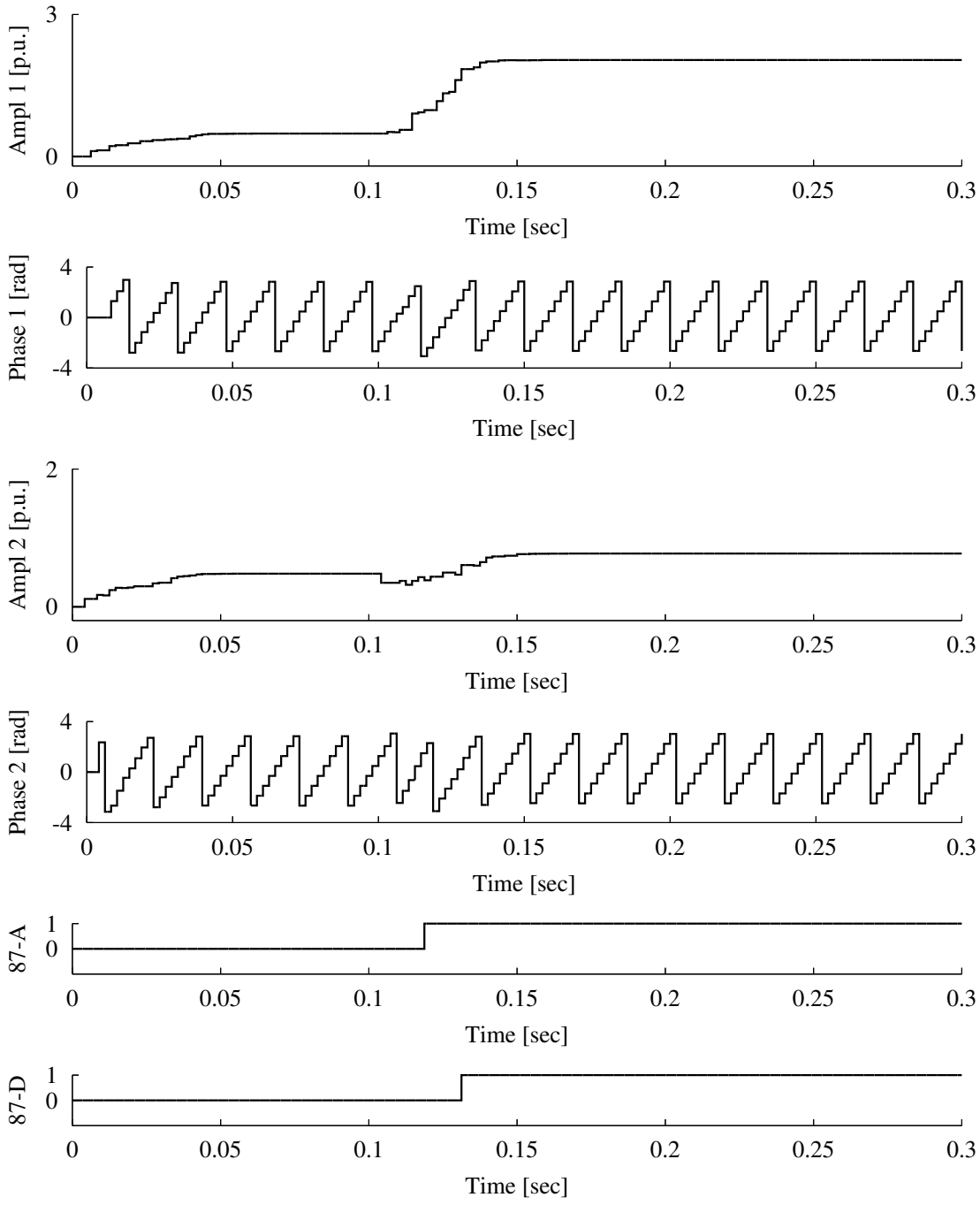

Figure B.49: GPS-LSE algorithm performance with 8 samples per cycle over slow network during a line-to-line fault at location F3

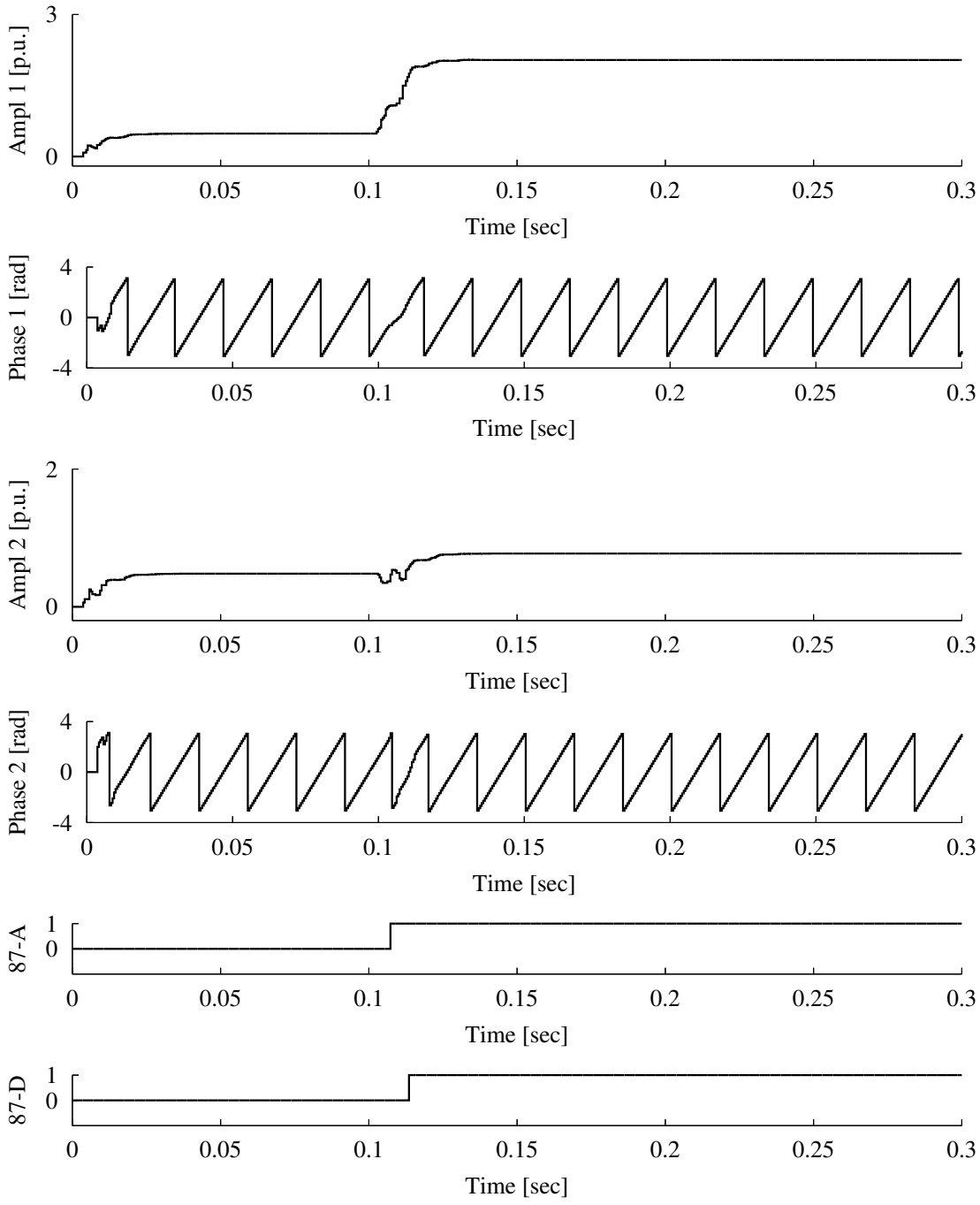

Figure B.50: GPS-LSE algorithm performance with 32 samples per cycle over slow network during a line-to-line fault at location F3

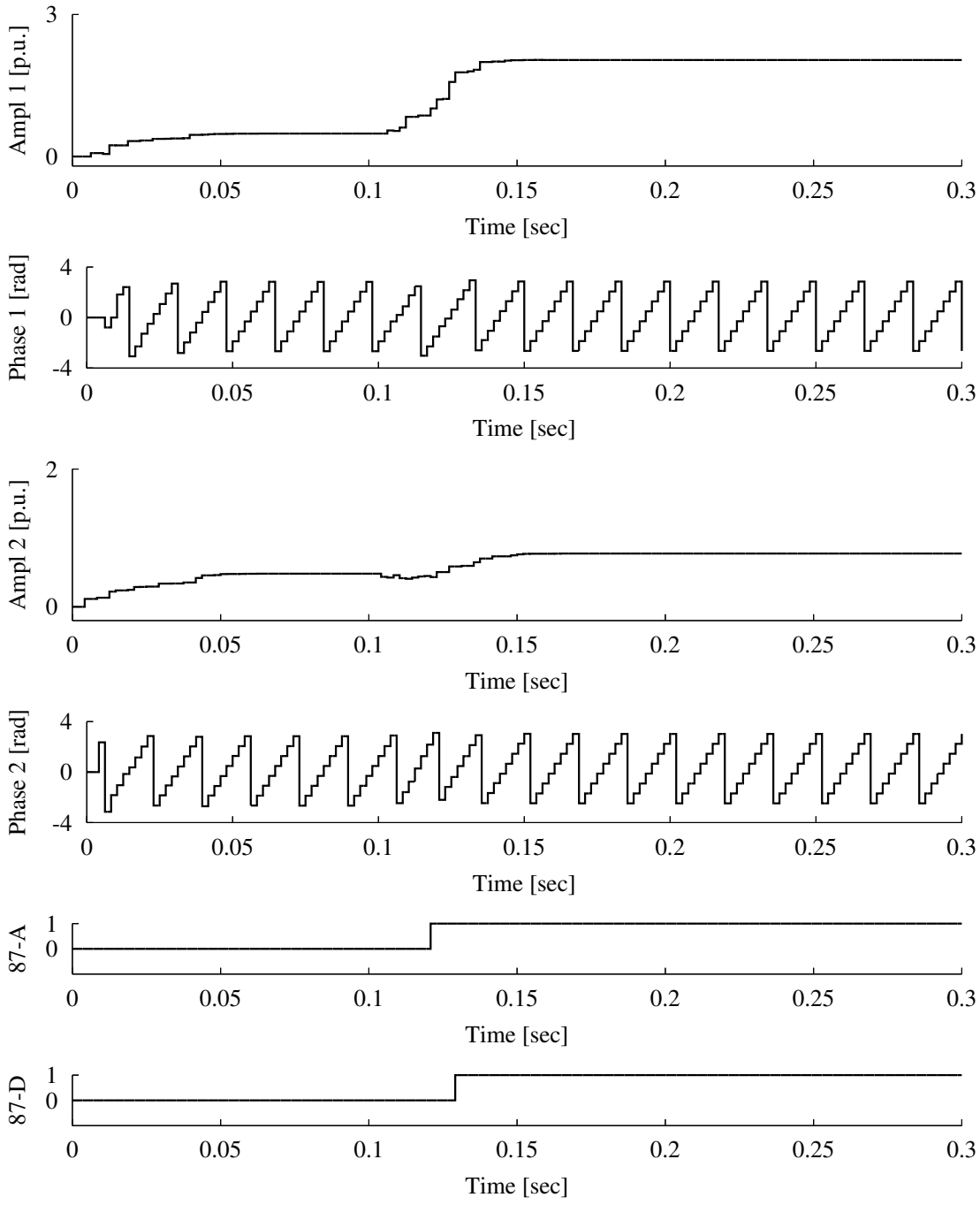

Figure B.51: GPS-LSE algorithm performance with 8 samples per cycle over fast network during a line-to-line fault at location F3

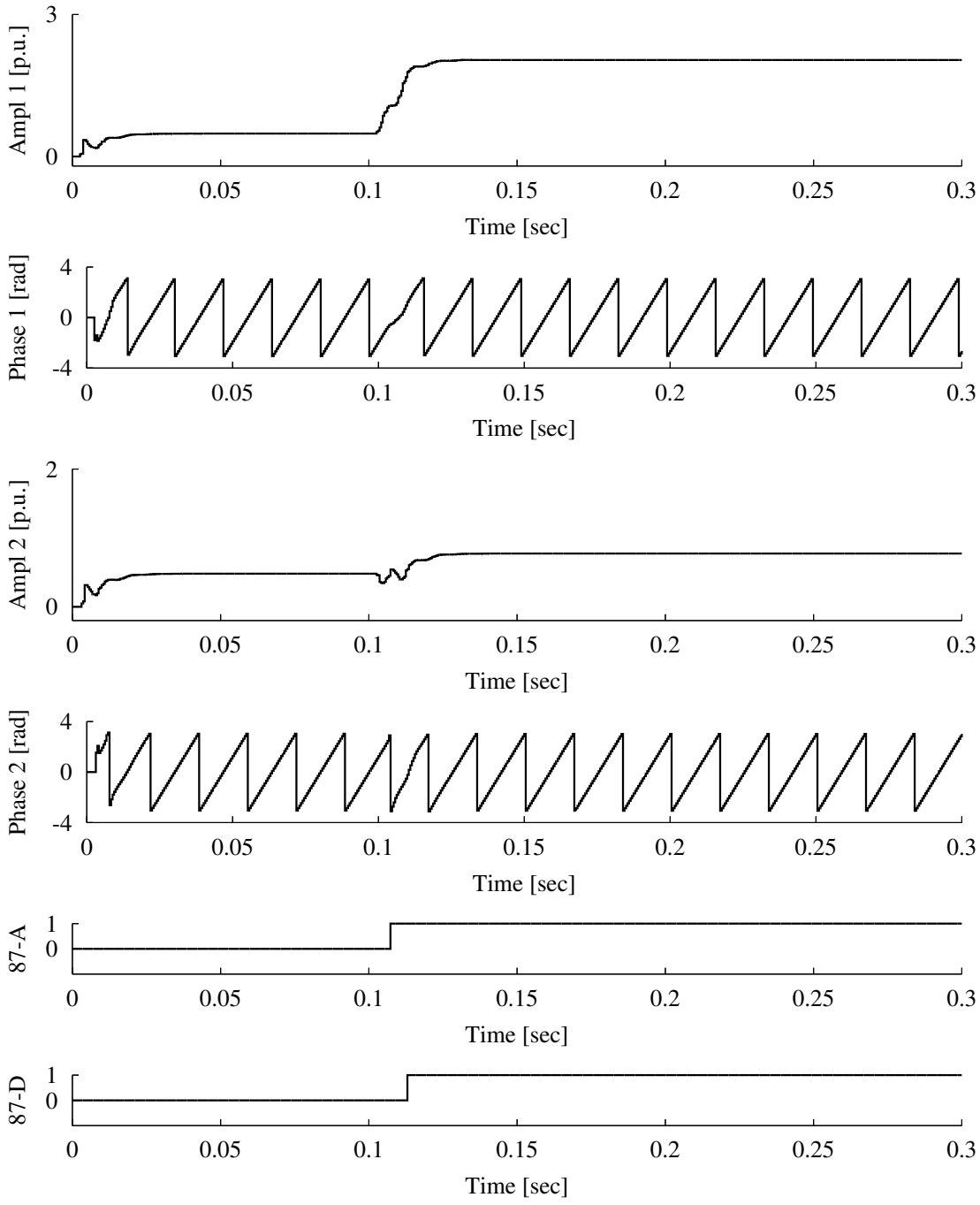

Figure B.52: GPS-LSE algorithm performance with 32 samples per cycle over fast network during a line-to-line fault at location F3

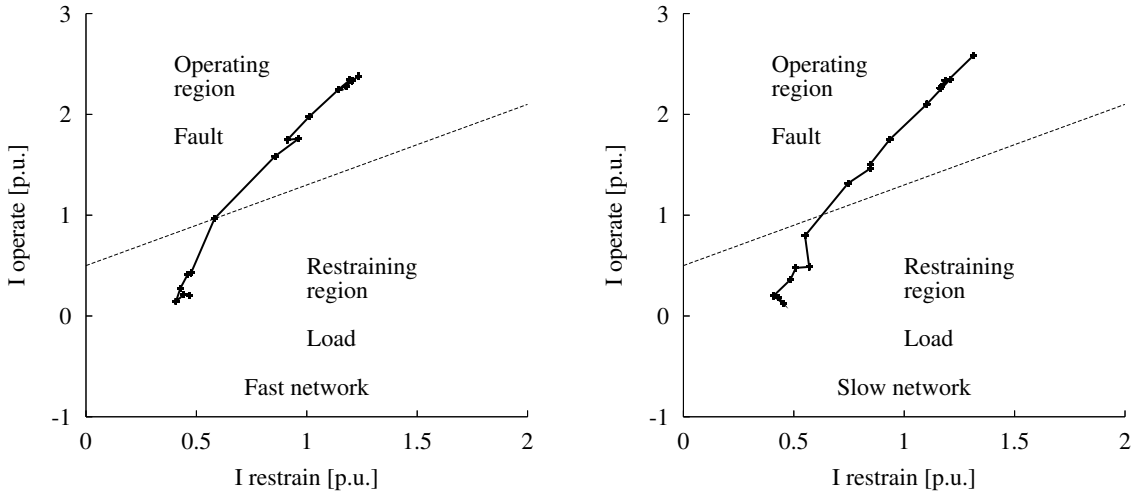

Figure B.53: Percentage differential protection performance of the FF algorithm with 8 samples per cycle during a line-to-line fault at location F3

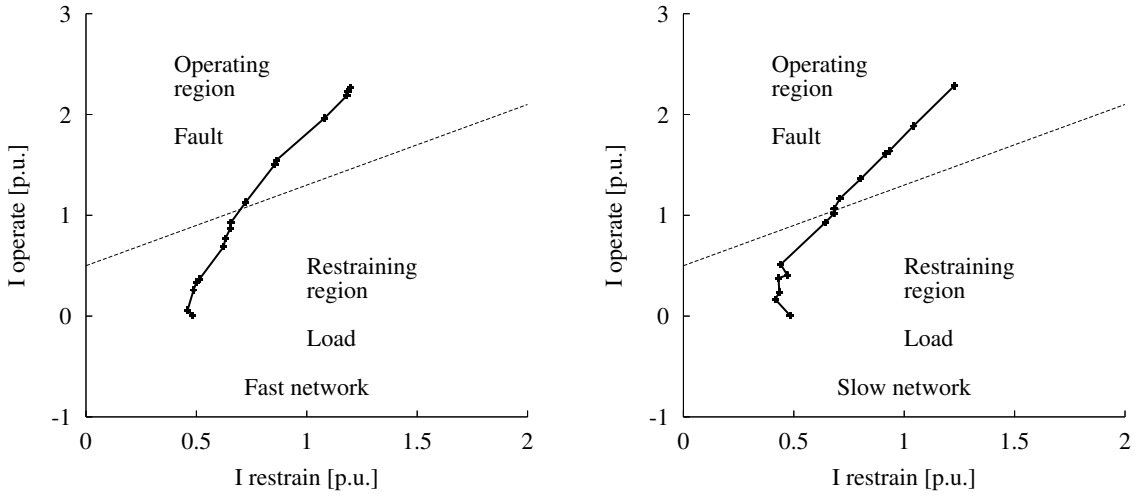

Figure B.54: Percentage differential protection performance of the GPS-LSE algorithm with 8 samples per cycle during a line-to-line fault at location F3

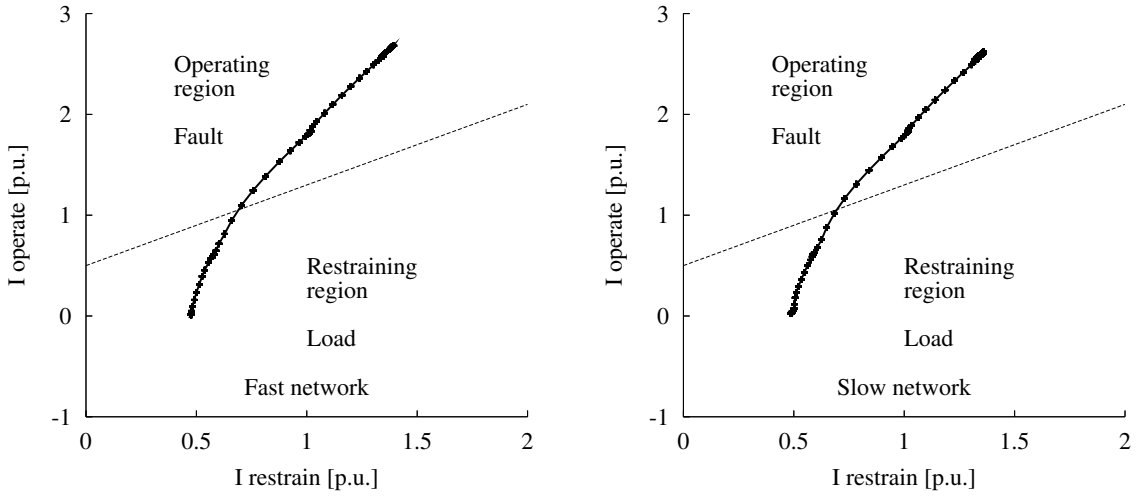

Figure B.55: Percentage differential protection performance of the FF algorithm with 32 samples per cycle during a line-to-line fault at location F3

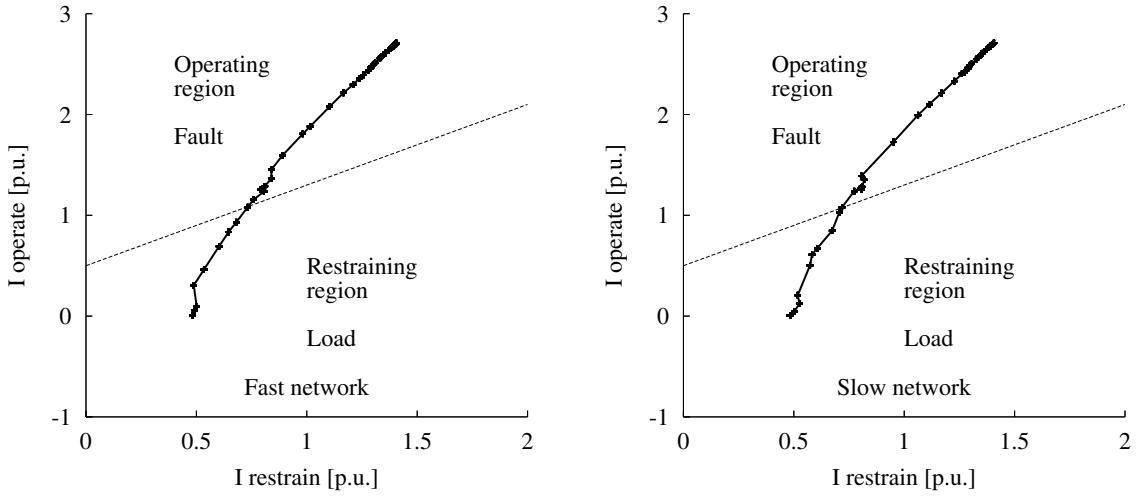

Figure B.56: Percentage differential protection performance of the GPS-LSE algorithm with 32 samples per cycle during a line-to-line fault at location F3

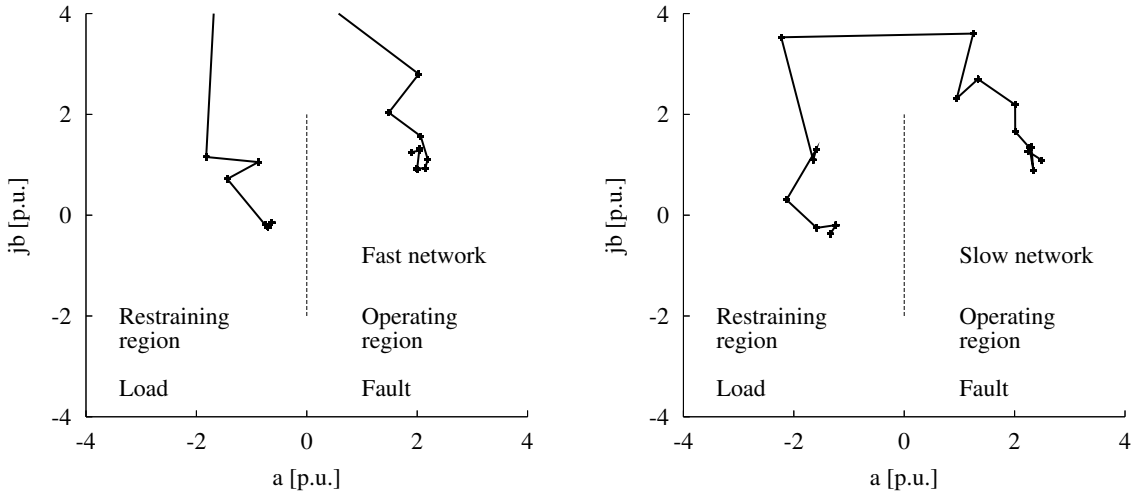

Figure B.57: Alpha-plane differential protection performance of the FF algorithm with 8 samples per cycle during a line-to-line fault at location F3

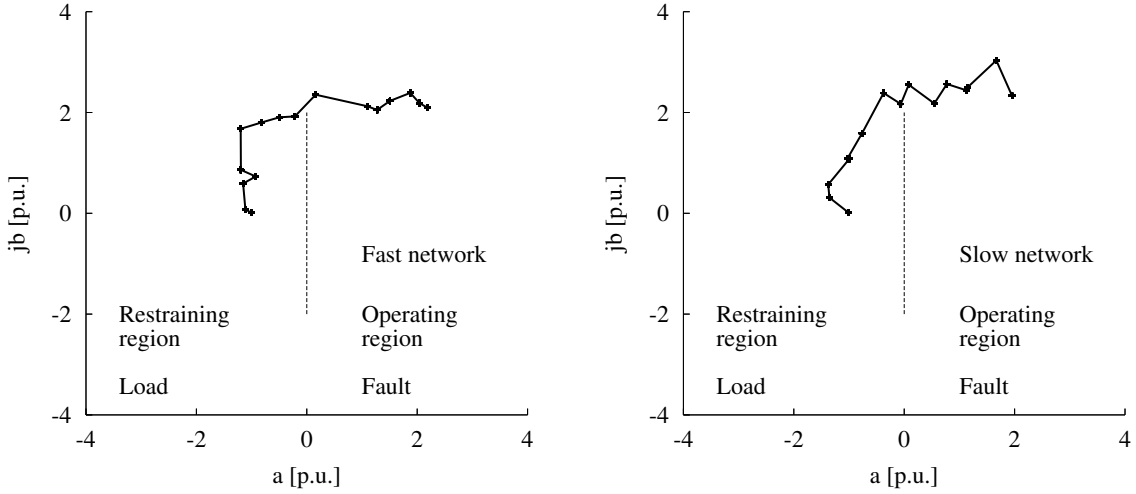

Figure B.58: Alpha-plane differential protection performance of the GPS-LSE algorithm with 8 samples per cycle during a line-to-line fault at location F3

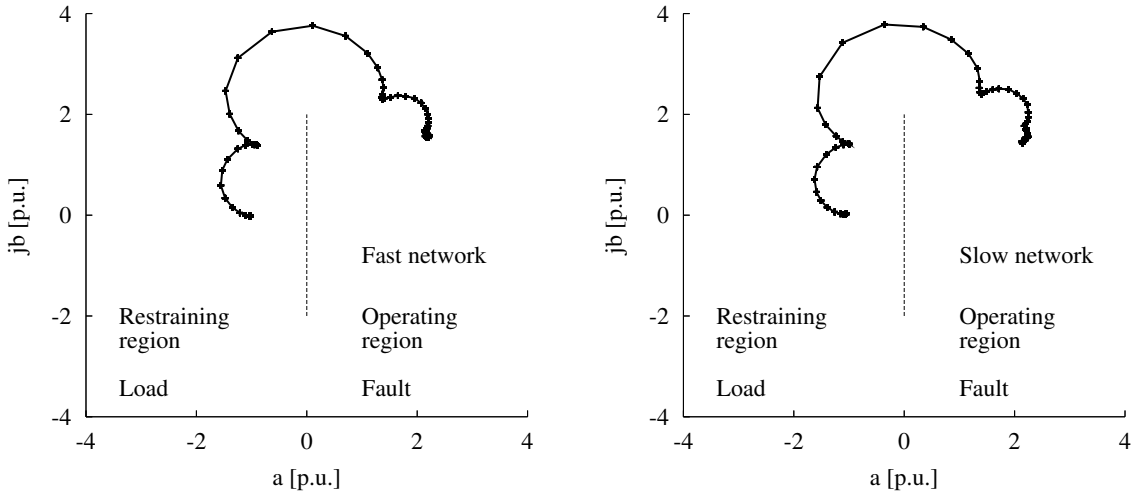

Figure B.59: Alpha-plane differential protection performance of the FF algorithm with 32 samples per cycle during a line-to-line fault at location F3

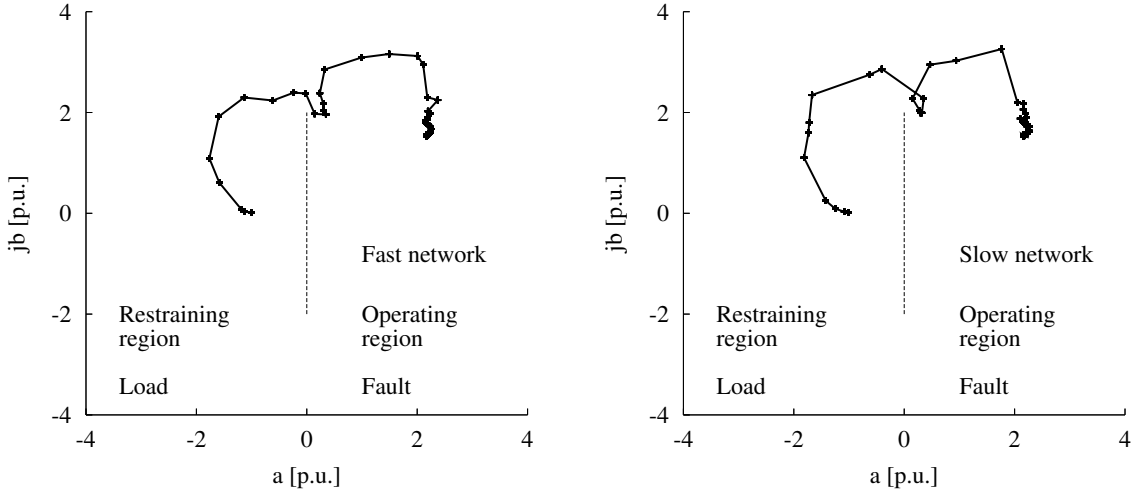

Figure B.60: Alpha-plane differential protection performance of the GPS-LSE algorithm with 32 samples per cycle during a line-to-line fault at location F3

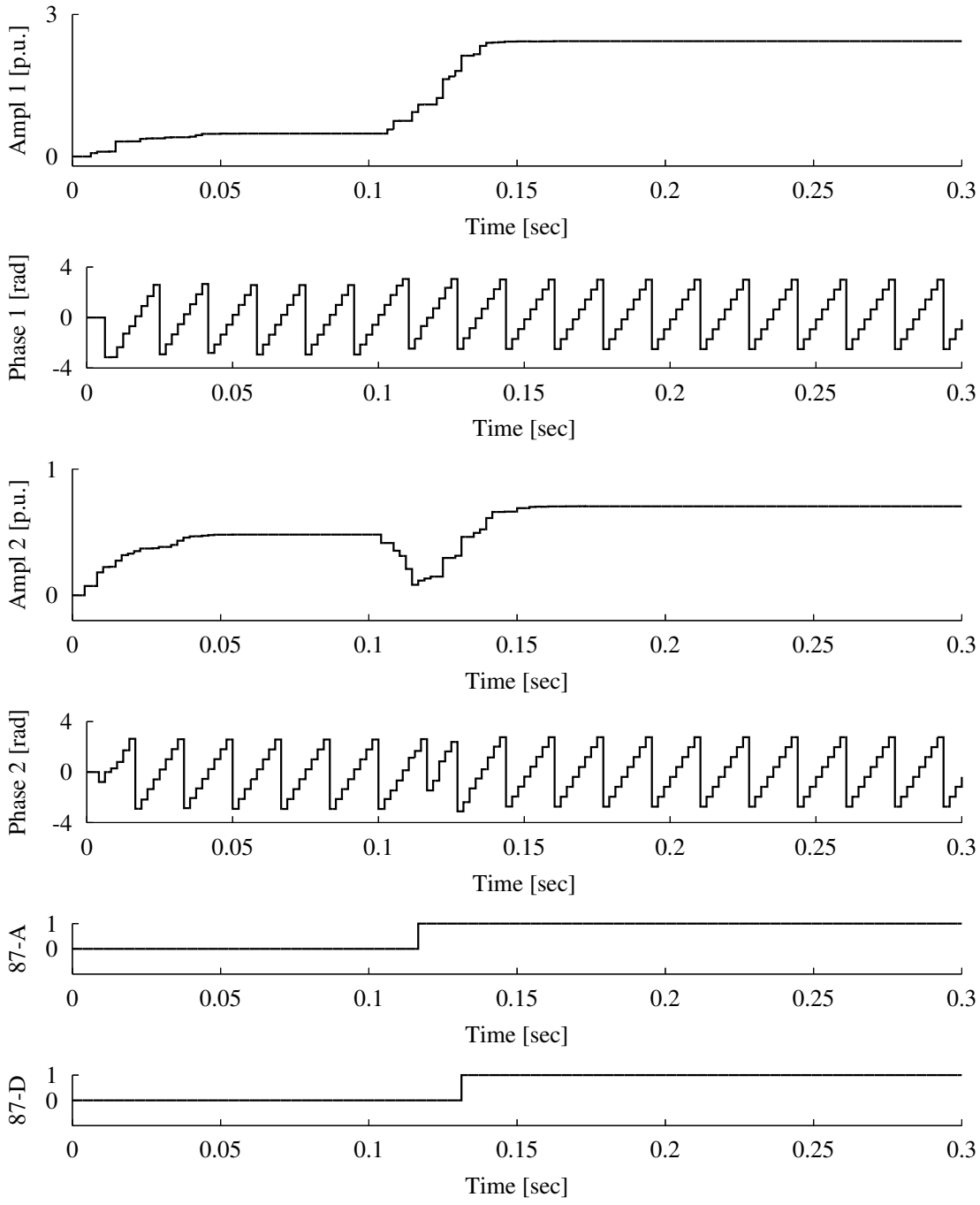

Figure B.61: GPS-LSE algorithm performance with 8 samples per cycle over slow network during a 3-line fault at location F3

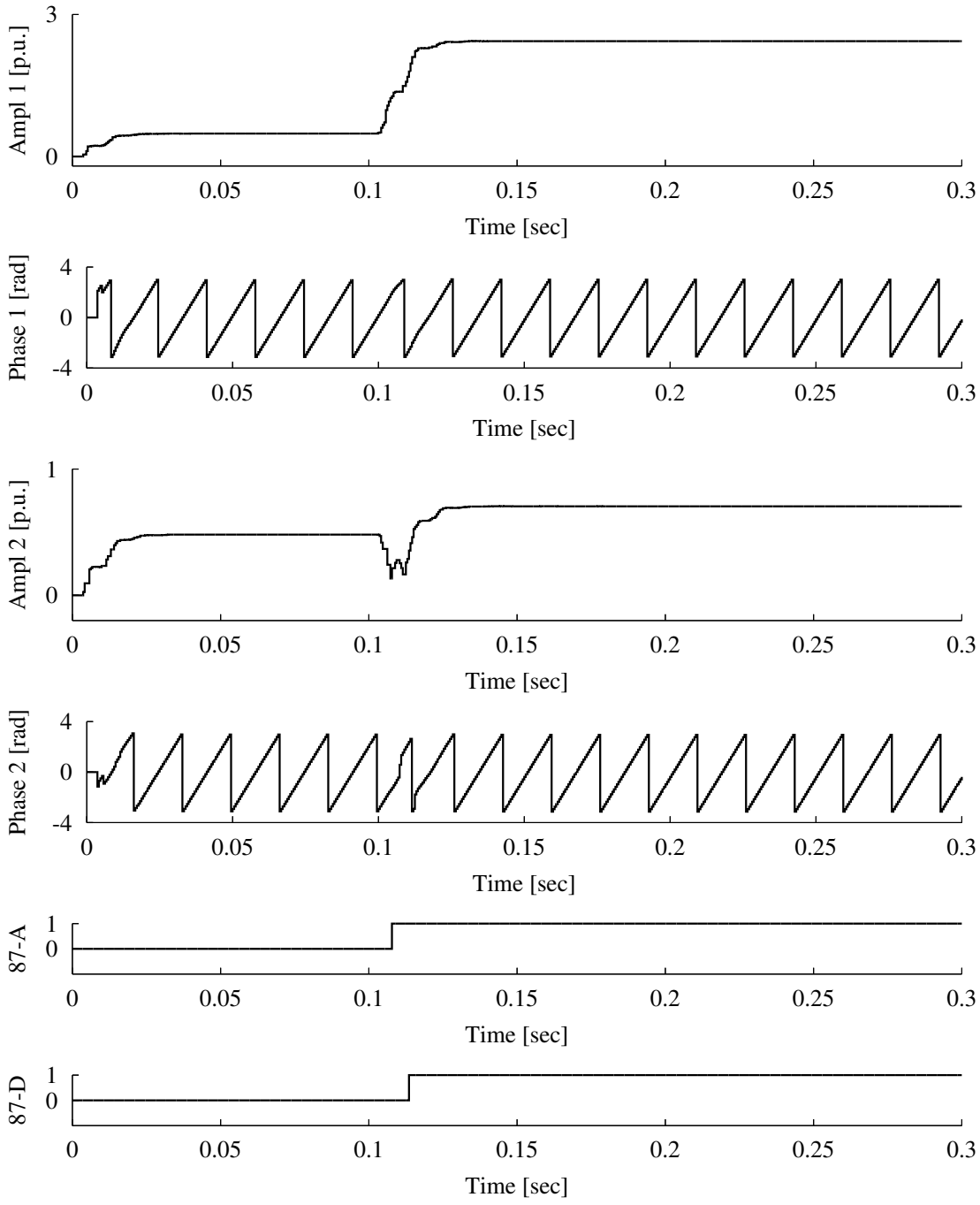

Figure B.62: GPS-LSE algorithm performance with 32 samples per cycle over slow network during a 3-line fault at location F3

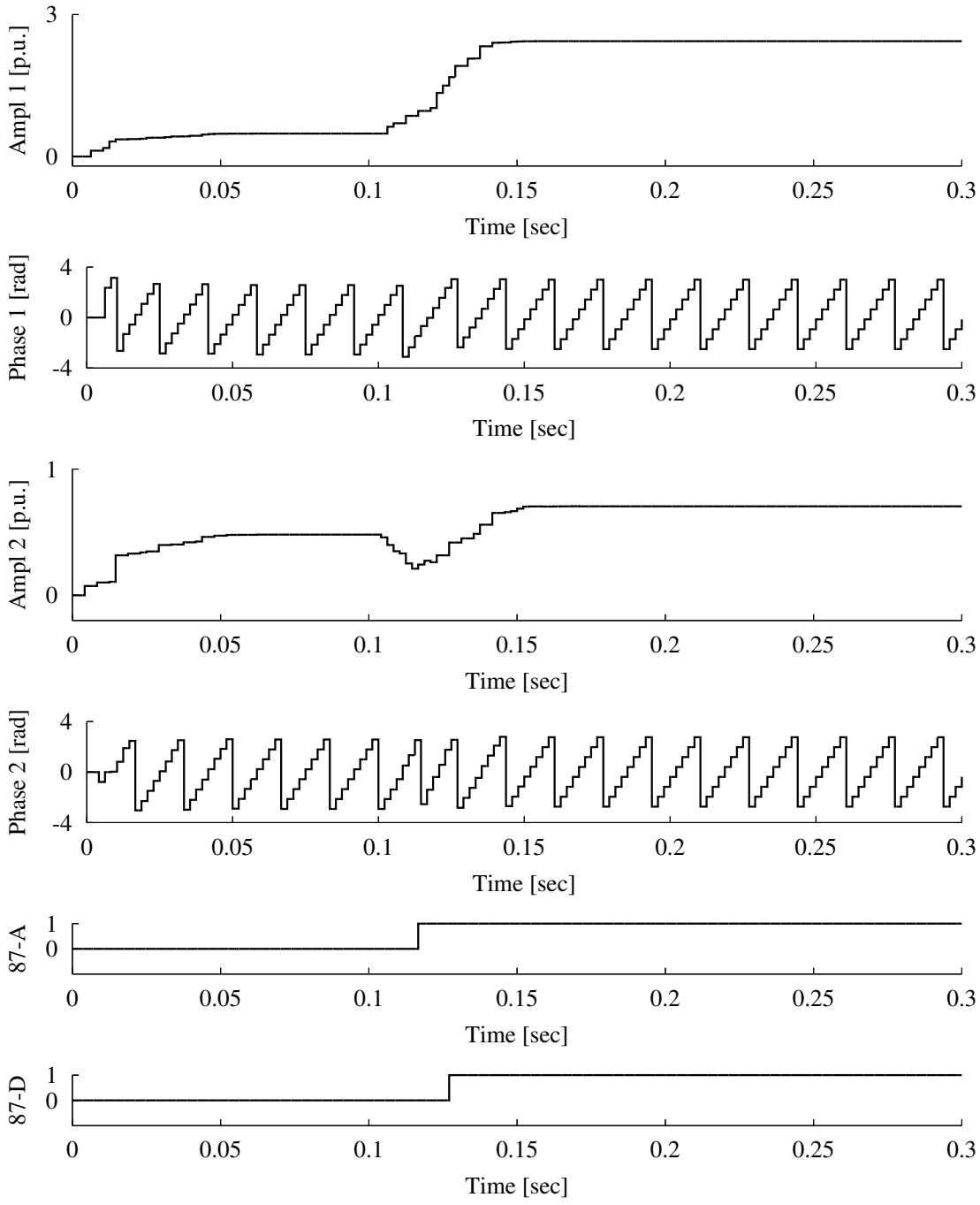

Figure B.63: GPS-LSE algorithm performance with 8 samples per cycle over fast network during a 3-line fault at location F3

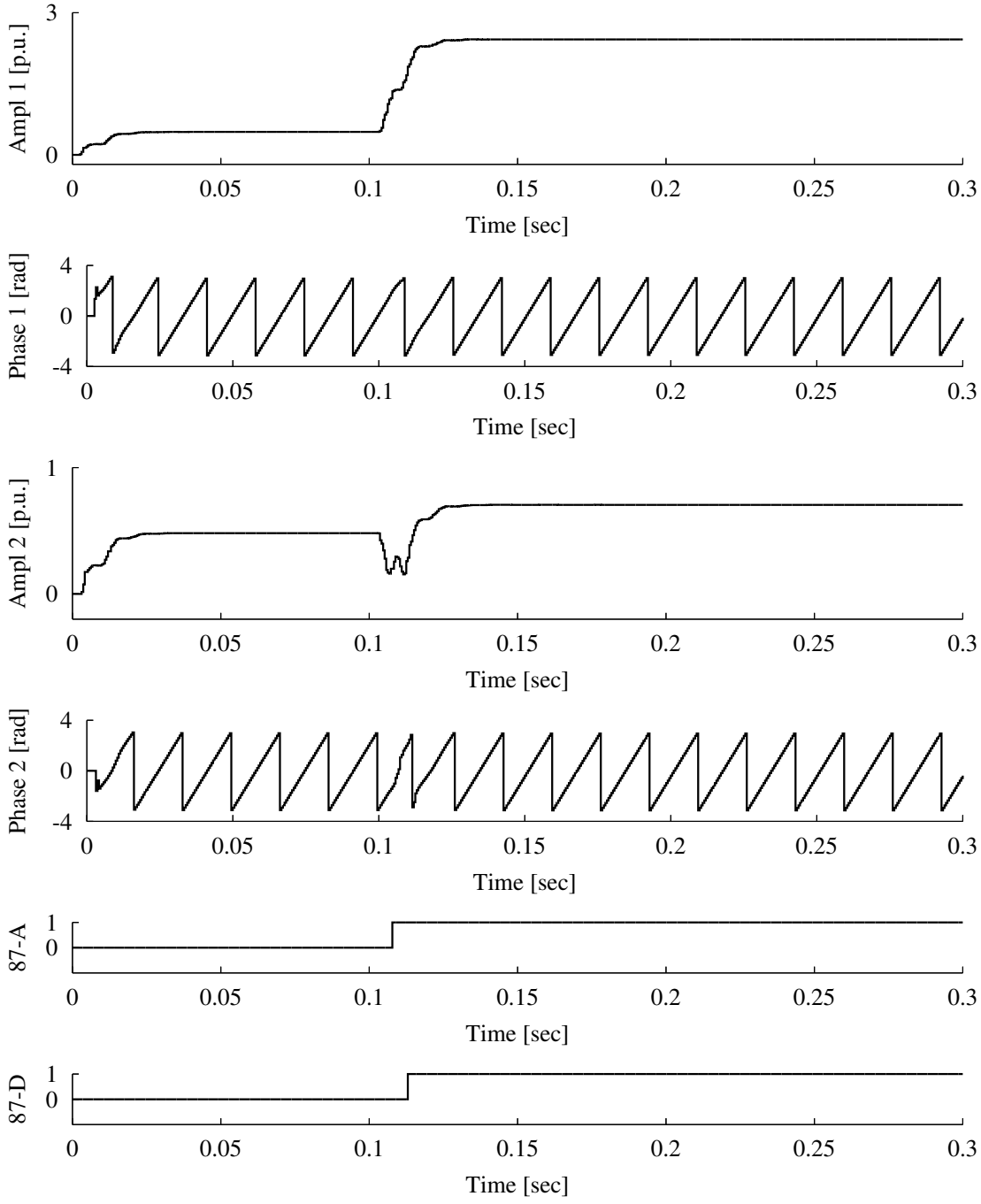

Figure B.64: GPS-LSE algorithm performance with 32 samples per cycle over fast network during a 3-line fault at location F3

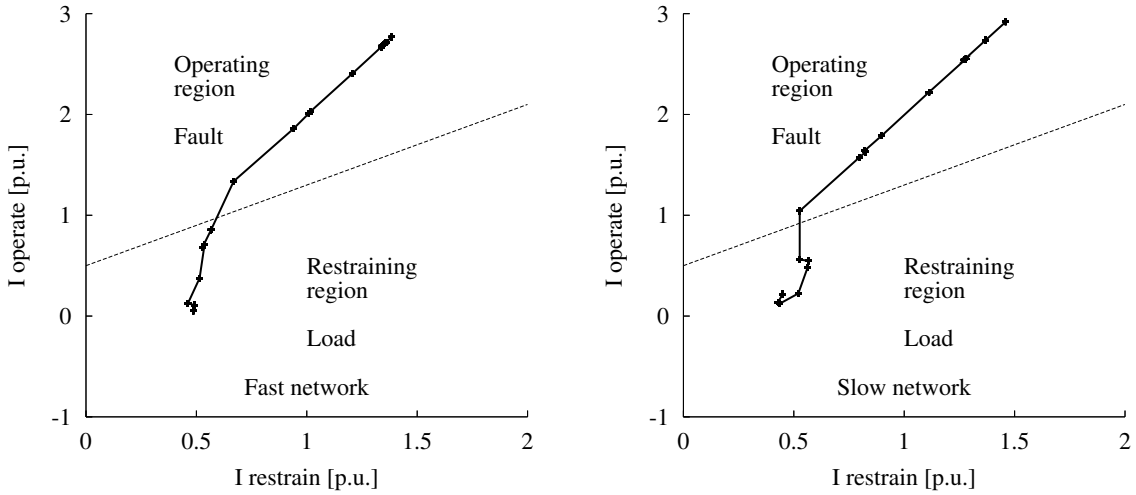

Figure B.65: Percentage differential protection performance of the FF algorithm with 8 samples per cycle during a 3-line fault at location F3

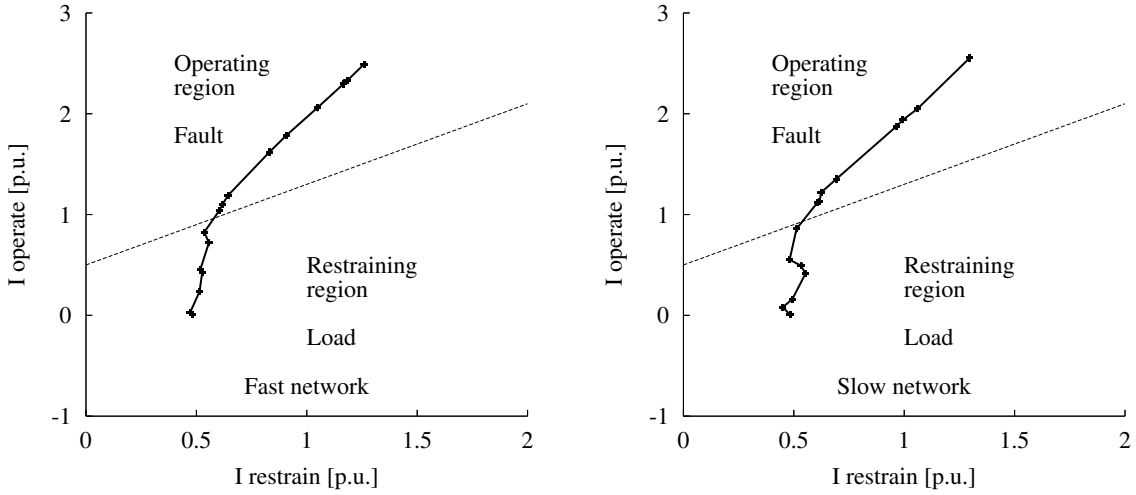

Figure B.66: Percentage differential protection performance of the GPS-LSE algorithm with 8 samples per cycle during a 3-line fault at location F3

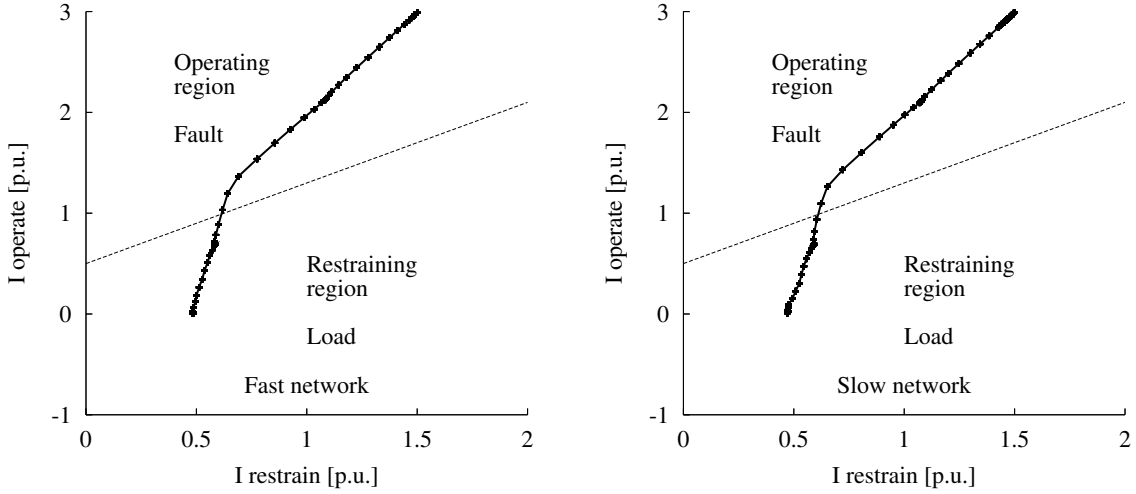

Figure B.67: Percentage differential protection performance of the FF algorithm with 32 samples per cycle during a 3-line fault at location F3

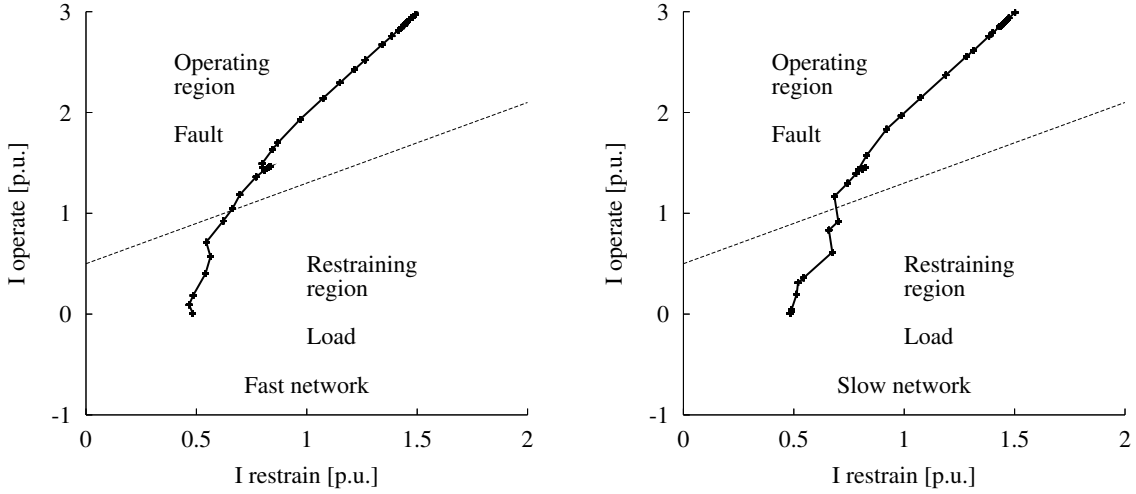

Figure B.68: Percentage differential protection performance of the GPS-LSE algorithm with 32 samples per cycle during a 3-line fault at location F3

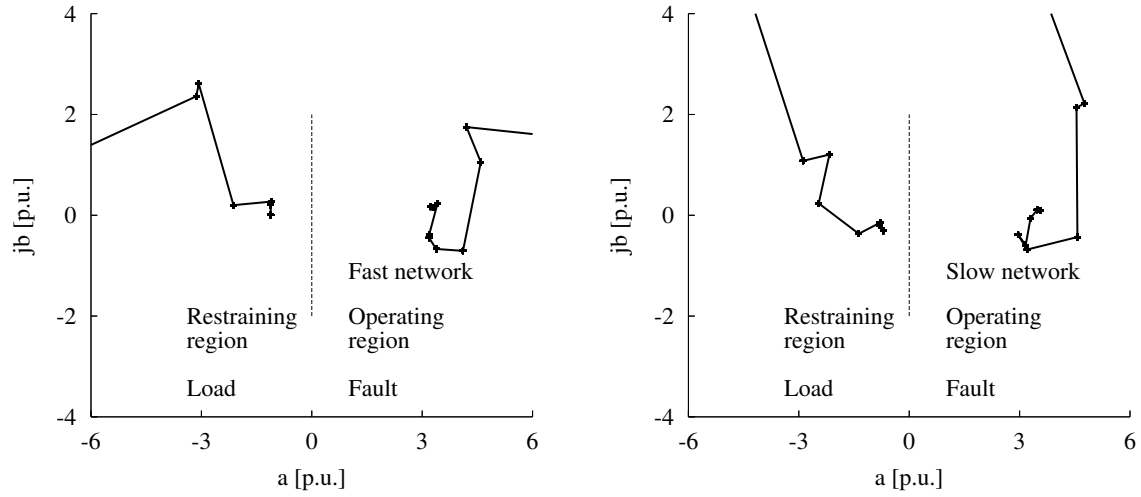

Figure B.69: Alpha-plane differential protection performance of the FF algorithm with 8 samples per cycle during a 3-line fault at location F3

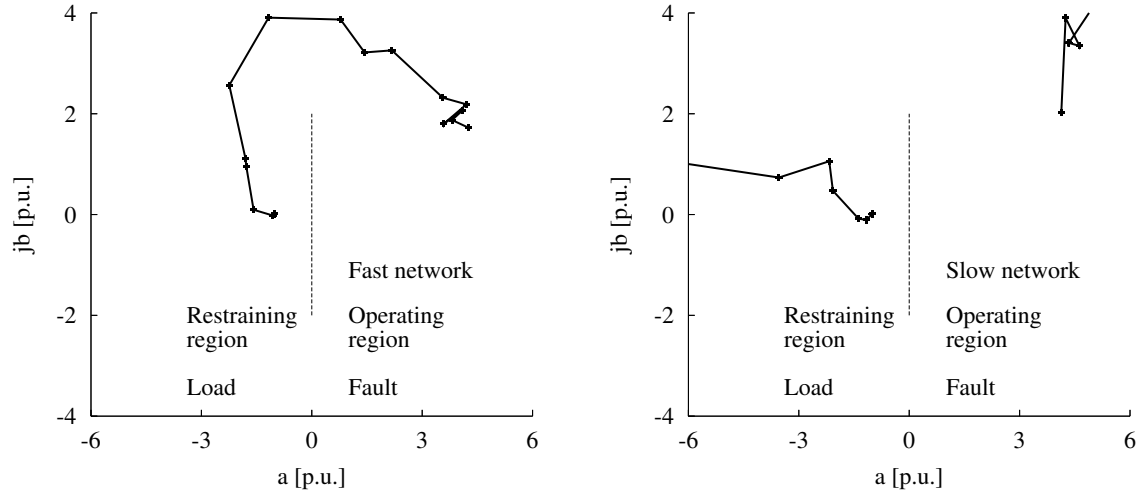

Figure B.70: Alpha-plane differential protection performance of the GPS-LSE algorithm with 8 samples per cycle during a 3-line fault at location F3

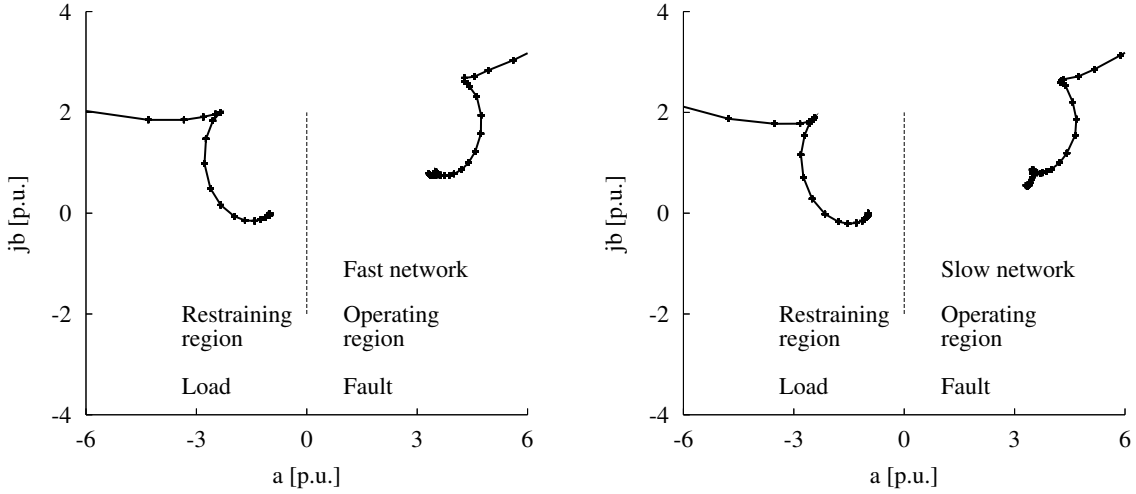

Figure B.71: Alpha-plane differential protection performance of the FF algorithm with 32 samples per cycle during a 3-line fault at location F3

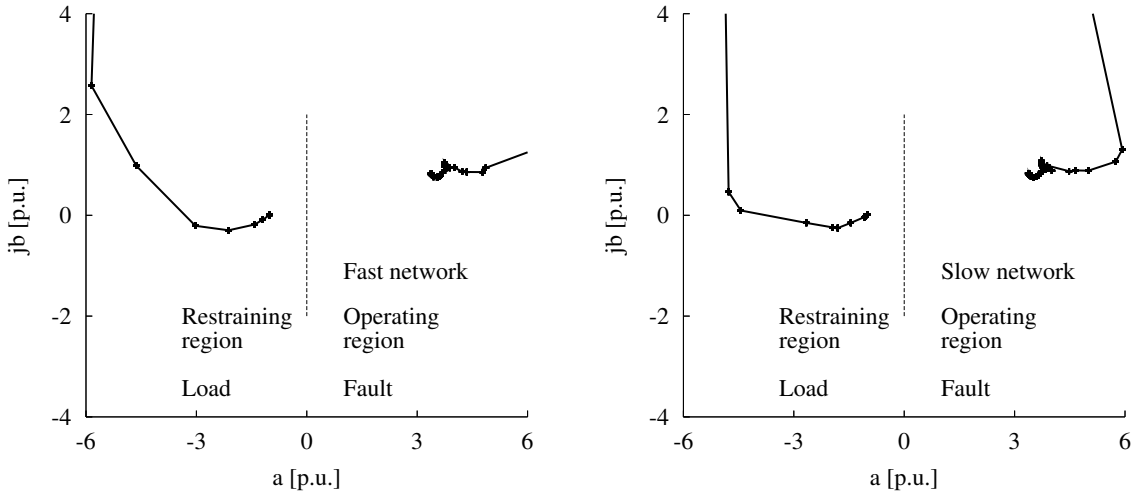

Figure B.72: Alpha-plane differential protection performance of the GPS-LSE algorithm with 32 samples per cycle during a 3-line fault at location F3

APPENDIX C

EFFECT OF CHANGING POWER SYSTEM PARAMETERS

The data transmission process is independent of the actual values of the measurements. Variable power system conditions and parameters do not affect the performance of the proposed digital relaying algorithm. The results presented in this appendix are obtained using the test system in Fig.(6.31), for a transmission line fault at location F2, using the modified system values shown in Tables (C.1) and (C.2).

Table C.1: Modified equivalent system parameters

System	Voltage [kV] L-L	Internal connection	Short circuit level [MVA]	X/R ratio	Initial phase angle [deg]
A	230	Yg	10,000	8	-5
B	138	Yg	1,500	6	-10

Table C.2: Modified test system load parameters

Station	Voltage [kV] L-L	Real load [MW]	Inductive load [MVAR]	Capacitive load [MVAR]
A	230	10	0	1.5
C	138	20	4	0

The results shown in Figs.(C.1) to (C.12) and Table (C.3) confirm the conclusions reached in the previous sections about the performance of the proposed digital relaying algorithm for integrated power system protection and control.

Table C.3: Test results for transmission line protection with modified system parameters

Algorithm	Fault type	Network	Samples	Trip time 87-D	Trip time 87-A	Sending s1	Sending s2	Receiving s1	Receiving s2
GPS-LSE	LG	Slow	8	0.03333	0.01667	0.02298	0.03974	0.08000	0.08049
		Fast	8	0.03333	0.01250	0.04347	0.05725	0.04249	0.04640
		Slow	32	0.01510	0.00625	0.03057	0.03101	0.01621	0.01639
		Fast	32	0.01354	0.00573	0.03067	0.03092	0.01610	0.01634
	LL	Slow	8	0.03333	0.01458	0.02563	0.03464	0.11305	0.11214
		Fast	8	0.02708	0.01458	0.01650	0.03084	0.05971	0.06621
		Slow	32	0.01354	0.00417	0.03049	0.02970	0.02790	0.02741
		Fast	32	0.01198	0.00417	0.02925	0.02906	0.02735	0.02691
	LLL	Slow	8	0.03333	0.01667	0.02266	0.03947	0.12422	0.12286
		Fast	8	0.02708	0.01667	0.03705	0.05258	0.04890	0.05073
		Slow	32	0.01354	0.00625	0.03280	0.03325	0.02880	0.02895
		Fast	32	0.01250	0.00573	0.03284	0.03307	0.02879	0.02911
FF	LG	Slow	8	0.02500	0.01250	3.41040	7.40947	7.42815	10.01991
		Fast	8	0.02500	0.01042	9.05628	13.70903	6.86656	8.17182
		Slow	32	0.01823	0.00938	1.09109	1.10695	2.22646	3.25150
		Fast	32	0.01771	0.00938	1.09276	1.23603	1.13255	1.46046
	LL	Slow	8	0.02292	0.01042	6.04501	6.00555	8.57170	12.95956
		Fast	8	0.01667	0.00625	6.09996	13.79091	6.32724	20.65620
		Slow	32	0.01719	0.01094	0.98257	1.55757	1.43801	3.16253
		Fast	32	0.01667	0.00885	0.59062	1.55224	0.77019	1.89825
	LLL	Slow	8	0.02292	0.01458	3.77992	6.51116	8.14738	11.46502
		Fast	8	0.01667	0.01042	8.48881	14.13781	6.76383	11.80595
		Slow	32	0.01667	0.00990	0.92511	0.97865	2.43553	3.74466
		Fast	32	0.01615	0.00938	0.98417	1.26310	0.95708	1.64864

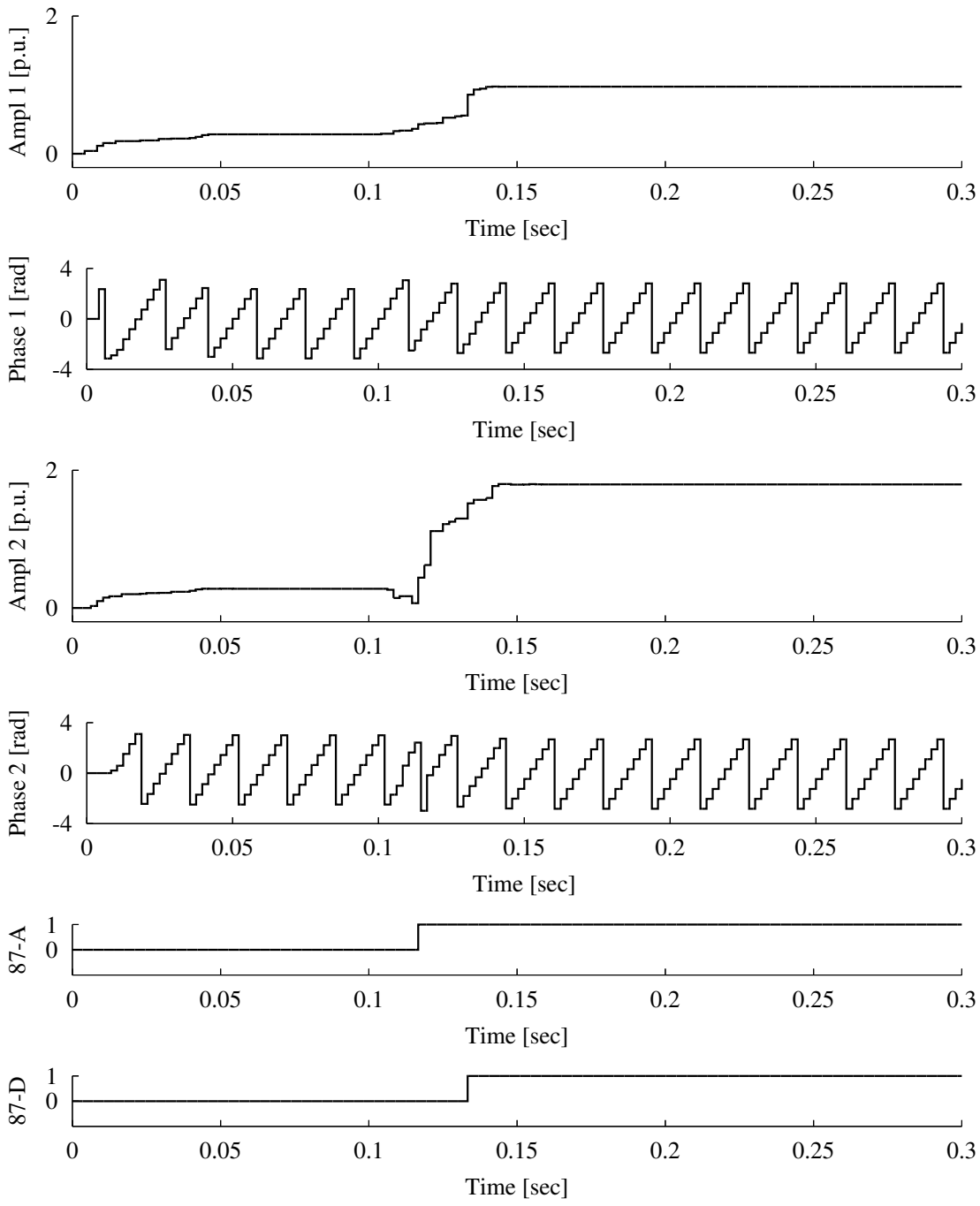

Figure C.1: GPS-LSE algorithm performance with 8 samples per cycle over slow network during a line-to-ground fault at location F2, modified power system parameters

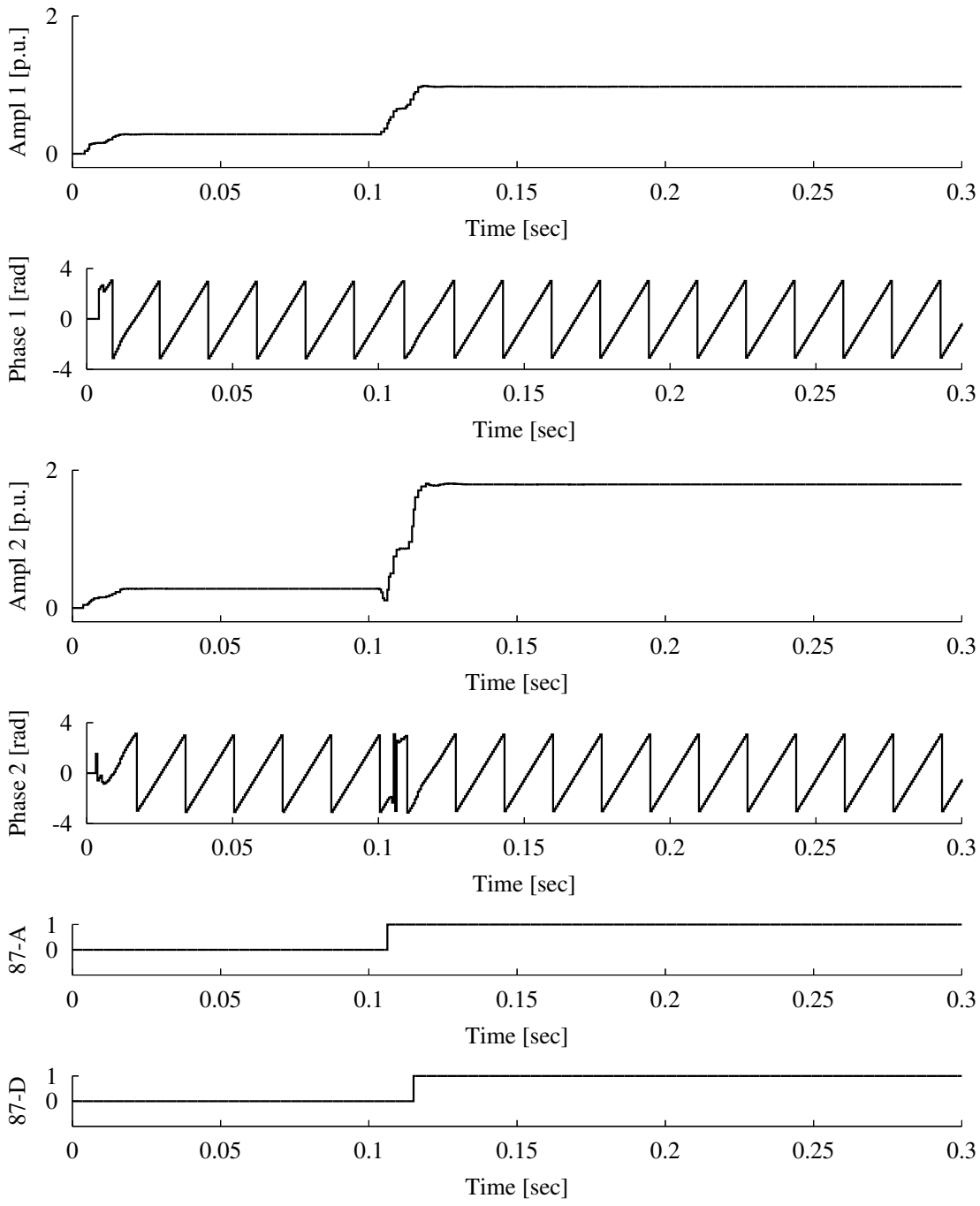

Figure C.2: GPS-LSE algorithm performance with 32 samples per cycle over slow network during a line-to-ground fault at location F2, modified power system parameters

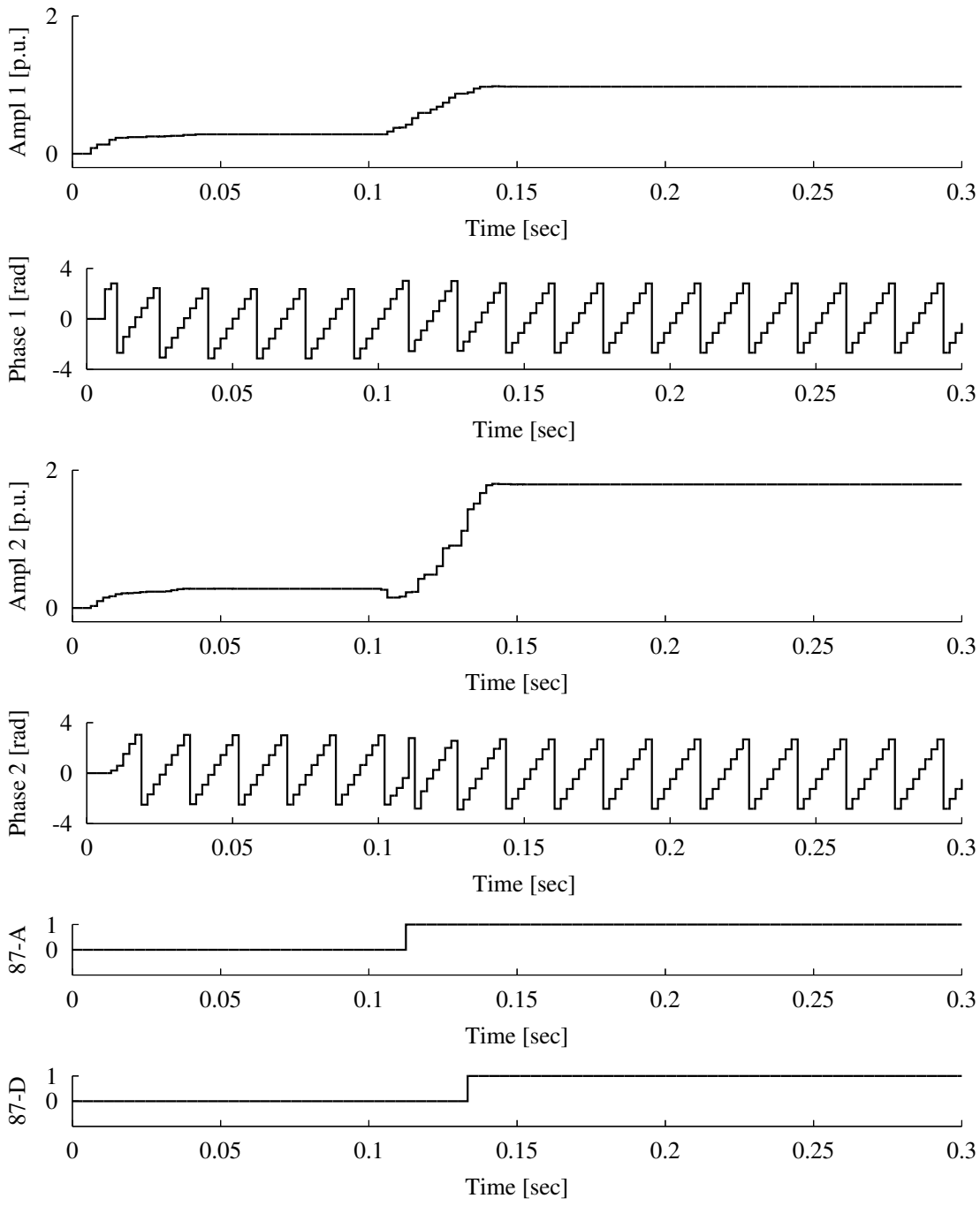

Figure C.3: GPS-LSE algorithm performance with 8 samples per cycle over fast network during a line-to-ground fault at location F2, modified power system parameters

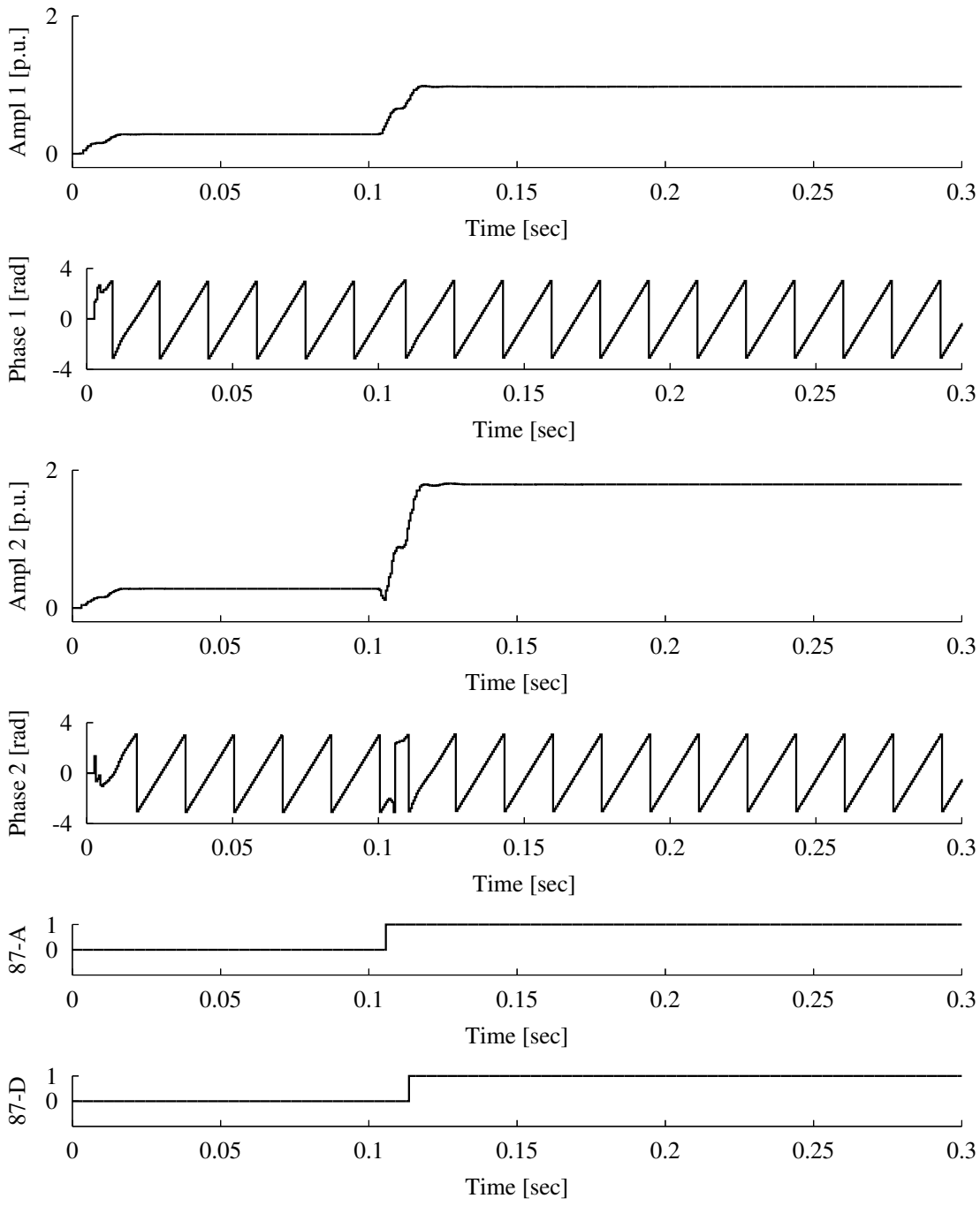

Figure C.4: GPS-LSE algorithm performance with 32 samples per cycle over fast network during a line-to-ground fault at location F2, modified power system parameters

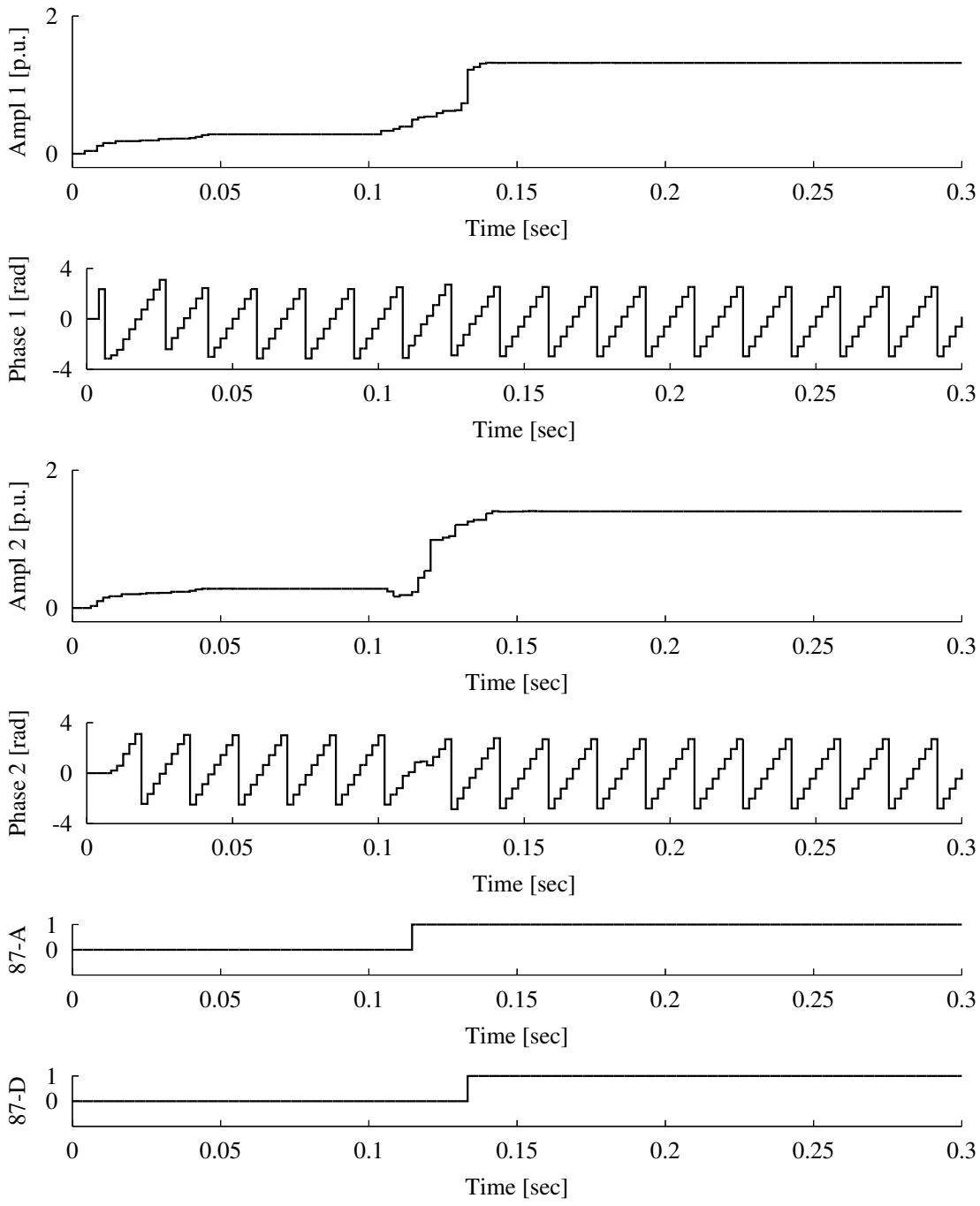

Figure C.5: GPS-LSE algorithm performance with 8 samples per cycle over slow network during a line-to-line fault at location F2, modified power system parameters

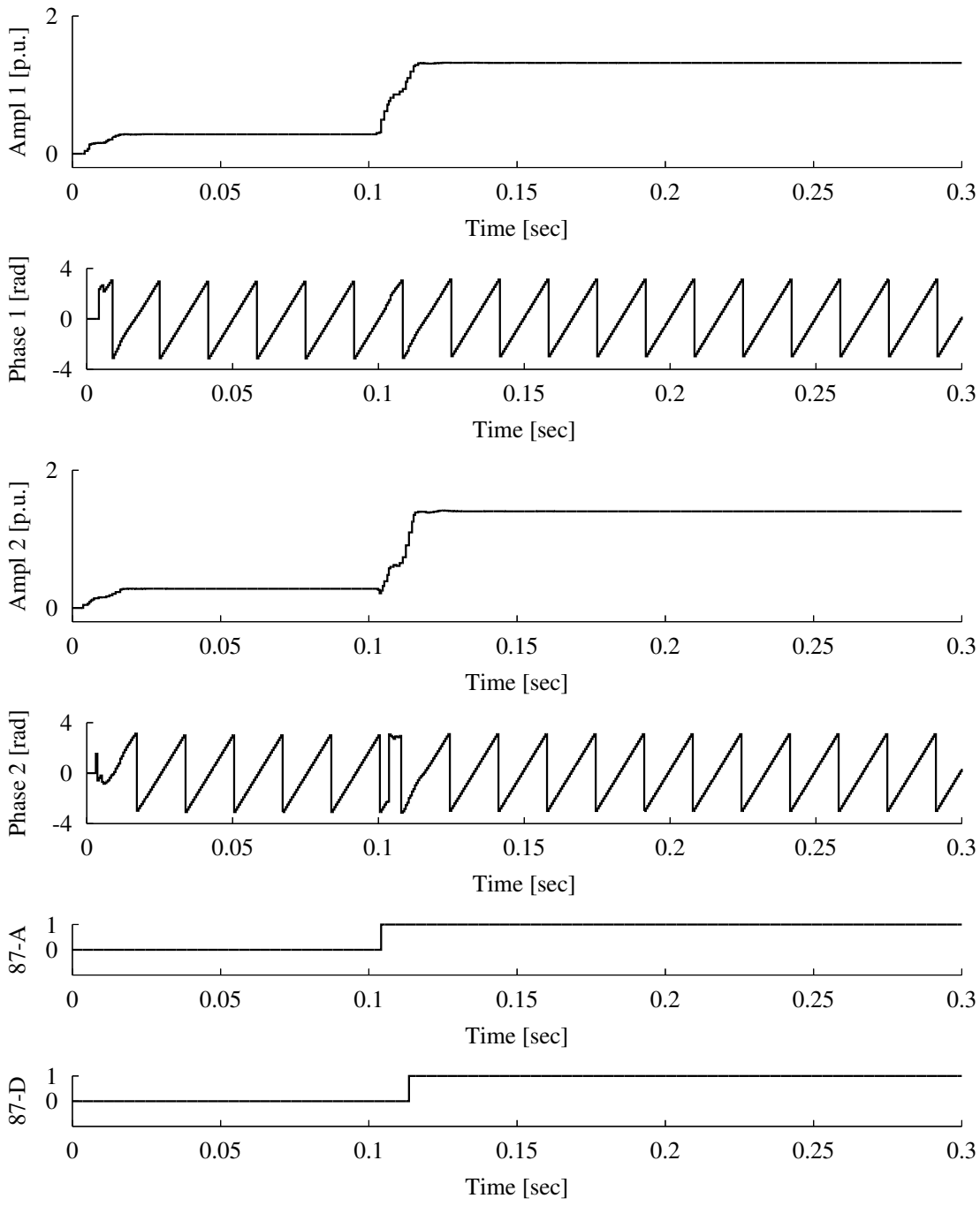

Figure C.6: GPS-LSE algorithm performance with 32 samples per cycle over slow network during a line-to-line fault at location F2, modified power system parameters

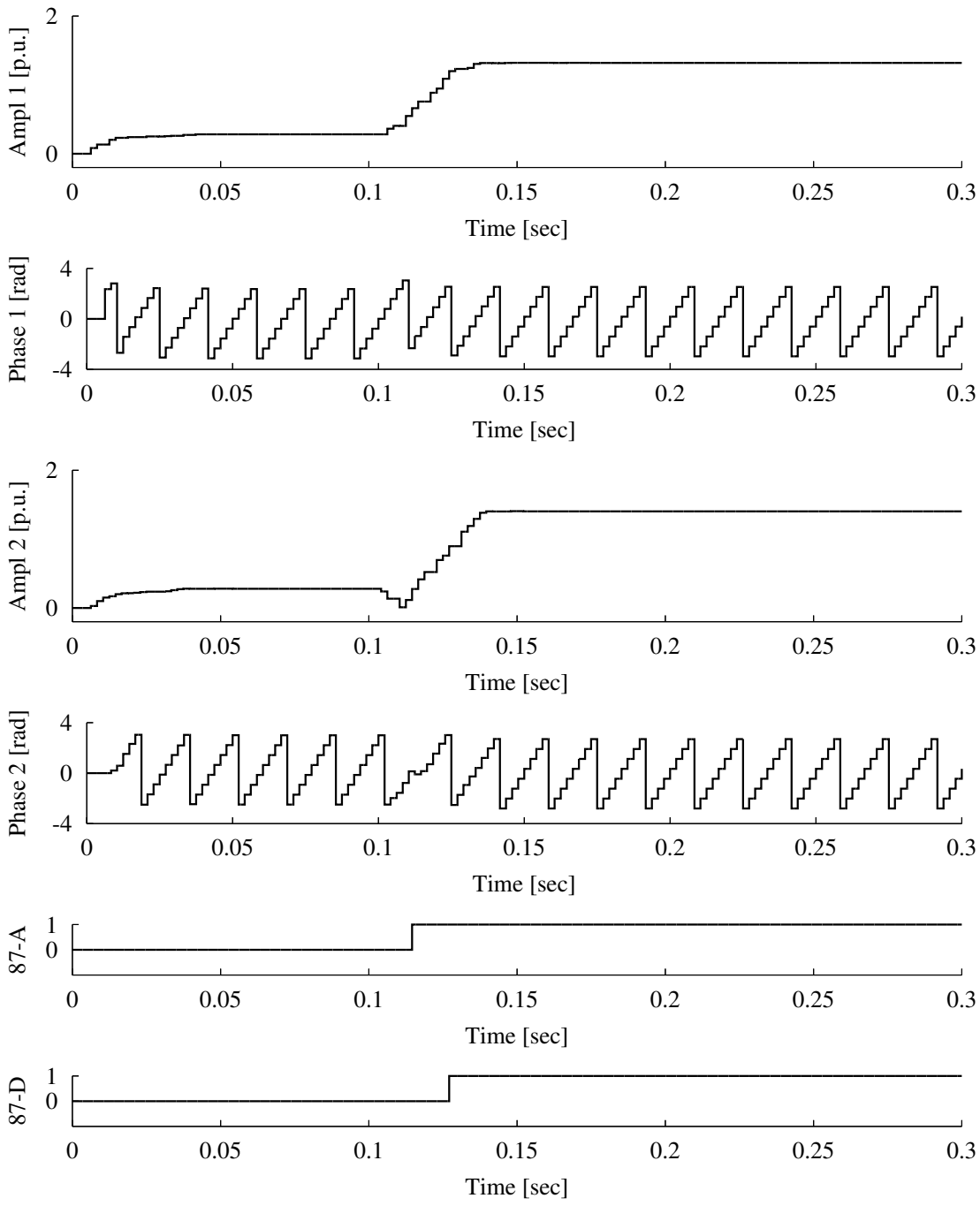

Figure C.7: GPS-LSE algorithm performance with 8 samples per cycle over fast network during a line-to-line fault at location F2, modified power system parameters

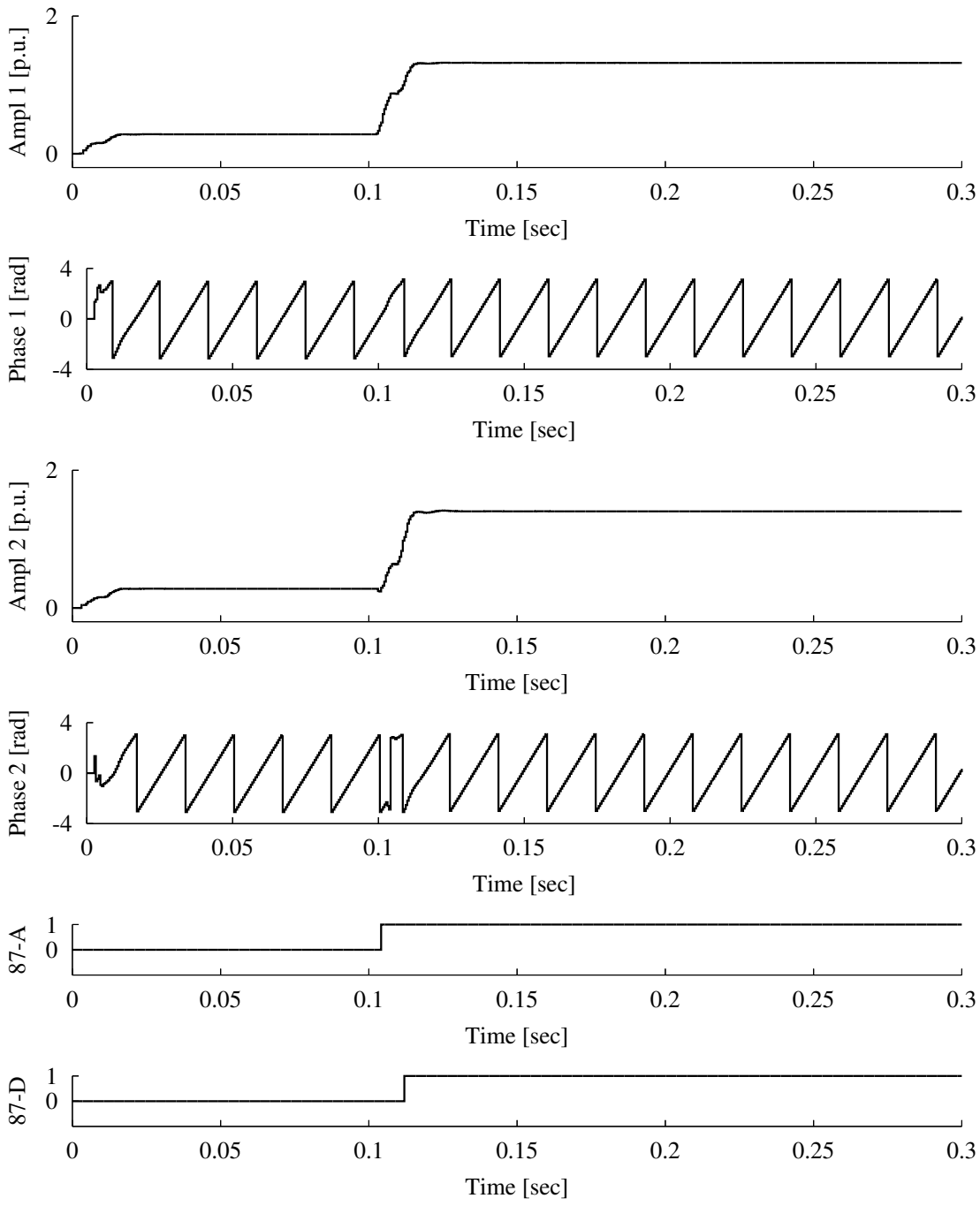

Figure C.8: GPS-LSE algorithm performance with 32 samples per cycle over fast network during a line-to-line fault at location F2, modified power system parameters

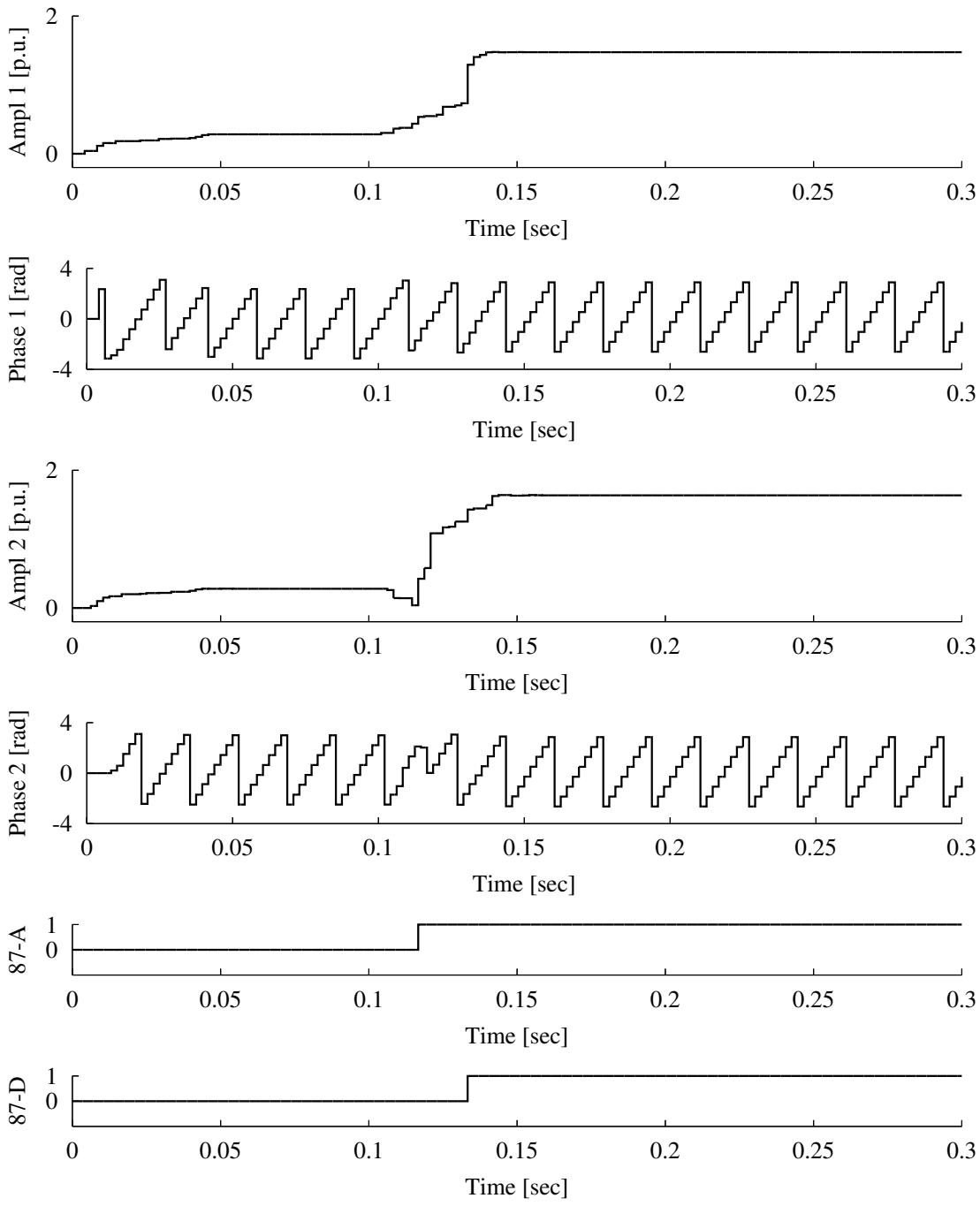

Figure C.9: GPS-LSE algorithm performance with 8 samples per cycle over slow network during a 3-line fault at location F2, modified power system parameters

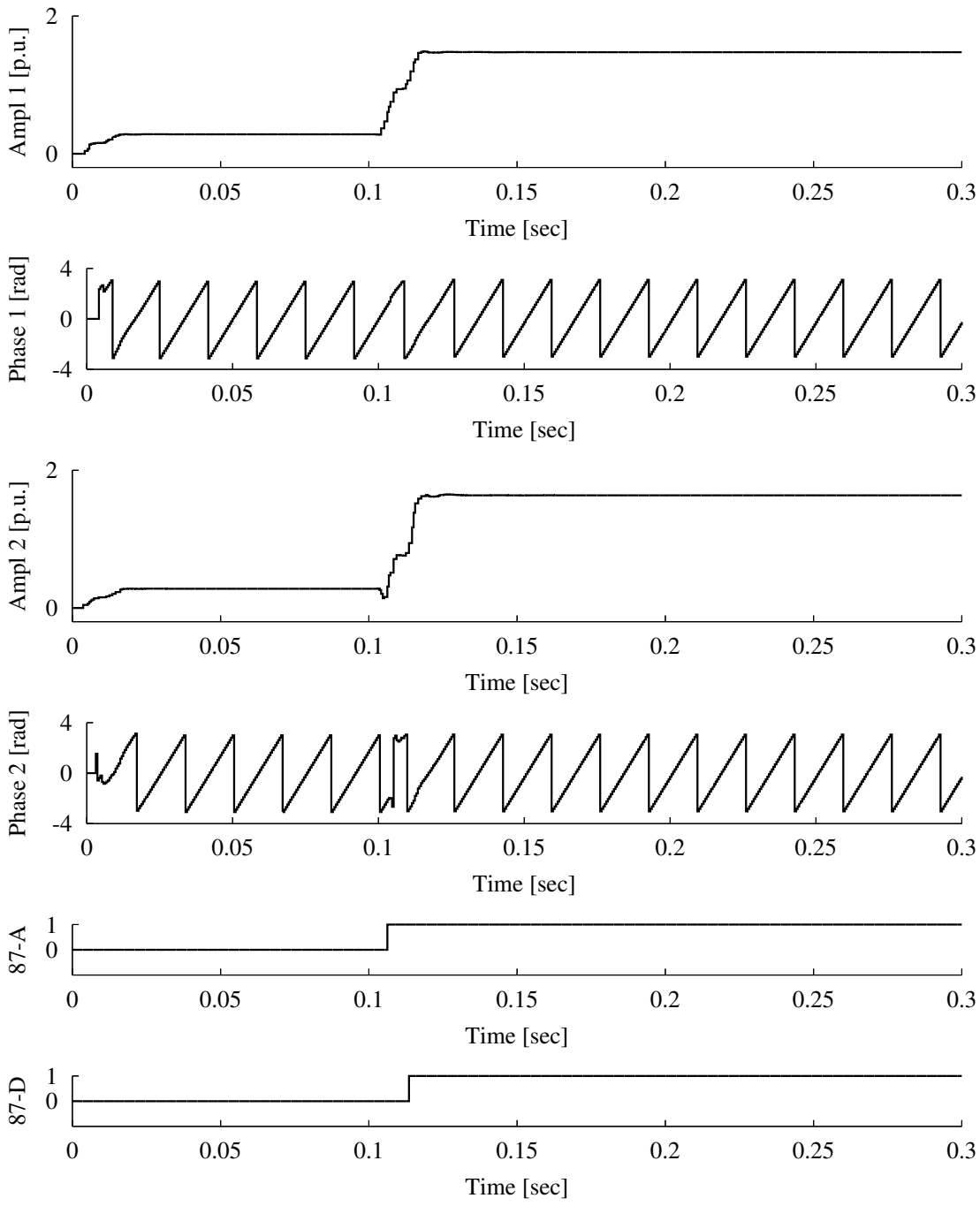

Figure C.10: GPS-LSE algorithm performance with 32 samples per cycle over slow network during a 3-line fault at location F2, modified power system parameters

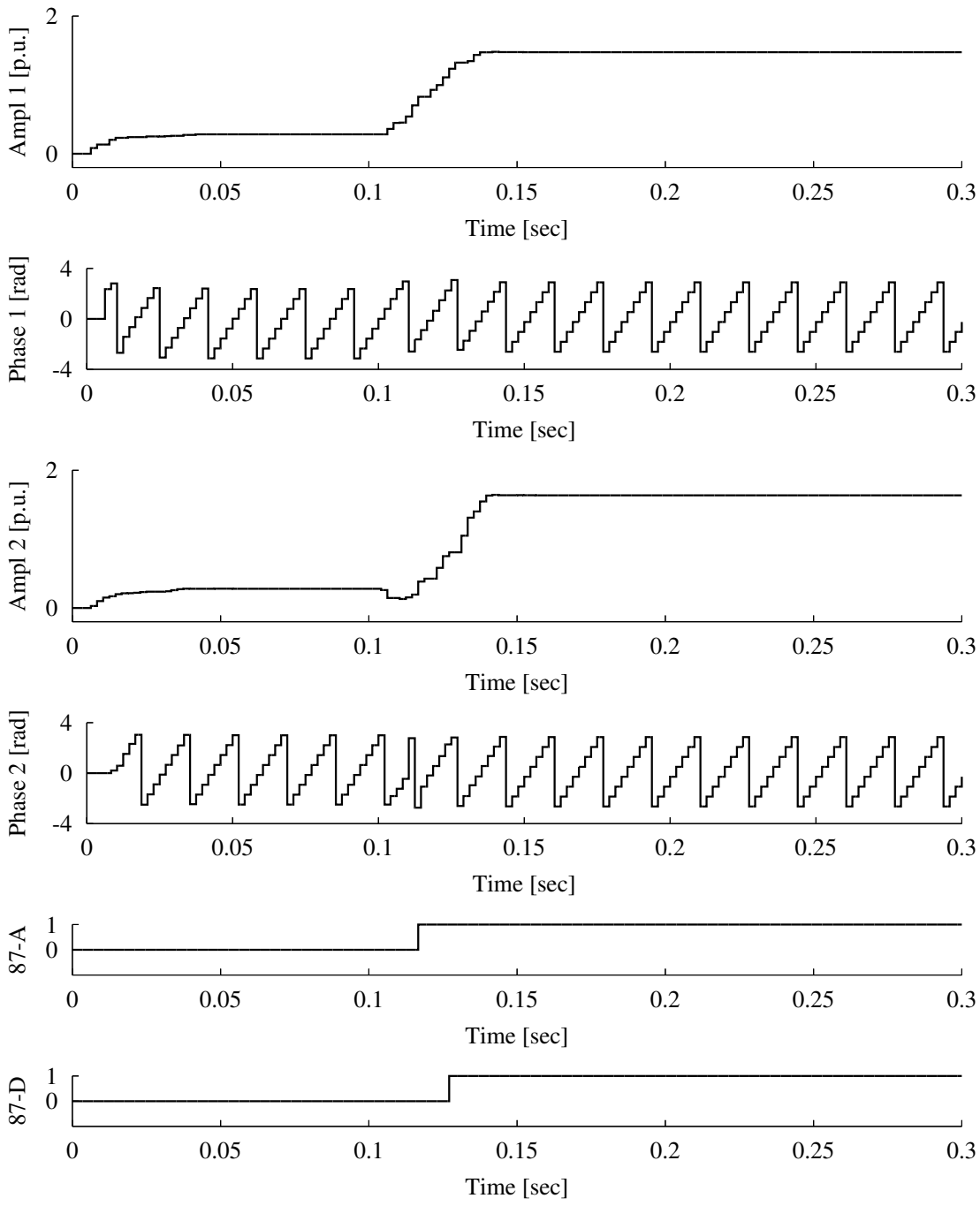

Figure C.11: GPS-LSE algorithm performance with 8 samples per cycle over fast network during a 3-line fault at location F2, modified power system parameters

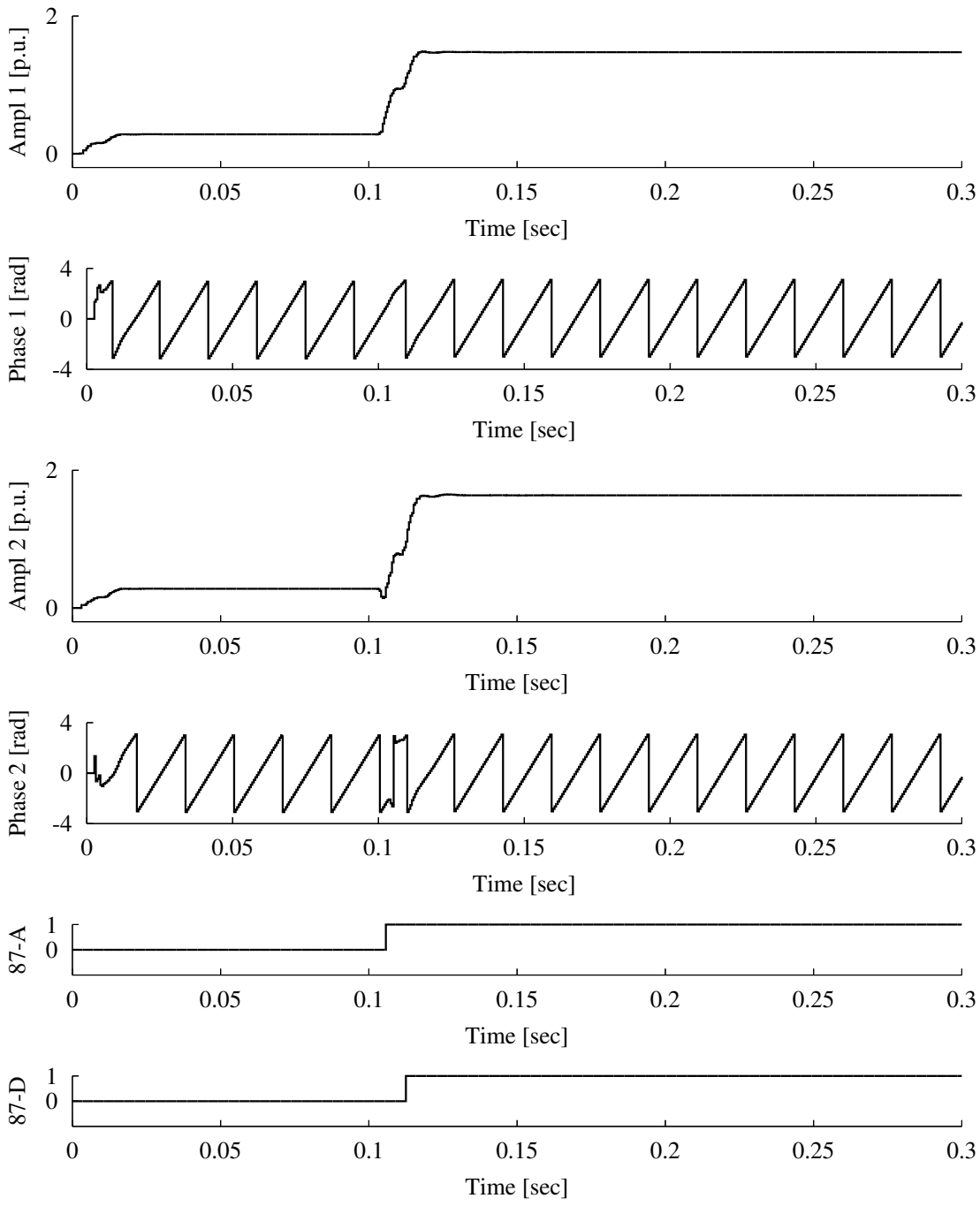

Figure C.12: GPS-LSE algorithm performance with 32 samples per cycle over fast network during a 3-line fault at location F2, modified power system parameters